XPF-ERCC1 protein complexes regulate 5´ DNA incision and XPC deubiquitylation in the Global Genome branch of Nucleotide Excision Repair

Dissertation zur Erlangung des Grades
"Doktor der Naturwissenschaften"

im Fachbereich Biologie
an der Johannes Gutenberg-Universität Mainz

Jens Michael Stadler

Geb. am 29.09.1987 in Pfullendorf, Deutschland

This work is dedicated to my wife Christine and my children Paul and Emma.

SUMMARY

The genome of cellular systems is under constant threat of genotoxic agents. Thus, efficient DNA damage repair is essential to maintain integrity and stability of the genome. Nucleotide excision repair (NER) represents one of the main cellular DNA repair pathways induced by UV light exposure. The global genome-NER branch counteracting lesions in transcriptionally silent DNA regions, is initiated by binding of the damage recognition factor XPC to DNA damage. The UV-DDB-CULA-RBX1 E3 ligase catalyzed polyubiquitylation of XPC after UV irradiation has been well studied. However, mechanistic insight into how ubiquitylated XPC regulates the GG-NER pathway is still lacking. Here, we show that ubiquitylated XPC is associated with a novel protein complex consisting of the heterodimeric ERCC1-XPF endonuclease and the deubiquitylase USP7 (also known as HAUSP). Interestingly, ERCC1-XPF enhances the deubiquitylation reaction of XPC *in vitro* and *in vivo*. We further demonstrate that USP7 competes with XPA for binding to the ERCC1-XPF endonuclease complex. Collectively our results provide evidence of two distinct ERCC1-XPF protein complexes that operate in 5' DNA incision or in XPC deubiquitylation thus coupling both processes in the GG-NER pathway.

ZUSAMMENFASSUNG

Das effiziente Beseitigen von DNA-Schäden ist für den Erhalt der Stabilität und Integrität des Genoms unverzichtbar. Aus diesem Grund gibt es eine Vielzahl von DNA-Reparaturmechanismen, die jeweils spezifisch charakteristische DNA-Schäden erkennen und reparieren. Bestrahlung mit UV-Licht verursacht hauptsächlich zwei spezifische DNA-Schäden, CPDs (Cyclobutan-Pyrimidindimere) und 6´-4´ Photoprodukte, die durch die Nukleotid-Exzisionsreparatur (NER) beseitigt werden. Der global genomweite Zweig der Nukleotidexzisions-Reparatur (GG-NER) wird durch die Bindung des Erkennungsproteins XPC an den DNA-Schaden initiiert. Die durch den UV-DDB-CULA-RBX1 Ligase Komplex katalysierte Polyubiquitylierung von XPC nach UV-Bestrahlung ist bereits gut dokumentiert. Es ist jedoch immer noch unklar, wie ubiquityliertes XPC den weiteren Verlauf der NER-Reaktion mechanistisch reguliert. Unsere Experimente zeigen, dass ubiquityliertes XPC mit einem neuen Protein-Komplex bestehend aus dem heterodimeren ERCC1-XPF-Komplex und der Deubiquitylase USP7 (auch bekannt als HAUSP), assoziiert ist. Interessanterweise beschleunigt ERCC1-XPF die Deubiquitylierungsreaktion von XPC sowohl *in vitro* als auch *in vivo*. Wir zeigen weiter, dass USP7 mit XPA um die Bindung an den ERCC1-XPF-Endonukleasekomplex konkurriert. Zusammenfassend betrachtet charakterisieren unsere Ergebnisse zwei unterschiedliche ERCC1-XPF-Protein-komplexe, die entweder in der 5'-DNA-Inzision oder in der Deubiquitylierung von XPC maßgeblich beteiligt sind. Da beide Proteinkomplexe auf ERCC1-XPF aufbauen, sind diese beiden Prozesse, der 5´-DNA-Einschnitt und die XPC Deubiquitylierung, in der NER-Reaktion miteinander gekoppelt.

TABLE OF CONTENTS

INTRODUCTION

THE NECESSITY FOR FAITHFUL DNA REPAIR

The formulation of the central dogma of molecular biology which defines the basis for all biological systems has been one of the most fundamental discoveries. Cells use their DNA as a template for the synthesis of RNA thereby transmitting the genetic information stored within the DNA. RNA is then further translated into proteins which precisely control and carry out all kinds of biological processes. Our DNA is assembled from small building blocks, nucleotides, which are composed of one of the four different nucleobases: adenine (A), guanine (G), cytosine (C) and thymine (T). The genetic information of DNA is encoded in the specific sequence of this four nucleobases. Any modification of the specific DNA sequence, and thereby in the instructions for the synthesis of proteins it encodes, can have deleterious effects on the cell´s function. DNA damage interferes with various essential cellular processes (such as transcription and DNA replication) and can potentially lead to mutations, chromosome aberrations or even cell death in case the amount of damaged DNA reaches a certain unrepairable threshold (Hoeijmakers, 2001; Friedberg et al., 2006). Thus, preserving and maintaining genome integrity and stability is one if not the most crucial function of a living cell.

TYPES OF DNA DAMAGE

DNA is constantly under attack by a plethora of damage-inducing agents, either derived from endogenous or exogenous sources, which can directly or indirectly induce the formation of DNA damage (see figure 1). As a first line of defense, many organisms express enzymes such as superoxide dismutase (SOD), catalase (CAT) and glutathione peroxidase which “detoxify” reactive oxygen species (ROS), released for example form the cellular respiratory chain or exogenously induced by UV irradiation (Rastogi et al., 2010). Additionally, scavenger molecules such as vitamin C (ascorbate), B and E as well as cysteine and glutathione quench radicals before they are able to react with and damage cellular proteins, lipids and DNA. Thus, these molecules play a role in preventing DNA damage (Ighodaro et al., 2018).

To counteract the deleterious effects of DNA damage, cells have evolved a wide variety of active DNA repair pathways that detect and repair such DNA lesions.

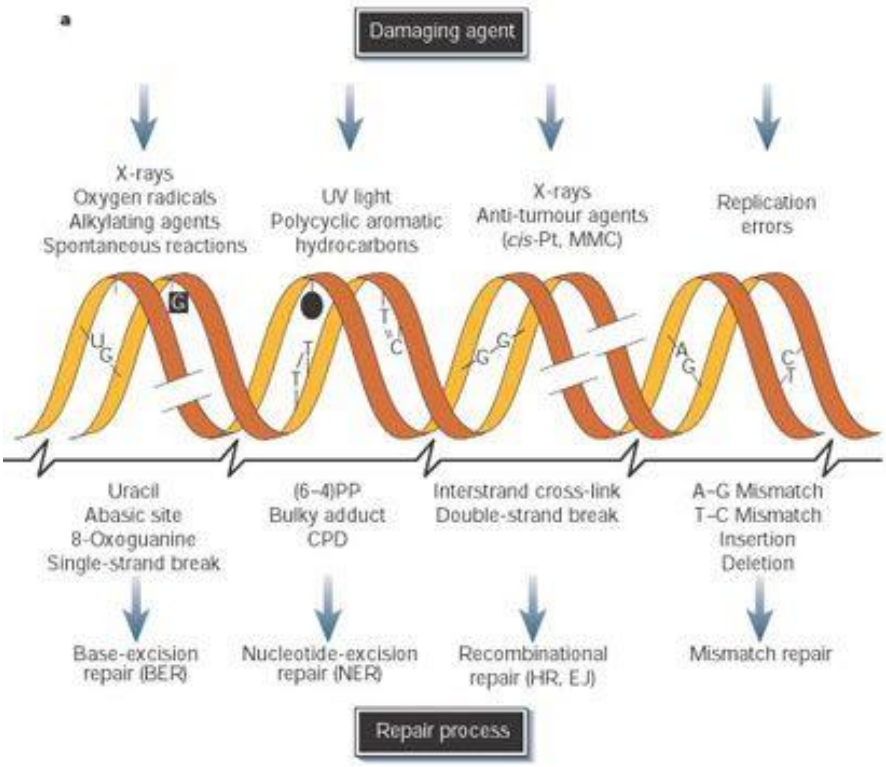

Figure 2: DNA damage and their counteracting repair mechanisms. Common DNA damage inducing agents derived from endogenous (spontaneous deamination, reactive oxygen species from cellular respiration) or exogenous (such as UV light) sources (top); examples of DNA lesions they induce (middle) and the respective DNA repair mechanism dealing with the repair of the DNA lesion (bottom). Abbreviations: cis-Pt and MMC, cisplatin and mitomycin C, respectively (both DNA crosslinking agents); (6-4)-PP and CPD, 6-4 photoproduct and cyclobutane pyrimidine dimer, respectively (both induced by UV light); BER and NER, Base excision and nucleotide excision repair, respectively; HR, homologous recombination, EH, end joining) (Figure adapted from Hoeijmakers, 2001).

Endogenous DNA Damage	DNA Lesions Generated	Number Lesions/Cell/Day	
Depurination	AP site	10000[a]	
Cytosine deamination	Base transition	100–500[a]	
SAM-induced methylation	3meA	600[a]	
	7meG	4000[a]	
	O^6meG	10–30[b]	
Oxidation	8oxoG	400–1500[c]	
Exogenous DNA Damage	Dose Exposure (mSv)	DNA Lesions Generated	Estimated Number Lesions/Cell
Peak hr sunlight	—	Pyrimidine dimers, (6–4) photoproducts	100,000/day[d]
Cigarette smoke	—	aromatic DNA adducts	45–1029[e]
Chest X-rays	0.02[f,g,h]	DSBs	0.0008[i]
Dental X-rays	0.005[f,g,h]	DSBs	0.0002[i]

Figure 1: Estimated numbers of DNA lesions per cell per day. (Figure adapted from Ciccia and Elledge, 2010). The values were estimated as described: (a) Lindahl and Barnes (2000), (b) Rydberg and Lindahl (1982), (c) Klungland et al., 1999, (d) Hoeijmakers (2009), (e) DNA adducts detected in the lung of smokers following 1-2 cigarette packs per day for approx.. 40 years (Philips et al., 1998),
(f) http://www.merck.com/mmhe/sec24/ch292/ch292a.html
(g)http://www.fda.gov/RadiationEmittingProducts/RadiationSafety/RadiationDoseReduction/ucm199994.htm#ft6
(h) Hall and Giaccia (2006).

One of the most frequently occurring and toxic DNA lesions are abasic sites which arise after spontaneous hydrolysis of the N-glycosidic bond between the deoxyribose and the respective base (Lindahl and Barnes, 2000; Ciccia and Elledge, 2010). This spontaneous hydrolysis reaction is markedly enhanced by chemical modification of DNA bases. Mostly driven by acid catalysis, the N-glycosidic bond between the deoxyribose and the purine bases adenine and guanine is less stable than the glycosidic bond with pyrimidine bases (cytosine and thymine) under physiological conditions, resulting in depurination occurring much more frequently than depyrimidination (Lindahl and Nyberg, 1972; Lindahl and Karlström, 1973). Furthermore, all DNA bases with an amine group, which excludes thymine, can undergo spontaneous deamination (Lindahl and Barnes, 2000). Interestingly, the rate of such spontaneous deamination processes is dramatically enhanced in single stranded-DNA (transient ssDNA for example during replication, transcription and recombination) compared to double stranded-DNA (Lindahl, 1993).

The deamination of cytosine to uracil occurs at a significant levels in cells and harbors mutagenic potential since the newly formed uracil base pairs with adenine. However, the majority of deamination products (such as uracil) are usually not found in DNA which greatly facilitates their recognition and removal by specific DNA glycosylases. Notably, an exception is 5-methylcytosine yielding thymine after spontaneous deamination. In addition, thymine DNA glycosylase (TDG), the enzyme removing thymine from T-G mismatches, is relatively inefficient (Cortazar et al., 2007). Therefore, 5´-mCpG sites can be considered as mutagenic hotspots reflected by the fact that the CG to TA transition at these sites is responsible for one third of point mutations associated with hereditary diseases in humans (Cooper et al., 2010, De Bont and van Larebeke, 2004). Reactive oxygen species derived from the cellular respiratory chain (O_2^-, H_2O_2, $^1O_2$, $OH\cdot$) can also lead to abasic sites as well as oxidized DNA bases such as formamidopyrimidine, thymine glycol (De Bont and van Larebeke, 2004; Hoeijmakers, 2009; Ciccia and Elledge, 2010). Besides DNA bases, ROS also attack the DNA phosphodiester-sugar backbone resulting in both single and double-strand breaks (Chatterjee and Walker, 2017). Another biologically significant oxidative DNA lesion is 8-oxo-guanine (7,8 dihydro-8-oxoguanine) formed from hydroxylation of the C-8 residue of guanine. 8-oxo-guanine is potentially mutagenic since this DNA lesion prefers to adopt the syn-conformation and thus, can pair incorrectly with adenine instead of cytosine (Chatterjee and Walker, 2017). Furthermore, DNA bases are also target of alkylation primarily mediated by the endogenous methyl-donor S-Adenosylmethionin (SAM) (Lindahl and Barnes, 2000). Collectively, it has been

estimated that a cell has to deal with 100 000 spontaneous DNA lesions per day (see figure 2; De Bont and van Larebeke, 2004; Ciccia and Elledge, 2010).

Besides the DNA lesions induced by endogenous cellular processes, DNA structure is also threatened by environmental damaging agents. Exogenous, environmental DNA damage can arise from both physical and chemical sources. Common physical genotoxic agents include ionizing radiation (IR) and the sun´s ultraviolet (UV) light, which stimulates the formation of two major DNA lesions, cyclobutane pyrimidine dimers (CPDs) and 6-4 photoproducts (6-4 PP). It has been estimated that a peak hour of sunlight can produce up to 100 000 DNA damage sites (CPDs and 6-4PPs) highlighting the sun´s powerful potential as genotoxic agent (see figure 2; Hoeijmakers, 2009). Even more energetic ionizing radiation (IR) such as cosmic radiation or Xrays (derived from medical treatments) is able to ionize atoms and molecules by displacing electrons which leads to the breakage of chemical bonds between atoms. Ionizing radiatuion (IR), either directly or indirectly through the generation of radicals and ROS inside the cell, produces single and double strand breaks (SSBs and DSBs, respectively) and induce oxidation of DNA bases (Hoeijmakers, 2001). Additionally, SSBs can also be formed indirectly by insufficient or impaired Base Excision repair (BER) (Ciccia and Elledge, 2010). Chemical agents used in cancer therapy are designed to cause overwhelming DNA damage to force cancer cells into apoptosis. Thus, these chemical agents can cause a wide variety of DNA lesions. Crosslinking agents such as mitomycin C (MMC), cisplatin (cis-Pt), psoralen and nitrogen mustard are covalently attached to DNA bases on the same strand (intrastrand crosslink) or to different DNA strands (interstrand crosslink) (Ciccia and Elledge, 2010). Additional modifications of cross-linking agents include DNA monoadducts and DNA protein crosslinks (Chatterjee and Walker, 2017). The alkylating agents methyl methanesulfonate (MMS) and temozolomide transfer alkyl groups to DNA bases. Other chemical agents, such as the topoisomerase inhibitors camptothecin (CPT) and etoposide inhibit topoisomerase I or II, respectively, resulting in trapped topoisomerase-DNA covalent complexes and the formation of SSBs. In case the trapped TOP1 cleavage complex is present on the leading strand, DSBs can be formed upon replication fork collision (Pommier et al., 2006; Xu et al., 2015). Polycyclic aromatic carbons (PAHs) including benzo(a)pyrene, probably the most prominent and best documented compound of this class of genotoxic agents, are commonly found in automobile exhaust, charred food and cigarette smoke and possess a high mutagenic and carcinogenic potential (Luch, 2009). Similar to other genotoxic agents such as aflatoxin and aminofluorene, benzo(a)pyrene is a pro-mutagen which is

enzymatically converted in its ultimate carcinogenic diol epoxide form, anti-BPDE (7,8-hydroxy-9α,10α-epoxy-7,8,9,10-tetrahydro-benzo(α)pyrene), by the action of the cytochrome P450 system in the liver (Chatterjee and Walker, 2017). Photo-oxidation, one electron oxidation, multiple ring-oxidation and nitrogen-reduction pathways are also known to activate the PAHs thereby leading to a broad spectrum of adducts and oxidative DNA damage (Harvey et al., 2005; Chatterjee and Walker, 2017).

Probably the most common environmental DNA damage-inducing agent is the sun´s UV light which is the leading cause of skin cancer in humans (Davies, 1995). The spectrum of UV irradiation ranges from 100 to 400 nm and can be subdivided, with increasing energy and mutagenic potential, into UV-A (400 – 320nm), UV-B (320 – 280nm) and UV-C (280nm – 100nm) components (D´Orazio et al., 2013; Schuch et al., 2018). Fortunately, oxygen and nitrogen molecules as well as ozone in the atmosphere completely absorb the UV-C fraction and the great majority (approximately 90%) of UV-B emitted from the sun (D´Orazio et al., 2013; Schuch et al., 2018). Consequently, only a small portion of the solar UV-B (10%) and almost the complete UV-A irradiation (90 – 95%) reach the earth´s surface and thus, are of relevance for cellular systems (Schuch et al., 2018). Inside living cells, proteins and DNA are primarily targeted by UV-induced damage due to their absorption characteristics and their abundance in cellular systems (Pattison and Davies, 2006). In general, UV light-triggered cellular damage is mediated by two distinct processes. DNA or proteins can directly absorb solar UV-B light (and UV-C in artificial systems) and their excitation can initiate subsequent chemical reactions (Pattison and Davies, 2006). Direct UV absorption of DNA, in particular 260 nm UV-C, characteristically results in the formation of DNA base dimers including cyclobutane pyrimidine dimers (CPDs) and pyrimidine (6-4) pyrimidone products (6-4 PPs) in an approximate ratio of 3:1 and their dewar isomers (Nakagawa et al., 1998). The second, indirect path involves endogenous or exogenous molecules (such as flavins, porphyrins including heme groups, pterins, NADH and the skin pigment melanin), and not DNA itself, that are excited upon photon absorption. Subsequently, the excited, highly reactive photosensitizers can induce damage for example by electron transfer and hydrogen abstraction resulting in the generation of ROS (H_2O_2, hydroxyl radical and $O_2^{\cdot -}$) and other free radicals (Pattison and Davies, 2006). An alternative mechanism is the direct energy transfer from the excited photosensitizer to molecular oxygen, yielding singulet oxygen ($^1O_2$) and subsequent damage to biomolecules (Schuch et al., 2018). Interestingly, UV-A

irradiation has been found to selectively induce guanine oxidation via $^1O_2$, thereby mainly generating 8-oxo-7,8-dihydroguanine (8-oxo-G) (Schuch et al., 2018; Cadet et al., 2015).

In proteins, the three amino acids tryptophane (single letter code W), tyrosine (Y) and phenylalanine (F) are responsible for the absorption of proteins in the UV spectrum based on their aromatic side chains, with an absorption maximum at 280 nm. Additionally, the peptide backbone (amide bond) also absorbs at around 215 nm.

In laboratory investigations, also including this study, 254 nm UV-C irradiation is thus routinely used for the induction of DNA damage based on the maximum absorption of DNA bases around 260 nm resulting in the specific induction of two major damage products, CPDs and 6-4-PPs (see figure 4) while minimizing damage occurring to cellular proteins (Schuch et al., 2018).

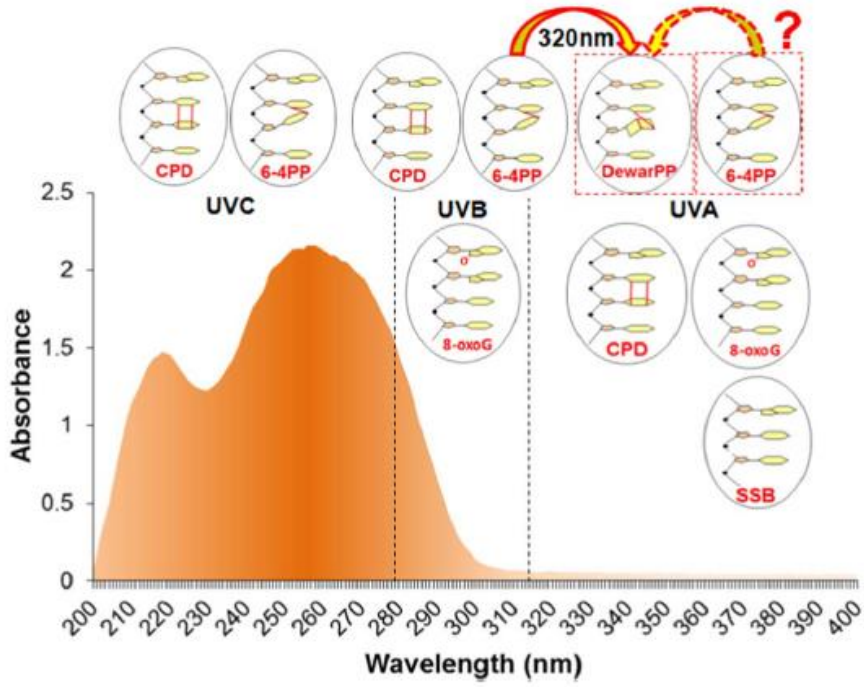

Figure 3: UV absorption spectrum of DNA and the main types of DNA lesions induced following irradiation by the respective UV fraction. DNA shows an absorption maximum around 260 nm. 6-4 PP are able to undergo photoisomerization to their Dewar valence isoform, most likely initiated by UV-A (and UV-B) irradiation since 6-4 PPs efficiently absorb at 320 nm. Abbreviations: CPD, cyclobutane pyrimidine dimer; 6-4 PP, pyrimidine (6-4) pyrimidone photoproducts; Dewar-PP, Dewar valence isomer; 8-oxo-G, 8-oxo-7,8-dihydroguanine; SSB, single strand breaks). (Figure taken from Schuch et al., 2018).

THE DNA DAMAGE RESPONSE AND CHECKPOINT ACTIVATION

The activities of this arsenal of cellular DNA repair pathways require a tight spatial, temporal and DNA damage specific regulation to avoid unnecessary and unwanted DNA structure alterations which might interfere with ongoing normal cellular processes (Ciccia and Elledge, 2010). This superior regulation unit in addition with the cellular DNA repair pathways is termed the DNA Damage Response (DDR) (Harper and Elledge, 2007; Jackson and Bartek, 2009; Ciccia and Elledge, 2010). The DDR coordinates and orchestrates DNA replication, DNA repair, cell cycle transitions and checkpoints, transcription and, in severe cases, triggers senescense or apoptotic cell death (Ciccia and Elledge, 2010; Blackford and Jackson, 2017). The DDR signaling is primarily initiated by three kinases ATM (ataxia telangiectasia mutated), ATR (AMT- and Rad3-related) and DNA-PKcs (DNA-dependent protein kinase catalytic subunit) which are recruited to the damage site by binding to specific factors and, subsequently, become activated (Ku70/80 recruits DNA-PKcs; ATM binds to the NBS1 subunit of the MRN complex; the ATRIP (ATR interacting protein)-ATR dimer senses DNA damage through ATRIP-recognition of RPA-coated ssDNA complexes; Falck et al., 2005) (Blackford and Jackson, 2017; Ciccia and Elledge, 2010). Upon activation, ATM and ATR trigger a signaling cascade by phosphorylating a variety of proteins, including the most notable factors, p53 and the downstream checkpoint kinases CHK1 and CHK2. CHK1 and CHK2 transmit the signal further via phosphorylation of the mitotic inhibitor kinase WEE1 and CDC25 phosphatases (see figure 5; Curtin, 2012; Hühn et al., 2013; Ciccia and Elledge, 2010). As a consequence, the activity of cyclin-dependent kinases (CDKs) is modulated resulting in the blockage of cell cycle of progression. Dependent on which of the CDKs is inhibited, the cell cycle is either arrested at the G1/S phase transition, in the intra-S phase or at the G2/M transition (Curtin, 2010). Importantly, the halt of the cell cycle progression ensures efficient DNA repair and thus, prevents DNA replication or mitosis in the presence of excessive DNA damage (Curtin, 2012; Hühn et al., 2013). For further details, please also see legend of figure 4.

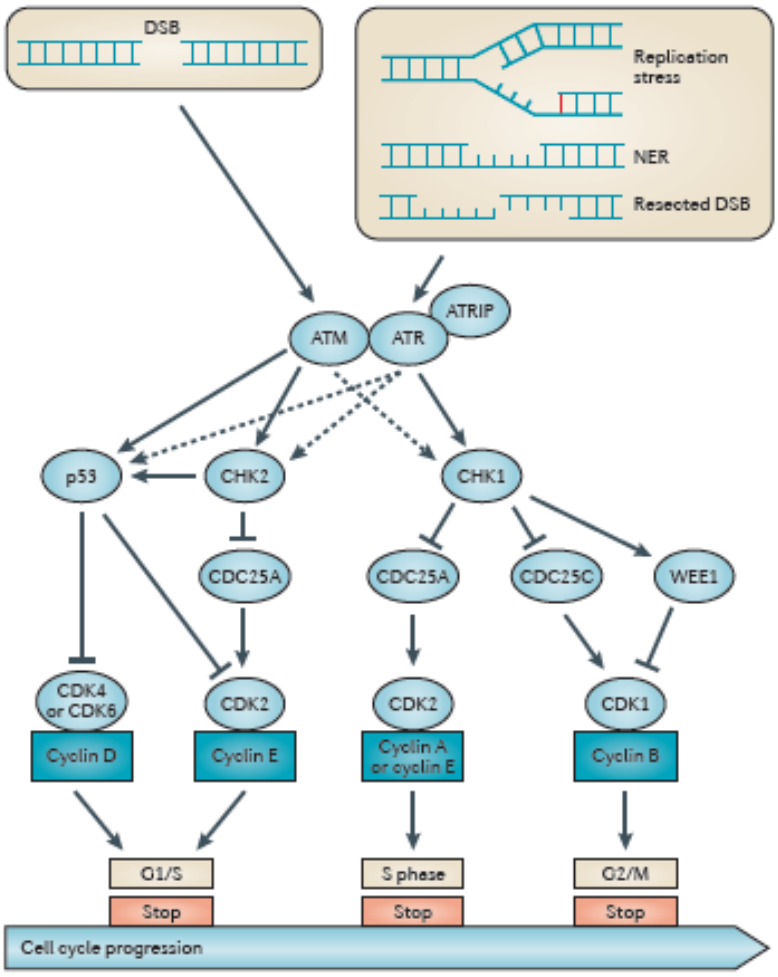

Figure 4: DNA damage and checkpoint signaling. ATM binds to the NBS1 subunit within the MRN complex at the DSB site and becomes activated. Upon activation, ATM triggers G1 signaling by phosphorylating, and thus activating, various proteins including CHK2 and p53. Activated p53 induces transcription of various target genes, including CDK inhibitors (p21, p27), DNA repair factors and pro-apoptotic factors resulting in growth and cell cycle arrest, efficient DNA repair and, in severe cases of excessive DNA damage, the induction of senescense or apoptotic cell death (Reinhardt and Schumacher, 2012). The ATM kinase is activated by ATRIP-dependent recruitment to RPA-coated ss-dsDNA junctions which arise at stalled replication forks, resected DSBs and are generated as intermediates during NER. Activated ATM initiates both intra-S phase and G2 checkpoint signaling by phosphorylation of CHK1. CHK1 further transmits the signal via phosphorylation of various targets including the mitotic inhibitor kinase WEE1 and the cell division cycle 25 (CDC25) phosphatase resulting in the coordinated inhibition of the cyclin-dependent kinase (CDK) activity, the main drivers of the cell cycle. Whereas phosphorylation activates WEE1, phosphorylation of CDC25, which stimulates CDK activity by removing inhibitory phosphate groups on CDKs, leads to its degradation (Curtin, 2012; Harvey et al., 2005). Notably, there is also crosstalk between the ATM-CHK2 axis and the ATR-CHK1 signaling pathway and that they share many substrates. ATRIP, ATR-interacting protein. Dashed arrows indicate secondary targets. (Figure taken form Curtin, 2012).

CELLULAR DNA REPAIR PATHWAYS

To ensure efficient removal of damaged DNA, cells have established a wide variety of DNA repair pathways (reviewed in De Bont and van Larebeke, 2004; Helleday et.al. 2014). The various DNA repair pathways are described in more detail in the following chapter.

Mismatch repair

The post-replicative Mismatch Repair (MMR) system is an evolutionarily conserved repair pathway that increases the fidelity of DNA replication by approximately 100 – 1000 fold (Kunkel and Erie, 2005). MMR removes misincorporated bases and insertion-deletion loops

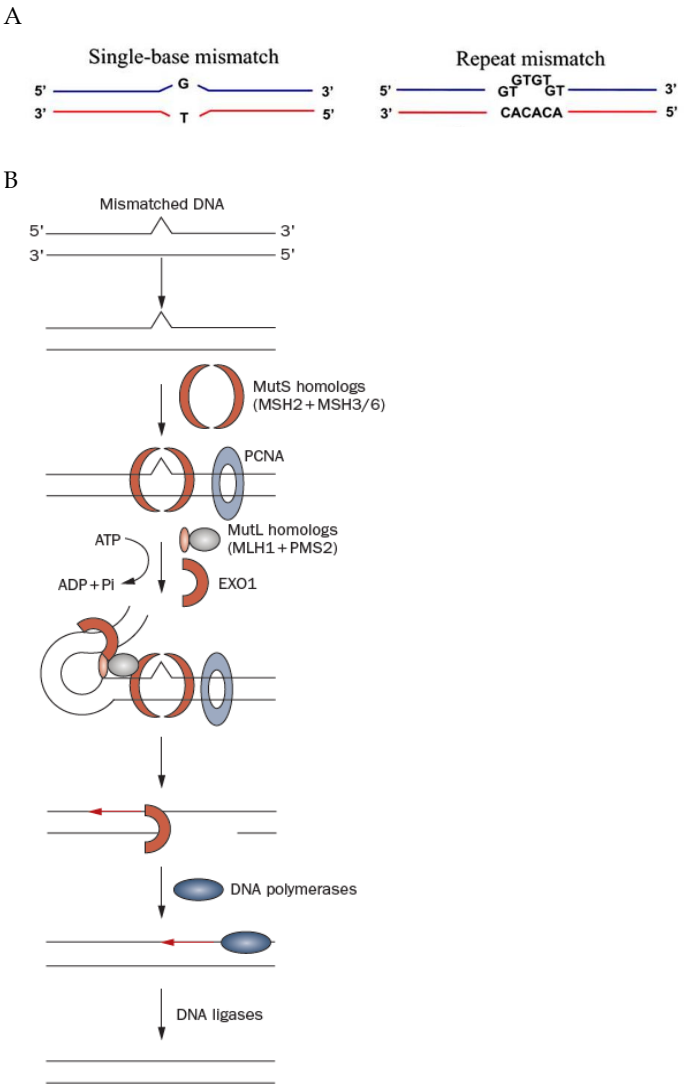

Figure 5: Mechanisms of Mismatch Repair in humans. (A) The MMR system recognizes base-base mismatches (left) and insertion-deletion loops (right). In humans, the MutSα heterodimer (complex of MSH2 and MSH6) detects base mismatches and one- to two-nucleotide IDLs, whereas the MutSβ complex composed of MSH2 and MSH3 recognize large IDLs. (Figure adapted from Banno et al., 2009). (B) Binding of MutS homologs to DNA mismatches or IDL´s triggers a structural change that is accompanied with the exchange of ADP towards ATP and binding of MutL homologs. The human MutL homologs further recruit downstream factors including PCNA and the exonuclease Exo1 with the subsequent excision of the damaged strand. The interactions of the complex mediate DNA looping and thus bringing both sites in close proximity. The resulting single-stranded gap is filled by DNA polymerase δ and the break is sealed by DNA ligase 1. Abbreviations: Exo1, exonuclease 1; PCNA, proliferating cell nuclear antigen. (Figure taken from Hewish et al., 2010).

(IDLs). IDLs can be formed by strand slippage events in repetitive DNA sequences such as microsatellites, a repeated DNA sequence motif composed of mono-, di-, or trinucleotide repeats (Jiricny 2006; Jiricny 2013). During DNA replication, both the primer as well as the template DNA strand in a microsatellite can occasionally dissociate and re-anneal incorrectly thereby creating IDLs (Kunkel 1993). The MMR system recognizes base-base mismatches and insertion-deletion loops. In humans, the MutSα heterodimer (complex of MSH2 and MSH6) detects base mismatches and one- to two-nucleotide IDLs, whereas the MutSβ complex composed of MSH2 and MSH3 recognize large IDLs (Kunkel and Erie, 2005). MutSα binds to a DNA base-base mismatch by inserting the GxFxE "reading head" into the DNA duplex. The insertion of the reading head triggers an ATP-dependant conformational change thereby converting MutSα into its sliding clamp form. The conversion to the clamp form is accompanied by an exchange of bound ADP to ATP and the recruitment of the MutL homologue (MLH) to form the ternary complex (Jiricny, 2013). Interestingly, in T. *aquaticus*, MutL binding to MutS immediately after its ATP-binding mediated structural changes traps MutS at the mismatch site before sliding (Qiu et al., 2015). Just recently, a study using a modified single molecule FRET approach suggests a model for MutSα MMR initiation where a coordinated, stepwise transition from a highly kinked, MutSα bound DNA complex towards the mobile clamp form of MutSα bound to unbent DNA (Le Blanc et al., 2018). Thus, combined and coordinated structural changes of MutSα, which are correlated to its nucleotide binding properties, and DNA seem to mediate MMR initiation (LeBlanc et al., 2018). So far, four human MutL homolog complexes have been identified, including its major player, the MutLα complex (MLH1 and PMS2 subuni) (Lipkin et al., 2000; Jiricny 2013). MutLα possesses endonuclease activity (within the PMS2 subunit) that is activated upon association with MutSα, a nicked mismatch-containing DNA heteroduplex and PCNA (Kadyrov et al., 2006). In this *in vitro* system, MutLα endonuclease activity was specifically directed towards the 3´ nicked strand of the heteroduplex and induced further single strand breaks particularly in the region between the nick and roughly 150 nucleotides past the mismatch. Furthermore, the generated nicks represent loading sites for EXO1 (Exonuclease 1) which cleaves the DNA between the MutLα-introduced nicks flanking the mismatch and the original 3´ nick with 5´-3´ directionality (Kadyrov et al., 2006). After removal of a DNA fragment containing the mismatch, Exo1 activity is inhibited pathing the way for DNA polymerase δ to fill the gaps followed by DNA ligase 1 mediated ligation (Peña-Diaz and Jiricny, 2012). Additionally, EXO1 catalyzes 5´

directed mismatch excision (which would not require MutLα endonuclease activity) creating a ssDNA gap stabilized by RPA. Subsequent DNA re-synthesis and ligation completes MMR.

The basis for strand discrimination of the MutLα endonuclease is its interaction with PCNA which is required for activation of the MutLα endonuclease (Pluciennik et al., 2010). PCNA is loaded by the clamp loader RFC (Replication factor C) at double- and single-stranded boundaries such as 3´ primer termini (and nicked circular DNA used in *in vitro* studies) and, more importantly, PCNA is always loaded on DNA facing its proximal site towards the DNA terminus (Pluciennik et al., 2010; McNally et al., 2010).

Since both MutSα and MutLα share a ring-like structure encircling the DNA, their ternary complex with PCNA has a fixed geometry and is not able to flip around. Finally, the latent MutLα endonuclease only resides in the PMS2 subunit of the heterodimer (Kadyrov et al., 2006). Collectively, this features guarantee that only the newly synthesized DNA strand has the correct orientation and, thus, will be cleaved βduring MMR (Jiricny, 2013).

Base excision repair

The individual DNA bases are also susceptible to damage via oxidation (ROS-induced), hydrolysis, deamination and alkylation. Indeed, these forms of base modifications represent a main source of DNA damage (Krokan and Bjoras, 2013). Such base lesions are repaired by the Base Excision Repair (BER) pathway by cleaving the damaged base, generation of a single strand breack which is then filled by DNA polymerase β and subsequently ligated (Dalhus et al., 2009; Krokan and Bjoras, 2013). The BER pathway is initiated by a collection of damage-specific DNA glycosylases which, upon target base recognition, cleave the modified base from the DNA backbone by hydrolyzing the N-glycosidic bond between the base and the 2´-deoxyribose leaving an abasic site behind (monofunctional glycosylase). The resulting abasic (apurinic or apyrimidinic) site, which is interestingly even more toxic than the initial modified base, is incised by an AP endonuclease such as APEX1 generating a single strand break. Alternatively, a bifunctional glycosylase possesses an additional 5´ deoxyribose-phosphate (dRP) lyase activity thus catalyzing both excision of the damaged base and the subsequent incision of the backbone. Finally, the one nucleotide gap is filled by DNA polymerase β and ligated (Krokan and Bjoras, 2013).

In some special cases as for O^6-methylguanine, repair occurs through direct reversal of the base modification, in this case via direct demethylation of O^6-methylguanine by the activity of O^6-alkylguanine methyltransferase (AGT or MGMT) (Sharma et al., 2009).

Double strand break repair

DNA double strand breaks (DSBs), arising for example from lesion-induced stalling of replication forks, represent one of the most dangerous types of DNA damage (Zeman and Cimprich, 2014). DSBs can potentially result in major chromosomal rearrangements and thus, need to be precisely repaired to maintain genome integrity (Ceccaldi et al., 2016).

The importance of DSB repair mechanisms for genome stability and integrity are highlighted by the fact that repair defects result in immune deficiencies and predisposition to cancer and neurodegenerative diseases (Aguilera and Gomez-Gonzalez, 2008). Even more severe, inherited DSB repair deficiencies lead to embryonic lethality and sterility (Aguilera and Gomez-Gonzalez, 2008; Ciccia and Elledge, 2010).

DSB repair is initiated by sensing and stabilization of the broken DNA ends by binding of the so-called MRN complex, which consists of MRE11, Rad50 and NBS1 (Petrini and Stracker, 2013; Hustedt and Durocher, 2017). Double strand break repair is further achieved by two main mechanism, homologous recombination (HR) and non-homologous end-joining (classical-NHEJ or c-NHEJ) (Kakarougkas and Jeggo, 2014; Blackford et al., 2017; Shilov and Ziv, 2013; Ceccaldi et al., 2016; Hustedt and Durocher, 2017). Both repair processes are considered to be mainly error-free. Besides these two main repair branches, two alternative error-prone DSB repair pathways, alternative end joining (alt-EJ) and single- strand annealing (SSA), have been discovered by the observation that yeast and mammalian cells ,although deficient in c-NHEJ, are still able to repair DSBs by using end joining (Ceccaldi et al., 2016). Recently, these alternative end joining pathways have attracted attention in regard of their widespread operation, dependent on the biological context, while contributing to genome rearrangements and oncogenic transformations (Ceccaldi et al., 2016).

The c-NHEJ mechanism involves direct joining of the two broken DNA ends by blunt end ligation which occurs independently of sequence homology (see figure 7; Chapman et al., 2012; Ceccaldi et al., 2016). Thus, c-NHEJ can theoretically occur during all phases of the cell cycle but is concentrated

in G0/G1 and G2 (Chiruvella et al., 2013; Ceccaldi et al., 2016). Notably, in dependence of the structure of the DSB substrate, c-NHEJ may require limited trimming (or gap filling) of the DNA ends prior to end joining resulting in loss of several nucleotides (Ceccaldi et al., 2016). Despite the potential loss of several nucleotides, the fast kinetics of c-NHEJ which can be completed in roughly 30 min in contrast to about 7 hours for homologous recombination, inhibits chromosomal translocations thereby playing a crucial role in protection of genome integrity (Mao et al., 2008; Ceccaldi et al., 2016).

C-NHEJ is initiated by binding of the ring-shaped Ku70/80 dimer to the broken DNA ends which blocks premature end processing (Chiruvella et al., 2013). The Ku70/80 heterodimer can be considered as a scaffold at which the downstream NHEJ factors can dock to facilitate their recruitment to the DSB site (Lieber, 2010). After binding, Ku70/80 recruits the catalytic subunit of the DNA dependant protein kinase (DNA-PKc) which bridges and orients both DSB ends in close proximity. DNA-PKc phosphorylate and thus activate additional factors including itself and the ARTEMIS nuclease. ARTEMIS is capable of incising a wide variety of DNA end structures and preferentially creates a blunt end or a 4-nt 3' overhang (Ma et al., 2002). After processing of the DNA termini, if required, the DNA ends are subsequently re-ligated by the DNA ligase IV-XRCC4-XLF (XRCC4-like factor) complex.

The alt-NHEJ mechanism is considered to be highly mutagenic since it uses microhomologies around the DSB site for repair. The initial end resection processes the DNA ends for about 20 base pairs generating a ssDNA patch that is able to hybridize with short complementary DNA stretches (Haber, 2008; Ceccaldi et al., 2016).

In contrast to c-NHEJ with minimal DNA end processing, repair of DSBs by HR, and also by the mutagenic pathways alt-EJ and SSA, requires extended DNA end resection leading to ssDNA overhangs (Ceccaldi et al., 2016). The initial phase of end resection, termed "end clipping", is catalyzed by the nucleases MRE11 within the MRN complex and CtIP which remove about 20 nucleotides from the DNA ends depending on the nature of the DSB (Ceccaldi et al., 2016). The removal of around 20 nucleotides is already sufficient to trigger the alt-EJ pathway. SSA and HR in particular require more extensive, long-range end resection in order to facilitate strand invasion. This extensive end resection step, mediated by DNA2 in complex with a helicase (BLM or WRN), CtIP and Exo1, commits cells to HR or SSA (Ceccaldi et al., 2016). Importantly, a further critical role

of CtIP might be the recruitment of BRCA1 which precludes the HR-inhibiting 53BP1-RIF complex from the DSB site thereby stimulating HR (Bunting et al., 2010). A pre-requisite for HR is the presence of a sister chromatid which serves as a template and thus, HR dominates in the mid-S and mid-G2 phases of the cell cycle (Ceccaldi et al., 2016). Interestingly, HR rarely employs the homologous chromatid as template (Kadyk et al., 1992; Helleday, 2010).

As mentioned above, one of the first factors recruited to DSBs is the Mre11-Rad50-Nbs1 (MRN) complex (see figure 7; Stracker and Petrini, 2011). In HR, after extensive end resection has occurred, the generated 3´ ssDNA overhang is stabilized by RPA which is lateron replaced by Rad51 forming a recombinase filament. A variety of factors including BRCA1 and BRCA2 facilitate this exchange (Carreira et al., 2009; Hustedt and Durocher, 2017). The Rad51 coated nucleofilament "searches" for the homologous DNA sequence and subsequently invades into the sister chromatid, facilitated by Rad51 mediated displacement of the complementary DNA strand, forming a D-loop structure (Sung and Klein, 2006; Ceccaldi et al., 2016). Re-synthesis of DNA (strand extension), resolution of the formed four way-transition Holliday junction, strand dissolution and ligation completes the HR pathway cycle.

The DNA end resection theme seems to be the determining factor committing cells to initiate a specific DSB repair process and represents the critical hub for the regulation of DSB repair via the cell cycle. The regulatory mechanisms influencing DNA end resection, such as the activity of cyclin-dependent kinases (CDK), are thus often referred to as pathway choice (Ira et al., 2004). For more detailed information about the question of pathway choice, I would like to refer the readers to two excellent reviews (Ceccaldi et al., 2016; Hustedt and Durocher, 2017).

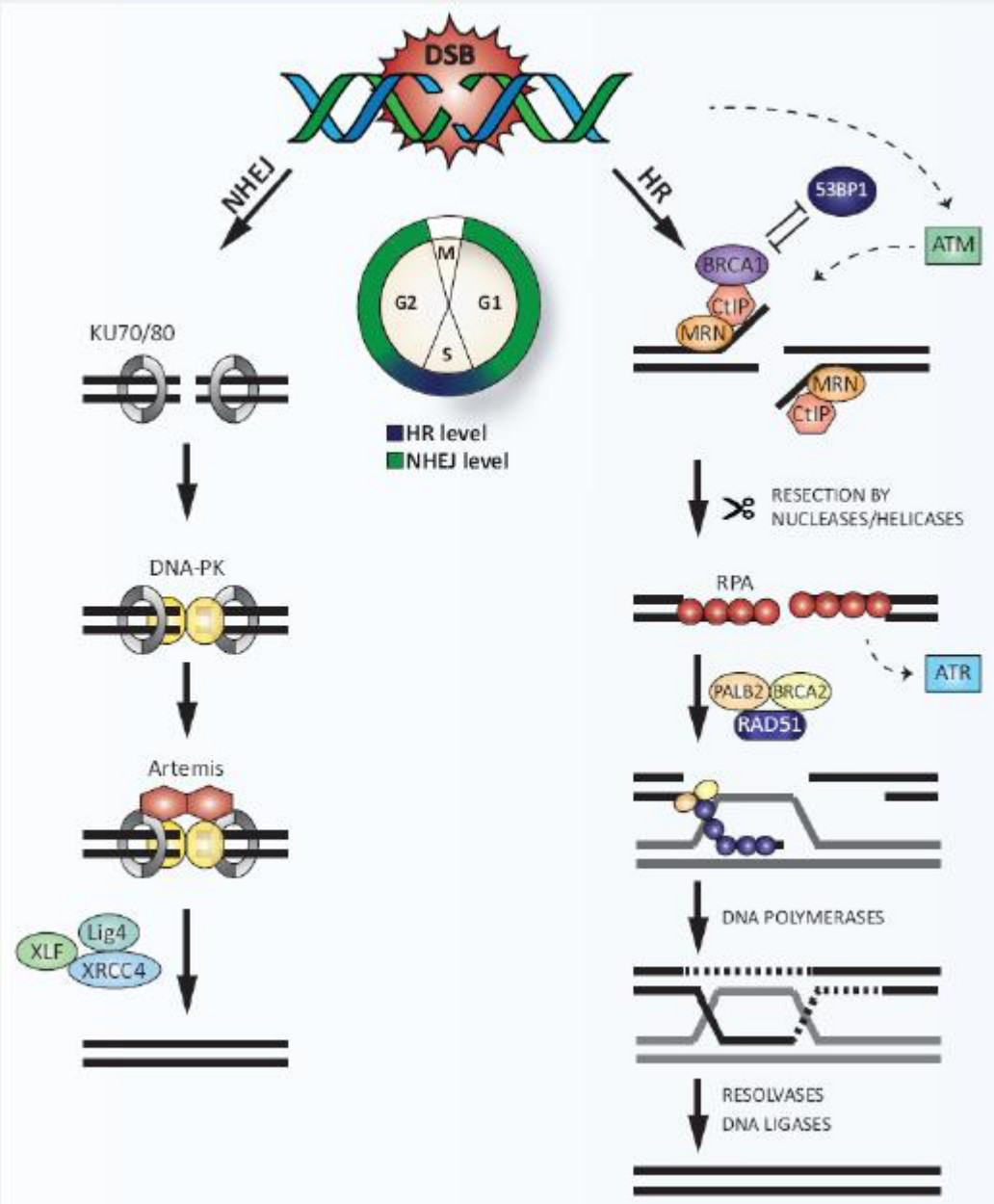

Figure 6: Repair of double strand breaks (DSBs) via homologous recombination (HR) and non-homologous end joining (NHEJ). Rapid binding of the broken DNA ends by the Ku70/80 heterodimer promotes NHEJ by recruiting DNA-PKcs to the DSB site. DNA ends are processed by the endonuclease ARTEMIS, followed by subsequent re-ligation mediated by a complex consisting of XLF, Ligase 4 and XRCC4. Alternatively, the MRN complex senses the DSB in competition with Ku70/80. The MRN complex in concert with CtIP trigger DNA end resection thereby promoting HR. 53BP1, a factor promoting end joining processes, antagonizes BRCA1 in DSB resection. Activation of ATR is triggered by extensive end resection and subsequent formation of RPA-coated ssDNA. RPA displacement and loading of Rad51 is mediated by BRCA1, BRCA2 and PALB2, resulting in the formation of the so-called Rad51 nucleo-protein filament. The Rad51 nucleoprotein filament invades into the respective homologous region of the sister chromatid. DNA re-synthesis and capturing of the other broken DNA end generates a Holliday junction which needs to be resolved. Finally, the DNA is sealed by ligases. (Figure taken from Hühn et al., 2013).

Nucleotide excision repair

Nucleotide excision repair (NER) is a highly versatile DNA repair pathway that counteracts helix-distorting and destabilizing lesions (Schärer, 2013). NER represents one of the multiple cellular DNA repair pathways which deals with helix distorting DNA lesions such as 6-4 photoproducts and cyclobutane pyrimidine dimers (CPDs), arising after exposure to ultraviolet (UV) light (de Laat et al., 1999). Defects in one of the NER proteins are associated with several human disorders including *Xeroderma Pigmentosum* (XP), *Cockayne syndrome* (CS) and *trichothiodystrophy* (TTD), resulting in skin cancer pre-disposition and neurodevelopmental abnormalities (Andressoo et al., 2006; Cleaver, 2009).

Mammalian NER consists of two sub-pathways that vary in the nature of DNA lesion recognition. Transcription-coupled NER (TC-NER) is limited to regions of ongoing transcription, where stalled RNA Polymerase II elicits the DNA damage response. Recognition of stalled RNA polymerase II is mediated by binding of the protein Cockayne syndrome B (CSB) protein which, in turn recruits CSA (Fousteri et al., 2006). Loading of CSA triggers the formation of the CSA-DDB1-CUL4A-RBX1 E3 ligase complex (Fousteri et al., 2006) which mediate a series of ubiquitylation events that regulate TC-NER progression (Groisman et al., 2003). Mutations which affect the function of CSA or CSB give rise to the Cockayne syndrome (CS) disorder mentioned above (Cleaver et al., 2009). Interestingly, fibroblasts from patients characterized by defective CSA or CSB proteins show only a minor impact on the overall NER activity, which is also reflected by the fact that CS does not lead to cancer predisposition (Cleaver et al., 2009; Andressoo et al., 2006). Thus, this suggests that GG-NER is able to compensate TC-NER deficiency to a certain extent and that CSA and CSB most likely have additional functions besides TC-NER (Fousteri and Mullenders, 2008).

In contrast, global genome NER (GG-NER) is initiated by the damage detectors XPC and DDB2 (XPE) which directly recognize DNA lesions. XPC specifically detects helix-distorting structures and hence represents a structure specific DNA binding factor (also the next chapter for further details; Riedl et al., 2003; Sugasawa et al., 1998). Together with the Rad23 homologues RAD23A or RAD23B, respectively, and centrin2 (Araki et al., 2001; Masutani et al., 1994) it exists in a trimeric complex that recognizes a variety of DNA lesions thereby triggering NER activity. The XPC-RAD23 complex rapidly dissociates after binding to the lesion site (Bergink et al., 2012; Hoogstraten et al., 2008; Sugasawa et al., 2001). Efficient recognition of CPDs and 6-4 photoproducts relies on DDB2 (Fitch et

al., 2003; Luijsterberg et al., 2007; Moser et al., 2005; Nishi et al., 2005, Tang et al., 2000). Loss of functional DDB2 causes reduced repair of CPDs and 6-4 photoproducts and hypersensitivity to UV-induced skin cancer (Alekseev et al., 2005; Rapic-Otrin et al., 2003).

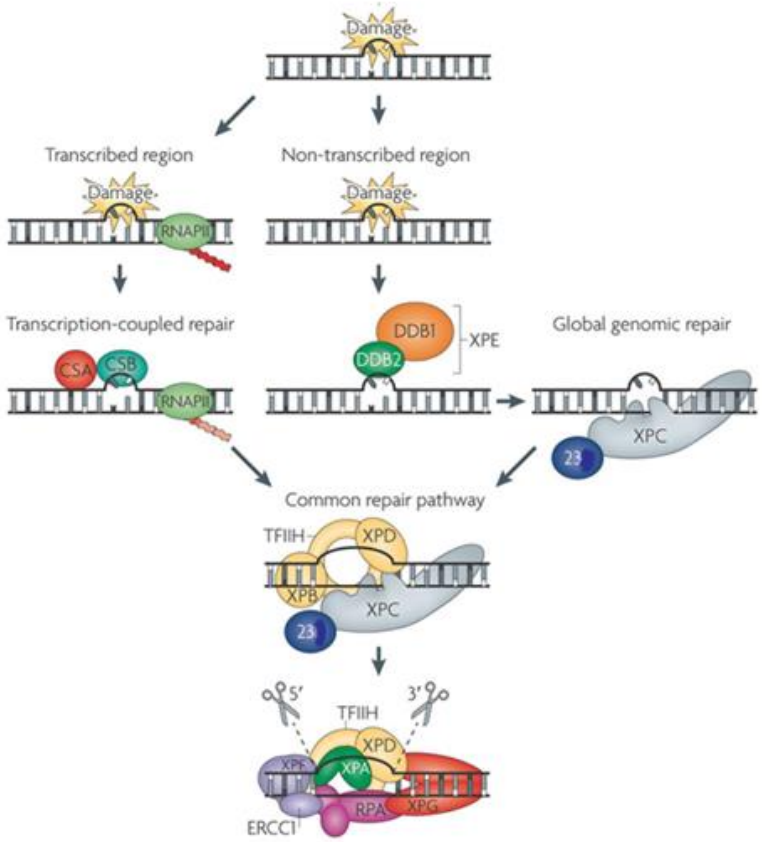

Figure 7: Overview of the basic steps in the two NER subpathways, TC-NER and GG-NER. The two subpathways use different strategies to detect the DNA damage. Whereas stalling of RNA polymerase II after encountering a lesion initiates TC-NER, the GG-NER subbranch employs two specific damage detection factors XPC and DDB2 which directly bind to UV-induced lesions. DDB2 recognizes CPDs in contrast to XPC which has a low affinity for the marginally-helix distorting CPDs. Binding of DDB2 to the lesion induces DNA bending and unwinding further facilitating recruitment of XPC to the damage site. In TC-NER, stalled RNA pol II recruits the proteins CSA and CSB. After damage recognition, the lesion is subjected to the same core machinery. TFIIH including its two helicase subunits XPB and XPD is recruited leading to opening of the DNA around the damage site. The helicase XPD, together with XPA, is involved in damage verification. XPA is a crucial factor in the incision complex and its absence is associated with severe NER defects. XPA interacts with almost allNER factors (apart from XPG) and is believed to act as a scaffold for correct positioning of the pre-incision complex (Sugitani et al., 2016). Finally, the endonucleases XPG and XPF catalyze the dual incision followed by re-synthesis of DNA and ligation by the XRCC1-DNA ligase 3 complex. (Figure taken from Cleaver et al., 2009).

DDB2 is a component of various E3 ligase complexes that, amongst others, catalyze the mono-ubiquitylation of histones H2A, H3 and H4 (Angers et al., 2006; Groisman et al., 2003; Guerrero-Santoro et al., 2008; Shiyanov et al., 1999; Wang et al., 2006). Likewise, the UV-RING1B complex brings about the mono-ubiquitylation of histone H2A at lysine 119 (Gracheva et al., 2016; Stadler and Richly, 2017) which generates a tethering platform for ZRF1 and contributes to the nuclear localization of GG-NER (Chitale and Richly, 2017). ZRF1 facilitates the conversion of the UV-RING1B complex into the UV-DDB-CUL4A complex by exchanging the Cullin and E3 ligase subunits (Gracheva et al., 2016; Papadopoulou and Richly, 2016). The UV-DDB-CUL4A-RBX1 complex catalyzes the polyubiquitylation of XPC, which increases its affinity for DNA *in vitro* and

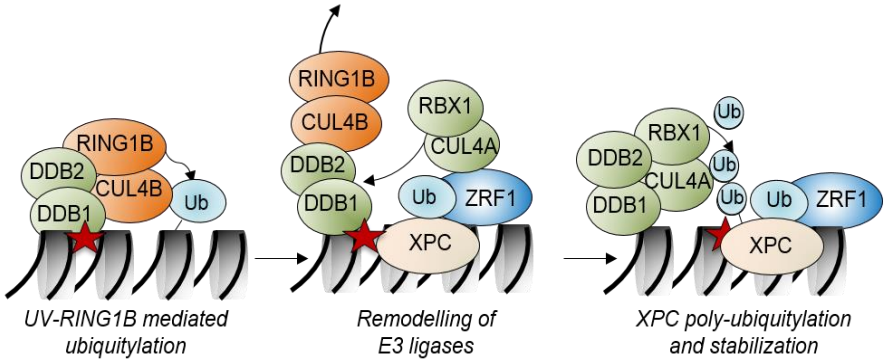

Figure 8: The Ubiquitylation cascade involved in the regulation of the damage recognition step of GG-NER. For further details see text. (Figure taken from Stadler and Richly, 2017).

contributes to its stable binding to photolesions (Sugasawa et al., 2005). Currently, it remains unclear whether the UV-DDB-CUL4A-RBX1 mediated polyubiquitylation has any function besides stabilization of XPC.

Following recognition, the lesion is verified by the repair factor XPA and by the generation of the TFIIH pre-incision complex. TFIIH opens the damaged chromatin for excision owing to the function of the two ATP-dependent helicases XPB and XPD (Compe and Egly, 2012). Finally, the endonucleases XPF and XPG excise the DNA surrounding the lesion, and the gap is filled by DNA polymerases (Fousteri and Mullenders, 2008; Marteijn et al., 2014). XPC ubiquitylation was recently shown to be involved in the recruitment of endonucleases to the DNA damage site. XPC is modified via K63-linked polyubiquitylation by the E3 ligase RNF111/Arkadia which is a prerequisite for the recruitment of XPG (Poulsen et al., 2013; van Cuijk et al., 2015). 5' incision of DNA is catalyzed by XPF-ERRC1. XPF together with ERCC1 forms a structure-specific endonuclease that cleaves the ssDNA/dsDNA junction of DNA structures such as hairpins, splayed arms and bubbles (Tripsianes et al., 2005; Tsodikov et al., 2005). XPF-ERCC1 is thought to be recruited to the damage site by XPA via specific interaction with ERCC1 (Croteau et al., 2008). Ubiquitylation of DNA repair factors is reversed by deubiquitylating enzymes, which

remove the covalently attached ubiquitin moieties from their substrates (Komander, 2010). One deubiquitylase (DUB), which acts during DNA replication, DSB repair and NER is USP7, a member of the Ubiquitin Specific Protease (USP) subgroup of DUBs (Lecona et al., 2016; Qian et al., 2015; Zlatanou et al., 2016; Zlatanou and Stewart, 2016). During TC-NER, USP7 operates in concert with UVSSA which recruits USP7 to the DNA damage site. Moreover, USP7 promotes deubiquitination of the CSB protein, thereby preventing UV-induced degradation of CSB (Schwertman et al., 2012; Schwertman et al., 2013). In GG-NER, USP7 was demonstrated to physically interact with XPC, even without UV irradiation, and to remove ubiquitin chains attached to XPC (He et al., 2014a). However, it is still not clear whether USP7 carries out an essential function during NER.

THE UBIQUITIOUS REGULATION OF GG-NER

As mentioned above, ubiquitylation processes play a crucial role in the regulation of the damage detection step of GG-NER. ZRF1 is recruited to sites of DNA damage by "reading" mono-ubiquitylated H2AK119 which is set by the UV-RING1B complex upon UV irradiation and facilitates the assembly of the UV-DDB E3 ligase complex (Gracheva et al., 2016; Papadopoulou and Richly, 2016).

Ubiquitylation, the post-translational modification of a lysine residue on a substrate protein by covalent attachment of ubiquitin, involves a cascade of three enzymatic reactions. First, the ubiquitin molecule is activated in an ATP consuming step by the E1 activating enzyme forming a thioester intermediate with the C-terminal glycine residue of ubiquitin and a cysteine of the E1 enzyme (Chitale and Richly, 2017). The activated ubiquitin molecule is then handed over to the E2 conjugating enzyme by a transesterification reaction. Finally, the E3 ubiquitin ligase promotes the covalent attachment of the activated ubiquitin molecule to its target protein via formation of an isopeptide bond (Messick and Greenberg, 2009). This results in mono-ubiquitination of the target protein. Repeating this cascade results in polyubiquitylation the target protein. Ubiquitin harbors seven internal lysine residues (and its N-terminus) which can be used for further prolongation of the ubiquitin chain. Importantly, the selection of one of the seven internal lysine residues for chain extension decides on the fate of the substrate protein (Messick and Greenberg, 2009). K48 linked polyubiquitylation of a substrate targets it for proteasomal degradation whereas poly-ubiquitin chains with K63-linkage are linked to signaling events (Messick and Greenberg, 2009).

Overall, ubiquitylation is one of the major regulatory mechanism of GG-NER and this processes are described in more detail in figure 9.

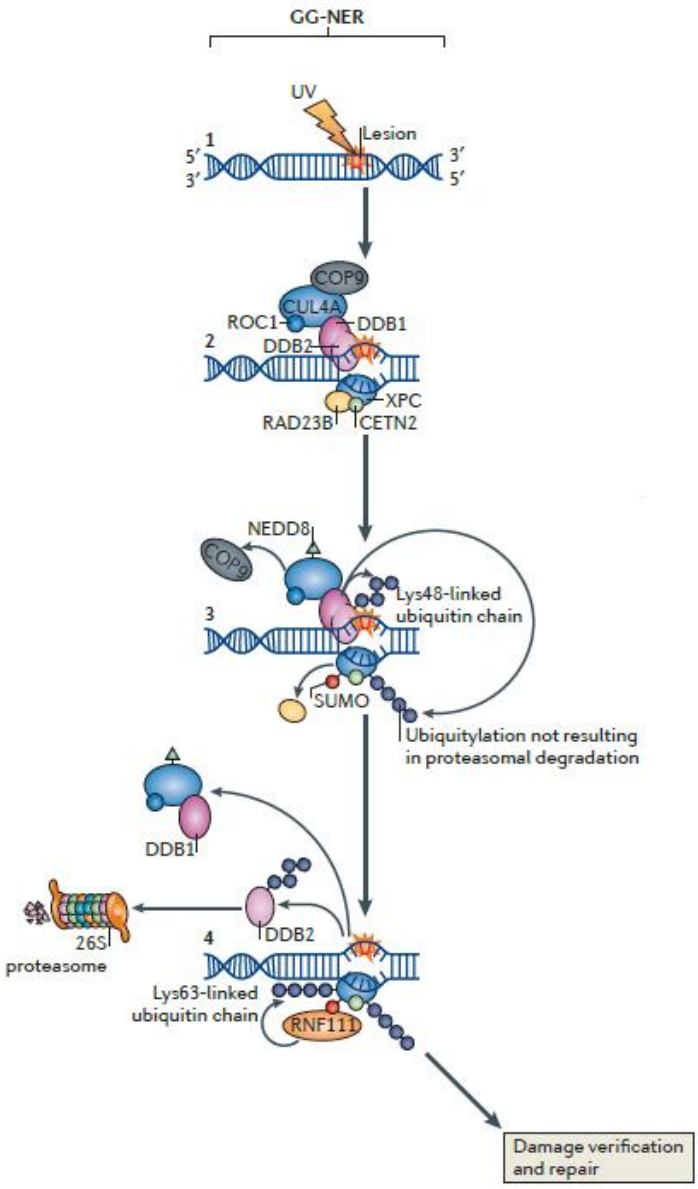

Figure 9: Regulation of GG-NER by ubiquitylation processes. GG-NER is initiated by binding of XPC and DDB2 as part of the UV-DDB complex to helix-destabilizing lesions (steps 1 and 2). ZRF1 (not shown) facilitates the assembly of the UV-DDB-CUL4A-RBX1 E3 ligase complex (see figure 8), which also interacts with the COP9 signalosome complex. Binding of this complex to DNA lesions triggers release of the COP9 signalosome. Finally, this results in neddylation of CUL4A by the ubiquitin-like modifier NEDD8, which in turn activates the UV-DD ligase complex for subsequent ubiquitylation of its targets, including DDB2 and XPC (step 3). Whereas K48-linked polyubiquitylated DDB2 is targeted for degradation, polyubiquitylation of XPC increases the binding affinity for damaged DNA. After lesion recognition by XPC, its binding partner Rad23 B is released form the complex (Step 3). In response to UV irradiation, XPC is also subjected to sumoylation which induces recruitment of a further E3 ligase, RNF111, through its SUMO-interacting motifs (SIM). RNF111 decorates XPC with a K63-linked polyubiquitin chain which is required for efficient NER. RNF111-dependant polyubiquitylation of XPC mediates its release from the damage site and enables efficient loading of XPG to the pre-incision complex (not shown). (Figure adapted from Marteijn et al., 2015).

DNA REPAIR IN THE CHROMATIN CONTEXT

As usual, things are more complicated as DNA in eukaryotic cells is highly organized and compacted in the form of chromatin established by the essential building block, the nucleosome (also see our review in Appendix 1; Stadler and Richly, 2017). Nucleosomes are assembled from an octamer of the four core histones (H2A, H2B, H3 and H4) around which the DNA is wrapped. The compact chromatin state represents major constraints for all cellular pathways, including DNA repair pathways, which require DNA as their substrate (Soria et al., 2012; Stadler and Richly, 2017). This already suggests that the chromatin configuration around the lesion site is subject to drastic remodeling processes in order increase the accessibility of DNA repair factors to the lesion site and to facilitate their removal (de Graaf et al., 2012). Nowadays, it has become clear that a plethora of DNA repair factors are interacting with proteins that are capable of mediating chromatin rearrangements, such as chromatin remodeling complexes (Lans et al., 2012). These findings aided in the formulation of the so-called "access-repair-restore" (ARR) which summarizes chromatin dynamics, a transient de-condensation to allow efficient DNA repair and the subsequent re-compaction, during DNA repair processes (Soria et al., 2012).

Nucleosomes are the essential structural units organizing DNA condensation and thus, one of the main factors determining the chromatin environment of a genomic region is its histone composition (Gurard-Levin et al., 2014). Re-shaping of a specific chromatin structure requires nucleosome and histone dynamics which can be induced by post-translational modifications (PTMs) of histone tails (Gurard-Levin et al., 2014; Polo, 2014). N- and C-terminal histone tails are crucial for both nucleosome stability and dynamics and their modification regulates the nucleosome-DNA as well as the nucleosome-nucleosome interactions (Iwasaki et al., 2013). Moreover, depending on the employed PTM, the outcome of such chromatin re-modeling processes can be completely different. Acetylation of histones is generally associated with de-compaction whereas modifications such as methylation shows a more ambiguous, context-specific outcome (Javaid and Choi, 2017). Alternatively, ATP-dependent chromatin remodeling complexes mediate re-arrangements of nucleosome structures by sliding or their eviction (Stadler and Richly, 2017, and references therein). In line with this, post-translational modifications as well as histone dynamics have been shown to have a crucial function in the modulation of the DDR (Polo, 2014; Gurard-Levin et al., 2014; Bartholomew, 2013). Thus, in the following paragraph, I would like to highlight both main strategies, PTM of histone tails and ATP-dependent chromatin remodeling, involved in chromatin dynamics

by focusing on the Nucleotide excision repair (NER) pathway. However, it has to be mentioned that the main strategies seem to be conserved among DNA repair pathways.

For further information, including chromatin re-modeling processes occurring during other repair processes such as DSB repair, I refer the readers to several excellent reviews (Kouzarides, 2007; Clapier et al., 2017; Stadler and Richly 2017, see Appendix 1; Bartholomew, 2013).

MECHANISMS REGULATING CHROMATIN STRUCTURE AROUND THE LESION

Considerably, the various cellular DNA repair pathways differ in their requirements for re-modeling of the chromatin region around the damage site. In regard to NER, TC-NER counteracts DNA lesions in actively transcribed genes. Transcription is already associated with a high degree of chromatin relaxation in the respective region which dramatically facilitates the access of the TC-NER repair machinery to the DNA, at least to some extent.

GG-NER, on the other hand, operates throughout the genome. Therefore, it is self-explaining that many DNA lesions are occurring in heterochromatic, highly organized chromatin regions which require fundamental chromatin re-modeling to allow efficient repair by NER. DDB2 and the UV-DDB complex are of central importance in stimulating an open chromatin conformation. This is also reflected by the finding that DDB2 is not essential for a reconstituted NER reaction *in vitro*, although it enhances the NER activity (Aboussekhra et al., 1995).

Global-genome nucleotide excision repair (GG-NER; left) is stimulated by an open chromatin environment which results from the activity of several chromatin remodelers and histone modifications. UV-DDB plays a crucial and central role in organizing the chromatin conformation during NER initiation. UV-DDB, which ubiquitylates core histones (H2A, H3 and H4), mediates chromatin PARylation (poly(ADP-ribosyl)ation) by direct association of DDB2 with PARP1 (poly(ADP-ribosyl) polymerase). Independent of DDB2, PARP1 has also been shown to interact with and to escort XPC to the damage site (Robu et al., 2017). DDB2-facilitated, PARP1-catalyzed PARylation of chromatin surrounding the DNA lesion promotes recruitment of the chromatin remodeler ALC1. The binding to PARylated PARP1 strongly stimulates ALC1 helicase activity (Ahel et al., 2009). Furthermore, DDB2 itself is decorated with PAR chains leading to stabilization of the protein and prolonged chromatin retention time (Pines et al., 2012). Furthermore, acetylation of

histones, which is generally associated with chromatin relaxation, stimulates NER. Acetylation of histones might potentially be catalyzed by the histone actelytransferases p300 and GCN5 (subunit of the STAGA complex) which are both recruited to UV-induced lesions. The SWI/SNF and INO80 ATP-dependent chromatin remodeler catalyze displacement of nucleosomes by eviction from chromatin or sliding inducing a more de-condensed chromatin environment and further, promote NER by interacting with and recruiting GG-NER initiation factors. Moreover, the UV-RING1B E3 ligase complex mediates ubiquitination of H2AK119 around the damage site in response to UV (not shown in the figure). This modification in turn serves as binding platform for the protein ZRF1 which facilitates the assembly of the UV-DDB E3 ligase complex (Gracheva et al., 2016). Additionally, ZRF1 recruits DICER to the damage site and both chromatin associated proteins impact on the chromatin conformation via PARP (Chitale and Richly, 2017). Interestingly, this activity of Dicer does not require its ribonuclease activity. DICER, apart from its catalytic function, contains various different domains which might be involved in the interaction with downstream factors that promote the chromatin relaxation (Chitale and Richly, 2017). The chromatin remodeler CHD1 is recruited to histone-assembled nucleosomal DNA in response to UV irradiation in a XPC-dependent manner (not shown in the figure). Furthermore, CHD1 was shown to facilitate substrate handover from XPC to the downstream acting TFIIH complex (Rüthemann et al., 2017).

In TC-NER (right), the chromatin structure is altered by the activity of histone modifiers, histone chaperones and chromatin remodeling proteins. CSB, containing a DNA-dependent ATPase domain, remodels nucleosomes *in vitro* and this activity is stimulated by the histone chaperones NAP1L1 (nucleosome assembly protein 1-like 1 and NAP1L4, which interact with CSB. Furthermore, CSB attracts the histone acetyltransferase complex p300 and the nucleosome binding protein high mobility group nucleosome-binding domain-containing protein 1 (HMGN1) to TC-NER initiation complexes. After lesion removal, chromatin state is modulated to ensure efficient transcription. The histone methyltransferase DOT1L might promote this modulation by setting transcriptionally activating histone marks. Moreover, the histone-chaperone FACT stimulates histone chaperones and chromatin remodeling proteins. CSB, containing a DNA-dependent SNF2 ATPase domain, remodels nucleosomes *in vitro* and this activity is stimulated by the histone chaperones NAP1L1 (nucleosome assembly protein 1-like 1 and NAP1L4, which interacts with CSB. Furthermore, CSB attracts the histone acetyltransferase complex p300 and the nucleosome binding protein high mobility group nucleosome-binding domain-containing protein 1 (HMGN1) to TC-

NER initiation complexes. After lesion removal, chromatin state is modulated to ensure efficient transcription. The histone methyltransferase DOT1L might promote this modulation by setting transcriptionally active histone marks. Moreover, the histone-chaperone FACT stimulates accelerated histone exchange thus facilitating transcription (Marteijn et al., 2015 and references therein).

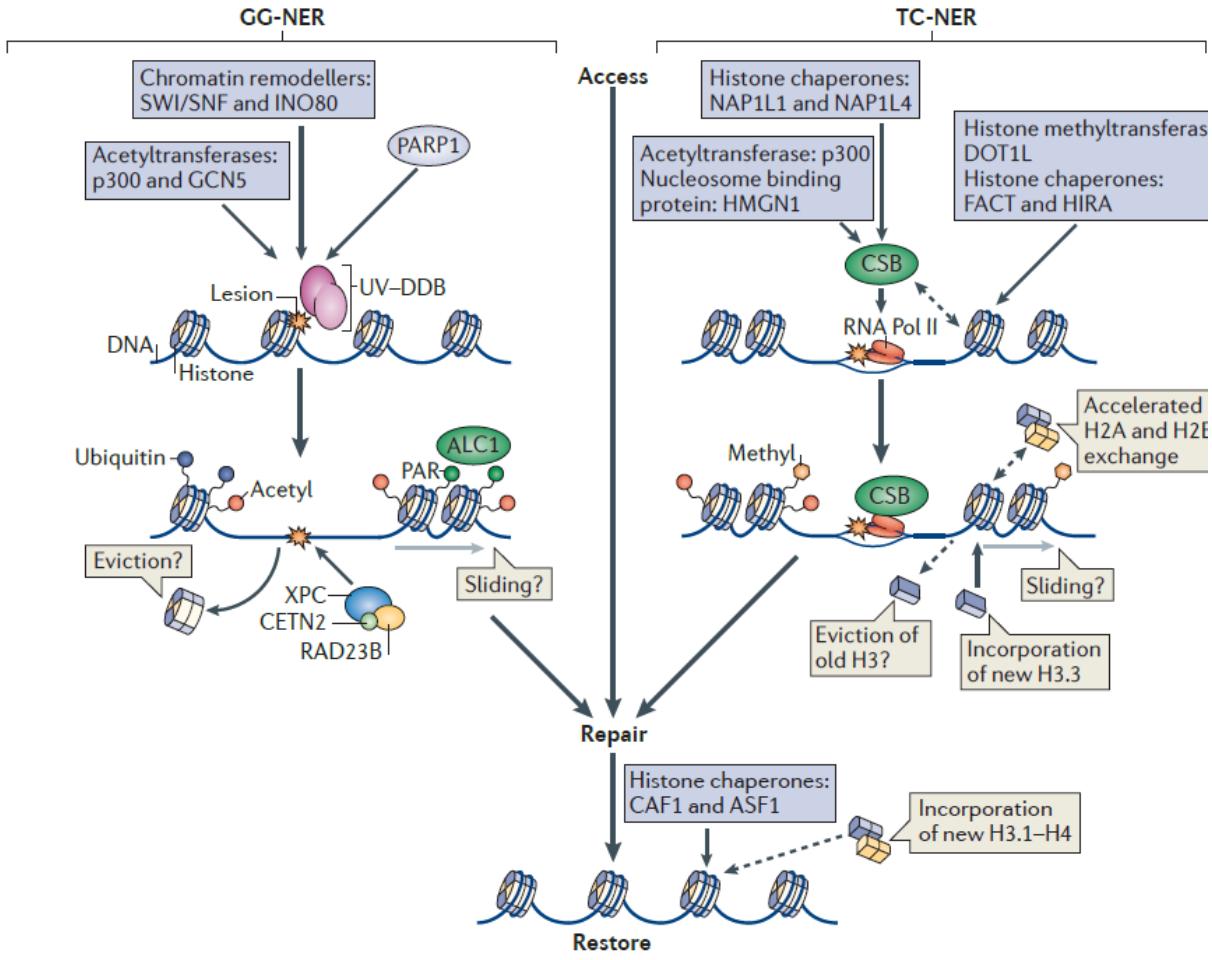

Figure 10: Chromatin dynamics around the lesion site in Nucleotide Excision repair. In accordance with the "Access-repair-restore" model, chromatin around the lesion site undergoes a transient relaxation to facilitate DNA repair. After removal of the lesion, the original chromatin state is restored. (Figure taken from Marteijn et al., 2015).

MECHANISMS OF DAMAGE DETECTION IN PROKARYOTES AND MAMMALS

General features of DNA damage

Apart from a few exceptions showing a stabilizing effect of DNA adducts, all DNA structures reported yet demonstrate that DNA damage in general causes local perturbation of the DNA duplex structure (reviewed in Lukin and De Los Santos, 2006). Consequently, the resulting suboptimal base stacking and decreased base pairing interactions around the lesion site leads to a destabilization of the DNA duplex. The destabilized DNA duplex shows enhanced conformational flexibility around the damage site. The increased backbone flexibility facilitates extrusion of lesion nucleotides, DNA bending and unwinding, and is also reflected by an increased mobility of DNA bases in direct proximity to the lesion which is also supported by molecular dynamics simulations (Barsky et al., 2007; Maillard et al., 2007; O´Neil et al., 2007).

Molecular dynamics simulations furthermore indicate that damage containing DNA structures show altered helical dynamics such as strand or base oscillations which are much more prominent and longer-lasting as compared to undamaged DNA (Barsky et al., 2007; O´Neil et al., 2007; Maillard et al., 2007). In the absence of DNA damage, the intact base stacking and base pairing interactions within the DNA duplex represent a high energy barrier and thus strongly disfavor the insertion of a hairpin and the concomitant flipping out of nucleotides from the helix (as will be discussed in more detail). Taken this into account, it has been suggested early on that DNA repair proteins use a common strategy to recognize DNA lesions based on sensing a reduction in DNA backbone rigidity originating from diminished base interactions (Chu and Yang, 2008; Maillard et al., 2007).

Basic strategies and common features of prokaryotic and eukaryotic DNA damage recognition: immersing in nature´s brilliantness and elegance

Cellular systems developed a plethora of repair pathways to counteract DNA damage. In contrast to the myriad of repair pathways, there are three basic mechanisms through which these repair pathways operate: direct DNA damage reversal, excision of single bases, nucleotides or oligonucleotides and recombination (Naegeli, 1997; Yang, 2008).

Due to the mechanistic diversity, cellular repair pathways rely on different molecular mechanisms to cope with the different structural requirements in order to recognize and process specific types of DNA damage.

Over the past twenty years, detailed structural information on damage recognition factors from various cellular repair pathways dramatically increased our understanding of how cells recognize specific types of DNA damage. Thus, I would like to describe and highlight the basic strategies and common features of damage recognition in both eukaryotes and prokaryotes.

"One enzyme – one damage" (Naegeli, 1997)

Characteristic examples for this type of damage recognition are the removal of CPDs by the prokaryotic FADH dependant photolyase enzyme, the O^6-methyl-guanine methyltransferase (MGMT, also known as AGT) that directly reverses methylation of guanine O^6, and the family of DNA glycosylases that remove altered, unnatural bases such as uracil resulting from deamination of cytosine. Such enzymes recognize damaged DNA by providing complementary surfaces and thereby interact specifically with their DNA lesion. In turn, this enzymes are just able to detect one specific DNA damage or a narrow range of chemically related DNA lesions as for thymine DNA glycosylase (Dalhus et al., 2009; Krokan and Bjoras, 2013).

Mechanistically, a long-standing question has been how DNA glycosylases, the damage detecting proteins in BER, are capable of precisely recognizing modified damaged bases that are buried and stacked within the double helical structure (Stivers, 2004). Furthermore, the specific recognition of certain types of damaged bases is even more stunning as the chemical structure of the modified base, in some cases such as 8-oxo-guanine, differ from its undamaged counterpart by only a single atom (Yang, 2008; Kuznetsova et al., 2013).

One of the best studied DNA glycosylases is uracil DNA glycosylase (UDG or UNG) which detects and cleaves uracil-containing DNA, either derived from misincorporation (UTP, dUTP) during DNA replication or from spontaneous deamination of cytosine (Parikh et al., 2000; Huffmann et al., 2005; Dalhus et al., 2009; Zharkov et al., 2010).

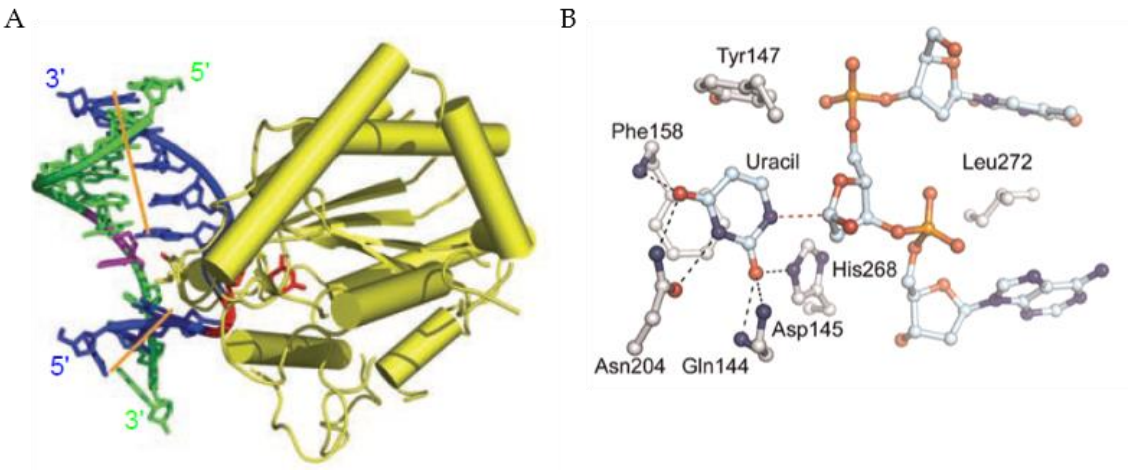

Figure 11: Structure of UDG-DNA complexes reveal key features for specific damage recognition: DNA segmentation and nucleotide flipping in a specialized binding pocket, DNA bending and unwinding. (A) Structure of wild-type UDG bound to DNA containing a U-G wobble base pair (PDB: 1EMJ; Parikh et al., 1998). Side chains forming "reading head" (L272, Y275, R276) by protruding into the DNA duplex are represented as sticks. Protein is depicted in yellow; the damaged and undamaged strand of the DNA duplex in blue and green, respectively; the lesion in red and the orphaned base pairing partner in magenta. DNA helical axis is represented in orange. (Figure taken from Yang, 2008) (B) Architecture of the uracil specific binding pocket and the active site residue D145. L272 stacked within the DNA duplex is also shown. The conserved uracil binding pocket is complementary in its shape, hydrogen bonding potential and electric charge distribution to the targeted uracil. The extruded uracil is sandwiched between F158 and H268. An extensive network of hydrogen bonding interactions involving both backbone amid N`s and side chain residues is established to all possible contacts of the uracil molecule. Asn204 plays a crucial role in uracil recognition by establishing Watson-Crick-like interactions with the uracil base. The shape of the binding pocket only accommodates pyrimidine nucleotides and thus, excludes purine bases. Whereas binding of thymine is rejected by steric clashes with Y147, cytosine is excluded by unfavorable H bond interactions involving its exocyclic amine group with Asn204 and the backbone amide-N of F158. (Figure adapted from Dalhus et al., 2009).

The structure of the UDG-DNA complex demonstrates that UDG uses three rigid loop structures for DNA binding that insert into both minor and major groove. The insertion of the loops induces kinking of DNA (about 45°) and concomitant flipping of the uracil base into the lesion binding pocket of the protein (see figure 7; Parikh et al., 1998; Dalhus et al., 2009). To facilitate extrusion of the lesion, the void in the base stack is filled by protein residues, in this case leucine 272 (Parikh et al., 1998; Parikh et al., 2000). Interestingly, when comparing the overall structure of the apo-form of UDG and its DNA bound structure, it becomes obvious that the protein undergoes a structural change upon target binding thereby forming the catalytically competent active site (Parikh et al., 1998; Zharkov et al., 2010). Bending of DNA is stimulated by three "Ser-Pro pinches" and one Gly-Ser loop which interact with the DNA backbone thereby compressing the distance between the 5´ and 3´ phosphate groups of the uracil nucleotide (Parikh et al., 1998). The protrusion of the nucleotide from the base stack occurs rather slow which indicates that normal bases might fail at

this step. Furthermore, the local backbone compression mechanism seems to be an elegant way for initial damage recognition since compression and DNA bending might be favored around the lesion site (such as a U-G mispair) and, this mechanism eliminates the requirement to flip out every single nucleotide from the double helix (Parikh et al., 1998; Zharkov et al., 2010).
The exact mechanism of UDG lesion recognition and the order of the different steps is still under debate.

By now, structures of a variety of DNA glycosylases as well as AP endonucleases from different species in complex with lesion-containing DNA are available. Collectively, comparison of these structures clearly reveal conserved, re-occurring features for lesion recognition of these remarkable enzymes including DNA segmentation, kinking and nucleotide flipping in a specialized complementary binding pocket. Additionally, the void in the DNA duplex is occupied in all cases by protein residues (primarily F, Y, L, I, M or R) which protrude into the DNA base stack (Dalhus et al., 2009; Yang, 2008).

Damage detection in NER: versatility by sensing destabilization and flexibility of DNA structures

The "one enzyme one damage" rule where specific DNA damage recognition was selectively achieved through complementary binding surfaces, comes with one drawback: it dramatically limits the range of DNA damage types which can efficiently be sensed and processed.

Due to the plethora of DNA damage-inducing agents that permanently threatens our DNA, it is not applicable to encode a single repair enzyme for each existing DNA damage. Thus, nature has established an excision repair mechanism which possess the key characteristic of being able to counteract a wide spectrum of covalent modifications of DNA bases. DNA adducts repaired by NER include 6´-4´ photoproducts and CPDs, the major lesions induced by UV light, protein-DNA crosslinks (Reardon and Sancar, 2006), as well as guanine cisplatin adducts and bulky benzo(a)pyrene or 2-acetylaminopyrene guanine modifications (Huang et al., 1996; Reardon and Sancar, 2003; Gillet and Schärer, 2006).

However, how are cells able to recognize such a diverse spectrum of DNA damage without a defined shape or common chemical nature with just a limited set of proteins. Mechanistic insight into this

question was provided by crystal structures of the damage recognition factors with (un)damaged DNA (Kuper and Kisker, 2012 and references therein).

Damage recognition of Rad4/ XPC: probing for single-stranded configurations in the undamaged DNA strand via insertion of a β-hairpin

In 2007, Min and Pavelitch solved the crystal structure of Rad4 (radiation sensitive), the yeast homologue of XPC, in complex with damaged DNA containing a CPD within a three base pair mismatch (which is specifically recognized by Rad4/XPC in contrast to a CPD alone (Sugasawa et al., 2001)) (Min and Pavelitch, 2007).

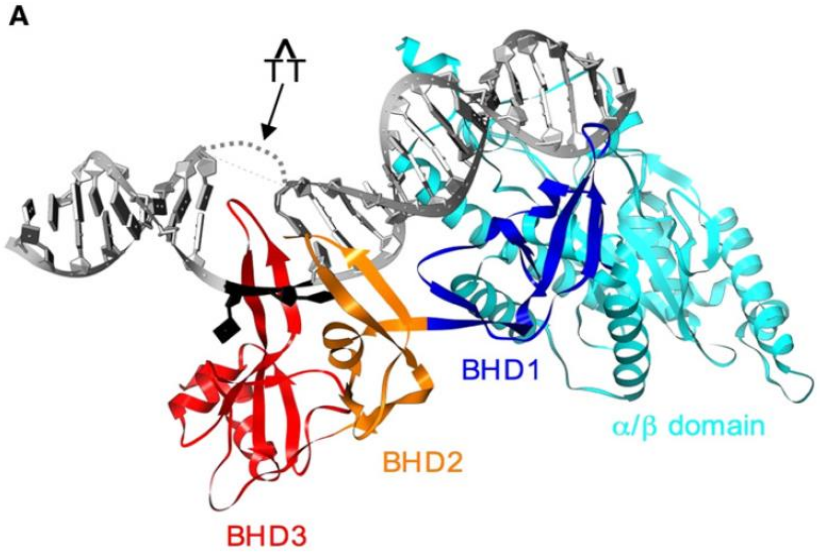

Figure 12: Ribbon diagram of Rad4 bound to damaged DNA containing a CPD lesion within a three base pair mismatch. The domain architecture of Rad4 is shown: the α/β domain (TDG domain) in cyan and BHD1-3 in blue, orange and and red, respectively. The two nucleotides opposite the DNA lesion stabilized by the BHD2-BHD3 groove are shown in black. Rad23 is omitted for clarity. (Figure taken from Schärer, 2007).

According to the crystal structure, Rad4 interact with the damaged DNA template with two modules. The TGD and BHD1 domain build an extensive network of backbone interactions with ribose and phosphate moieties whereas the BHD2 in cooperation with BHD3 form a hand-like structure which bind to a 4 bp segment including the CPD (see figure 5 and 6 for more details; Schärer 2006, Min and Pavelitch, 2007). Insertion of the BHD3 beta-hairpin in the major groove of the destabilized DNA duplex completely displaces the two base pairs including the CPD lesion (see

figure 6). On the other hand, Rad4 stabilizes this flipping out feature of the DNA lesion by specifically interacting with two expelled nucleotides opposite the DNA lesion on the undamaged strand with a BHD2-BHD3 groove. Additionally, the side chains of F599 and T604 replace the expelled nucleotides on the undamaged strand by establishing π stacking and van der Waals contacts, respectively, to their adjacent bases . This binding mode, the flipping out of two nucleotides on the undamaged strand, leads to a distortion of the geometry of the DNA helix which includes an approximately 42 degree kink, stretching and unwinding of the DNA duplex. Ironically, the damage detection factor Rad4 does not contact the DNA lesion directly and this theme, however, builds the basis for the broad target spectrum of GG-NER.

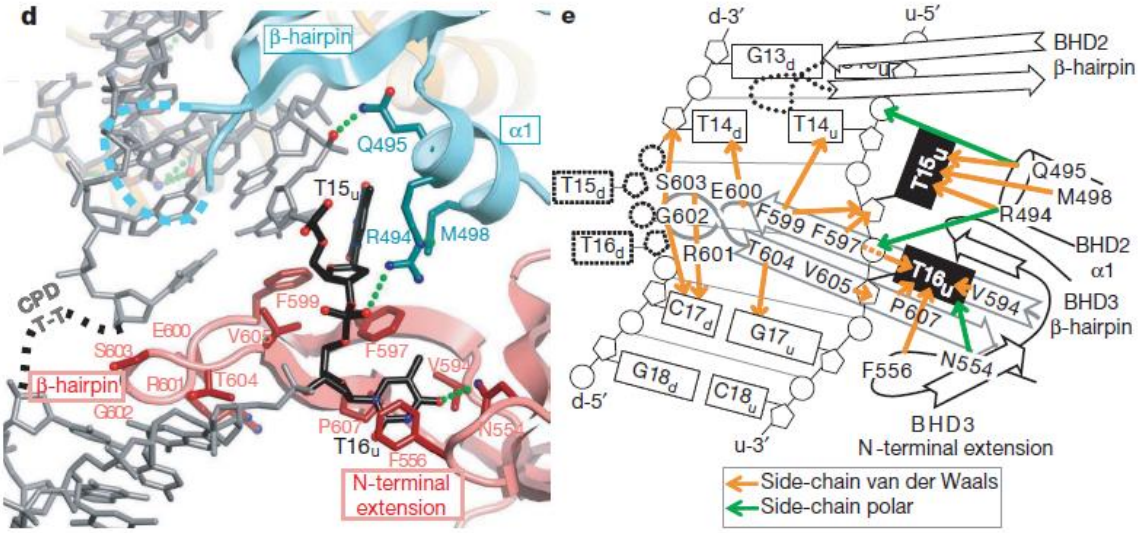

Figure 13: Cooperative binding of the Rad4 BHD2-BHD3 hairpin interface to a 4 bp DNA sequence including the CPD lesion. (left) Representation of important amino acid side chains that contact the DNA. The BHD2 hairpin is shown in cyan, the BHD3 hairpin invading the DNA duplex from the major groove is shown in red and the expelled thymidines on the undamaged DNA strand are marked in black. Importantly, the thymidine T16u(ndamaged) interacts exclusively with the BHD3 hairpin and is stabilized in its conformation by stacking between V594, F597 and P607 from one face, and F556 on the other side including V605 packing to the ribose moiety. The other flipped out thymidine, T15u, interact with both BHD2 and BHD3. M498 and the aliphatic portions of R494 and Q495 establish van der Waals contacts with T15u, whereas the BHD3 side chains F597 and F599 interact with the ribose group. Notably, the side chains of F599 and T604 establish π stacking and van der Waals contacts, respectively, to their non-flipped adjacent bases (T14u and G17u) on the undamaged strand. Thus, F599 and T604 "replace" the thymine bases T15u and T16u in the DNA helix thereby facilitating their flipping out. **(right)** Schematic representation of the Rad4-DNA interaction network around the damage site shown in the left panel (figure adapted from Min and Pavelitch, 2007; Maillard et al., 2007)

In summary, Rad4 recognizes DNA lesions which distort and thus, alter and destabilize the DNA helical structure thereby providing increased flexibility and single stranded character of the DNA bases around the damage site (Schärer, 2007). Mechanistically, Rad4 is a structure-specific rather than a damage-specific recognition factor.

Importantly, a key feature of the Rad4 binding mechanism is the fact that the lesion-induced distortion and destabilization of the DNA helix strongly favor the flipping out of the CPD lesion as well as their complementary bases opposite the DNA lesion on the undamaged strand. In other words, the DNA lesion has to weaken the DNA duplex conformation significantly in order to allow recognition by Rad4. Unfortunately, most but not all DNA lesions lead to a reduction in the stability of the DNA helical structure. A prototype of a DNA lesion which only marginally alter and destabilize the DNA duplex conformation is a CPD lesion (Lukin and de Los Santos, 2006).

Further experiments revealed the presence of an additional damage recognition factor, the DNA damage binding protein 1 (DDB1)-DDB2 heterodimer, which binds to CPDs and 6-4 PPs with high affinity and recruits XPC to the damage site (Fitch et al., 2003; Wakasugi et al., 2002). Scrima and colleagues solved crystal structures of human DDB (DDB1 in complex with DDB2) and human DDB1 in complex with the DDB2 orthologe from zebrafish, which are overall very similar (Scrima et al., 2008; also see figure 15)). DNA is held exclusively by the DDB2 subunit which contacts the DNA template via several loops within its WD40 β propeller domain (Scrima et al., 2008; Fischer et al., 2011). As for Rad4, damage recognition by DDB2 involves insertion of a strongly conserved three residue hairpin (F371, Q372,H373) which invades the DNA through the minor groove site. The β hairpin insertion triggers separation of the damaged and undamaged DNA strands, resulting in a minor groove widening to 18 Angstrom and partial unwinding of the DNA around the lesion (23° for 6-4 PPs, 12,6° for CPD lesion (Scrima et al., 2008; Fischer et al., 2011)). Due to the large footprint of the invading hairpin, the photolesion nucleotides are forced to flip out from the DNA duplex in a binding pocket formed by hydrophobic and aromatic residues. The profile and the structure of the binding pocket restricts the size and the chemical properties of lesions that fit in the pocket. The overall complementarity between the photodimer surface and the binding pocket is partial thus leaving the lesion largely exposed to solvent and explaining its ability to accommodate various lesions such as 6-4 PPs, CPDs, cisplatin intrastrand crosslinks and even abasic sites. On one side, the extrahelical conformation of the CPD is further stabilized by the hairpin residues Q372 and H373 which interact with the unpaired opposing adenine bases and stack with the DNA bases flanking the photodimer on the damaged strand. On the other side, the conformation of the compressed phosphodiester backbone (from 7 to around 6 Angstrom) of the photodimer, a structural characteristic of photolesions as well as cisplatine intrastrand crosslinks (Gelasco and Lippard, 1998), is stabilized by hydrogen bonds and salt bridges with a lysine residue (K168) as well as Q372 within the hairpin. Finally, the interactions of DDB2 with both strands induce bending of the DNA duplex

for approximately 40° (F371 and F447 push the undamaged strand away whereas P191 (not shown in figure 8) at the edge of the photodimer binding pocket distorts the damaged strand). The bending and unwinding of damaged DNA around the lesion site triggered by DDB2 binding facilitate recruitment of XPC to the damage site and efficient handover (Koch et al., 2016).

Discrepancy between the damage recognition of Rad4 and DDB2: lesion specificity

As revealed by the structural information of UV-DDB and Rad4 in complex with damaged DNA, DDB2 probes more specifically for photolesion-induced, characteristic alterations of the DNA structure. The protein recognizes a structural attribute caused by the lesion, the compression of the lesion phosphodiester backbone, through hydrogen bonding and electrostatic interactions with a lysine residue. Additionally, DDB2 contains a shallow binding pocket for the extruded photolesion which further stabilizes the damaged nucleotides in the extrahelical conformation whereas Rad4 does notinteract with the disordered DNA lesion. The most fundamental key difference in damage recognition of the two proteins is the extrusion of the non-paired DNA bases opposite the DNA lesion on the undamaged strand observed for Rad4. DNA damage which substantially perturb and destabilize the DNA double-helical structure facilitate the flipping out of the orphaned bases on the undamaged strand opposite the lesion due to weakenend hydrogen bonding and stacking interactions. However, the DNA bases opposite a CPD lesion are largely stacked within the DNA duplex and even retain interstrand hydrogen bonding interactions (Lukin and deLos Santos, 2006). Consequently, these DNA bases on the undamaged strand are not flipped out from the duplex when complexed with UV-DDB. In summary, the three main features described enables UV-DDB, in contrast to Rad4, to recognize lesions that cause minimal destabilization of the DNA duplex.

In short, UV-DDB is a rather substrate-specific damage recognition factor whereas Rad4 employs an indirect, structure-specific readout to detect DNA damage. Thus, the damage recognition strategy of UV-DDB ideally complement the binding of XPC and further highlight the different roles of both proteins within the recognition process.

Usually not noticed, another key feature of damage recognition via a β-hairpin is that it directly distinguishes the DNA strand containing the lesion which is crucial for further processing and repair by the NER machinery (Kuper and Kisker, 2012).

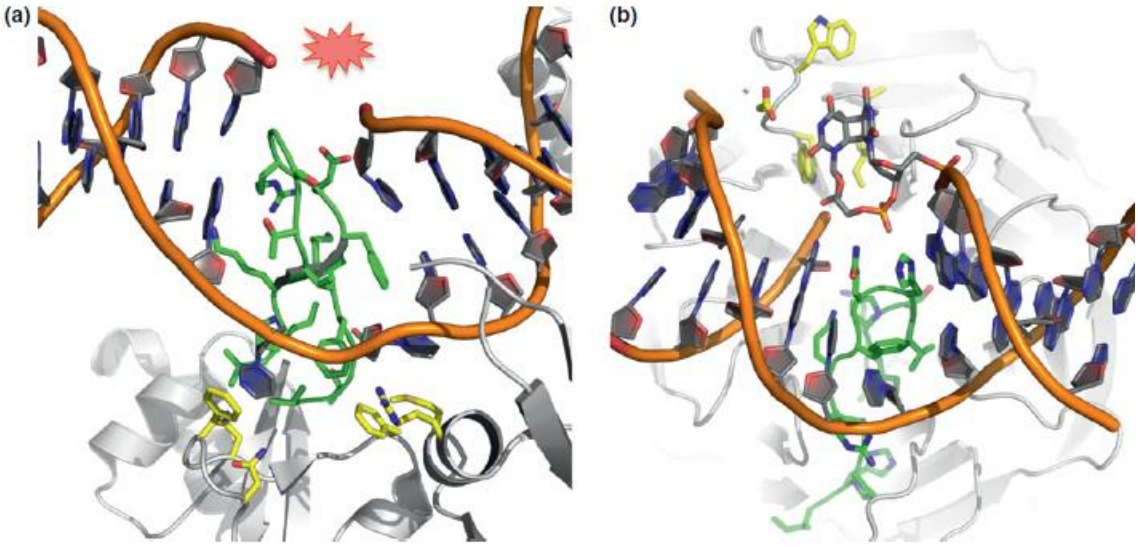

Figure 14: Molecular basis of distinct damage recognition strategies used by Rad4 and DDB2. β-hairpin structures of XPC (a) and DDB2 (b) in complex with damaged DNA. The β-hairpin is marked in green and the residues are shown as stick models. The overall protein is represented in gray and shown as cartoon. Amino acid residues involved in specific lesion recognition (for DDB2) or unspecific base and backbone interactions (for XPC) are shown in yellow. The disordered expelled damage for the Rad4 DNA complex is colored as a red mark whereas the CPD lesion in the DDB2 DNA structure is shown as stick representation and colored in CPK. (Figure taken from Kuper and Kisker, 2012).

Damage recognition in prokaryotic NER: DNA shape matters! - revealing DNA distortion by ATP coupled-conformational changes

In *E. coli*, the NER pathway is driven by three proteins termed UvrA, UvrB and UvrC (Truglio et al., 2006). UvrA and UvrB are involved in damage recognition and verification whereas damage removal and re-synthesis of DNA is carried out by UvrC (Truglio et al., 2006).

Whereas the key feature of lesion recognition for both Rad4 and UV-DDB is the detection of damage-triggered destabilization of the DNA duplex which facilitates wedging of a β-hairpin into the DNA helix, damage detection by UvrA-UvrB follows a different path.

In vivo, the UvrA-UvrB complex exits as a hetero-tetramer containing two molecules of both subunits ($UvrA_2$-$UvrB_2$) (Kisker et al., 2013). Interestingly, UvrA belongs to the ABC ATPase family, also including the MutS protein involved in Mismatch repair, and is unique among DNA repair

proteins (Jaciuk et al., 2011). The UvrA protomer contains two ATP binding sites termed I and II. Importantly, two specific protein domains, signature domain I and II, respectively, are directly inserted into the respective ATP binding domain (Jaciuk et al., 2011; Pakotiprapha et al., 2012). In 2011, a crystal structure of the UvrA homodimer from *T. maritima* bound to a DNA segment containing a fluoresceine-adducted thymidine gave first insight into the damage recognition mechanism employed by the prokaryotic NER machinery (Jaciuk et al., 2011). Crystallized in the absence of UvrB, the structure reveals that UvrA does not contact the lesion directly and there is no evidence for a flipping out feature (Jaciuk et al., 2011). Importantly, UvrA establishes an open-tray conformation and the most significant UvrA-DNA interactions, which are far away from the damage site, reside in the signature domain II (Jaciuk et al., 2011; Pakotiprapha et al., 2012).

Interestingly, the structure of *T. maritima* UvrA dimer also demonstrates that the signature domain II harbors a β-hairpin which, however, does not mediate any direct interactions to the DNA duplex (Jaciuk et al., 2011; Kuper and Kisker, 2012). In 2012, Pakotiprapha and colleagues reported a novel structure of $UvrA_2$-$UvrB_2$ from *Geobacillus stearothermophilus* in which UvrA is also able to adopt a so-called closed-groove conformation thereby forming a deep and narrow DNA binding surface which only accommodates native, undamaged DNA (Pakotiprapha et al., 2012). In contrast, the previously observed open-tray conformation can also bind damaged DNA besides native DNA (Jaciuk et al., 2011). Interestingly, the two observed UvrA forms are highly dependent on the position of the signature domain II which, in turn, is coupled to nucleotide bound state of the ATPase domain (Pakotiprapha et al., 2008). Furthermore, the closed-groove conformation of UvrA within the complex reveals the importance of the signature domain II as central hub for protein-protein interactions among UvrB, the proximal ATP binding site and DNA (Pakotiprapha et al., 2012). Thus, the signature domain II is in an ideal position for transmitting nucleotide-dependant conformational changes which directly influence the interaction network. Based on the observed structural configurations, a damage recognition mechanism has been proposed. Initially, the $UvrA_2$-$UvrB_2$ complex most likely binds to DNA in its open tray form since the open tray form allows binding to both damaged and undamaged DNA. The encounter with DNA triggers a conformational change of the signature domains, thus provoking the interconversion from the open tray configuration towards the closed groove state. If native DNA has been encountered, the narrowing of the DNA binding surface in the closed groove configuration can be fully accomplished thus signaling that the encountered DNA is un-damaged and triggering its rejection. Subsequently, the UvrA-UvrB complex relaxes back to the open tray form ready for a further DNA binding event. However, in the

case of lesion DNA showing structural distortion, the interconversion is blocked by the deformed DNA duplex which results in a trapped UvrA-UvrB complex in the partially open or open tray conformation. The trapping leads to a productive, stabilized protein-DNA complex. Subsequently, UvrA dissociates from DNA accompanying with the translocation of UvrB, most likely via its reported 5´ to 3´ helicase and single stranded DNA translocase activity (Oh and Grossmann, 1989; Moolenaar et al., 1994), along the DNA to replace UvrA at the damage site. Interestingly, it has been suggested that a further, ATP hydrolysis-dependant conformational switch of the signature domain II renders UvrA incapable of binding to either DNA or UvrB and thus stimulates release of UvrA from the pre-incision complex (Pakotiprapha et al., 2012).

Dissociation of UvrA leaves a symmetric complex of two UvrB molecules, one on each DNA strand, behind. Thus, initial damage recognition of UvrA does not discriminate between the damaged and the undamaged DNA strand (Kuper and Kisker, 2012). Moreover, since UvrA does not contact the actual lesion, the presence of a DNA lesion has to be verified in order to increase specificity of the NER reaction. In both mentioned processes, discrimination of the damaged DNA strand and lesion verification, UvrB plays a crucial role. Interestingly, UvrB employs a re-occuring theme to facilitate both tasks, a β hairpin structure (Truglio et al., 2006; Kisker et al., 2013).

Collectively, both prokaryotic and eukaryotic NER share the basic concept of sensing an altered, deformed double helical structure although it is achieved by completely distinct mechanisms. Whereas eukaryotic damage recognition by Rad4 and the DDB1-DDB2 complex employ a β-hairpin structure which invades the DNA duplex, prokaryotic UvrA recognizes damaged DNA duplexes showing a distorted backbone structure by sensing their limited probability to undergo protein mediated, ATP-driven structural changes.

Potential mechanism for XPD damage verification

The described, indirect lesion recognition read-outs employed by NER do not include interactions with the actual DNA lesion. Moreover, proteins such as TBP (TATA-box binding protein) and transcription factors are also able to bend DNA upon binding which might lead to the erroneous interpretation as DNA damage (Yang, 2008). Thus, the presence of a DNA lesion needs to be verified

after initiation to prevent unspecific incision events and to increase the specificity of the NER reaction.

The SF2 helicase XPD, a subunit within the TFIIH complex, has been implicated in damage verification in eukaryotic NER, based on the observation that XPD scans the lesion-containing DNA strand and is stalled by its encountering (Li et al., 2015; Mathieu et al., 2013; Kuper and Kisker, 2012). The archaeal as well as human XPD contain a 4Fe4S cluster (Wolski et al., 2008; Rudolf et al., 2006). The presence of the iron-sulfur cluster is a structural pre-requisite for XPD´s helicase activity since the FeS domain contains the set of amino acids essential for unwinding of dsDNA (Honda et al., 2009). However, besides its structural importance, the FeS domain might have further functions in damage verification. Further studies imply that the FeS domain plays an important role in ssDNA binding and that single residues in the FeS domain act as regulators of the helicase activity (Pugh et al., 2011; Kuper et al., 2011). Consequently, this further suggests that the FeS domain might be involved in damage verification. Interestingly, the chemical properties of FeS clusters, which also involve oxidation-reduction cycles, would allow additional functions. Indeed, dramatic similarities between XPD and the endonucleases MutY and Endo III which also harbors FeS clusters. The adenine DNA glycosylase MutY and Endo III participate in base excision repair (Kuper and Kisker, 2013). Importantly, structures provide evidence that the FeS cluster, although not directly involved in excision catalysis, is placed in close proximity to the DNA backbone and that a conserved arginine pair bridges the DNA backbone and the FeS cluster (Wolski et al., 2008; Thayer et al., 1995; Fromme et al., 2004). Such an assembly is also found in human and archaeal XPD proteins where the FeS cluster is bridged to the DNA backbone by a tyrosine-arginine motif (Mathieu et al., 2013). Interestingly, upon DNA binding, the FeS clusters from MutY and Endo III get oxidized from the Fe^{2+} to the Fe^{3+} state and the electron is used for charge transport along the DNA (DNA-CT) through the π-stacked bases of a DNA strand (Boal et al., 2005). Remarkably, the presence of a DNA lesion disrupts proper π stacking of the DNA bases and thus blocks the electron transport along the DNA and the electron "returns" to the FeS cluster (Kuper and Kisker, 2012; Zwang et al., 2018; for further information about DNA-CT please see the review of Zwang et al., 2018). Notably, it has been shown that proteins in the oxidized state bind more tightly to DNA (Merino et al., 2008) and thus, this redox signaling mechanism seems to be an efficient way of damage verification (Boal et al., 2009).

MATERIAL AND METHODS

Cell lines and transfections

HEK293T, U2OS, U2OS 2-6-3 and the U2OS cells carrying the K63 ubiquitin replacement system (kindly provided by Zhijian Chen) were cultured in DMEM (Life Technologies, Gibco) supplemented with L-glutamine (Gibco), Penicillin/Streptomycin (Gibco) and 10% FBS (Gibco) at 37°C and 5% CO_2. The medium for U2OS 2-6-3 cells was additionally contained 100 µg/mL hygromycin (Sigma Aldrich) to maintain stable insertion of the LacO cassette. MRC5 (AG05965), XPF-complemented (XP2YO(SV) complemented with HA-tagged human wild-type XPF cDNA (Staresincic et al, 2009), XPF (GM08437; XP2YO(SV)), untransformed CSA and XPA patient MRC5 (GM00710) fibroblasts were purchased from Coriell Cell Repositories and cultured in DMEM supplemented with 15% FBS, L-glutamine and Penicillin/ Streptomycin.

Transfection of HEK293T cells was performed using Polyethylenimine (Polysciences; 4mg/mL PEI dissolved in 0,2N HCl pH 4) and U2OS cells were transfected with Lipofectamine (Invitrogen) according to the manufacturer´s instructions. The following plasmids were used in this study: $^{His\text{-}HA\text{-}GFP}$XPC; pCMV2b ^{FLAG}XPF; ^{mCherry}XPF; pEGFP-C1 ^{GFP}XPF; pCI-neo ^{FLAG}USP7 (pCI-neo ^{FLAG}HAUSP was a gift from Bert Vogelstein (Addgene #16655)); pcDNA-DEST53 ^{GFP}USP7; pcDNA-DEST53 $^{FLAG\text{-}STREP}$USP7; ^{mCherry}USP7; ^{mCherry}USP7-LacR; GFP binding protein (GBP)-LacR; pcDNA-DEST53 $^{FLAG\text{-}STREP}$ERCC1; pEGFP-C1 ^{GFP}XPA; pcDNA-DEST53 $^{FLAG\text{-}STREP}$XPA. The ORFs of the generated constructs were verified by sequencing before usage.

The bacterial ^{GST}AMSH expression plasmid and the pEGFP-N1 ^{HA}VX3KO^{GFP} vector were a kind gift from Hans-Peter Wollscheid and Christian Renz, respectively.

Gene knockdown with shRNA

HEK293T shControl, shZRF1 and shRING1B were described previously and generated by transduction of HEK293T cells with retrovirus vector containing the shRNA against ZRF1 or RING1B (Richly et al., 2010). Gene knockdown in HEK293T, U2OS and MRC5 fibroblasts was performed by introduction of pLKO.1-shRNA plasmids (either purchased from Sigma Aldrich-Aldrich or generated in the laboratory) targeting the respective gene using the 3rd generation lentivirus system.

pLKO-1 plasmids contained the following shRNA sequences (Sigma Aldrich):

Gene	*TRC code*	*Sequence*
NMC	TRC1/1.5	CCGGCAACAAGATGAAGAGCACCAACTCG AGTTGGTGCTCTTCATCTTGTTGTTTTT
DDB2	TRCN0000083995	CCGGGCTGAAGTTTAACCCTCTCAACTCGA GTTGAGAGGGTTAAACTTCAGCTTTTTG
ZRF1	TRCN0000254058	CCGGCTGGAAGAACCAAGATCATTACTCG AGTAATGATCTTGGTTCTTCCAGTTTTTG
RING1B	TRCN0000033697	CCGGGCCAGGATCAACAAGCACAATCTCG AGATTGTGCTTGTTGATCCTGGCTTTTTG
XPC	TRCN0000307193	CCGGGCAACAGCAAAGGGAAAGAAACTCG AGTTTCTTTCCCTTTGCTGTTGCTTTTTG

The generated pLKO-1 shRNA vectors contained the following sequences targeting the indicated human gene:

Gene target	*Sequence (5´ to 3´)*
USP7	CCAGCTAAGTATCAAAGGAAACTCGAGTTTCCTTTGATACTTAGCTGG
RBX1	ACTTCCACTGCATCTCTCGCTCTCGAGAGCGAGAGATGCAGTGGAAG
XPA	GTGATATGAAACTCTACTTAACTCGAGTTAAGTAGAGTTTCATATCAC
CSB	GCGGTTAAGGAGATGGAATAACTCGAGTTATTCCATCTCCTTAACCGC
XPF	GCGCAAGAGTATCAGTGATTTCTCGAGAAATCACTGATACTCTTGCGC

In brief, the pLKO-1 empty TRC cloning vector (a kind gift from David Root (Addgene plasmid #10878)) was digested with AgeI and EcoRI releasing a 1,9 kb stuffer. Two complementary oligos containing the shRNA sequence including the complementary sticky ends were annealed and ligated into the digested pLKO-1 vector. Further details regarding the pLKO-1 vector and a cloning guide can be found here: www.addgene.org/plko. All vectors were verified by sequencing before usage. Viral particles were produced in HEK293T cells. Briefly, HEK293 T were transfected with 6 µg of pLKO.1 shRNA vector, 3 µg pMDLg/pRRE (Addgene), 3 µg pRSV-Rev (Addgene) and 3 µg pMD2.G (Addgene) using polyethylenimine (PEI). Medium was collected 48h and 72h post transfection and filtered through a 0.45mm PDVF filter to remove any HEK293T cells.

Generation of knockdown cells stably expressing shRNA

In brief, 1 mL media containing the respective viral particles and 4 µg/mL polybrene (Sigma Aldrich) was added to cells grown in 6 well plates and passaged 24 hours before the first transduction. Transduction was facilitated by centrifugation (1000 rpm, RT, 30 min). Subsequently, 2 mL fresh media was added to the cells and plates were transferred back to the incubator. The procedure described was repeated the following day resulting in two transduction rounds.

For UDS, cells were serum starved for 24 hours and then immediately used for experiments.

For the generation of the single and double knockdown U2OS cell lines (used in the MTT assay) and the HEK293T knockdown cell lines, medium was replaced the day after the second transduction and cells were incubated one day for recovery. Cells were then selected for 3 days with 2 µg/mL puromycin (Sigma Aldrich) until all control cells were dead. Cells were further grown for 1-2 days and subsequently used for experiments.

Antibodies used in this study

Antibodies used in this study were ZRF1 (NBP2-12802; Novus Biologicals), RING1B clone (D22F2, 5694, rabbit; Cell Signaling), XPA (GTX103168, mouse; Genetex), XPA (FL-273, rabbit; Santa Cruz), H2B (V119 8135, mouse; Cell Signaling), FLAG (mouse and rabbit; Sigma Aldrich), CPD (mouse; CosmoBio), HA (C29F4, rabbit; Cell Signaling), XPB (S-19, rabbit; Santa Cruz), USP7 (#4833, , rabbit, Cell Signaling), XPF (MS-1385-P0, mouse, NeoMarkers and A301-315A, rabbit, Bethyl Laboratories), XPC (ab6264, mouse, Abcam or A301-121A, rabbit, Bethyl Laboratories) and anti-ubiquitin Lys63 specific, clone Apu3 (#05-1308, rabbit, Merck Millipore).

Chromatin association assays

HEK293T cells were irradiated with UV and crosslinked by 1% formaldehyde at the indicated time points after UV irradiation. Assays were essentially performed as published (Richly et al., 2010). Briefly, the cell pellet was resuspended in Buffer A (100mM Tris (pH 7.5), 5mM $MgCl_2$, 60mM KCl, 125mM NaCl, 300mM sucrose, 1% NP-40; 0.5mM DTT) and kept on ice for 10 min. After centrifugation, nuclei pellet was lysed in a hypotonic solution (3mM EDTA, 0,2mM EGTA, 1mM DTT) twice. The chromatin containing pellet was solubilized in 2x Lämmli buffer (125mM Tris (pH 7,5), 4% SDS (w/v), 20% glycerol (v/v), 4% 2-mercaptoethanol and 0,02% Bromophenol Blue),

sonicated and boiled to reverse the crosslinking. All experiments were repeated at least three times. Band intensities from Western blots were measured using the ImageLab (Biorad) software.

Cell survival assay (MTT assay)

Cell viability was determined by the 3-(4,5-dimethylthiazol-2-yl)-2,5-diphenyltetrazolium bromide (MTT, Sigma Aldrich) colorimetric assay as described in Sun et al., 2002. In brief, 7000 cells were plated in 96-well plates and exposed to UV 24 hours after passaging. Cell survival was assessed 48 hours after UV exposure by measuring conversion of MTT to formazan product.

Immunoprecipitations and affinity purifications

Cells were treated with UV (UV-C at 15 J/m^2 using a CL-1000 UV-C cross-linker (UVP)) and harvested 1 hour after UV exposure (unless stated otherwise). Cells were resuspended in buffer A (10 mM HEPES pH 7.9, 1,5 mM $MgCl_2$, 10 mM KCl) supplemented with 1 mM PMSF, 5 mM N-Ethylmaleimide (NEM, Sigma Aldrich) and Protease inhibitors (Roche)) and homogenized by 10 strokes in a Dounce homogenizer with a B-type pestle. After centrifugation (2500 rpm, 4 min at 4°C), nuclei were resuspended in lysis buffer (20mM Hepes, 150mM NaCl, 2,5mM EGTA, 2mM EDTA, 0,1% Triton X-100 containing 1mM PMSF, 10mM NEM and Protease inhibitors (Roche)). Subsequently, Sm Nuclease (Benzonase equivalent; provided by our in-house Protein Production Core Facility) and 6,5mM $MgCl_2$ were added. Samples were incubated at for 1 hour at 4°C with gentle rotation. To verify DNA cleavage efficiency, DNA from extracts was analyzed by agarose gel electrophoresis. Only samples containing DNA of around 150 bp (representing mono nucleosomes) were used in the experiments. Protein extracts were then subjected to centrifugation (20.000g, 4 °C, 10 min) and the supernatant was incubated with anti-bodies overnight at 4°C. After incubation with Protein A agarose beads for 2 hours at 4°C, the immune complexes were washed extensively in lysis buffer and material retained on the beads was subjected to Western blotting.

Affinity purifications using FLAG-M2 agarose beads (Sigma Aldrich), anti-HA agarose beads (Sigma Aldrich), NiNTA agarose beads (Quiagen) and StrepTactin sepharose beads (IBA Lifesciences) were performed using essentially the protocol stated for immunoprecipitations.

Purifications involving a GFP tag were performed with GFP-Trap® agarose beads (Chromotek) according to the manufacturer's instructions.

Purification of ^{FLAG}USP7 and ^{FLAG}XPF/$^{FLAG\text{-}STREP}$ERCC1 protein complexes

In brief, HEK293T cells transiently expressing the respective protein were harvested, washed with 1x PBS and lysed in buffer A. Nuclei were pelleted by centrifugation, lysed in lysis buffer and sonicated with a Bioruptor device for 20 min (30 sec on/off; High setting). After high speed centrifugation, lysate was incubated with the respective beads overnight. Beads were washed extensively with lysis buffer containing 1M NaCl and proteins were eluted with either 2,5mM Desthiobiotin (StrepTactin beads, Iba Lifesciences) or 200µg/mL FLAG peptide (Sigma Aldrich) for FLAG affinity purifications according to manufacturer´s instructions. Eluate was concentrated using Amicon Ultra 0,5 mL centrifugal filters (Sigma Aldrich) and re-buffered with 50mM Hepes (pH 7,5), 137mM NaCl, 1mM DTT and 12% glycerol using a NAP5 column (GE Healthcare). Aliquots were snap-frozen and stored at -80°C until usage. To verify purity, 5 to 10 µL of the purified protein fractions were subjected to Western Blotting and both probed with the respective antibodies and detected by Coomassie staining.

Recombinant full-length His_6-tagged XPA (aa 2-293) was purchased from MyBioSource (Catalog number: MBS966967).

Preparation of cell extracts

Cells were collected by scraping (HEK293T) or by trypsinization (U2OS and MRC5 fibroblasts). The cell pellet was resuspended in 2x Laemmli buffer, sonicated (10 min with 30s on/off) and boiled for 10 min at 95°C. After centrifugation at maximum speed, whole cell extracts were subjected to Western blotting and probed with the indicated antibodies.

DNA cleavage assay

Standard reaction mixtures (25 µl final volume) contained 45 ng of annealed stem loop DNA ((Sijbers et al., 1996); purchased PAGE purified from Sigma Aldrich; 5´ GCCAGCGCTCGGTTTTTTTTTTTTTTTTTTTTCCGAGCGCTGGC 3´) and 150 ng of purified ERCC1-XPF complexes. To allow complex formation, the respective proteins were incubated on ice

for 30 min with XPF-ERCC1 complexes before addition of 2x reaction buffer (final concentrations (1x): 50mM Tris-HCl (pH 8.0), 0,25mM $MnCl_2$, 0,1mg/ml bovine serum albumin, and 0,5mM 2-mercaptoethanol) containing the stem loop DNA substrate. After incubation at 29°C for 2 and 4 hours, respectively, aliquots were taken and the reaction was stopped immediately with 2x Formamide Loading buffer (80% formamide and 0,02% Bromophenol Blue in 1x TBE buffer). Samples were heated at 95°C for 3 min, cooled-down on ice and subsequently separated on a denaturing 14% polyacrylamide gel followed by GelRed staining of the DNA fragments.

In vitro deubiquitylation assay with K63 ubiquitin chains

The respective proteins were incubated with 40ng purified $^{FLAG\text{-}STREP}$USP7 for 30 min on ice before adding to the reaction buffer (50mM Hepes (pH 7,5), 150mM NaCl) containing K63 ubiquitin chains (purchased from Boston Biochem) and 5mM DTT in a final volume of 25 µL. The reaction was incubated at 37°C, aliquots were taken at the respective time points, immediately mixed with 2x Laemmli buffer to stop the deubiquitylation reaction and subsequently analyzed by Western Blotting.

In vitro deubiquitylation of immunoprecipitated XPC complexes

HEK293T cells expressing $^{His6\text{-}HA}$XPC were UV irradiated and collected 1 hour post UV irradiation. His_6-HA tagged XPC was purified with NiNTA agarose beads or anti-HA agarose beads following the protocol described above. For the AMSH deubiquitylation experiment, a washing buffer with 150 mM NaCl was used whereas the washing buffer for the *in vitro* deubiquitylation assay with the purified USP7 and ERCC1-XPF complexes contained 1M NaCl to remove all XPC bound proteins.

After three washing steps, XPC complexes retained on NiNTA agarose beads were resuspended in deubiquitylation buffer (50mM Tris (pH 7,5), 5mM NaCl and 5mM $MgCl_2$) and incubated with purified ^{GST}AMSH (1,5 µg) for the indicated time at 37°C with gentle shaking and occasional mixing by pipetting. After three washing steps, samples were mixed with 2x Laemmli buffer and analyzed by Western Blotting with the indicated antibodies.

For the *in vitro* XPC deubiquitylation assay, immunoprecipitated ^{HA}XPC on HA agarose beads was resuspended in deubiquitylation buffer (50 mM Hepes (pH 7,5), 150 mM NaCl, 0,05% Triton X-100)

containing 2mM DTT after washing and divided in new tubes. The indicated proteins were pre-mixed on ice and incubated for 30 min to allow complex formation before adding to the purified XPC fraction. The amounts used in the assay were: 800 ng GST as control (lane 1); 200ng $^{FLAG\text{-}STREP}$USP7 with either 600 ng GST (lane 2) or 600 ng purified ^{FLAG}XPF/ $^{FLAG\text{-}STREP}$ERCC1 complexes (n(USP7)/ n(XPF/ERCC1) = 1 : 3; lane 3). The samples were incubated at 37°C for 2,5 hours with gentle shaking, mixed with 2x Laemmli buffer and analyzed by Western Blotting with the indicated antibodies.

Competition experiments using ^{FLAG}K63-TUBEs

HEK239T cells expressing ^{HA}XPC were UV irradiated and collected 1 hour post UV irradiation. HA-tagged XPC was purified with anti-HA agarose beads (Sigma Aldrich) following the immunoprecipitation protocol stated above. After three washing steps, 15 µg ^{FLAG}K63-TUBEs were added to the respective samples and incubated for 3 hours at 4°C with gentle rotation. Beads were washed 3 times and the purified fraction was subjected to immunoblotting and probed with the indicated antibodies.

In vitro competition assays using purified proteins

Purified ^{STREP}ERCC1-XPF protein complexes were bound to StrepTactin beads either alone or in the presence of XPA. Binding was performed overnight at 4°C under gentle rotation. After washing the complexes were incubated with purified proteins at a specific amount of substance. The relative amounts of substance (n) are shown in the respective experiments. After intensive washing, proteins bound to the beads were assessed by immunoblotting and incubated with the indicated antibodies.

Fluorescence microscopy

Experiments were performed with U2OS or U2OS 2-6-3 cells. Cells were exposed to localized UV damage (100 J/m^2) using a micropore membrane with 5µm pore size as described in (Katsumi et al., 2001). In brief, cells were washed three times with 1x PBS. Micropore membranes pre-soaked in PBS were carefully placed on the cell layer, superfluous PBS was aspirated and cells were irradiated at 100 J/m^2. At 30 min post UV irradiation, pre-extraction was performed with CSK buffer (10mM Pipes (pH 7,4), 100mM NaCl, 300mM sucrose and 3mM $MgCl_2$) supplemented with 0.2% Triton X-

100 for 5 min on ice followed by fixation with 4% PFA for 10 min at room temperature. Cells were stained with XPA (Novus Biologicals) or XPC (Cell Signaling) antibodies overnight at 4°C. Staining of CPDs was performed following manufacturer´s instructions. After washing, coverslips were incubated with Alexa-488 fluorophore-conjugated secondary antibodies (Life technologies) and mounted in Vectashield with DAPI. Images were acquired with the LAS AF software (Leica) using a TCS SP5 confocal microscope (Leica) with a 63x/1.4 oil immersion objective at room temperature. For co-localization studies, about 100 lesions were counted per condition.

Unscheduled DNA synthesis (UDS)

MRC5 fibroblasts were transduced with lentiviral particles containing the respective shRNAs. XPA fibroblasts (GM00710) were used as a positive control. The day after the second viraltransduction, cells were serum starved for 24 hours, irradiated with UV light (20 J/m^2) and incubated with 10 μM EdU (Thermo Fisher) for 2 hours at 37°C in the incubator. Alexa-555-azide (Thermo Fisher) was conjugated to EdU using the Click-reaction. The coverslips were mounted in Vectashield with DAPI. Images were acquired with the LAS AF software (Leica) using an AF-7000 widefield microscope (Leica) with a 63x/1.4 oil immersion objective and an ORCA CCD camera (Hamamatsu). Images were analyzed using ImageJ. DAPI was used to define nuclei and EdU intensity within nuclei was measured after background subtraction. 150-300 nuclei were analyzed per sample. Mean intensities of +UV and –UV conditions for all cells were calculated and used to estimate the DNA repair occurring in the particular sample.

AIM OF THIS STUDY

In the course of NER, the UV DDB-Cul4A-RBX1 E3 ligase complex catalyzes poly-ubiquitylation of XPC in response to UV irradiation. The Richly laboratory previously published a report, where I also contributed (see Appendix 1), demonstrating that ZRF1 is an essential factor involved in the ubiquitin signaling cascade in the damage recognition step of GG-NER. In more detail, we demonstrated that ZRF1 facilitates the assembly of the final UV-DDB-CUL4A-RBX1 E3 ligase complex by mediating the exchange of the RING1B-CUL4B module with the CUL4A-RBX1 complex. Poly-ubiquitylation of XPC has been shown to enhance the DNA binding affinity of XPC *in vitro* and stabilize the protein at the damage site. However, the function of the poly-ubiquitin chain decorating XPC as well as its topology remains unknown.

Thus, the aim of my PhD thesis is to characterize the mechanistic function of the poly-ubiquitin chain on XPC within the GG-NER cascade. More specifically, my PhD thesis addresses the following questions:

- What is the function of the poly-ubiquitin chain tagging XPC in the context of NER?
- Is the XPC K63 poly-ubiquitin chain important for the recruitment of NER downstream factors?
- Which protein factors interpret the poly-ubiquitin chain on XPC?
- How are this interaction partners involved in the regulation of NER?

RESULTS

K63-linked ubiquitylation of XPC mediates XPF recruitment to DNA damage sites

Previous work had demonstrated that polyubiquitylation mediated by the UV-CUL4A E3 ligase complex is essential to stabilize XPC at the DNA damage site (Sugasawa, 2005). However, the exact configuration of the UV-CUL4A E3 ligase catalyzed polyubiquitin chain decorating XPC and how the polyubiquitin signal is interpreted in the course of DNA repair still remains elusive. Our laboratory had reported earlier that knockdown of either ZRF1 or RING1B caused a prominent reduction of XPC ubiquitylation (Gracheva et al., 2016). To better understand the nature of the ubiquitin chains decorating XPC we carried out immunoprecipitations with HA-tagged XPC in control, ZRF1 (shZRF1) and RING1B (shRING1B) knockdown HEK293T cell lines after UV irradiation (Figure 15A). We observed that ubiquitylation of XPC was abolished when depleting cells for RING1B or ZRF1. Next, we speculated that the polyubiquitin signal might provide a binding platform for NER factors operating downstream XPC. When immunoprecipitating ^{HA}XPC from nuclear protein extracts of UV XPC. When immunoprecipitating ^{HA}XPC from nuclear protein extracts of UV irradiated control or ZRF1 knockdown cells we observed a dramatic decrease of XPF binding after depleting ZRF1 whereas XPB levels remained unchanged (Figure 15B). The TFIIH helicase subunit XPB serves as control in this case since it has been demonstrated that XPC recruits TFIIH to damage sites via interaction of an acidic string region of XPC with the TFIIH subunit p62 (Okuda et al., 2015; Okuda et al, 2017). When performing time course chromatin association experiments in shZRF1 and control HEK293T (Figure 15C), we noticed a drastic decrease of XPF levels at chromatin upon knockdown of ZRF1. To substantiate this finding we overexpressed a K63 Ubiquitin mutant (K63R) in HEK293T cells to inhibit the formation of K63-linked polyubiquitin chains (Figure 15D). We carried out a UV time course and examined chromatin fractions from cells of ZRF1. To substantiate this finding we overexpressed a K63 Ubiquitin mutant (K63R) in HEK293T cells to inhibit the formation of K63-linked polyubiquitin chains. We carried out a UV time course and examined chromatin fractions from cells either expressing the mutant or wildtype ubiquitin.

We observed diminished ubiquitylation of XPC and as a consequence, a reduction of XPC levels over time. This is in accordance with an earlier report which revealed that the ubiquitylation of XPC is required for stabilization of the protein at the damage site (Sugasawa et al., 2005). Notably and in agreement with our previous findings, XPF levels at chromatin decreased abruptly. To further support this idea we performed competition

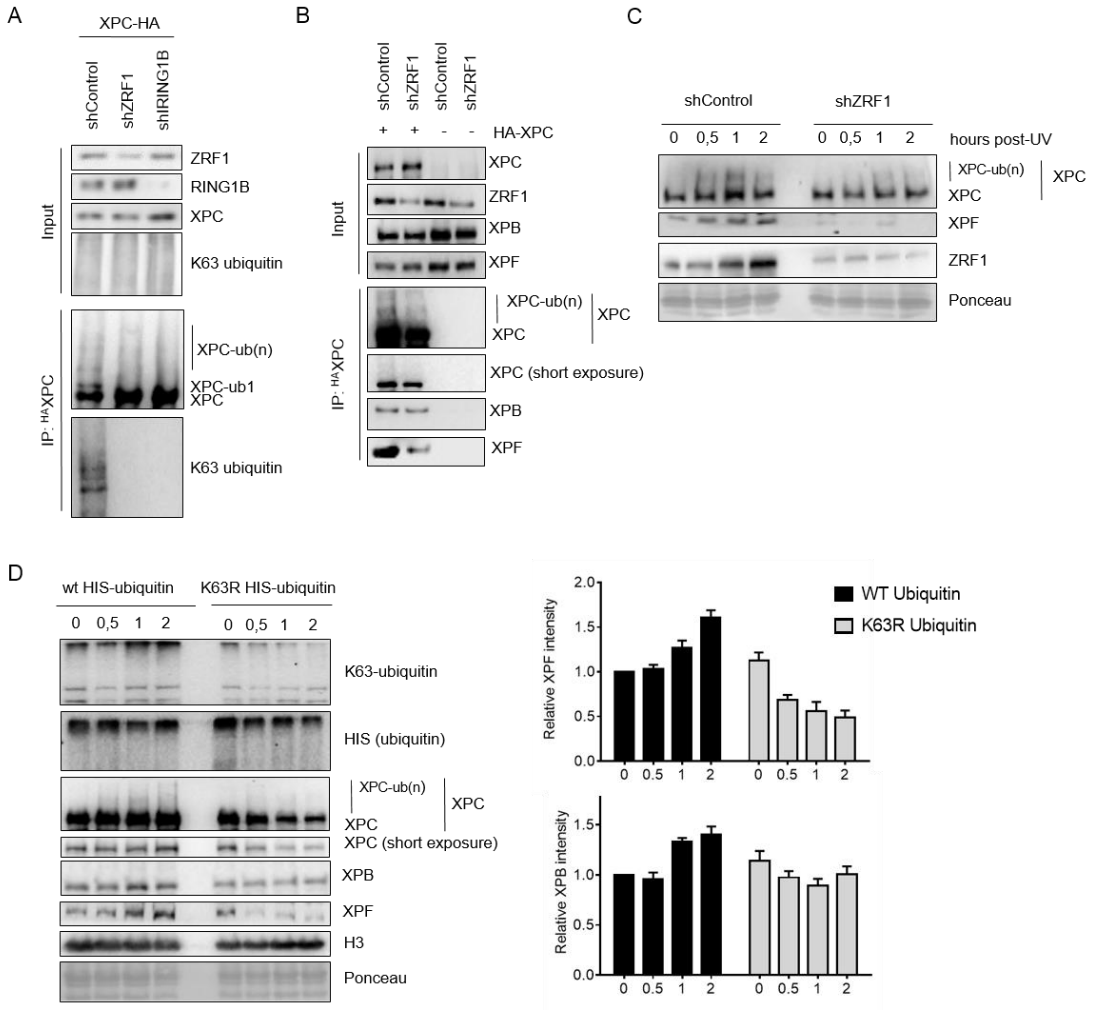

Figure 15: XPC is subjected to K63-linked polyubiquitylation in response to UV irradiation which is required for chromatin recruitment of XPF. Immunoprecipitations reveal that XPC is modified by a K63-linked ubiquitin chain. HA-tagged XPC was expressed in control and knockdown cell lines. One hour after UV irradiation, ^{HA}XPC was immunoprecipitated and XPC and K63-ubiquitin levels were assessed by immunoblotting with the indicated antibodies. (B) Knockdown of ZRF1 reduces the association of XPF and XPC. Immunoprecipitations of HA-tagged XPC in control and ZRF1 knockdown cells collected one hour after UV exposure. Immunoprecipitates were assessed by immune-blotting with the indicated antibodies. (C) Knockdown of ZRF1 strongly diminishes XPC ubiquitylation and subsequent recruitment of XPF to chromatin. Chromatin was purified from control and shZRF1 HEK293T cells at the respective time points after UV irradiation followed by immunoblotting with the indicated antibodies. (D) K63-linked poly-ubiquitylation stabilizes XPC and impacts the recruitment of both XPF and XPB to chromatin. Chromatin was purified from HEK293T cells overexpressing wildtype ubiquitin or a K63R ubiquitin mutant at the indicated time points after UV exposure. Chromatin was analyzed by immunoblotting with the indicated antibodies. Intensities were calculated by using the ImageLab software.

experiments employing purified ^{FLAG}K63-TUBE peptides. Tandem ubiquitin binding entities (TUBEs) consist of tandem ubiquitin interacting motifs (tUIM) separated by structured linker regions enabling tight and specific binding to K63-linked polyubiquitin chains (Sims et al., 2012). With regard to their specific association with K63-linked poly-ubiquitin chains, ^{FLAG}K63-TUBE peptides compete with other factors for binding to the K63 polyubiquitin chain decorating XPC. To this end we purified ^{HA}XPC from nuclear extracts of control and ZRF1 knockdown cells using anti-HA agarose beads and subsequently incubated the precipitated XPC fraction with an excess of ^{FLAG}K63-TUBEs (Figure 16A).

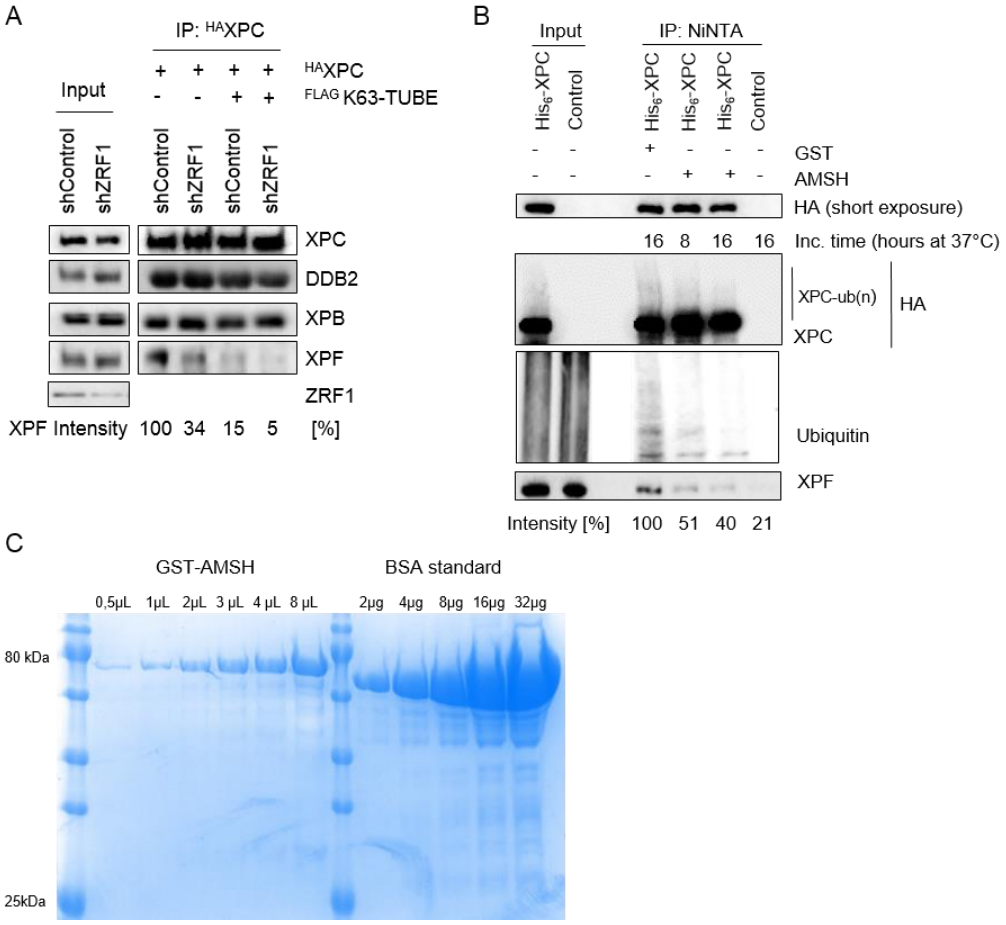

Figure 16: K63-linked polyubiquitylation of XPC regulates the association with XPF. (A) XPF-XPC association is mediated by the K63-linked polyubiquitin chain. ^{HA}XPC expressed in control or ZRF1 knockdown HEK293T cells was purified with anti-HA beads and subsequently treated with an excess of K63-TUBE peptides. XPC complexes retained on the beads were analyzed by immunoblotting with the indicated antibodies. (B) Association of XPC and XPF depends on K63-linked XPC polyubiquitylation. ^{His6}XPC was immunoprecipitated from HEK293T and, after washing, incubated with the K63-specific deubiquitylase AMSH for the indicated time at 37°C. After washing, XPC protein complexes retained on the NiNTA beads were assessed by immunoblotting with the indicated antibodies. (C) ^{GST}AMSH purified from E. coli was analyzed in Coomassie stained gels. A BSA standard curve was included to facilitate concentration determination of the purified ^{GST}AMSH fraction.

Knockdown of ZRF1 alone caused a reduction of XPF association (34% compared to control). Likewise, incubation of the precipitate with K63-TUBEs reduced XPF binding in control conditions (15%). XPF abundance in the precipitate from ZRF1 knockdown cells simultaneously treated with K63-TUBEs was nearly abolished (5%) suggesting that XPF specifically associates with K63 ubiquitylated XPC. To further support this finding, we purified HIS-tagged XPC from nuclear extracts of HEK293T cells and incubated the precipitate with either GST or recombinant ^{GST}AMSH, a K63-specific deubiquitylase (McCullough et al., 2004) (Figures 16B and C). We observed a significant stepwise reduction of XPF association (51% XPF-XPC association after 8 hours; 40% after 16 hours incubation) with increasing incubation time. The fact that AMSH is able to degrade poly-ubiquitin chains decorating XPC further confirms the presence of a K63-linked polyubiquitin chain. Next, we assessed the co-localization of XPF and K63-ubiquitylated XPC at DNA damage sites to investigate whether poly-ubiquitylated XPC plays a role in the loading of XPF to the damage site (Figure 17). To this end we performed immunefluorescence experiments in control and shZRF1 U2OS cells after exposition to UV light in a localized manner (Figure 17A). XPF co-localized with CPDs in 65% of the control cells. In contrast, depletion of ZRF1, as monitored by immunoblotting (Figure 17D), reduces the co-localization of XPF with CPDs (32,7%) pointing to a role of K63 ubiquitin chains in the recruitment or stabilization of XPF at the DNA damage site. Similarly, co-localization of XPA and XPF in response to UV-induced localized DNA damage is significantly reduced in shZRF1 U2OS cells (Figure 17B). To corroborate these data we used a U2OS replacement system in which cells are depleted of endogenous wildtype ubiquitin while expressing wildtype ubiquitin or a K63R mutant ectopically after tetracycline induction (Xu et al., 2009). When inducing localized DNA damage we observed robust co-localization of XPF with CPDs in the presence of wildtype ubiquitin (58,8 %) (Figure 17C). In cells expressing the K63R mutant we observed a reduced co-localization (32,2%). Taken together, these data suggest that XPF recruitment to DNA damage foci is, besides other potential recruitment mechanisms, regulated via K63-ubiquitylated XPC.

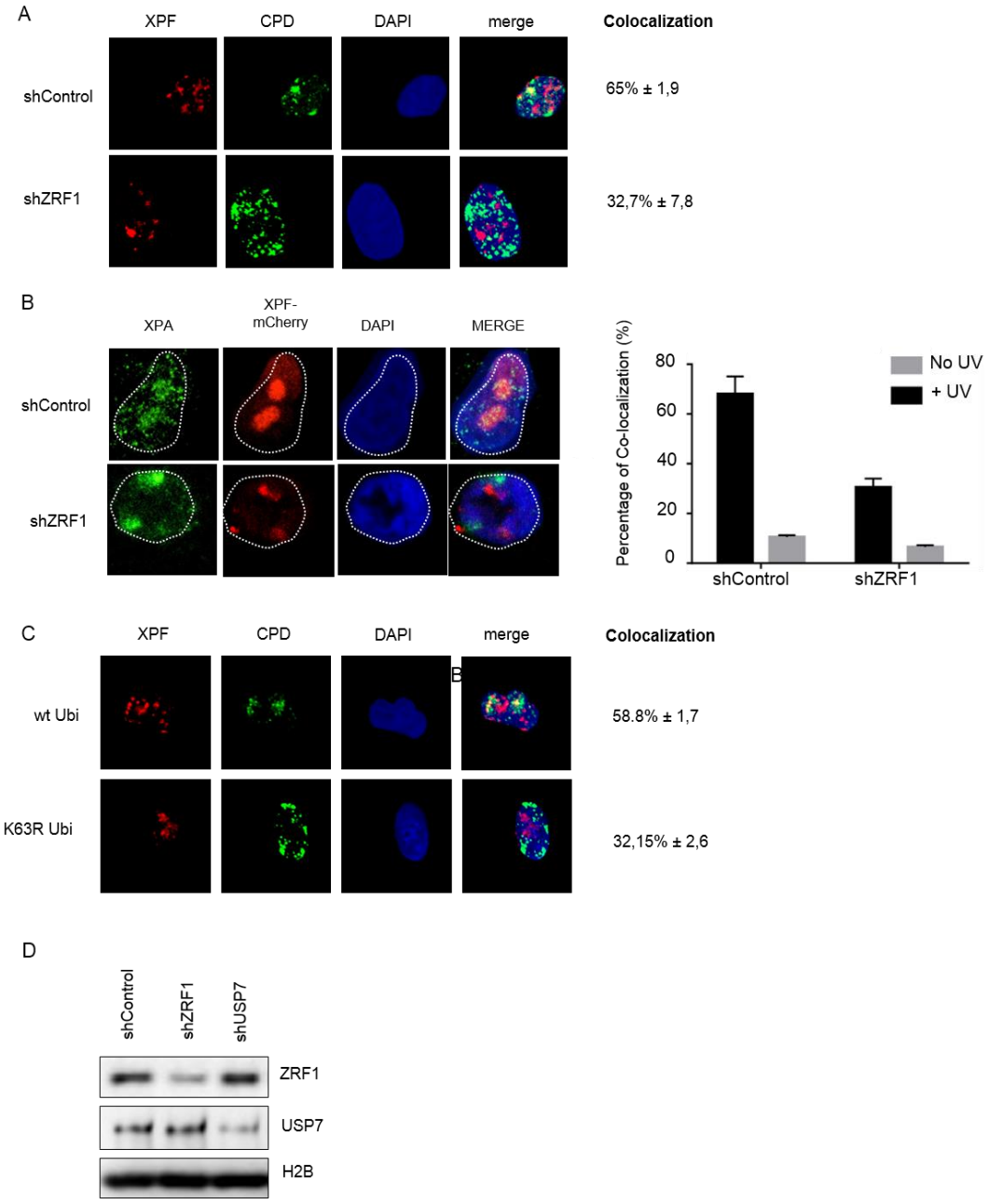

Figure 17: Besides other potential loading mechanisms, recruitment of XPF to UV-induced DNA damage foci is regulated by K63-linked polyubiquitylation of XPC. (A) Control and ZRF1 knockdown U2OS expressing ^{mCherry}XPF were exposed to localized UV irradiation. Staining with CPD antibodies was performed to visualize DNA damage sites. In about 65% of control cells and 59% of the cells expressing wildtype ubiquitin, we observed a co-localization of the damage site marked by CPD staining and XPF. In contrast, in the K63R background as well as ZRF1 knockdown only about 32% of co-localization was observed. (B) Control and ZRF1 knockdown U2OS expressing ^{mCherry}XPF were exposed to localized UV irradiation. In about 65 % of control cells, we observed a co-localization of the damage site marked by XPA and ^{mCherry}XPF. In contrast, only about 35 % of co-localization was observed when ZRF1 levels are diminished. (C) Tetracycline-inducible ubiquitin knockdown U2OS cells expressing either wild-type Ubiquitin or K63R Ubiquitin (see main text for details) transfected with ^{mCherry}XPF were exposed to localized UV irradiation. Staining with CPD antibodies was performed to visualize DNA damage sites. In about 59% of the cells expressing wildtype ubiquitin, we observed a co-localization of the damage site marked by CPD staining and XPF. In contrast, in the K63R background only about 32% of co-localization was observed. (D) ZRF1 knockdown level of the respective U2Os cell line used for the immunofluorescense studies as revealed by immunoblotting of a whole cell lysate and probing with the indicated antibodies.

XPF interacts with the deubiquitylase USP7 and both proteins regulate XPC ubiquitylation

To better understand the potential link of XPF with XPC, we analyzed chromatin from HEK293T XPF knockdown cells (shXPF) and control cells after UV irradiation (Figure 18A). We noted that global XPC ubiquitylation levels were enhanced in shXPF cells compared to the levels in control cells. We reasoned that this increased XPC ubiquitylation in XPF knockdown conditions might likely be due to a reduced deubiquitylation activity. It has previously been shown that the deubiquitylase USP7 directly binds and deubiquitylates XPC (He et al., 2014b) and we confirmed a function for USP7 in editing XPC ubiquitin chains by either overexpressing ^{GFP}USP7 or by knocking down USP7 (shUSP7) in HEK293T cells (Figures 18B and 18C). Given the specific association of XPF with ubiquitylated XPC (Figure 15-17) and the function of USP7 in removing the K63 ubiquitin chains decorating XPC, we next asked whether USP7 and XPF interact *in vivo*. To address this question we carried out endogenous immunoprecipitations with USP7 antibodies (Figure 18D) after UV irradiation of HEK293T cells. We observed a robust interaction of both proteins in this experiment. To support our data we assessed the interaction of XPF and USP7 by using a lactose repressor (LacR) based system for tethering proteins to a defined chromosome region *in vivo* (Belmont and Straight, 1998; Janicki et al., 2004). These assays make use of a human U2OS 2-6-3 cell line, containing 200 copies of a LacO containing cassette (total array size ≈ 4Mbp) (Janicki et al., 2004). We expressed a ^{GFP}LacR fusion of XPF and analyzed the co-localization of a ^{mCherry}USP7 fusion protein (Figures 18E-G). We observed co-localization of both proteins in about 77% of the analyzed cells. Likewise, USP7-mCherry-LacR tethered to the array showed co-localization with XPF-GFP in about 80% of the analyzed cells. These data demonstrate that XPF and USP7 stably interact. Next, we investigated whether the binding of XPF with USP7 was dependent on the presence of XPC or the XPC ubiquitin chains. Hence, we performed ^{FLAG}XPF immunoprecipitations from control, RBX1 knockdown (shRBX1) and XPC knockdown (shXPC) HEK 293T cells expressing ^{FLAG}XPF after UV irradiation (Figures 19A and B).

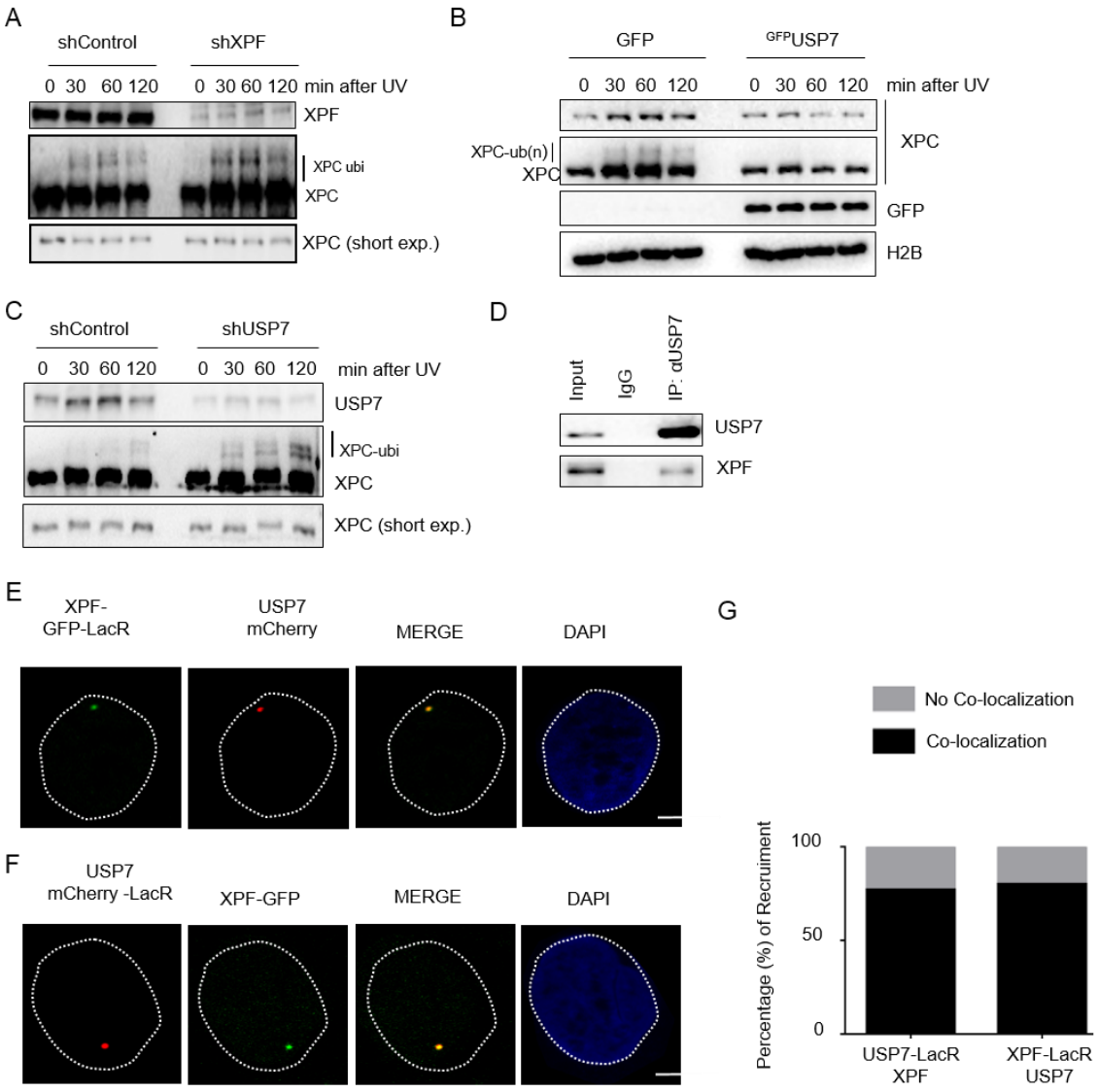

Figure 18: XPF interacts with the deubiquitylase USP7 and both proteins regulate XPC ubiquitylation. (A) XPF plays a role in the turnover of K63 polyubiquitylated XPC. Chromatin was purified from XPF knockdown and control HEK293T cells after UV irradiation at the indicated time points. XPC levels were analyzed by immunoblotting with the indicated antibodies. (B) USP7 catalyzes XPC deubiquitylation in response to UV exposure. Overexpression of GFPUSP7 in HEK293T cells causes accelerated deubiquitylation of XPC. Chromatin was purified after PFA fixation and XPC levels were analyzed by immunoblotting with the indicated antibodies. (B) Knockdown of USP7 leads to accumulation of XPC ubiquitylation levels. Control and USP7 knockdown cells were collected at the indicated time points after UV irradiation and whole cell extracts were prepared as described. Protein levels were analyzed by immunoblotting with the indicated antibodies. (D) USP7 interacts with XPF. Endogenous immunoprecipitation with USP7 antibodies from HEK293T. Protein levels were analyzed by immunoblotting with the indicated antibodies.(E) – (G) XPF and USP7 interact when associated to chromatin. LacR fusions of USP7 or XPF were tethered to the LacO array in U2OS 2-6-3 cells and the respective other protein was expressed (USP7-mCherry; XPF-GFP). In both cases proteins co-localize in about 75% of the cells analyzed.

We noticed that the levels of USP7 in the coprecipitate remained unchanged despite strongly diminished XPC ubiquitylation levels or even total XPC levels regarding XPC knockdown

conditions. Furthermore, ^{STREP}USP7 purifications in XPF patient fibroblasts (XP2YO(SV)) and the XPF complemented control fibroblasts demonstrated the interaction of USP7 with XPF (Figure 19C). Next, we analyzed the association of XPF with ubiquitylated XPC in control and shUSP7 HEK293T cells after UV irradiation (Figure 19D). Interestingly, we only

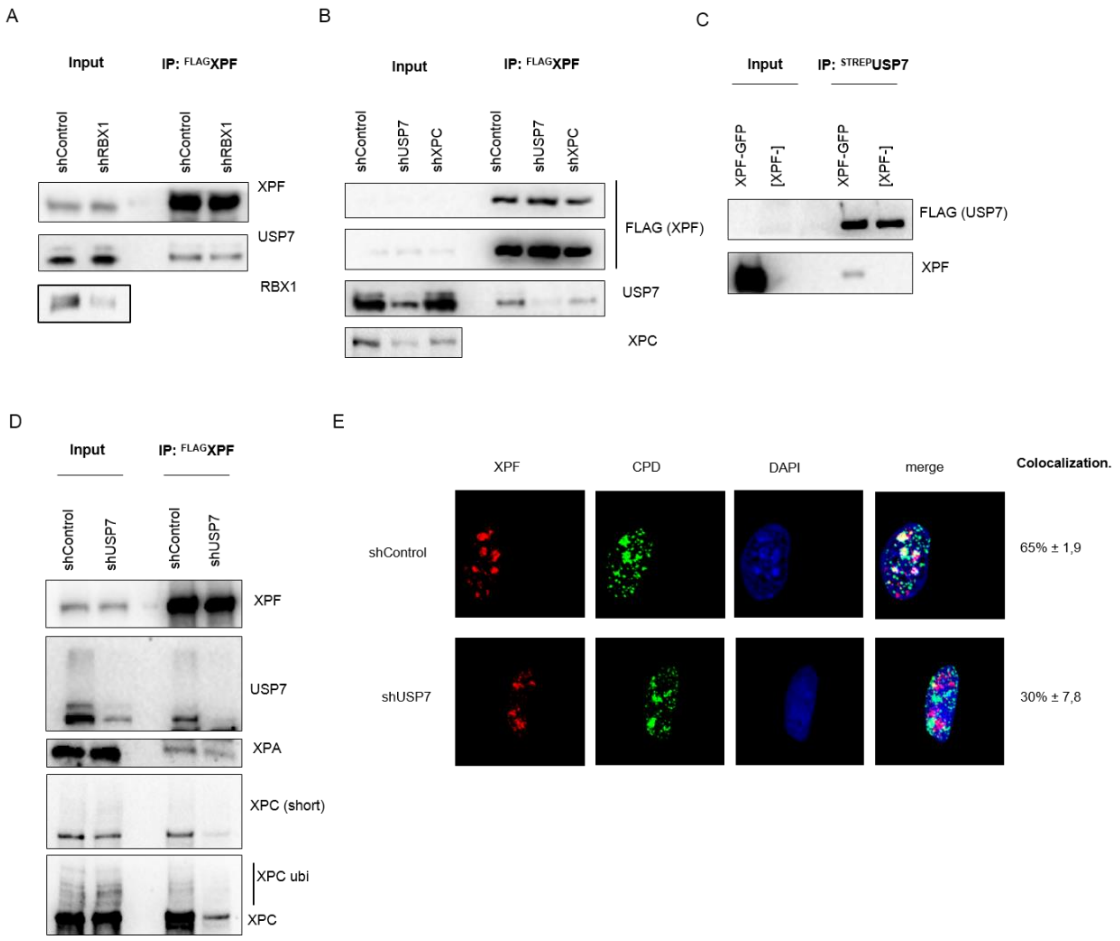

Figure 19: USP7 mediates association of XPF with polyubiquitylated XPC. (A) Binding of XPF and USP7 is independent of XPC polyubiquitylation. ^{FLAG}XPF was expressed in control and RBX1 knockdown cells. One hour after UV irradiation, ^{FLAG}XPF was immune-precipitated and the purified material was analyzed by immunoblotting with the indicated antibodies. (B) USP7 and XPF interact irrespectively of the presence of XPC. Immunoprecipitations of ^{FLAG}XPF in control, USP7 and XPC knockdown cells collected one hour after UV irradiation. Immunoprecipitates were assessed by immunoblotting with the indicated antibodies. (C) USP7 binds to XPF. Purification of ^{STREP}USP7 in XPF complemented fibroblasts and XPF patient fibroblasts after UV exposure. Immunoprecipitates were analyzed by immunoblotting with the indicated antibodies. (D) USP7 mediates association of XPF with polyubiquitylated XPC. ^{FLAG}XPF was expressed in control and USP7 knockdown HEK293T cells. ^{FLAG}XPF was immunoprecipitated one hour post UV exposure and the purified material was analyzed by immunoblotting with the indicated antibodies. (E) Recruitment of XPF to the damage site is (partially) regulated by USP7. Control and USP7 knockdown U2OS cells expressing ^{mCherry}XPF were exposed to localized UV irradiation. Staining with CPD antibodies was performed to visualize DNA damage sites. In about 65% of control cells, we observed a co-localization of the damage site marked by CPD staining and XPF. In contrast, about 30% of co-localization was observed in USP7 knockdown cells.

observed ubiquitylated XPC in the control fraction suggesting that the presence of USP7 is a prerequisite for the association of XPF with both ubiquitylated and unmodified XPC. Finally, we analyzed the recruitment of XPF to DNA damage sites (marked by CPD staining) in USP7 knockdown U2OS (Figure 19E, Figure 17D represents the USP7 knockdown level). We found significant co-localization of XPF and CPDs (65%) in control cells whereas the co-localization was diminished in the USP7 knockdown background (30%) suggesting that localization of XPF to the damage site is at least partially mediated by USP7. Taken together these results suggest that XPF and USP7 interact independently of both XPC and XPC ubiquitylation and that USP7 seems to bridge the association of XPF with ubiquitylated XPC. Our findings strongly point towards an important role for USP7 in GG-NER.

USP7 operates in both TC-NER and GG-NER pathways

USP7 plays an important role during TC-NER. Our data and previously published work suggest a novel function of USP7 in GG-NER. To monitor GG-NER, we performed unscheduled DNA synthesis (UDS) experiments. The vast majority of UV lesions is repaired by GG-NER, hence the measured UDS signals mainly reflect GG-NER activity (Limsirichaikul et al., 2009). We measured UDS in control, USP7 knockdown (shUSP7) and RBX1 knockdown (shRBX1) MRC5 fibroblasts and included XPA and CSA patient fibroblasts as a further reference point (Figure 20A). Knockdown of USP7, RBX1 or XPA caused a significant reduction of EdU incorporation. In contrast, depletion of CSA did not show a reduction in UDS activity. These data indicate a role for USP7 in GG-NER. To further assess the role of USP7 in both NER sub-pathways, GG-NER and TC-NER, we conducted an epistasis analysis employing UDS. Additionally, we monitored the knockdown levels of each of the factors for the respective experiments (Figure 20D). We performed UDS in CSB (shCSB; TC-NER), DDB2 (shDDB2, GG-NER), USP7 (shUSP7) knockdown and control fibroblasts (Figure 20B). We further analyzed fibroblasts with a simultaneous knockdown of CSB and USP7 (shCSB-shUSP7) or DDB2 and USP7 (shDDB2-shUSP7) (Figure 20B). Single knockdown of CSB led to a slight reduction of EdU incorporation whereas single

knockdown of USP7 caused a significant decrease in EdU incorporation. Simultaneous knockdown of CSB and USP7 showed an even stronger reduction of EdU incorporation when compared to either of the single knockdown conditions. Simultaneous knockdown of both DDB2 and USP7 showed only a slight reduction when compared to the single knockdown conditions in agreement with the idea that the contribution of USP7 to TC-NER is hardly measured by UDS. In sum, these data suggest that USP7 functions in both NER sub-pathways, TC-NER and GG-NER.

To strengthen our data we performed MTT cell proliferation assays using the single and double knockdown conditions introduced before (Figure 20C, Figure 20E represents the knockdown levels of the respective protein). We observed a slight decrease in the absorbance of the formazan product in CSB knockdown conditions in comparison to control cells. Single knockdown of either USP7 or DDB2 showed a similar decrease of absorbance as compared to control and CSB knockdown cells, an observation also revealed in the UDS experiment (see Figure 20B). Simultaneous knockdown of USP7 and CSB showed a further reduction of absorbance when compared to single knockdown conditions again reflecting the findings of the EdU incorporation (see Figure 20B). In particular, the reduction observed by comparing CSB single knockdown and CSB-USP7 knockdown cells suggest that CSB and USP7 operate in different cellular pathways. Simultaneous knockdown of DDB2 and USP7 showed a further reduction of absorbance when compared to the single knockdown conditions suggesting that USP7 operates in different cellular pathways controlling cell proliferation. Taken together, these data show that USP7 is required in both NER sub-branches for efficient repair of UV-induced DNA lesions and that its function in NER has a profound impact on cell proliferation.

A

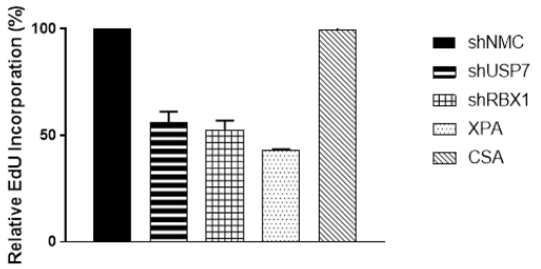
Relative EdU Incorporation (%)
100
50
0
shNMC
shUSP7
shRBX1
XPA
CSA

B

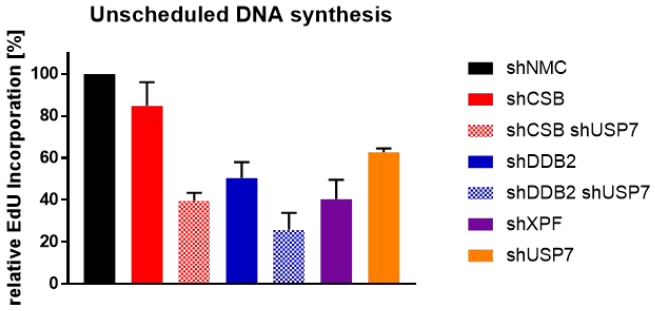
Unscheduled DNA synthesis
relative EdU Incorporation [%]
100
80
60
40
20
0
shNMC
shCSB
shCSB shUSP7
shDDB2
shDDB2 shUSP7
shXPF
shUSP7

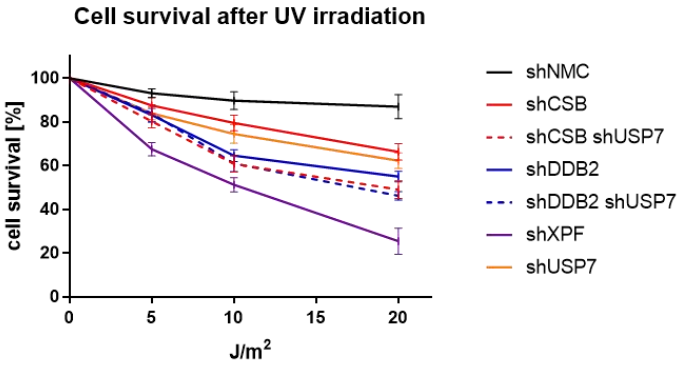
Cell survival after UV irradiation
cell survival [%]
100
80
60
40
20
0
0
5
10
15
20
J/m2
shNMC
shCSB
shCSB shUSP7
shDDB2
shDDB2 shUSP7
shXPF
shUSP7

D

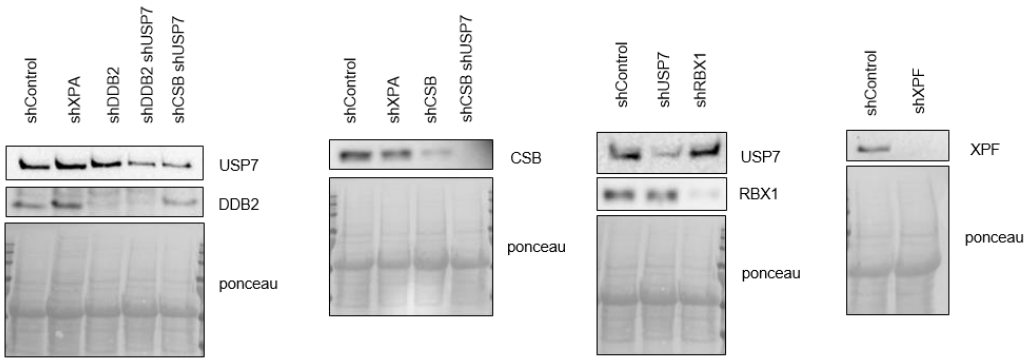
shControl
shXPA
shDDB2
shDDB2 shUSP7
shCSB shUSP7
USP7
DDB2
ponceau
shControl
shXPA
shCSB
shCSB shUSP7
CSB
ponceau
shControl
shUSP7
shRBX1
USP7
RBX1
ponceau
shControl
shXPF
XPF
ponceau

E

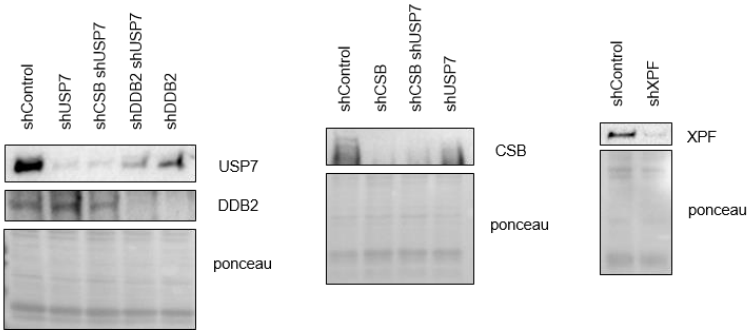
shControl
shUSP7
shCSB shUSP7
shDDB2 shUSP7
shDDB2
USP7
DDB2
ponceau
shControl
shCSB
shCSB shUSP7
shUSP7
CSB
ponceau
shControl
shXPF
XPF
ponceau

Figure 20: USP7 operates in both NER subpathways, TC-NER and GG-NER. (A) UDS reveals an essential function for USP7 in GG-NER. The relative EdU incorporation was measured in control, USP7 and RBX1 knockdown fibroblasts. NER-deficient XPA and TC-NER deficient CSA fibroblasts were analyzed as further controls. (B) USP7 is required in both branches of NER for efficient repair of UV-induced lesions. The relative EdU incorporation was measured in control, USP7, XPF, CSB, DDB2, CSB USP7 and DDB2 USP7 knockdown MRC5 fibroblasts. XPA patient fibroblasts were assessed as control. (C) USP7 has a dramatic impact on cell survival after UV irradiation. Control, USP7, XPF, CSB, DDB2, CSB USP7 and DDB2 USP7 knockdown U2OS were treated with the indicated UV-C doses and further incubated for 48 hours. Cell survival was measured by measuring conversion of MTT to the formazan product. For UDS experiments, MRC5 fibroblasts were treated with lentiviral particles containing the respective shRNA. Knockdown levels of the respective proteins were analyzed 24 hours after viral infection. Cells were collected, whole cell extracts were prepared as described and analyzed by immunoblotting with the indicated antibodies. (D) Knockdown levels of the respective MRC5 knockdown cell lines used for UDS assays. Cells were collected, whole cell extracts were prepared as described and analyzed by immunoblotting with the indicated antibodies. (E) Knockdown levels of the respective U2OS knockdown cell lines used for MTT assays. Cells were collected, whole cell extracts were prepared as described and analyzed by immunoblotting with the indicated antibodies.

USP7 competes with XPA to form a protein complex with XPF-ERCC1

XPF forms a heterodimer with ERCC1 and hence we were interested to find out whether USP7 might form a protein complex with XPF-ERCC1. Thus, we purified USP7 and XPF-ERCC1 complexes from HEK293T cells via FLAG affinity purification (^{FLAG}USP7) and STREP-Tactin affinity purification ($^{FLAG\text{-}STREP}$ERCC1) (Figure 21A) to perform *in vitro* binding assays. First, we incubated purified ERCC1-XPF bound to STREP-Tactin beads and control (empty) beads in pulldown experiments with purified USP7 (Figure 21C). We observed specific binding of USP7 to ERCC1-XPF complexes. Similarly, XPA had previously been shown to interact with the ERCC1 subunit of the ERCC1-XPF endonuclease complex and we reconfirmed this interaction by *in vitro* pulldown experiments using commercially available recombinant ^{His6}XPA (Figure 21B). To find out whether XPA and USP7 might have overlapping binding sites on ERCC1-XPF protein complexes we carried out a competition experiment by using immobilized ERCC1-XPF as bait (Figure 21D). We now doubled the USP7 concentration stepwise while keeping the XPA concentration unchanged. We observed enhanced binding of USP7 and reduced binding of XPA with ERCC1-XPF while increasing USP7 levels to equimolar (n=1) concentrations. Accordingly, when applying ^{His6}XPA immobilized on NiNTA beads as a binding matrix, we observed a reduced interaction of ERCC1-XPF with XPA after gradually increasing USP7 levels (Figure 21G).

These data suggest that USP7 has a stronger binding affinity towards ERCC1-XPF than XPA. Hence, we tested this hypothesis *in vivo* by pulling down ERCC1-XPF complexes from HEK293T cells while expressing ^{GFP}XPA at low levels and overexpressing ^{FLAG}USP7 (Figure 21E). In control conditions, without USP7 overexpression, we only monitored incorporation of both endogenous and ectopically expressed XPA into the ERCC1-XPF heterodimer. However, upon overexpression of USP7, we noticed a strong reduction of XPA and ^{GFP}XPA

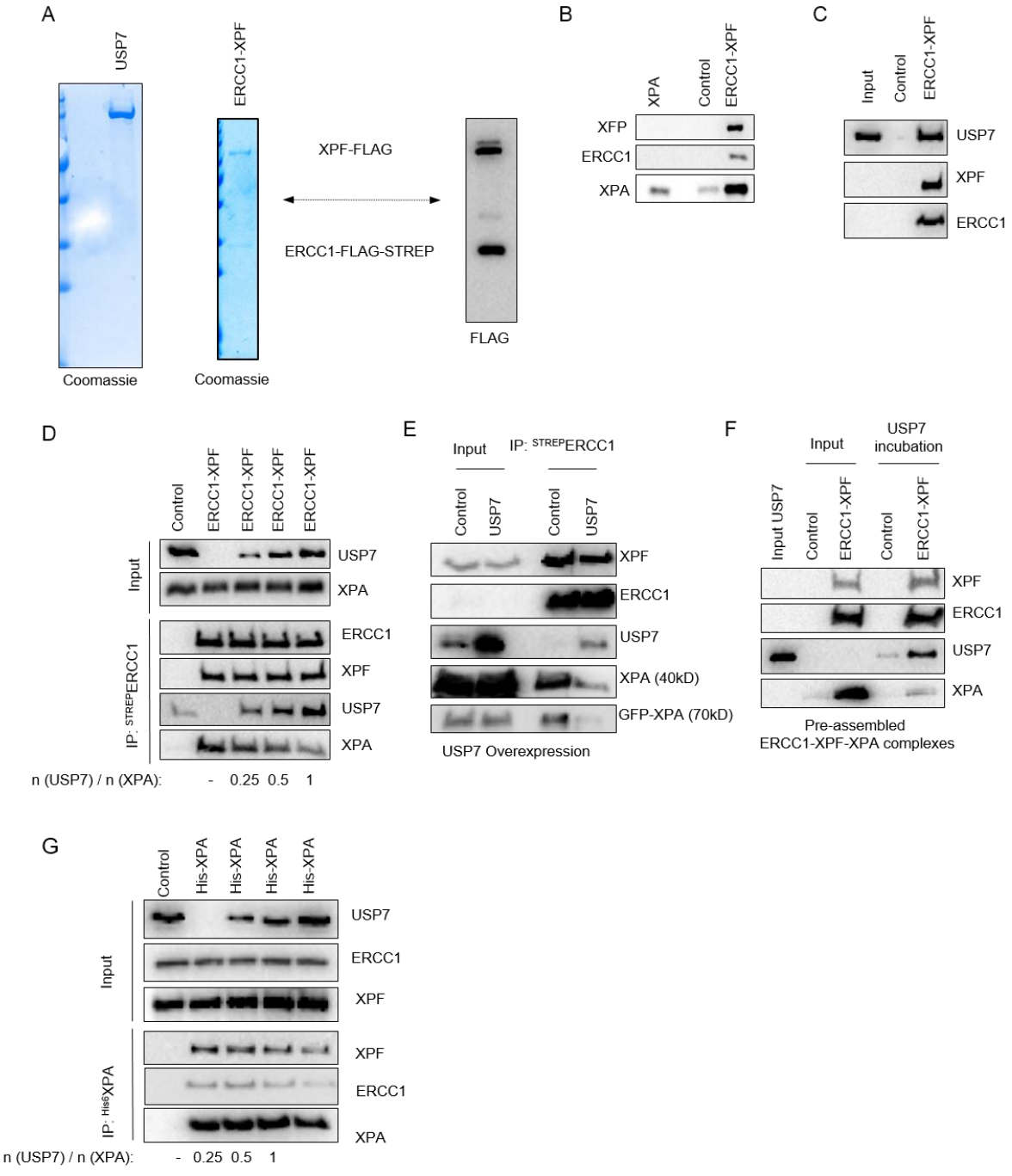

Figure 21 USP7 competes with XPA for binding to ERCC1-XPF complexes in vivo and in vitro. (A) USP7 and ERCC1-XPF complexes purified from HEK293T cells were analyzed in Coomassie stained gels and immunoblotting with FLAG antibodies. (B) XPA strongly interacts with purified ERCC1-XPF complexes in vitro. Pulldown assays with ERCC1-XPF and control beads assessing binding of purified XPA. Input represents 10% of XPA used in pulldowns. (C) USP7 interacts with ERCC1-XPF complexes *in vitro*. Pulldown assays with ERCC1-XPF and control beads assessing binding of purified USP7. Input represents 2% of USP7 used in the pulldown. (D) USP7 competes with XPA for binding to XPF-ERCC1. XPF-ERCC1 complexes were immobilized on StrepTactin beads and incubated with equimolar amounts of XPA and increasing amounts of USP7. USP7 levels were doubled stepwise reaching a fourfold molar excess of USP7 over the other components (relative molarity of USP7: 1:0, 1:1; 1:2; 1:4). Precipitate material was subjected to Western Blotting and probed with the indicated antibodies. (E) USP7 dislodges XPA from XPF-ERCC1 complexes *in vivo*. Immunoprecipitation of ^{FLAG}XPF-^{STREP}ERCC1 from HEK293T cells additionally expressing low levels of ^{GFP}XPA and overexpression of ^{GFP}USP7 using StrepTactin beads. Purified fraction was subjected to Western Blotting and probed with the indicated antibodies. (F) USP7 binds to pre-assembled XPF-ERCC1-XPA complexes and promotes dislocation of XPA from these complexes *in vitro*. ERCC1-XPF complexes were immobilized on StrepTactin beads and incubated with XPA for 2 hours at 4°C under gentle rotation. After washing, USP7 was added to the pre-assembled ERCC1-XPF-XPA complexes. (G) USP7 competes with XPA for binding to XPF-ERCC1 in vitro. XPA was immobilized on NiNTA beads and incubated with equimolar amounts of ERCC1-XPF complexes and increasing amounts of USP7. USP7 levels were doubled stepwise reaching a fourfold molar excess of USP7 over the other components (relative molarity of USP7: 1:0, 1:1; 1:2; 1:4). Precipitate material was subjected to Western Blotting and probed with the indicated antibodies.

in the co-precipitate while USP7 was modestly incorporated into the protein complex. These data suggest that USP7 has a higher binding affinity towards ERCC1-XPF than XPA and that USP7 potentially associates with ERCC1-XPF only transiently *in vivo*. To underline this finding we performed *in vitro* experiments to test whether XPA might be dislocated from ERCC1-XPF by USP7 (Figure 21F). To this end we assembled ERCC1-XPF-XPA protein complexes on STREP-Tactin beads and incubated them with an equimolar amount of USP7. We observed a dislocation of XPA and simultaneous association of USP7 with ERCC1-XPF complexes reflecting our previous results. Collectively, these data suggest that the ERCC1-XPF endonuclease complex forms two distinct protein complexes and that USP7 likely dislocates XPA from the ERCC1-XPF heterodimer.

ERCC1-XPF protein complexes cause deubiquitylation of XPC and DNA incision

Next, we dissected the function of the distinct ERCC1-XPF protein complexes. First, we analyzed the potential function of ERCC1-XPF-USP7 protein complexes. To this end we overexpressed HA-tagged XPC and ^{FLAG}XPF in HEK293T cells (Figure 22A). When performing XPC immunoprecipitations in the presence of enhanced levels of XPF we observed a drastic reduction of XPC ubiquitylation in comparison to control conditions. This

reduction was neither due to diminished amounts of USP7 nor reduced levels of the CUL4A E3 ubiquitin ligase. To test a direct involvement of ERCC1-XPF in USP7 mediated deubiquitylation we carried out deubiquitylation assays *in vitro*.

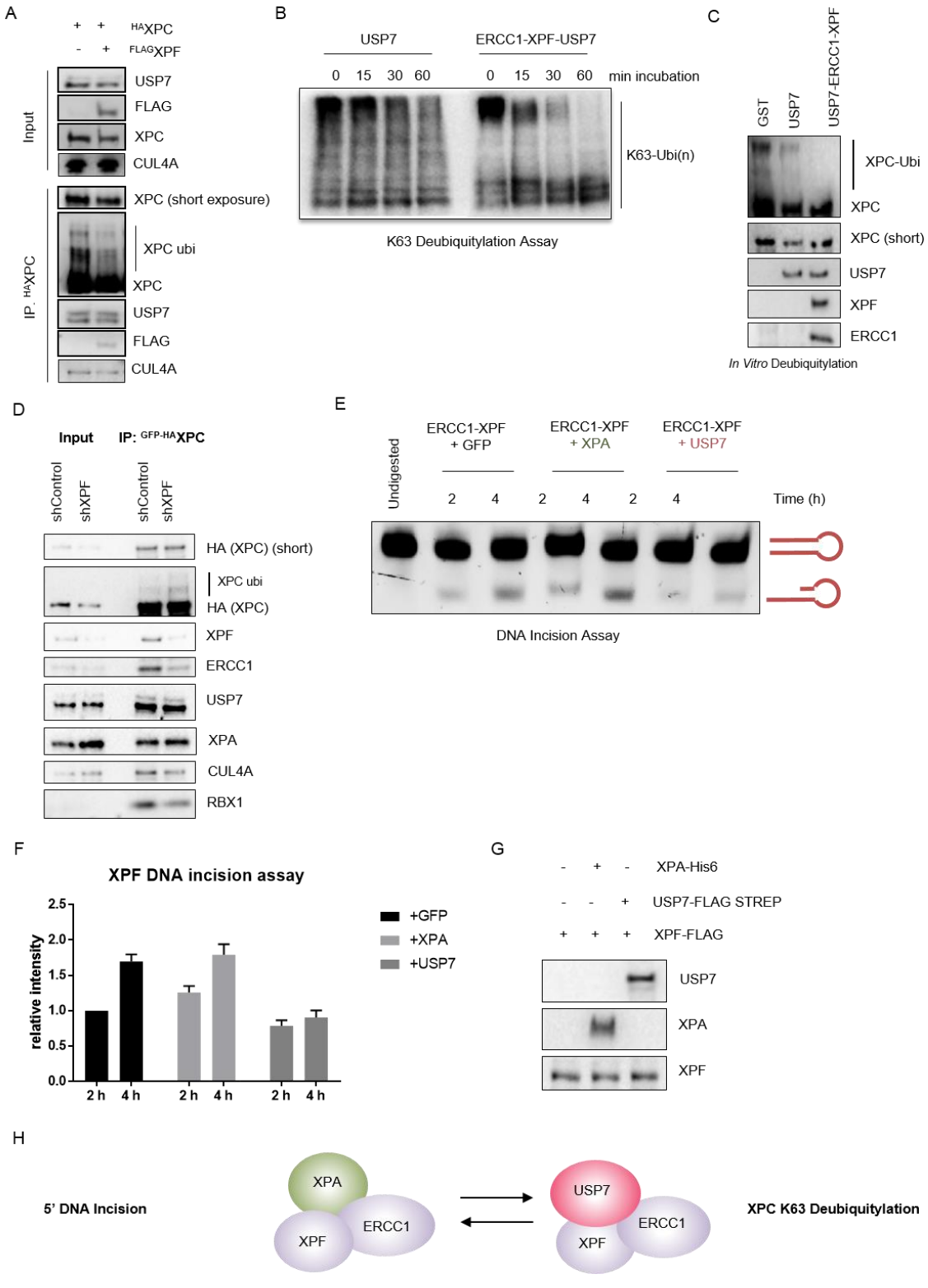

Figure 22: Two distinct XPF-ERCC1 protein complexes mediate 5´ DNA incision and XPC deubiquitination in GG-NER. (A) Overexpression of ^{FLAG}XPF accelerates USP7 mediated deubiquitination of XPC. Immuno-precipitation of ^{HA}XPC from HEK293T cells additionally expressing either ^{FLAG}XPF or the empty FLAG vector. Purified material was subjected to Western Blotting and probed with the indicated antibodies. (B) USP7 catalyzed cleavage of K63-linked polyubiquitin chains is facilitated by XPF-ERCC1 *in vitro*. Purified USP7 was pre-incubated with ERCC1-XPF or GST (control) for 30 min on ice. K63 ubiquitin chains were added and reactions were incubated at 37°C for the indicated times and immunoblotted with ubiquitin antibodies. (C) XPF-ERCC1 stimulates USP7-mediated deubiquitination of XPC *in vitro*. Immunoprecipitation of HA-tagged XPC from HEK293T cells collected one hour post-UV exposure. After washing, beads were divided and incubated with the indicated pre-assembled proteins at 37°C. Subsequently, the material was subjected to immunoblotting with the indicated antibodies. (D) Absence of XPF results in increased XPC ubiquitylation levels despite unaltered XPC bound USP7 levels. Immunoprecipitation of ^{HA}XPC in control and XPF knockdown cells one hour after UV exposure. The purified fractions were subjected to immunoblotting with the indicated antibodies. Input levels correspond to 0,5%. (E) USP7 drastically inhibits XPF incision activity on a stem loop oligonucleotide *in vitro*. Similar amounts of purified XPF-ERCC1 complexes, as monitored by immunoblotting in (G), were incubated with GST (as control), XPA or USP7, respectively, for 30min on ice. The stem loop substrate was added to the pre-assembled complexes and incubated at 29°C. Aliquots were taken at the respective time points and analyzed by 7M urea denaturing PAGE following visualization of DNA fragments with GelRed. (F) Graphical representation of the estimated band intensities corresponding to the respective cleaved DNA fragments from the DNA incision assay described in (E). Band intensities were determined with the BioRad Image Lab software. (H) Model illustrating the distinct XPF-ERCC1 protein complexes and their function in the GG-NER pathway.

We incubated K63-linked ubiquitin chains with either USP7 alone or the ERCC1-XPF-USP7 protein complex and monitored cleavage of K63 ubiquitin chains over time (Figures 22B). Interestingly, we observed that the deubiquitylation reaction was enhanced in the presence of the protein complex as compared to USP7 alone confirming our previous result (Figure 22B). To unequivocally demonstrate that ERCC1-XPF protein complexes stimulate USP7 activity towards polyubiquitylated XPC we examined the deubiquitylation of XPC *in vitro*. We immunoprecipitated XPC including the pool of ubiquitylated XPC from HEK293T cells after UV exposure and incubated the precipitate with GST (control), USP7 or the ERCC1-XPF-USP7 protein complex (Figure 22C). We observed the strongest reduction of polyubiquitylated XPC levels in the presence of the protein complex despite equivalent USP7 levels used in the assay. Furthermore, we analyzed XPC ubiquitylation levels in XPF knockdown HEK293T cells (shXPF) (Figure 22D). After immunoprecipitating HA-tagged XPC we noticed that depletion of XPF (shXPF) leads to increased amounts of ubiquitylated XPC despite unaltered USP7 levels and slightly decreased CUL4A-E3 ligase levels.

Finally, we tested both protein complexes for their DNA cleavage activity which is mediated by XPF within the ERCC1-XPF complex. The DNA incision assay was performed on a stem loop DNA structure as published previously (Sijbers et al., 1996). The stem loop DNA substrate was incubated with either ERCC1-XPF and GFP, ERCC1-XPF-XPA or ERCC1-

XPF-USP7 (Figure 22E-G). ERCC1-XPF catalyzed 5` incision of the DNA substrate resulting in a 9-10 bp shortened oligo fragment. For the XPA containing complex we observed a slightly enhanced incision as compared to the control (GFP). In contrast, XPF-ERCC1 protein complexes containing USP7 showed drastically reduced DNA cleavage suggesting that USP7 inhibits the nuclease activity of XPF. Taken together, our data indicate that ERCC1-XPF can establish two different protein complexes with distinct functions (Figure 22H). In combination with USP7, ERCC1-XPF enhances XPC deubiquitylation whereas ERCC1-XPF is only able of catalyzing 5´ DNA incision in the presence of XPA, but not USP7.

DISCUSSION

In the GG-NER sub-branch, DNA lesions are directly recognized by the main damage detector XPC. XPC probes the DNA for lesion-induced helical distortions, which are associated with an improved single stranded character of the DNA around the lesion (Min and Pavletich, 2007). Lesion recognition of XPC is essential for the assembly of the core NER factors and for the progress of the NER reaction (Volker et al., 2001). XPC is poly-ubiquitylated by the UV-DDB-CUL4A-RBX1 E3 ligase thereby stabilizing the protein at the DNA damage site (Sugasawa et al, 2005). The linkage type of this poly-ubiquitin chain on XPC is still unknown. Due to the fact that the UV-DDB-CUL4A-RBX1 complex decorates DDB2 with a Our data suggests that the UV-DDB-CUL4A-RBX1 catalyzed poly-ubiquitin chain decorating XPC is indeed a K63-linked polyubiquitin chain (Figures 15A and D). Similarly, in a previous report it was shown that the E3 ligase RNF111/Arkadia brings about a K63-linked ubiquitylation of XPC (Poulsen et al., 2013). Although both E3 ligases decorate XPC with a K63-linked polyubiquitin chain, they have opposing effects. The UV-DDB-CUL4A-RBX1 mediated ubiquitylation stabilizes XPC and enhances its DNA binding affinity *in vitro* (Sugasawa et al., 2005) whereas the ubiquitylation catalyzed by RNF111/Arkadia has been shown to be crucial for XPC release from the damage site (Poulson et al., 2013). We first examined whether the DDB-CUL4A complex mediated K63-ubiquitylation of XPC plays a role in the recruitment of downstream DNA repair factors to the damage site. Surprisingly, we noticed specific recruitment of the XPF-ERCC1 endonuclease complex to XPC in a K63 ubiquitylation dependent fashion after UV exposure (Figure 1). XPF does not contain any known ubiquitin binding domain and thus the question arises whether the association of XPF with the XPC K63-ubiquitin chains is bridged by other factors or whether it might have a rather transient function in the regulation of the XPC ubiquitylation and deubiquitylation cycle. To address this question we analyzed XPC ubiquitylation levels in XPF knockdown conditions. We noted a strong conservation of XPC ubiquitylation levels pointing towards a potential function in XPC deubiquitylation. A previous report demonstrated that USP7 catalyzes the deubiquitylation of XPC during GG-

NER (He et al., 2014b). In agreement with this report, we observed a physical interaction of USP7 and XPF suggesting a common function of both factors in the XPC deubiquitylation process. In line with this finding, XPF association with polyubiquitylated XPC requires the presence of USP7 as demonstrated by ^{FLAG}XPF purifications in control and USP7 knockdown cells (Figure 2D). In addition, localization of XPF to DNA damage sites is at least partially dependent on USP7 (Figure 2E). Taken together these data indicate that XPF and USP7 interact and that USP7 seems to bridge the association of XPF with ubiquitylated XPC. Thus, our results strongly imply an important role of USP7 in GG-NER. Our results in addition with published work suggest that USP7 operates in both NER sub-pathways. By performing UDS and cell survival assays, we unequivocally demonstrated that USP7 has a function in GG-NER besides its well documented role in TC-NER (Schwertman et al., 2012). The 5' DNA incision in the course of the NER reaction is known to be mediated by the XPF-ERCC1 heterodimer where XPF harbors the nuclease activity. Therefore, a role for XPF or ERCC1-XPF in the XPC deubiquitylation process is quite unexpected. To gain further insight into the interaction network of XPC, USP7 and XPF-ERCC1 and to define a molecular mechanism for the function of XPF in XPC deubiquitylation, *in vitro* experiments with purified proteins were performed. Interestingly, we found that ERCC1-XPF interacts with USP7 *in vitro*. It is well established that ERCC1-XPF associates with XPA through the ERCC1 subunit of the heterodimeric complex (Croteau et al., 2008). Thus we asked whether USP7 and XPA might have overlapping binding sites on ERCC1-XPF. In competition experiments we demonstrated that both XPA and USP7 associate with XPF-ERCC1 complexes with overlapping binding sites and, furthermore, that USP7 has a stronger binding affinity towards ERCC1-XPF than XPA (Figure 4B). In accordance, overexpression of USP7 causes a dislocation of XPA from ERCC1-XPF complexes *in vivo* confirming our *in vitro* data (Figure 4C). *In vitro* dislocation assays with pre-assembled ERCC1-XPF-XPA complexes further support this finding (Figure 4D). Various published reports suggested that XPA recruits ERCC1-XPF to the DNA damage site (Riedl et al., 2003; Volker et al., 2001). Whereas XPA might have a function in recruitment of ERCC1-XPF and potentially in the DNA incision process, our results clearly point toward a mechanism in which ERCC1-XPF complexes

might be remodelled at the DNA damage site to give rise to further protein complex that operates during XPC deubiquitylation. To be able to dissect the functions of the two distinct XPF-ERCC1 protein complexes, we performed *in vitro* deubiquitylation and DNA cleavage assays with purified proteins. USP7 shows accelerated cleavage of K63-linked ubiquitin chains in the presence of ERCC1-XPF as compared to incubation with USP7 alone (Figure 5B). More importantly, when employing ubiquitylated XPC purified from HEK293T cells as substrate, we noticed an enhanced deubiquitylation activity of the USP7-XPF-ERCC1 complex (Figure 5C). Additionally, these results reflect our findings when investigating XPC ubiquitylation levels in XPF knockdown background (Figures 2A and 5D) or after overexpressing XPF (Figure 5A). Thus, we speculate that the ERCC1-XPF endonuclease might stabilize USP7 at the damage site and that the binding of XPF-ERCC1 triggers the catalytic activity of USP7 in an allosteric fashion. In other words, USP7 seems to remain catalytically inactive *in vivo* until XPF-ERCC1 is incorporated forming the active USP7-ERCC1-XPF deubiquitylating complex. Finally, we investigated the function of both protein complexes in 5' DNA incision assays *in vitro*. Our data clearly demonstrate that XPF catalyzed DNA incision occurs normally when ERCC1-XPF associates with XPA. In contrast, ERCC1-XPF mediated incision was critically reduced in the presence of USP7. One hypothesis to explain this observation is that USP7 blocks the entry of the DNA into the active site of the heterodimer, which is plausible given its molecular weight of about 133 kDa. Alternatively, the interaction with USP7 might induce a structural change of the complex thereby inhibiting the association of the ERCC1-XPF heterodimer with DNA.

Taken together, our data reveals the existence of two distinct protein complexes that use ERCC1-XPF as a binding platform. An interesting point is that 5´DNA incision and XPC deubiquitylation are obviously coupled. Further evidence strongly supporting our finding of a coupled mechanism for both processes arises from a previous report (Staresincic et al., 2009). In immunofluorescense experiments with XPF deficient (XP2YO(SV)) fibroblasts stably expressing wild-type XPF or a catalytically inactive XPF mutant (XPF D676A), Staresincic and co-workers demonstrated that XPC co-localizes with catalytically inactive

XPF and, importantly, both proteins persist at the damage site even at three hours after local UV irradiation. In contrast, the co-localization of XPC with wild-type XPF observed at 30 min could no longer be detected at three hours after local UV exposure indicating that XPC and XPF are not present anymore at the damage site. Additionally, XPC remained stably tethered at the damage site in XPF deficient fibroblasts both at 30 min and at three hours in response to local UV irradiation. Collectively, their results suggest that the ERCC1-XPF catalyzed 5´ DNA incision in GG-NER has to occur prior to cleavage of the K63-linked polyubiquitin chain on XPC (Staresincic et al., 2009). USP7 mediated deubiquitylation of XPC is essential for efficient progression of the NER reaction and XPC removal from the damage site at later stages of the NER reaction.

This work suggests that the ERCC1-XPF catalyzed 5´ DNA incision in GG-NER has to occur prior to cleavage of the polyubiquitin chain on XPC. USP7 mediated deubiquitylation of XPC is essential for efficient progression of the NER reaction and XPC removal from the damage site at later stages of the NER reaction. Given the strong affinity of USP7 towards ERCC1-XPF and its potential to displace XPF-ERCC1 bound XPA, one might speculate that XPA recruits ERCC1-XPF, supports 5´ DNA incision and that USP7 dislocates XPA to degrade the XPC K63-polyubiquitin chain set by the DDB-CUL4A E3 ligase complex. However the exact mechanism might be, our data clearly shows that USP7 mediated deubiquitylation of XPC is required for the efficient removal of UV-induced DNA lesions by the GG-NER branch. Future research will certainly reveal the underlying molecular mechanism and the impact of XPC deubiquitylation on downstream repair even

CONCLUSION

In this study, we show that 5' incision of damaged DNA is linked with the deubiquitylation of XPC. Our data suggests that XPF-ERCC1 forms a protein complex with XPA that is capable of incising DNA. The deubiquitylase USP7 competes with XPA for binding to XPF-ERCC1 establishing a novel protein complex that catalyzes the degradation of K63-ubiquitylated XPC *in vivo* and *in vitro*. Hence, our new findings reveal the existence of two separate functions of XPF-ERCC1 and shed new light on the orchestration of GG-NER.

REFERENCES

Aboussekhra, A.; Biggerstaff, M.; Shivji, M. K.; Vilpo, J. A.; Moncollin, V.; Podust, V. N. et al. (1995): Mammalian DNA nucleotide excision repair reconstituted with purified protein components. In *Cell* 80 (6), pp. 859–868.

Aguilera, Andrés; Gómez-González, Belén (2008): Genome instability. A mechanistic view of its causes and consequences. In *Nature reviews. Genetics* 9 (3), pp. 204–217. DOI: 10.1038/nrg2268.

Ahel, Dragana; Horejsí, Zuzana; Wiechens, Nicola; Polo, Sophie E.; Garcia-Wilson, Elisa; Ahel, Ivan et al. (2009): Poly(ADP-ribose)-dependent regulation of DNA repair by the chromatin remodeling enzyme ALC1. In *Science (New York, N.Y.)* 325 (5945), pp. 1240–1243. DOI: 10.1126/science.1177321.

Alekseev, Sergey; Kool, Hanneke; Rebel, Heggert; Fousteri, Maria; Moser, Jill; Backendorf, Claude et al. (2005): Enhanced DDB2 expression protects mice from carcinogenic effects of chronic UV-B irradiation. In *Cancer research* 65 (22), pp. 10298–10306. DOI: 10.1158/0008-5472.CAN-05-2295.

Andressoo, Jaan-Olle; Hoeijmakers, Jan H. J.; Mitchell, James R. (2006): Nucleotide excision repair disorders and the balance between cancer and aging. In *Cell cycle (Georgetown, Tex.)* 5 (24), pp. 2886–2888. DOI: 10.4161/cc.5.24.3565.

Angers, Stephane; Li, Ti; Yi, Xianhua; MacCoss, Michael J.; Moon, Randall T.; Zheng, Ning (2006): Molecular architecture and assembly of the DDB1-CUL4A ubiquitin ligase machinery. In *Nature* 443 (7111), pp. 590–593. DOI: 10.1038/nature05175.

Araki, M.; Masutani, C.; Takemura, M.; Uchida, A.; Sugasawa, K.; Kondoh, J. et al. (2001): Centrosome protein centrin 2/caltractin 1 is part of the xeroderma pigmentosum group C complex that initiates global genome nucleotide excision repair. In *The Journal of biological chemistry* 276 (22), pp. 18665–18672. DOI: 10.1074/jbc.M100855200.

Bannister, Andrew J.; Kouzarides, Tony (2011): Regulation of chromatin by histone modifications. In *Cell research* 21 (3), pp. 381–395. DOI: 10.1038/cr.2011.22.

Banno, Kouji; Yanokura, Megumi; Kobayashi, Yusuke; Kawaguchi, Makiko; Nomura, Hiroyuki; Hirasawa, Akira et al. (2009): Endometrial cancer as a familial tumor. Pathology and molecular carcinogenesis (review). In *Current genomics* 10 (2), pp. 127–132. DOI: 10.2174/138920209787847069.

Barsky, D.; Foloppe, N.; Ahmadia, S.; Wilson, D. M.; MacKerell, A. D. (2000): New insights into the structure of abasic DNA from molecular dynamics simulations. In *Nucleic acids research* 28 (13), pp. 2613–2626. DOI: 10.1093/nar/28.13.2613.

Bartholomew, Blaine (2014): Regulating the chromatin landscape. Structural and mechanistic perspectives. In *Annual review of biochemistry* 83, pp. 671–696. DOI: 10.1146/annurev-biochem-051810-093157.

Batty, D.; Rapic'-Otrin, V.; Levine, A. S.; Wood, R. D. (2000): Stable binding of human XPC complex to irradiated DNA confers strong discrimination for damaged sites. In *Journal of molecular biology* 300 (2), pp. 275–290. DOI: 10.1006/jmbi.2000.3857.

Belmont, A. S.; Straight, A. F. (1998): In vivo visualization of chromosomes using lac operator-repressor binding. In *Trends in cell biology* 8 (3), pp. 121–124.

Bergink, Steven; Toussaint, Wendy; Luijsterburg, Martijn S.; Dinant, Christoffel; Alekseev, Sergey; Hoeijmakers, Jan H. J. et al. (2012): Recognition of DNA damage by XPC coincides with disruption of the XPC-RAD23 complex. In *The Journal of cell biology* 196 (6), pp. 681–688. DOI: 10.1083/jcb.201107050.

Biswas, Mithun; Voltz, Karine; Smith, Jeremy C.; Langowski, Jörg (2011): Role of histone tails in structural stability of the nucleosome. In *PLoS computational biology* 7 (12), e1002279. DOI: 10.1371/journal.pcbi.1002279.

Blackford, Andrew N.; Jackson, Stephen P. (2017): ATM, ATR, and DNA-PK. The Trinity at the Heart of the DNA Damage Response. In *Molecular cell* 66 (6), pp. 801–817. DOI: 10.1016/j.molcel.2017.05.015.

Boal, Amie K.; Genereux, Joseph C.; Sontz, Pamela A.; Gralnick, Jeffrey A.; Newman, Dianne K.; Barton, Jacqueline K. (2009): Redox signaling between DNA repair proteins for efficient lesion detection. In *Proceedings of the National Academy of Sciences of the United States of America* 106 (36), pp. 15237–15242. DOI: 10.1073/pnas.0908059106.

Boal, Amie K.; Yavin, Eylon; Lukianova, Olga A.; O'Shea, Valerie L.; David, Sheila S.; Barton, Jacqueline K. (2005): DNA-bound redox activity of DNA repair glycosylases containing 4Fe-4S clusters. In *Biochemistry* 44 (23), pp. 8397–8407. DOI: 10.1021/bi047494n.

Boer, J. de; Hoeijmakers, J. H. (2000): Nucleotide excision repair and human syndromes. In *Carcinogenesis* 21 (3), pp. 453–460.

Bont, Rinne de; van Larebeke, Nik (2004): Endogenous DNA damage in humans. A review of quantitative data. In *Mutagenesis* 19 (3), pp. 169–185.

Bunting, Samuel F.; Callén, Elsa; Wong, Nancy; Chen, Hua-Tang; Polato, Federica; Gunn, Amanda et al. (2010): 53BP1 inhibits homologous recombination in Brca1-deficient cells by blocking resection of DNA breaks. In *Cell* 141 (2), pp. 243–254. DOI: 10.1016/j.cell.2010.03.012.

Buterin, T.; Hess, M. T.; Luneva, N.; Geacintov, N. E.; Amin, S.; Kroth, H. et al. (2000): Unrepaired fjord region polycyclic aromatic hydrocarbon-DNA adducts in ras codon 61 mutational hot spots. In *Cancer research* 60 (7), pp. 1849–1856.

Cadet, Jean; Douki, Thierry; Ravanat, Jean-Luc (2015): Oxidatively generated damage to cellular DNA by UVB and UVA radiation. In *Photochemistry and photobiology* 91 (1), pp. 140–155. DOI: 10.1111/php.12368.

Carreira, Aura; Hilario, Jovencio; Amitani, Ichiro; Baskin, Ronald J.; Shivji, Mahmud K. K.; Venkitaraman, Ashok R.; Kowalczykowski, Stephen C. (2009): The BRC repeats of BRCA2 modulate the DNA-binding selectivity of RAD51. In *Cell* 136 (6), pp. 1032–1043. DOI: 10.1016/j.cell.2009.02.019.

Chang, Debbie J.; Cimprich, Karlene A. (2009): DNA damage tolerance. When it's OK to make mistakes. In *Nature chemical biology* 5 (2), pp. 82–90. DOI: 10.1038/nchembio.139.

Chapman, J. Ross; Taylor, Martin R. G.; Boulton, Simon J. (2012): Playing the end game. DNA double-strand break repair pathway choice. In *Molecular cell* 47 (4), pp. 497–510. DOI: 10.1016/j.molcel.2012.07.029.

Chatterjee, Nimrat; Walker, Graham C. (2017): Mechanisms of DNA damage, repair, and mutagenesis. In *Environmental and molecular mutagenesis* 58 (5), pp. 235–263. DOI: 10.1002/em.22087.

Chiruvella, Kishore K.; Liang, Zhuobin; Wilson, Thomas E. (2013): Repair of double-strand breaks by end joining. In *Cold Spring Harbor perspectives in biology* 5 (5), a012757. DOI: 10.1101/cshperspect.a012757.

Chitale, Shalaka; Richly, Holger (2017): DICER and ZRF1 contribute to chromatin decondensation during nucleotide excision repair. In *Nucleic acids research* 45 (10), pp. 5901–5912. DOI: 10.1093/nar/gkx261.

Chitale, Shalaka; Richly, Holger (2017): Nuclear organization of nucleotide excision repair is mediated by RING1B dependent H2A-ubiquitylation. In *Oncotarget* 8 (19), pp. 30870–30887. DOI: 10.18632/oncotarget.16142.

Chu, Gilbert; Yang, Wei (2008): Here comes the sun. Recognition of UV-damaged DNA. In *Cell* 135 (7), pp. 1172–1174. DOI: 10.1016/j.cell.2008.12.015.

Ciccia, Alberto; Elledge, Stephen J. (2010): The DNA damage response. Making it safe to play with knives. In *Molecular cell* 40 (2), pp. 179–204. DOI: 10.1016/j.molcel.2010.09.019.

Clapier, Cedric R.; Iwasa, Janet; Cairns, Bradley R.; Peterson, Craig L. (2017): Mechanisms of action and regulation of ATP-dependent chromatin-remodelling complexes. In *Nature reviews. Molecular cell biology* 18 (7), pp. 407–422. DOI: 10.1038/nrm.2017.26.

Cleaver, J. E. (1977): Nucleosome structure controls rates of excision repair in DNA of human cells. In *Nature* 270 (5636), pp. 451–453.

Cleaver, James E.; Lam, Ernest T.; Revet, Ingrid (2009): Disorders of nucleotide excision repair. The genetic and molecular basis of heterogeneity. In *Nature reviews. Genetics* 10 (11), pp. 756–768. DOI: 10.1038/nrg2663.

Compe, Emmanuel; Egly, Jean-Marc (2012): TFIIH. When transcription met DNA repair. In *Nature reviews. Molecular cell biology* 13 (6), pp. 343–354. DOI: 10.1038/nrm3350.

Cooper, David N.; Mort, Matthew; Stenson, Peter D.; Ball, Edward V.; Chuzhanova, Nadia A. (2010): Methylation-mediated deamination of 5-methylcytosine appears to give rise to mutations causing human inherited disease in CpNpG trinucleotides, as well as in CpG dinucleotides. In *Human genomics* 4 (6), pp. 406–410.

Cortázar, Daniel; Kunz, Christophe; Saito, Yusuke; Steinacher, Roland; Schär, Primo (2007): The enigmatic thymine DNA glycosylase. In *DNA repair* 6 (4), pp. 489–504. DOI: 10.1016/j.dnarep.2006.10.013.

Croteau, Deborah L.; Peng, Ye; van Houten, Bennett (2008): DNA repair gets physical. Mapping an XPA-binding site on ERCC1. In *DNA repair* 7 (5), pp. 819–826. DOI: 10.1016/j.dnarep.2008.01.018.

Dalhus, Bjørn; Laerdahl, Jon K.; Backe, Paul H.; Bjørås, Magnar (2009): DNA base repair--recognition and initiation of catalysis. In *FEMS microbiology reviews* 33 (6), pp. 1044–1078. DOI: 10.1111/j.1574-6976.2009.00188.x.

Davies, R. J. (1995): Royal Irish Academy Medal Lecture. Ultraviolet radiation damage in DNA. In *Biochemical Society transactions* 23 (2), pp. 407–418.

Dip, Ramiro; Camenisch, Ulrike; Naegeli, Hanspeter (2004): Mechanisms of DNA damage recognition and strand discrimination in human nucleotide excision repair. In *DNA repair* 3 (11), pp. 1409–1423. DOI: 10.1016/j.dnarep.2004.05.005.

D'Orazio, John; Jarrett, Stuart; Amaro-Ortiz, Alexandra; Scott, Timothy (2013): UV radiation and the skin. In *International journal of molecular sciences* 14 (6), pp. 12222–12248. DOI: 10.3390/ijms140612222.

Falck, Jacob; Coates, Julia; Jackson, Stephen P. (2005): Conserved modes of recruitment of ATM, ATR and DNA-PKcs to sites of DNA damage. In *Nature* 434 (7033), pp. 605–611. DOI: 10.1038/nature03442.

Fishel, Richard (2015): Mismatch repair. In *The Journal of biological chemistry* 290 (44), pp. 26395–26403. DOI: 10.1074/jbc.R115.660142.

Fitch, Maureen E.; Nakajima, Satoshi; Yasui, Akira; Ford, James M. (2003): In vivo recruitment of XPC to UV-induced cyclobutane pyrimidine dimers by the DDB2 gene product. In *The Journal of biological chemistry* 278 (47), pp. 46906–46910. DOI: 10.1074/jbc.M307254200.

Fousteri, Maria; Mullenders, Leon H. F. (2008): Transcription-coupled nucleotide excision repair in mammalian cells. Molecular mechanisms and biological effects. In *Cell research* 18 (1), pp. 73–84. DOI: 10.1038/cr.2008.6.

Fousteri, Maria; Vermeulen, Wim; van Zeeland, Albert A.; Mullenders, Leon H. F. (2006): Cockayne syndrome A and B proteins differentially regulate recruitment of chromatin remodeling and repair factors to stalled RNA polymerase II in vivo. In *Molecular cell* 23 (4), pp. 471–482. DOI: 10.1016/j.molcel.2006.06.029.

Friedberg, Errol C. (2006): DNA repair and mutagenesis. 2nd ed. Washington, D.C: ASM Press. Available online at http://site.ebrary.com/id/10430836.

Fromme, J. Christopher; Banerjee, Anirban; Huang, Susan J.; Verdine, Gregory L. (2004): Structural basis for removal of adenine mispaired with 8-oxoguanine by MutY adenine DNA glycosylase. In *Nature* 427 (6975), pp. 652–656. DOI: 10.1038/nature02306.

Geacintov, Nicholas E.; Broyde, Suse (2017): Repair-Resistant DNA Lesions. In *Chemical research in toxicology* 30 (8), pp. 1517–1548. DOI: 10.1021/acs.chemrestox.7b00128.

Gelasco, A.; Lippard, S. J. (1998): NMR solution structure of a DNA dodecamer duplex containing a cis-diammineplatinum(II) d(GpG) intrastrand cross-link, the major adduct of the anticancer drug cisplatin. In *Biochemistry* 37 (26), pp. 9230–9239. DOI: 10.1021/bi973176v.

Ghosal, Gargi; Chen, Junjie (2013): DNA damage tolerance. A double-edged sword guarding the genome. In *Translational cancer research* 2 (3), pp. 107–129. DOI: 10.3978/j.issn.2218-676X.2013.04.01.

Gillet, Ludovic C. J.; Schärer, Orlando D. (2006): Molecular mechanisms of mammalian global genome nucleotide excision repair. In *Chemical reviews* 106 (2), pp. 253–276. DOI: 10.1021/cr040483f.

Graaf, Carolyn A. de; van Steensel, Bas (2013): Chromatin organization. Form to function. In *Current opinion in genetics & development* 23 (2), pp. 185–190. DOI: 10.1016/j.gde.2012.11.011.

Groisman, Regina; Polanowska, Jolanta; Kuraoka, Isao; Sawada, Jun-ichi; Saijo, Masafumi; Drapkin, Ronny et al. (2003): The ubiquitin ligase activity in the DDB2 and CSA complexes is differentially regulated by the COP9 signalosome in response to DNA damage. In *Cell* 113 (3), pp. 357–367.

Guerrera, G.; Melina, D.; Falappa, P.; Baruffi, E.; Musumeci, V.; Capaldi, L.; Intonti, F. (1987): Gli aneurismi da miceti. Descrizione di un caso di pseudoaneurisma dell'aorta toracica in corso di candidosi sistemica. In *Minerva cardioangiologica* 35 (9), pp. 499–504.

Guerrero-Santoro, Jennifer; Kapetanaki, Maria G.; Hsieh, Ching L.; Gorbachinsky, Ilya; Levine, Arthur S.; Rapić-Otrin, Vesna (2008): The cullin 4B-based UV-damaged DNA-binding protein ligase binds to UV-damaged chromatin and ubiquitinates histone H2A. In *Cancer research* 68 (13), pp. 5014–5022. DOI: 10.1158/0008-5472.CAN-07-6162.

Guibert, J.; Destrée, D.; Konopka, C.; Acar, J. (1986): Ciprofloxacin in the treatment of urinary tract infection due to enterobacteria. In *European journal of clinical microbiology* 5 (2), pp. 247–248.

Gunz, D.; Hess, M. T.; Naegeli, H. (1996): Recognition of DNA adducts by human nucleotide excision repair. Evidence for a thermodynamic probing mechanism. In *The Journal of biological chemistry* 271 (41), pp. 25089–25098.

Gupta, Shikha; Gellert, Martin; Yang, Wei (2011): Mechanism of mismatch recognition revealed by human MutSβ bound to unpaired DNA loops. In *Nature structural & molecular biology* 19 (1), pp. 72–78. DOI: 10.1038/nsmb.2175.

Gurard-Levin, Zachary A.; Quivy, Jean-Pierre; Almouzni, Geneviève (2014): Histone chaperones. Assisting histone traffic and nucleosome dynamics. In *Annual review of biochemistry* 83, pp. 487–517. DOI: 10.1146/annurev-biochem-060713-035536.

Haber, James E. (2008): Alternative endings. In *Proceedings of the National Academy of Sciences of the United States of America* 105 (2), pp. 405–406. DOI: 10.1073/pnas.0711334105.

Hainaut, P.; Hollstein, M. (2000): p53 and human cancer. The first ten thousand mutations. In *Advances in cancer research* 77, pp. 81–137.

Hardeland, U.; Bentele, M.; Lettieri, T.; Steinacher, R.; Jiricny, J.; Schär, P. (2001): Thymine DNA glycosylase. In *Progress in nucleic acid research and molecular biology* 68, pp. 235–253.

Harper, J. Wade; Elledge, Stephen J. (2007): The DNA damage response. Ten years after. In *Molecular cell* 28 (5), pp. 739–745. DOI: 10.1016/j.molcel.2007.11.015.

Harvey, Stacy L.; Charlet, Alyson; Haas, Wilhelm; Gygi, Steven P.; Kellogg, Douglas R. (2005): Cdk1-dependent regulation of the mitotic inhibitor Wee1. In *Cell* 122 (3), pp. 407–420. DOI: 10.1016/j.cell.2005.05.029.

Harvey, Ronald G.; Dai, Qing; Ran, Chongzhao; Lim, Keunpoong; Blair, Ian; Penning, Trevor M. (2005): SYNTHESES OF ADDUCTS OF ACTIVE METABOLITES OF CARCINOGENIC POLYCYCLIC AROMATIC HYDROCARBONS WITH 2′-DEOXYRIBONUCLEOSIDES. In *Polycyclic Aromatic Compounds* 25 (5), pp. 371–391. DOI: 10.1080/10406630500447019.

He, Jinshan; Zhu, Qianzheng; Sharma, Nidhi; Wani, Gulzar; Han, Chunhua; Qian, Jiang et al. (2014): Abstract 2391. USP7 deubiquitinates XPC in response to ultraviolet light irradiation. In *Cancer research* 74 (19 Supplement), p. 2391. DOI: 10.1158/1538-7445.AM2014-2391.

He, Jinshan; Zhu, Qianzheng; Wani, Gulzar; Sharma, Nidhi; Han, Chunhua; Qian, Jiang et al. (2014): Ubiquitin-specific protease 7 regulates nucleotide excision repair through deubiquitinating XPC protein and preventing XPC protein from undergoing ultraviolet light-induced and VCP/p97 protein-regulated proteolysis. In *The Journal of biological chemistry* 289 (39), pp. 27278–27289. DOI: 10.1074/jbc.M114.589812.

Heinen, Christopher D. (2016): Mismatch repair defects and Lynch syndrome. The role of the basic scientist in the battle against cancer. In *DNA repair* 38, pp. 127–134. DOI: 10.1016/j.dnarep.2015.11.025.

Helleday, Thomas (2010): Homologous recombination in cancer development, treatment and development of drug resistance. In *Carcinogenesis* 31 (6), pp. 955–960. DOI: 10.1093/carcin/bgq064.

Hewish, Madeleine; Lord, Christopher J.; Martin, Sarah A.; Cunningham, David; Ashworth, Alan (2010): Mismatch repair deficient colorectal cancer in the era of personalized treatment. In *Nature reviews. Clinical oncology* 7 (4), pp. 197–208. DOI: 10.1038/nrclinonc.2010.18.

Heyer, Wolf-Dietrich (2015): Regulation of recombination and genomic maintenance. In *Cold Spring Harbor perspectives in biology* 7 (8), a016501. DOI: 10.1101/cshperspect.a016501.

Hoeijmakers, J. H. (2001): Genome maintenance mechanisms for preventing cancer. In *Nature* 411 (6835), pp. 366–374. DOI: 10.1038/35077232.

Hoeijmakers, Jan H. J. (2009): DNA damage, aging, and cancer. In *The New England journal of medicine* 361 (15), pp. 1475–1485. DOI: 10.1056/NEJMra0804615.

Honda, Masayoshi; Park, Jeehae; Pugh, Robert A.; Ha, Taekjip; Spies, Maria (2009): Single-molecule analysis reveals differential effect of ssDNA-binding proteins on DNA translocation by XPD helicase. In *Molecular cell* 35 (5), pp. 694–703. DOI: 10.1016/j.molcel.2009.07.003.

Hoogstraten, Deborah; Bergink, Steven; Ng, Jessica M. Y.; Verbiest, Vincent H. M.; Luijsterburg, Martijn S.; Geverts, Bart et al. (2008): Versatile DNA damage detection by the global genome nucleotide excision repair protein XPC. In *Journal of cell science* 121 (Pt 17), pp. 2850–2859. DOI: 10.1242/jcs.031708.

Hsieh, Peggy; Zhang, Yongliang (2017): The Devil is in the details for DNA mismatch repair. In *Proceedings of the National Academy of Sciences of the United States of America* 114 (14), pp. 3552–3554. DOI: 10.1073/pnas.1702747114.

Huang, J. C.; Hsu, D. S.; Kazantsev, A.; Sancar, A. (1994): Substrate spectrum of human excinuclease. Repair of abasic sites, methylated bases, mismatches, and bulky adducts. In *Proceedings of the National Academy of Sciences of the United States of America* 91 (25), pp. 12213–12217.

Huffman, Joy L.; Sundheim, Ottar; Tainer, John A. (2005): DNA base damage recognition and removal. New twists and grooves. In *Mutation research* 577 (1-2), pp. 55–76. DOI: 10.1016/j.mrfmmm.2005.03.012.

Hühn, Daniela; Bolck, Hella A.; Sartori, Alessandro A. (2013): Targeting DNA double-strand break signalling and repair. Recent advances in cancer therapy. In *Swiss medical weekly* 143, w13837. DOI: 10.4414/smw.2013.13837.

Ighodaro, O. M.; Akinloye, O. A. (2018): First line defence antioxidants-superoxide dismutase (SOD), catalase (CAT) and glutathione peroxidase (GPX). Their fundamental role in the entire antioxidant defence grid. In *Alexandria Journal of Medicine* 54 (4), pp. 287–293. DOI: 10.1016/j.ajme.2017.09.001.

Ira, Grzegorz; Pellicioli, Achille; Balijja, Alitukiriza; Wang, Xuan; Fiorani, Simona; Carotenuto, Walter et al. (2004): DNA end resection, homologous recombination and DNA damage checkpoint activation require CDK1. In *Nature* 431 (7011), pp. 1011–1017. DOI: 10.1038/nature02964.

Iwasaki, Wakana; Miya, Yuta; Horikoshi, Naoki; Osakabe, Akihisa; Taguchi, Hiroyuki; Tachiwana, Hiroaki et al. (2013): Contribution of histone N-terminal tails to the structure and stability of nucleosomes. In *FEBS open bio* 3, pp. 363–369. DOI: 10.1016/j.fob.2013.08.007.

Jackson, Stephen P.; Bartek, Jiri (2009): The DNA-damage response in human biology and disease. In *Nature* 461 (7267), pp. 1071–1078. DOI: 10.1038/nature08467.

Janicki, Susan M.; Tsukamoto, Toshiro; Salghetti, Simone E.; Tansey, William P.; Sachidanandam, Ravi; Prasanth, Kannanganattu V. et al. (2004): From silencing to gene expression. Real-time analysis in single cells. In *Cell* 116 (5), pp. 683–698.

Javaid, Nasir; Choi, Sangdun (2017): Acetylation- and Methylation-Related Epigenetic Proteins in the Context of Their Targets. In *Genes* 8 (8). DOI: 10.3390/genes8080196.

Jiricny, Josef (2006): The multifaceted mismatch-repair system. In *Nature reviews. Molecular cell biology* 7 (5), pp. 335–346. DOI: 10.1038/nrm1907.

Jiricny, Josef (2013): Postreplicative mismatch repair. In *Cold Spring Harbor perspectives in biology* 5 (4), a012633. DOI: 10.1101/cshperspect.a012633.

Kadyk, L. C.; Hartwell, L. H. (1992): Sister chromatids are preferred over homologs as substrates for recombinational repair in Saccharomyces cerevisiae. In *Genetics* 132 (2), pp. 387–402.

Kadyrov, Farid A.; Dzantiev, Leonid; Constantin, Nicoleta; Modrich, Paul (2006): Endonucleolytic function of MutLalpha in human mismatch repair. In *Cell* 126 (2), pp. 297–308. DOI: 10.1016/j.cell.2006.05.039.

Kakarougkas, A.; Jeggo, P. A. (2014): DNA DSB repair pathway choice. An orchestrated handover mechanism. In *The British journal of radiology* 87 (1035), p. 20130685. DOI: 10.1259/bjr.20130685.

Katsumi, S.; Kobayashi, N.; Imoto, K.; Nakagawa, A.; Yamashina, Y.; Muramatsu, T. et al. (2001): In situ visualization of ultraviolet-light-induced DNA damage repair in locally irradiated human fibroblasts. In *The Journal of investigative dermatology* 117 (5), pp. 1156–1161. DOI: 10.1046/j.0022-202x.2001.01540.x.

Kisker, Caroline; Kuper, Jochen; van Houten, Bennett (2013): Prokaryotic nucleotide excision repair. In *Cold Spring Harbor perspectives in biology* 5 (3), a012591. DOI: 10.1101/cshperspect.a012591.

Knobel, Philip A.; Marti, Thomas M. (2011): Translesion DNA synthesis in the context of cancer research. In *Cancer cell international* 11, p. 39. DOI: 10.1186/1475-2867-11-39.

Koch, Sandra C.; Simon, Nina; Ebert, Charlotte; Carell, Thomas (2016): Molecular mechanisms of xeroderma pigmentosum (XP) proteins. In *Quarterly reviews of biophysics* 49, e5. DOI: 10.1017/S0033583515000268.

Komander, David (2010): Mechanism, specificity and structure of the deubiquitinases. In *Sub-cellular biochemistry* 54, pp. 69–87. DOI: 10.1007/978-1-4419-6676-6_6.

Kouzarides, Tony (2007): Chromatin modifications and their function. In *Cell* 128 (4), pp. 693–705. DOI: 10.1016/j.cell.2007.02.005.

Kunkel, T. A. (1993): Nucleotide repeats. Slippery DNA and diseases. In *Nature* 365 (6443), pp. 207–208. DOI: 10.1038/365207a0.

Kunkel, T. A. (2009): Evolving views of DNA replication (in)fidelity. In *Cold Spring Harbor symposia on quantitative biology* 74, pp. 91–101. DOI: 10.1101/sqb.2009.74.027.

Kunkel, Thomas A. (2011): Balancing eukaryotic replication asymmetry with replication fidelity. In *Current opinion in chemical biology* 15 (5), pp. 620–626. DOI: 10.1016/j.cbpa.2011.07.025.

Kunkel, Thomas A.; Erie, Dorothy A. (2015): Eukaryotic Mismatch Repair in Relation to DNA Replication. In *Annual review of genetics* 49, pp. 291–313. DOI: 10.1146/annurev-genet-112414-054722.

Kuper, Jochen; Kisker, Caroline (2012): Damage recognition in nucleotide excision DNA repair. In *Current opinion in structural biology* 22 (1), pp. 88–93. DOI: 10.1016/j.sbi.2011.12.002.

Kuper, Jochen; Wolski, Stefanie C.; Michels, Gudrun; Kisker, Caroline (2012): Functional and structural studies of the nucleotide excision repair helicase XPD suggest a polarity for DNA translocation. In *The EMBO journal* 31 (2), pp. 494–502. DOI: 10.1038/emboj.2011.374.

Kuznetsova, Alexandra A.; Kuznetsov, Nikita A.; Ishchenko, Alexander A.; Saparbaev, Murat K.; Fedorova, Olga S. (2014): Step-by-step mechanism of DNA damage recognition by human 8-oxoguanine DNA glycosylase. In *Biochimica et biophysica acta* 1840 (1), pp. 387–395. DOI: 10.1016/j.bbagen.2013.09.035.

Laat, W. L. de; Jaspers, N. G.; Hoeijmakers, J. H. (1999): Molecular mechanism of nucleotide excision repair. In *Genes & development* 13 (7), pp. 768–785.

Lans, Hannes; Marteijn, Jurgen A.; Vermeulen, Wim (2012): ATP-dependent chromatin remodeling in the DNA-damage response. In *Epigenetics & chromatin* 5, p. 4. DOI: 10.1186/1756-8935-5-4.

LeBlanc, Sharonda J.; Gauer, Jacob W.; Hao, Pengyu; Case, Brandon C.; Hingorani, Manju M.; Weninger, Keith R.; Erie, Dorothy A. (2018): Coordinated protein and DNA conformational changes govern mismatch repair initiation by MutS. In *Nucleic acids research* 46 (20), pp. 10782–10795. DOI: 10.1093/nar/gky865.

Lecona, Emilio; Rodriguez-Acebes, Sara; Specks, Julia; Lopez-Contreras, Andres J.; Ruppen, Isabel; Murga, Matilde et al. (2016): USP7 is a SUMO deubiquitinase essential for DNA replication. In *Nature structural & molecular biology* 23 (4), pp. 270–277. DOI: 10.1038/nsmb.3185.

Lee, Yuan-Cho; Cai, Yuqin; Mu, Hong; Broyde, Suse; Amin, Shantu; Chen, Xuejing et al. (2014): The relationships between XPC binding to conformationally diverse DNA adducts and their excision by the human NER system. Is there a correlation? In *DNA repair* 19, pp. 55–63. DOI: 10.1016/j.dnarep.2014.03.026.

Li, Chia-Lung; Golebiowski, Filip M.; Onishi, Yuki; Samara, Nadine L.; Sugasawa, Kaoru; Yang, Wei (2015): Tripartite DNA Lesion Recognition and Verification by XPC, TFIIH, and XPA in Nucleotide Excision Repair. In *Molecular cell* 59 (6), pp. 1025–1034. DOI: 10.1016/j.molcel.2015.08.012.

Lieber, Michael R. (2010): The mechanism of double-strand DNA break repair by the nonhomologous DNA end-joining pathway. In *Annual review of biochemistry* 79, pp. 181–211. DOI: 10.1146/annurev.biochem.052308.093131.

Limsirichaikul, Siripan; Niimi, Atsuko; Fawcett, Heather; Lehmann, Alan; Yamashita, Shunichi; Ogi, Tomoo (2009): A rapid non-radioactive technique for measurement of repair synthesis in primary human fibroblasts by incorporation of ethynyl deoxyuridine (EdU). In *Nucleic acids research* 37 (4), e31. DOI: 10.1093/nar/gkp023.

Lindahl, T. (1993): Instability and decay of the primary structure of DNA. In *Nature* 362 (6422), pp. 709–715. DOI: 10.1038/362709a0.

Lindahl, T.; Barnes, D. E. (2000): Repair of endogenous DNA damage. In *Cold Spring Harbor symposia on quantitative biology* 65, pp. 127–133.

Lindahl, T.; Karlström, O. (1973): Heat-induced depyrimidination of deoxyribonucleic acid in neutral solution. In *Biochemistry* 12 (25), pp. 5151–5154.

Lindahl, T.; Nyberg, B. (1972): Rate of depurination of native deoxyribonucleic acid. In *Biochemistry* 11 (19), pp. 3610–3618.

Lipkin, S. M.; Wang, V.; Jacoby, R.; Banerjee-Basu, S.; Baxevanis, A. D.; Lynch, H. T. et al. (2000): MLH3. A DNA mismatch repair gene associated with mammalian microsatellite instability. In *Nature genetics* 24 (1), pp. 27–35. DOI: 10.1038/71643.

Luch, Andreas (2009): On the impact of the molecule structure in chemical carcinogenesis. In *EXS* 99, pp. 151–179.

Luijsterburg, Martijn S.; Goedhart, Joachim; Moser, Jill; Kool, Hanneke; Geverts, Bart; Houtsmuller, Adriaan B. et al. (2007): Dynamic in vivo interaction of DDB2 E3 ubiquitin ligase with UV-damaged DNA is independent of damage-recognition protein XPC. In *Journal of cell science* 120 (Pt 15), pp. 2706–2716. DOI: 10.1242/jcs.008367.

Lukin, Mark; Los Santos, Carlos de (2006): NMR structures of damaged DNA. In *Chemical reviews* 106 (2), pp. 607–686. DOI: 10.1021/cr0404646.

Ma, Yunmei; Pannicke, Ulrich; Schwarz, Klaus; Lieber, Michael R. (2002): Hairpin opening and overhang processing by an Artemis/DNA-dependent protein kinase complex in nonhomologous end joining and V(D)J recombination. In *Cell* 108 (6), pp. 781–794.

Mahaney, Brandi L.; Meek, Katheryn; Lees-Miller, Susan P. (2009): Repair of ionizing radiation-induced DNA double-strand breaks by non-homologous end-joining. In *The Biochemical journal* 417 (3), pp. 639–650. DOI: 10.1042/BJ20080413.

Maillard, Olivier; Camenisch, Ulrike; Clement, Flurina C.; Blagoev, Krastan B.; Naegeli, Hanspeter (2007): DNA repair triggered by sensors of helical dynamics. In *Trends in biochemical sciences* 32 (11), pp. 494–499. DOI: 10.1016/j.tibs.2007.08.008.

Maillard, Olivier; Solyom, Szilvia; Naegeli, Hanspeter (2007): An aromatic sensor with aversion to damaged strands confers versatility to DNA repair. In *PLoS biology* 5 (4), e79. DOI: 10.1371/journal.pbio.0050079.

Mao, Zhiyong; Bozzella, Michael; Seluanov, Andrei; Gorbunova, Vera (2008): Comparison of nonhomologous end joining and homologous recombination in human cells. In *DNA repair* 7 (10), pp. 1765–1771. DOI: 10.1016/j.dnarep.2008.06.018.

Marteijn, Jurgen A.; Lans, Hannes; Vermeulen, Wim; Hoeijmakers, Jan H. J. (2014): Understanding nucleotide excision repair and its roles in cancer and ageing. In *Nature reviews. Molecular cell biology* 15 (7), pp. 465–481. DOI: 10.1038/nrm3822.

Masutani, C.; Sugasawa, K.; Yanagisawa, J.; Sonoyama, T.; Ui, M.; Enomoto, T. et al. (1994): Purification and cloning of a nucleotide excision repair complex involving the xeroderma pigmentosum group C protein and a human homologue of yeast RAD23. In *The EMBO journal* 13 (8), pp. 1831–1843.

Mathieu, Nadine; Kaczmarek, Nina; Rüthemann, Peter; Luch, Andreas; Naegeli, Hanspeter (2013): DNA quality control by a lesion sensor pocket of the xeroderma pigmentosum group D helicase subunit of TFIIH. In *Current biology : CB* 23 (3), pp. 204–212. DOI: 10.1016/j.cub.2012.12.032.

McAteer, K.; Jing, Y.; Kao, J.; Taylor, J. S.; Kennedy, M. A. (1998): Solution-state structure of a DNA dodecamer duplex containing a Cis-syn thymine cyclobutane dimer, the major UV photoproduct of DNA. In *Journal of molecular biology* 282 (5), pp. 1013–1032. DOI: 10.1006/jmbi.1998.2062.

McCullough, John; Clague, Michael J.; Urbé, Sylvie (2004): AMSH is an endosome-associated ubiquitin isopeptidase. In *The Journal of cell biology* 166 (4), pp. 487–492. DOI: 10.1083/jcb.200401141.

Mehta, Anuja; Haber, James E. (2014): Sources of DNA double-strand breaks and models of recombinational DNA repair. In *Cold Spring Harbor perspectives in biology* 6 (9), a016428. DOI: 10.1101/cshperspect.a016428.

Merino, Edward J.; Boal, Amie K.; Barton, Jacqueline K. (2008): Biological contexts for DNA charge transport chemistry. In *Current opinion in chemical biology* 12 (2), pp. 229–237. DOI: 10.1016/j.cbpa.2008.01.046.

Messick, Troy E.; Greenberg, Roger A. (2009): The ubiquitin landscape at DNA double-strand breaks. In *The Journal of cell biology* 187 (3), pp. 319–326. DOI: 10.1083/jcb.200908074.

Miyahara, H.; Suzuki, H. (1987): Pre- and post-junctional effects of adenosine triphosphate on noradrenergic transmission in the rabbit ear artery. In *The Journal of physiology* 389, pp. 423–440.

Moolenaar, G. F.; Visse, R.; Ortiz-Buysse, M.; Goosen, N.; van de Putte, P. (1994): Helicase motifs V and VI of the Escherichia coli UvrB protein of the UvrABC endonuclease are essential for the formation of the preincision complex. In *Journal of molecular biology* 240 (4), pp. 294–307. DOI: 10.1006/jmbi.1994.1447.

Moser, Jill; Volker, Marcel; Kool, Hanneke; Alekseev, Sergei; Vrieling, Harry; Yasui, Akira et al. (2005): The UV-damaged DNA binding protein mediates efficient targeting of the nucleotide excision repair complex to UV-induced photo lesions. In *DNA repair* 4 (5), pp. 571–582. DOI: 10.1016/j.dnarep.2005.01.001.

Naegeli, Hanspeter (2013): Mechanisms of DNA Damage Recognition in Mammalian Cells. New York, NY: Springer (Molecular Biology Intelligence Unit Ser).

Nakagawa, A.; Kobayashi, N.; Muramatsu, T.; Yamashina, Y.; Shirai, T.; Hashimoto, M. W. et al. (1998): Three-dimensional visualization of ultraviolet-induced DNA damage and its repair in human cell nuclei. In *The Journal of investigative dermatology* 110 (2), pp. 143–148. DOI: 10.1046/j.1523-1747.1998.00100.x.

Nishi, Ryotaro; Alekseev, Sergey; Dinant, Christoffel; Hoogstraten, Deborah; Houtsmuller, Adriaan B.; Hoeijmakers, Jan H. J. et al. (2009): UV-DDB-dependent regulation of nucleotide excision repair kinetics in living cells. In *DNA repair* 8 (6), pp. 767–776. DOI: 10.1016/j.dnarep.2009.02.004.

Oh, E. Y.; Grossman, L. (1989): Characterization of the helicase activity of the Escherichia coli UvrAB protein complex. In *The Journal of biological chemistry* 264 (2), pp. 1336–1343.

Okuda, Masahiko; Kinoshita, Minoru; Kakumu, Erina; Sugasawa, Kaoru; Nishimura, Yoshifumi (2015): Structural Insight into the Mechanism of TFIIH Recognition by the Acidic String of the Nucleotide Excision Repair Factor XPC. In *Structure (London, England : 1993)* 23 (10), pp. 1827–1837. DOI: 10.1016/j.str.2015.07.009.

Okuda, Masahiko; Nakazawa, Yuka; Guo, Chaowan; Ogi, Tomoo; Nishimura, Yoshifumi (2017): Common TFIIH recruitment mechanism in global genome and transcription-coupled repair subpathways. In *Nucleic acids research* 45 (22), pp. 13043–13055. DOI: 10.1093/nar/gkx970.

O'Neil, Lauren L.; Grossfield, Alan; Wiest, Olaf (2007): Base flipping of the thymine dimer in duplex DNA. In *The journal of physical chemistry. B* 111 (40), pp. 11843–11849. DOI: 10.1021/jp074043e.

Pagès, Vincent; Fuchs, Robert P. P. (2002): How DNA lesions are turned into mutations within cells? In *Oncogene* 21 (58), pp. 8957–8966. DOI: 10.1038/sj.onc.1206006.

Papadopoulou, Thaleia; Richly, Holger (2016): On-site remodeling at chromatin. How multiprotein complexes are rebuilt during DNA repair and transcriptional activation. In *BioEssays : news and reviews in molecular, cellular and developmental biology* 38 (11), pp. 1130–1140. DOI: 10.1002/bies.201600094.

Parikh, S. S.; Walcher, G.; Jones, G. D.; Slupphaug, G.; Krokan, H. E.; Blackburn, G. M.; Tainer, J. A. (2000): Uracil-DNA glycosylase-DNA substrate and product structures. Conformational strain promotes catalytic efficiency by coupled stereoelectronic effects. In *Proceedings of the National Academy of Sciences of the United States of America* 97 (10), pp. 5083–5088.

Pattison, David I.; Davies, Michael J. (2006): Actions of ultraviolet light on cellular structures. In *EXS* (96), pp. 131–157.

Peña-Diaz, Javier; Jiricny, Josef (2012): Mammalian mismatch repair. Error-free or error-prone? In *Trends in biochemical sciences* 37 (5), pp. 206–214. DOI: 10.1016/j.tibs.2012.03.001.

Pfeifer, Gerd P.; You, Young-Hyun; Besaratinia, Ahmad (2005): Mutations induced by ultraviolet light. In *Mutation research* 571 (1-2), pp. 19–31. DOI: 10.1016/j.mrfmmm.2004.06.057.

Pines, Alex; Vrouwe, Mischa G.; Marteijn, Jurgen A.; Typas, Dimitris; Luijsterburg, Martijn S.; Cansoy, Medine et al. (2012): PARP1 promotes nucleotide excision repair through DDB2 stabilization and recruitment of ALC1. In *The Journal of cell biology* 199 (2), pp. 235–249. DOI: 10.1083/jcb.201112132.

Polo, Sophie E. (2015): Reshaping chromatin after DNA damage. The choreography of histone proteins. In *Journal of molecular biology* 427 (3), pp. 626–636. DOI: 10.1016/j.jmb.2014.05.025.

Pommier, Yves; Barcelo, Juana M.; Rao, V. Ashutosh; Sordet, Olivier; Jobson, Andrew G.; Thibaut, Laurent et al. (2006): Repair of topoisomerase I-mediated DNA damage. In *Progress in nucleic acid research and molecular biology* 81, pp. 179–229. DOI: 10.1016/S0079-6603(06)81005-6.

Poulsen, Sara L.; Hansen, Rebecca K.; Wagner, Sebastian A.; van Cuijk, Loes; van Belle, Gijsbert J.; Streicher, Werner et al. (2013): RNF111/Arkadia is a SUMO-targeted ubiquitin ligase that facilitates the DNA damage response. In *The Journal of cell biology* 201 (6), pp. 797–807. DOI: 10.1083/jcb.201212075.

Pugh, Robert A.; Wu, Colin G.; Spies, Maria (2012): Regulation of translocation polarity by helicase domain 1 in SF2B helicases. In *The EMBO journal* 31 (2), pp. 503–514. DOI: 10.1038/emboj.2011.412.

Qian, J.; Pentz, K.; Zhu, Q.; Wang, Q.; He, J.; Srivastava, A. K.; Wani, A. A. (2015): USP7 modulates UV-induced PCNA monoubiquitination by regulating DNA polymerase eta stability. In *Oncogene* 34 (36), pp. 4791–4796. DOI: 10.1038/onc.2014.394.

Qiu, Ruoyi; Sakato, Miho; Sacho, Elizabeth J.; Wilkins, Hunter; Zhang, Xingdong; Modrich, Paul et al. (2015): MutL traps MutS at a DNA mismatch. In *Proceedings of the National Academy of Sciences of the United States of America* 112 (35), pp. 10914–10919. DOI: 10.1073/pnas.1505655112.

Ramanathan, B.; Smerdon, M. J. (1989): Enhanced DNA repair synthesis in hyperacetylated nucleosomes. In *The Journal of biological chemistry* 264 (19), pp. 11026–11034.

Rapić-Otrin, Vesna; Navazza, Valentina; Nardo, Tiziana; Botta, Elena; McLenigan, Mary; Bisi, Dawn C. et al. (2003): True XP group E patients have a defective UV-damaged DNA binding protein complex and mutations in DDB2 which reveal the functional domains of its p48 product. In *Human molecular genetics* 12 (13), pp. 1507–1522.

Rastogi, Rajesh P.; Richa; Kumar, Ashok; Tyagi, Madhu B.; Sinha, Rajeshwar P. (2010): Molecular mechanisms of ultraviolet radiation-induced DNA damage and repair. In *Journal of nucleic acids* 2010, p. 592980. DOI: 10.4061/2010/592980.

Reardon, Joyce T.; Sancar, Aziz (2003): Recognition and repair of the cyclobutane thymine dimer, a major cause of skin cancers, by the human excision nuclease. In *Genes & development* 17 (20), pp. 2539–2551. DOI: 10.1101/gad.1131003.

Reardon, Joyce T.; Sancar, Aziz (2006): Repair of DNA-polypeptide crosslinks by human excision nuclease. In *Proceedings of the National Academy of Sciences of the United States of America* 103 (11), pp. 4056–4061. DOI: 10.1073/pnas.0600538103.

Reinhardt, H. Christian; Schumacher, Björn (2012): The p53 network. Cellular and systemic DNA damage responses in aging and cancer. In *Trends in genetics : TIG* 28 (3), pp. 128–136. DOI: 10.1016/j.tig.2011.12.002.

Richly, Holger; Rocha-Viegas, Luciana; Ribeiro, Joana Domingues; Demajo, Santiago; Gundem, Gunes; Lopez-Bigas, Nuria et al. (2010): Transcriptional activation of polycomb-repressed genes by ZRF1. In *Nature* 468 (7327), pp. 1124–1128. DOI: 10.1038/nature09574.

Riedl, Thilo; Hanaoka, Fumio; Egly, Jean-Marc (2003): The comings and goings of nucleotide excision repair factors on damaged DNA. In *The EMBO journal* 22 (19), pp. 5293–5303. DOI: 10.1093/emboj/cdg489.

Robu, Mihaela; Shah, Rashmi G.; Purohit, Nupur K.; Zhou, Pengbo; Naegeli, Hanspeter; Shah, Girish M. (2017): Poly(ADP-ribose) polymerase 1 escorts XPC to UV-induced DNA lesions during nucleotide excision repair. In *Proceedings of the National Academy of Sciences of the United States of America* 114 (33), E6847-E6856. DOI: 10.1073/pnas.1706981114.

Rudolf, Jana; Makrantoni, Vasso; Ingledew, W. John; Stark, Michael J. R.; White, Malcolm F. (2006): The DNA repair helicases XPD and FancJ have essential iron-sulfur domains. In *Molecular cell* 23 (6), pp. 801–808. DOI: 10.1016/j.molcel.2006.07.019.

Rüthemann, Peter; Balbo Pogliano, Chiara; Codilupi, Tamara; Garajovà, Zuzana; Naegeli, Hanspeter (2017): Chromatin remodeler CHD1 promotes XPC-to-TFIIH handover of nucleosomal UV lesions in nucleotide excision repair. In *The EMBO journal* 36 (22), pp. 3372–3386. DOI: 10.15252/embj.201695742.

Schärer, Orlando D. (2013): Nucleotide excision repair in eukaryotes. In *Cold Spring Harbor perspectives in biology* 5 (10), a012609. DOI: 10.1101/cshperspect.a012609.

Schuch, André Passaglia; Moreno, Natália Cestari; Schuch, Natielen Jacques; Menck, Carlos Frederico Martins; Garcia, Camila Carrião Machado (2017): Sunlight damage to cellular DNA. Focus on oxidatively generated lesions. In *Free radical biology & medicine* 107, pp. 110–124. DOI: 10.1016/j.freeradbiomed.2017.01.029.

Schwertman, Petra; Lagarou, Anna; Dekkers, Dick H. W.; Raams, Anja; van der Hoek, Adriana C.; Laffeber, Charlie et al. (2012): UV-sensitive syndrome protein UVSSA recruits USP7 to regulate transcription-coupled repair. In *Nature genetics* 44 (5), pp. 598–602. DOI: 10.1038/ng.2230.

Schwertman, Petra; Vermeulen, Wim; Marteijn, Jurgen A. (2013): UVSSA and USP7, a new couple in transcription-coupled DNA repair. In *Chromosoma* 122 (4), pp. 275–284. DOI: 10.1007/s00412-013-0420-2.

Sharma, Soniya; Salehi, Fateme; Scheithauer, Bernd W.; Rotondo, Fabio; Syro, Luis V.; Kovacs, Kalman (2009): Role of MGMT in tumor development, progression, diagnosis, treatment and prognosis. In *Anticancer research* 29 (10), pp. 3759–3768.

Shiloh, Yosef; Ziv, Yael (2013): The ATM protein kinase. Regulating the cellular response to genotoxic stress, and more. In *Nature reviews. Molecular cell biology* 14 (4), pp. 197–210. DOI: 10.1038/nrm3546.

Shiyanov, P.; Nag, A.; Raychaudhuri, P. (1999): Cullin 4A associates with the UV-damaged DNA-binding protein DDB. In *The Journal of biological chemistry* 274 (50), pp. 35309–35312.

Sijbers, A. M.; Laat, W. L. de; Ariza, R. R.; Biggerstaff, M.; Wei, Y. F.; Moggs, J. G. et al. (1996): Xeroderma pigmentosum group F caused by a defect in a structure-specific DNA repair endonuclease. In *Cell* 86 (5), pp. 811–822.

Sims, Joshua J.; Scavone, Francesco; Cooper, Eric M.; Kane, Lesley A.; Youle, Richard J.; Boeke, Jef D.; Cohen, Robert E. (2012): Polyubiquitin-sensor proteins reveal localization and linkage-type dependence of cellular ubiquitin signaling. In *Nature methods* 9 (3), pp. 303–309. DOI: 10.1038/nmeth.1888.

Skorvaga, Milan; Theis, Karsten; Mandavilli, Bhaskar S.; Kisker, Caroline; van Houten, Bennett (2002): The beta -hairpin motif of UvrB is essential for DNA binding, damage processing, and UvrC-mediated incisions. In *The Journal of biological chemistry* 277 (2), pp. 1553–1559. DOI: 10.1074/jbc.M108847200.

Soria, Gaston; Polo, Sophie E.; Almouzni, Geneviève (2012): Prime, repair, restore. The active role of chromatin in the DNA damage response. In *Molecular cell* 46 (6), pp. 722–734. DOI: 10.1016/j.molcel.2012.06.002.

Stadler, Jens; Richly, Holger (2017): Regulation of DNA Repair Mechanisms. How the Chromatin Environment Regulates the DNA Damage Response. In *International journal of molecular sciences* 18 (8). DOI: 10.3390/ijms18081715.

Staresincic, Lidija; Fagbemi, Adebanke F.; Enzlin, Jacqueline H.; Gourdin, Audrey M.; Wijgers, Nils; Dunand-Sauthier, Isabelle et al. (2009): Coordination of dual incision and repair synthesis in human nucleotide excision repair. In *The EMBO journal* 28 (8), pp. 1111–1120. DOI: 10.1038/emboj.2009.49.

Stivers, James T. (2004): Site-specific DNA damage recognition by enzyme-induced base flipping. In *Progress in nucleic acid research and molecular biology* 77, pp. 37–65. DOI: 10.1016/S0079-6603(04)77002-6.

Stracker, Travis H.; Theunissen, Jan-Willem F.; Morales, Monica; Petrini, John H. J. (2004): The Mre11 complex and the metabolism of chromosome breaks. The importance of communicating and holding things together. In *DNA repair* 3 (8-9), pp. 845–854. DOI: 10.1016/j.dnarep.2004.03.014.

Sugasawa, K.; Ng, J. M.; Masutani, C.; Iwai, S.; van der Spek, P. J.; Eker, A. P. et al. (1998): Xeroderma pigmentosum group C protein complex is the initiator of global genome nucleotide excision repair. In *Molecular cell* 2 (2), pp. 223–232.

Sugasawa, K.; Okamoto, T.; Shimizu, Y.; Masutani, C.; Iwai, S.; Hanaoka, F. (2001): A multistep damage recognition mechanism for global genomic nucleotide excision repair. In *Genes & development* 15 (5), pp. 507–521. DOI: 10.1101/gad.866301.

Sugasawa, Kaoru; Okuda, Yuki; Saijo, Masafumi; Nishi, Ryotaro; Matsuda, Noriyuki; Chu, Gilbert et al. (2005): UV-induced ubiquitylation of XPC protein mediated by UV-DDB-ubiquitin ligase complex. In *Cell* 121 (3), pp. 387–400. DOI: 10.1016/j.cell.2005.02.035.

Sugitani, Norie; Sivley, Robert M.; Perry, Kelly E.; Capra, John A.; Chazin, Walter J. (2016): XPA. A key scaffold for human nucleotide excision repair. In *DNA repair* 44, pp. 123–135. DOI: 10.1016/j.dnarep.2016.05.018.

Sun, Nian Kang; Kamarajan, Pachiyappan; Huang, Haimei; Chao, Chuck C-K (2002): Restoration of UV sensitivity in UV-resistant HeLa cells by antisense-mediated depletion of damaged DNA-binding protein 2 (DDB2). In *FEBS letters* 512 (1-3), pp. 168–172.

Sung, Patrick; Klein, Hannah (2006): Mechanism of homologous recombination. Mediators and helicases take on regulatory functions. In *Nature reviews. Molecular cell biology* 7 (10), pp. 739–750.

Tang, J. Y.; Hwang, B. J.; Ford, J. M.; Hanawalt, P. C.; Chu, G. (2000): Xeroderma pigmentosum p48 gene enhances global genomic repair and suppresses UV-induced mutagenesis. In *Molecular cell* 5 (4), pp. 737–744.

Thayer, M. M.; Ahern, H.; Xing, D.; Cunningham, R. P.; Tainer, J. A. (1995): Novel DNA binding motifs in the DNA repair enzyme endonuclease III crystal structure. In *The EMBO journal* 14 (16), pp. 4108–4120.

Theis, K.; Skorvaga, M.; Machius, M.; Nakagawa, N.; van Houten, B.; Kisker, C. (2000): The nucleotide excision repair protein UvrB, a helicase-like enzyme with a catch. In *Mutation research* 460 (3-4), pp. 277–300.

Tripsianes, Konstantinos; Folkers, Gert; Ab, Eiso; Das, Devashish; Odijk, Hanny; Jaspers, Nicolaas G. J. et al. (2005): The structure of the human ERCC1/XPF interaction domains reveals a complementary role for the two proteins in nucleotide excision repair. In *Structure (London, England : 1993)* 13 (12), pp. 1849–1858. DOI: 10.1016/j.str.2005.08.014.

Truglio, James J.; Karakas, Erkan; Rhau, Benjamin; Wang, Hong; DellaVecchia, Matthew J.; van Houten, Bennett; Kisker, Caroline (2006): Structural basis for DNA recognition and processing by UvrB. In *Nature structural & molecular biology* 13 (4), pp. 360–364. DOI: 10.1038/nsmb1072.

Tsodikov, Oleg V.; Enzlin, Jacquelin H.; Schärer, Orlando D.; Ellenberger, Tom (2005): Crystal structure and DNA binding functions of ERCC1, a subunit of the DNA structure-specific endonuclease XPF-ERCC1. In *Proceedings of the National Academy of Sciences of the United States of America* 102 (32), pp. 11236–11241. DOI: 10.1073/pnas.0504341102.

van Cuijk, Loes; van Belle, Gijsbert J.; Turkyilmaz, Yasemin; Poulsen, Sara L.; Janssens, Roel C.; Theil, Arjan F. et al. (2015): SUMO and ubiquitin-dependent XPC exchange drives nucleotide excision repair. In *Nature communications* 6, p. 7499. DOI: 10.1038/ncomms8499.

Volker, M.; Moné, M. J.; Karmakar, P.; van Hoffen, A.; Schul, W.; Vermeulen, W. et al. (2001): Sequential assembly of the nucleotide excision repair factors in vivo. In *Molecular cell* 8 (1), pp. 213–224.

Wakasugi, Mitsuo; Kawashima, Aki; Morioka, Hiroshi; Linn, Stuart; Sancar, Aziz; Mori, Toshio et al. (2002): DDB accumulates at DNA damage sites immediately after UV irradiation and directly stimulates nucleotide excision repair. In *The Journal of biological chemistry* 277 (3), pp. 1637–1640. DOI: 10.1074/jbc.C100610200.

Wang, Hengbin; Zhai, Ling; Xu, Jun; Joo, Heui-Yun; Jackson, Sarah; Erdjument-Bromage, Hediye et al. (2006): Histone H3 and H4 ubiquitylation by the CUL4-DDB-ROC1 ubiquitin ligase facilitates cellular response to DNA damage. In *Molecular cell* 22 (3), pp. 383–394. DOI: 10.1016/j.molcel.2006.03.035.

Wolski, Stefanie C.; Kuper, Jochen; Hänzelmann, Petra; Truglio, James J.; Croteau, Deborah L.; van Houten, Bennett; Kisker, Caroline (2008): Crystal structure of the FeS cluster-containing nucleotide excision repair helicase XPD. In *PLoS biology* 6 (6), e149. DOI: 10.1371/journal.pbio.0060149.

Wong, Isaac; Lundquist, Amy J.; Bernards, Andrew S.; Mosbaugh, Dale W. (2002): Presteady-state analysis of a single catalytic turnover by Escherichia coli uracil-DNA glycosylase reveals a "pinch-pull-push" mechanism. In *The Journal of biological chemistry* 277 (22), pp. 19424–19432. DOI: 10.1074/jbc.M201198200.

Xu, Yang; Her, Chengtao (2015): Inhibition of Topoisomerase (DNA) I (TOP1). DNA Damage Repair and Anticancer Therapy. In *Biomolecules* 5 (3), pp. 1652–1670. DOI: 10.3390/biom5031652.

Xu, Ming; Skaug, Brian; Zeng, Wenwen; Chen, Zhijian J. (2009): A ubiquitin replacement strategy in human cells reveals distinct mechanisms of IKK activation by TNFalpha and IL-1beta. In *Molecular cell* 36 (2), pp. 302–314. DOI: 10.1016/j.molcel.2009.10.002.

Yang, Wei (2008): Structure and mechanism for DNA lesion recognition. In *Cell research* 18 (1), pp. 184–197. DOI: 10.1038/cr.2007.116.

Yeo, Jung-Eun; Khoo, Andy; Fagbemi, Adebanke F.; Schärer, Orlando D. (2012): The efficiencies of damage recognition and excision correlate with duplex destabilization induced by acetylaminofluorene adducts in human nucleotide excision repair. In *Chemical research in toxicology* 25 (11), pp. 2462–2468. DOI: 10.1021/tx3003033.

Yu, Hongtao (2002): Environmental carcinogenic polycyclic aromatic hydrocarbons. Photochemistry and phototoxicity. In *Journal of environmental science and health. Part C, Environmental carcinogenesis & ecotoxicology reviews* 20 (2), pp. 149–183. DOI: 10.1081/GNC-120016203.

Zeman, Michelle K.; Cimprich, Karlene A. (2014): Causes and consequences of replication stress. In *Nature cell biology* 16 (1), pp. 2–9. DOI: 10.1038/ncb2897.

Zharkov, Dmitry O.; Mechetin, Grigory V.; Nevinsky, Georgy A. (2010): Uracil-DNA glycosylase. Structural, thermodynamic and kinetic aspects of lesion search and recognition. In *Mutation research* 685 (1-2), pp. 11–20. DOI: 10.1016/j.mrfmmm.2009.10.017.

Zlatanou, A.; Sabbioneda, S.; Miller, E. S.; Greenwalt, A.; Aggathanggelou, A.; Maurice, M. M. et al. (2016): USP7 is essential for maintaining Rad18 stability and DNA damage tolerance. In *Oncogene* 35 (8), pp. 965–976. DOI: 10.1038/onc.2015.149.

Zlatanou, Anastasia; Stewart, Grant S. (2016): Damaged replication forks tolerate USP7 to maintain genome stability. In *Molecular & cellular oncology* 3 (1), e1063571. DOI: 10.1080/23723556.2015.1063571.

Zwang, Theodore J.; Tse, Edmund C. M.; Barton, Jacqueline K. (2018): Sensing DNA through DNA Charge Transport. In *ACS chemical biology* 13 (7), pp. 1799–1809. DOI: 10.1021/acschembio.8b00347.

APPENDIX

Stadler J, Richly H. **Regulation of DNA Repair Mechanisms: How the Chromatin Environment Regulates the DNA Damage Response.**
Int J Mol Sci. 2017 Aug 5;18(8).
pii: E1715. doi: 10.3390/ijms18081715. Review. PubMed PMID: 28783053

Regulation of DNA Repair Mechanisms: How the Chromatin Environment Regulates the DNA Damage Response.

International Journal of
Molecular Sciences

MDPI

Review

Regulation of DNA Repair Mechanisms: How the Chromatin Environment Regulates the DNA Damage Response

Jens Stadler [1,2] and Holger Richly [1,*]

[1] Laboratory of Molecular Epigenetics, Institute of Molecular Biology (IMB), Ackermannweg 4, 55128 Mainz, Germany; j.stadler@imb-mainz.de
[2] Faculty of Biology, Johannes Gutenberg University, 55099 Mainz, Germany
* Correspondence: h.richly@imb-mainz.de; Tel.: +49-(0)-6131-3921440

Received: 14 June 2017; Accepted: 2 August 2017; Published: 5 August 2017

Abstract: Cellular DNA is constantly challenged by damage-inducing factors derived from exogenous or endogenous sources. In order to maintain genome stability and integrity, cells have evolved a wide variety of DNA repair pathways which counteract different types of DNA lesions, also referred to as the DNA damage response (DDR). However, DNA in eukaryotes is highly organized and compacted into chromatin representing major constraints for all cellular pathways, including DNA repair pathways, which require DNA as their substrate. Therefore, the chromatin configuration surrounding the lesion site undergoes dramatic remodeling to facilitate access of DNA repair factors and subsequent removal of the DNA lesion. In this review, we focus on the question of how the cellular DNA repair pathways overcome the chromatin barrier, how the chromatin environment is rearranged to facilitate efficient DNA repair, which proteins mediate this re-organization process and, consequently, how the altered chromatin landscape is involved in the regulation of DNA damage responses.

Keywords: DNA repair; chromatin; histone marks; ubiquitin; nucleotide excision repair (NER); DSB repair

1. Introduction

Genome integrity is permanently challenged by both exogenous and endogenous factors. In eukaryotes, damaged DNA is recognized and repaired by a variety of complex cellular pathways, which are referred to as the DNA damage response (DDR) [1,2]. The DNA damage response is characterized by the well-timed recruitment and removal of specific DNA repair factors and ancillary proteins, which mediate the recognition, verification, and repair of the lesion. However, DNA repair in eukaryotes occurs not simply on "naked" DNA. Eukaryotic genomes are organized and compacted into chromatin established by the essential building block, the nucleosome, which is generated from an octamer of the four core histones (H2A, H2B, H3, H4) around which the DNA is wrapped. Additionally, the mammalian genome is organized in specific chromatin structures that are characterized by signatures of histone and DNA modifications, specific histone variants, chromatin-associated factors, and nucleosome occupancy [3]. Thus, all cellular pathways, including the DNA damage response, which rely on DNA as their substrate, have to respond to and overcome this major constraint limiting the access of DNA repair factors, which is crucial for efficient recognition and removal of DNA lesions [4,5]. The importance of chromatin rearrangements and chromatin dynamics during the process of DNA repair was first indicated by nuclease digestion assays of damaged DNA in UV-C-irradiated fibroblasts in which replication was blocked by hydroxyurea treatment. Chromatin regions with active nucleotide excision repair (NER) were more prone to be digested by micrococcal

nuclease treatment indicating that these regions have been rearranged to a more relaxed state and are, thus, more sensitive to nuclease treatment compared to compacted chromatin [6,7].

Another breakthrough regarding the question of how cells recognize and counteract DNA lesions in the context of chromatin, and how the chromatin landscape is altered to facilitate efficient DNA repair, emerged when human fibroblasts were pulse-labelled with (3H) deoxy-thymidine directly after UV irradiation and transferred into nonradioactive medium for recovery for different time points [7]. Interestingly, it was observed that the sensitivity of the incorporated nucleotides towards nuclease digestion decreased progressively depending on the time of recovery after UV irradiation and pulse-labelling and that, after a certain time of recovery, the original level of nuclease resistance was restored in the repaired DNA regions [7]. These findings built the first principles of the so-called "access-repair-restore" (ARR) model which highlights the frame conditions for the dynamic chromatin environment during DNA repair processes [5]. This model summarizes the transient de-condensation of chromatin structures to facilitate recognition and repair of DNA lesions. After the DNA lesion is removed, chromatin is reorganized and compacted to its original state. However, recent data also points out that new histones can be deposited during the restore section illustrating that the epigenetic memory allows some degree of plasticity [8]. Chromatin relaxation, as well as its re-condensation after removal of the DNA lesion, is a highly-regulated, ATP-consuming process, which requires the action of so-called chromatin remodeling complexes. Chromatin remodelers can be classified into four subfamilies depending on their domain organization: the imitation switch (ISWI), the chromodomain DNA helicase-binding (CHD), the switch/sucrose non-fermentable (SWI/SNF), and the INO80 subfamily. Furthermore, the four subfamilies can also be separated on a functional level since the different subfamilies preferentially catalyze specific functions. The SWI/SNF family of remodelers primarily conducts functions related to chromatin accessibility, which includes unwrapping of DNA coiled around nucleosomes, nucleosome re-positioning by the sliding of nucleosomes along the DNA, and partial (e.g., H2A-H2B dimer) or complete nucleosome eviction. In particular, access remodelers of the SWI/SNF subfamily can gain access to binding sites for transcription factors at promoter regions and can restore accessibility for DNA repair factors [9].

The core histones consist of a globular domain and unstructured N-terminal tails which both can be modified by histone-modifying enzymes. Such covalent modifications comprise of acetylation, methylation, phosphorylation, PARylation, and ubiquitylation [10]. To better understand the underlying principles of these chromatin alterations and the involvement of non-coding RNAs in DNA repair, research in the last decade has focused on the contribution of the chromatin environment during genome surveillance. In this review we will cover the role of histone phosphorylation, ubiquitylation, and PARylation of DNA repair factors since these modifications are intimately linked to DNA damage signaling pathways and also play crucial roles for granting access to DNA lesions via remodeling of the chromatin conformation. Furthermore, we will elucidate on novel functions of small non-coding RNAs in the DDR focusing on the events of chromatin that facilitate double-strand break (DSB) repair and nucleotide excision repair (NER).

2. Repairing Damaged DNA: NER and DSB Repair

Chromatin reorganization and de-condensation plays a crucial role within all cellular processes which use DNA as their substrate, including transcription, replication, and DNA repair pathways. For instance, one of the several DNA repair pathways relying on conformational changes of chromatin is base excision repair (BER). BER is specifically important in the removal of damaged and altered DNA bases induced by spontaneous hydrolysis of cytosine to uracil, for example, deaminating and alkylating agents or reactive oxygen species released from the cellular respiratory chain. In this review, however, we will focus on the DNA damage response and, further, on double-strand break (DSB) repair and nucleotide excision repair (NER), the DNA repair pathways which handle and remove the most toxic DNA lesions.

Nucleotide excision repair (NER) is an essential DNA repair pathway that counteracts bulky and helix-distorting DNA lesions. The main types of lesions repaired by NER are 6-4 photoproducts and cyclobutane pyrimidine dimers (CPDs), which are caused by exposure to UV light or several chemical agents [11]. NER operates in two sub-pathways, which differ in the nature of lesion recognition. Transcription coupled-NER (TC-NER) operates in transcriptionally-active genes, where stalled Polymerase II elicits the DNA damage response [12]. The global genomic NER branch (GG-NER) deals with lesions in any chromatin environment. In contrast to the TC-NER sub-pathway, in GG-NER DNA lesions are directly recognized by the two damage recognition factors, DDB2 and XPC [13]. After lesion recognition, both sub-pathways converge and lesion verification, unwinding of the DNA, excision of the lesion-containing strand, and refilling of the DNA gap are carried out by the same core machinery. Verification of the DNA lesion is carried out by the repair factor XPA and via the generation of the pre-excision complex, which consists of the TFIIH transcription factor complex with its helicase subunits XPB and XPD. Subsequently, the DNA lesion is excised by the endonucleases XPF and XPG, and the gap is filled by DNA polymerases [12,13]. As detailed below, damage recognition is accompanied by changes in the chromatin conformation and by chromatin signaling pathways that build on phosphorylation, ubiquitylation, and PARylation events. Such chromatin-associated pathways halt the cell cycle and facilitate the DNA damage response (DDR).

Among the most detrimental DNA damages are double-strand breaks (DSBs), which may cause severe genome rearrangements. DSBs are repaired by either error-free homologous recombination (HR) or the error-prone non-homologous end joining (NHEJ) [2,14]. NHEJ involves minimal processing of the damaged DNA and re-ligation of the processed ends. Damage recognition in NHEJ requires the Ku70/80 DNA-binding complex, which binds the broken DNA end and recruits other proteins to facilitate the processing and ligation of the broken ends. Amongst the proteins recruited by Ku to the damage site is DNA-PK, a serine/threonine protein kinase, which induces conformational changes within the damage recognition complex that allows end-processing enzymes to operate on the ends of the double-strand break [15]. DNA-PK also acts in concert with the protein kinase ataxia-telangiectasia, mutated (ATM), and ATM and Rad3-related protein (ATR) to phosphorylate factors that are essential in the DNA damage checkpoint. Further, Ku directly interacts with XRCC4, which recruits specific DNA end processing enzymes to the damage site to generate DNA ends compatible for ligation. Lastly, Ku and XRCC4 associate with the DNA ligase IV complex and localize it to the processed DNA ends for re-ligation [16–18]. HR depends on a resection process that involves the generation of single-stranded DNA (ssDNA) intermediates. The ssDNA tails are recognized by RPA, which is then replaced by Rad51. The Rad51-containing nucleoprotein filament searches for, and invades a homologous sequence from the sister chromatid generating a D-loop. After strand invasion DNA polymerase extends the end of the invading strand leading to the formation of holiday junctions. After resolving the intermediates the remaining ssDNA gaps and nicks are repaired by DNA polymerase and DNA ligase. More detailed information on HR repair mechanisms are available in several excellent reviews [19,20]. Sister chromatids and, hence, HR exist only in the S and G2 phases of the cell cycle. In contrast, NHEJ predominates in the G1 phase of the cell cycle. However, how cells choose between HR and NHEJ repair pathways is still elusive [21]. Analogously to NER, chromatin signaling and the regulation of both DSB repair sub-pathways are dependent on phosphorylation, ubiquitylation, and PARylation of factors.

3. Phosphorylation Cascades Regulate the DDR

One essential means of signaling during the DNA damage response are phosphorylation events. The damage response at double strand breaks (DSBs) commences with the activation of two specific kinases, the ataxia telangiectasia mutated (ATM) kinase and the ATM and rad3-related (ATR) kinase, which stimulate DNA repair and mediate either apoptosis or checkpoint activation through p53-mediated mechanisms [22]. The main regulator of ATM activation is the MRE11-RAD50-NBS1 (MRN) complex. The MRN complex is one of the first factors which recognize the DSB and plays

an essential role in processing of DSBs before repair by either HR or NHEJ is carried out [23]. Notably, PARP1-mediated PARylation events play an important role in the early recruitment of the MRN complex to DSBs highlighting the concerted action, as well as the crosstalk between different post-translational modification processes which mediate chromatin re-organization events [24]. Activation of ATM by the MRN complex causes the phosphorylation of a plethora of factors comprising proteins involved in checkpoint activation such as the checkpoint kinase 2 (CHK2), p53 and DNA-repair proteins, like the breast cancer type 1 susceptibility protein (BRCA1) and the p53 binding protein 1 (53BP1) [1,2]. An important target for the ATM kinase is the histone variant H2A.X (H2AX) (Figure 1A). Phosphorylated H2AX (γH2AX), which occurs early during the DNA damage response, generates a binding platform for the mediator of the DNA damage checkpoint protein 1 (MDC1) [25]. MDC1 is constitutively phosphorylated within its SDT domain by the casein kinase 2 (CK2). This phosphorylation, in turn, creates a binding site for other repair proteins, including the MRN-ATM complex, which brings about the bidirectional spreading of γH2AX for hundreds of kilo-bases along the chromatin fiber emanating from the DSB [26,27]. MDC1 also recruits the ubiquitin E3 ligases RNF8 and RNF168 (Figure 1A), which ubiquitylates histone H2A and the linker histone H1 and facilitates loading of effectors, such as 53BP1 and BRCA1 [28,29]. In contrast to ATM, ATR is activated by a broad spectrum of genomic insults and replication problems [30]. Common to these insults is the generation of single-stranded DNA (ssDNA), which results in the loading of the single-stranded DNA binding protein replication protein A (RPA) [31]. RPA acts as a recruitment platform for ATR via its binding partner ATRIP [32]. ATM and ATR have a plethora of common substrates regulating different cellular functions. Whereas both enzymes for example phosphorylate H2AX, other substrates are predominantly phosphorylated by one specific kinase [22].

It is still largely unresolved how ATR and ATM elicit the damage response upon UV light-induced DNA damage. However, it seems that damage signaling upon UV exposure is dependent on both ATR and ATM. Importantly, H2AX phosphorylation as a major DNA damage marker is predominantly catalyzed by the ATR kinase and occurs in the G1 and S phases of the cell cycle [33–35]. However, ATM was also shown to be activated in response to UV-induced DNA damage resulting in phosphorylation of H2AX [36]. Hence, both ATR and ATM are rapidly recruited to DNA lesions following UV-irradiation. Recruitment of both kinases is dependent on the damage recognition factors XPC, DDB2, and XPA only during the G1 phase [37,38]. In contrast, in the S phase, when the UV lesions mainly generate stalled replication forks with long single-stranded DNA, ATR and ATM recruitment to damage loci and subsequent H2AX phosphorylation are likely mediated by different factors. Therefore, UV-induced recruitment of ATR and ATM differ in S and G1 phases owing to the existence of different types of DNA lesions, which facilitate the assembly of different DNA repair factors involved in the process of repair and checkpoint activation.

Taken together, the DNA damage response relies on protein kinase cascades which mediate phosphorylation of DNA repair factors and histones. Phosphorylated substrates operate as binding platforms for effector proteins and regulate the assembly of protein complexes at chromatin. Further, phosphorylation of H2AX is linked to H2A-ubiquitylation and, hence, will likely have an impact on the chromatin conformation. It remains to be seen whether phosphorylation events also crosstalk to other chromatin modifications during the DDR.

4. Driving the DDR by Ubiquitylation

Ubiquitin is a small, conserved, regulatory protein that is expressed in almost all tissues of eukaryotic organisms. Ubiquitylation, the attachment of ubiquitin molecules to a substrate protein, can affect the fate and the function of the substrate in various ways. Ubiquitylation of a target protein can trigger its proteasomal degradation; it may alter its cellular localization, affect the enzymatic activity, and facilitate or prevent protein interactions [39–41]. An essential histone modification at DNA damage loci is the ubiquitylation of histone H2A, the H2A histone variant H2AX and the linker histone H1 [29,42,43] (Figure 1A). H2A ubiquitylation has been investigated intensively during DSB repair.

Ubiquitin-mediated signaling at DSBs is initiated by MDC1-dependent recruitment of the ubiquitin E3 ligase RNF8, which, in concert with Ubc13, catalyzes K63-linked poly-ubiquitylation of histone H1 (Figure 1A) [44]. Ubiquitylated histone H1 subsequently mediates recruitment of the E3 ligase RNF168 to the damage site which, together with RNF8, catalyzes both mono- and poly-ubiquitylation of histones H2A and H2AX at lysine 13–15 [28,42,43,45]. Such ubiquitylated histones also play an essential role in regulating the DSB repair pathway choice by provoking the recruitment of the effector proteins BRCA1 and 53BP1 to the damage site. BRCA1 promotes homologous recombination and is recruited to damaged chromatin through its binding partner within the BRCA1-A complex RAP80, a UBD-containing protein, likely tethering to ubiquitylated histone H2A [46–48].

This essential function of BRCA1 in HR is considered one of the major mechanisms contributing to its tumor suppression activity. In contrast, 53BP1 is an essential mediator of NHEJ [49]. Recruitment of 53BP1 to DSBs occurs in a two-pronged fashion and depends on its Tudor domains and on an ubiquitin binding motif [50]. 53BP1 tethers to H4K20 dimethyl marks at damaged chromatin [51,52] and specifically reads RNF168-catalysed H2AK15 ubiquitylation [50]. In parallel to the RNF8-RNF168 pathway, the E3 ligase RING1B catalyzes mono-ubiquitylation of histone H2A at lysine 119 [43,53–55], which presumably heterochromatinizes regions surrounding the damage site [56]. Ubiquitylation processes are also a prominent feature of chromatin signalling in NER (Figure 1B). During GG-NER, different E3 ligases were demonstrated to catalyze ubiquitylation of histone H2A. Here, H2A-ubiquitylation is brought about by the E3 ligase RNF8, the UV-DDB-CUL4A/B complexes and the UV-RING1B complex [57–61] (Figure 1B). The UV-RING1B complex, which consists of the subunits DDB1, DDB2, CUL4B, and the E3 ligase RING1B, operates early during DNA damage recognition [61]. It specifically catalyzes the ubiquitylation of lysine 119 of histone H2A, which provides a tethering platform for the H2A-ubiquitin binding protein ZRF1. ZRF1 removes the CUL4B-RBX1 subunits from the UV-RING1B complex and facilitates the incorporation of CUL4A-RBX1, thus mediating the generation of the UV-DDB CUL4A complex at the damage site [61]. The latter catalyzes the poly-ubiquitylation of the DNA damage recognition factor XPC, which stabilizes XPC at chromatin [62]. Hence, the ubiquitylation status of XPC probably acts like a timing device that determines the transition from damage recognition to damage verification [63]. Mono-ubiquitylation at histone H2A is additionally catalyzed by the RING-containing E3 ligase RNF8, which likely does not affect NER directly but rather links it with the DSB-repair pathway [59]. Ubiquitylation events in TC-NER are less well understood and concern poly-ubiquitylation of DNA repair factors rather than ubiquitylation events at chromatin (Figure 1C). In TC-NER, stalled RNA Pol II initiates lesion recognition by recruiting CSB [64]. Notably, CSB, together with DDB1, either one of the scaffold proteins CUL4A or CUL4B, and the E3 ubiquitin ligase RBX1, form another ubiquitin E3 ligase complex. This complex fine-tunes the advance of TC-NER by ubiquitylation of CSB and subsequent proteasomal degradation. CSB ubiquitin chains are cleared by the deubiquitinase USP7, which is recruited to the damage site via the UV-stimulated scaffold protein A (UVSSA) [65–67]. UVSSA and USP7 antagonize proteasomal degradation of CSB at the damage site (Figure 1C). In addition, ubiquitylation and degradation of the Pol II subunit RBP1 is a complex two-step process that involves the E3 ubiquitin ligase NEDD4 and the Elongin A ubiquitin ligase [68,69] (Figure 1C). Taken together, predominantly poly-ubiquitylation events participate in the regulation of TC-NER. It still needs to be addressed whether ubiquitylation events at chromatin contribute to TC-NER and whether they provide a binding platform facilitating the recruitment of effector proteins as in GG-NER.

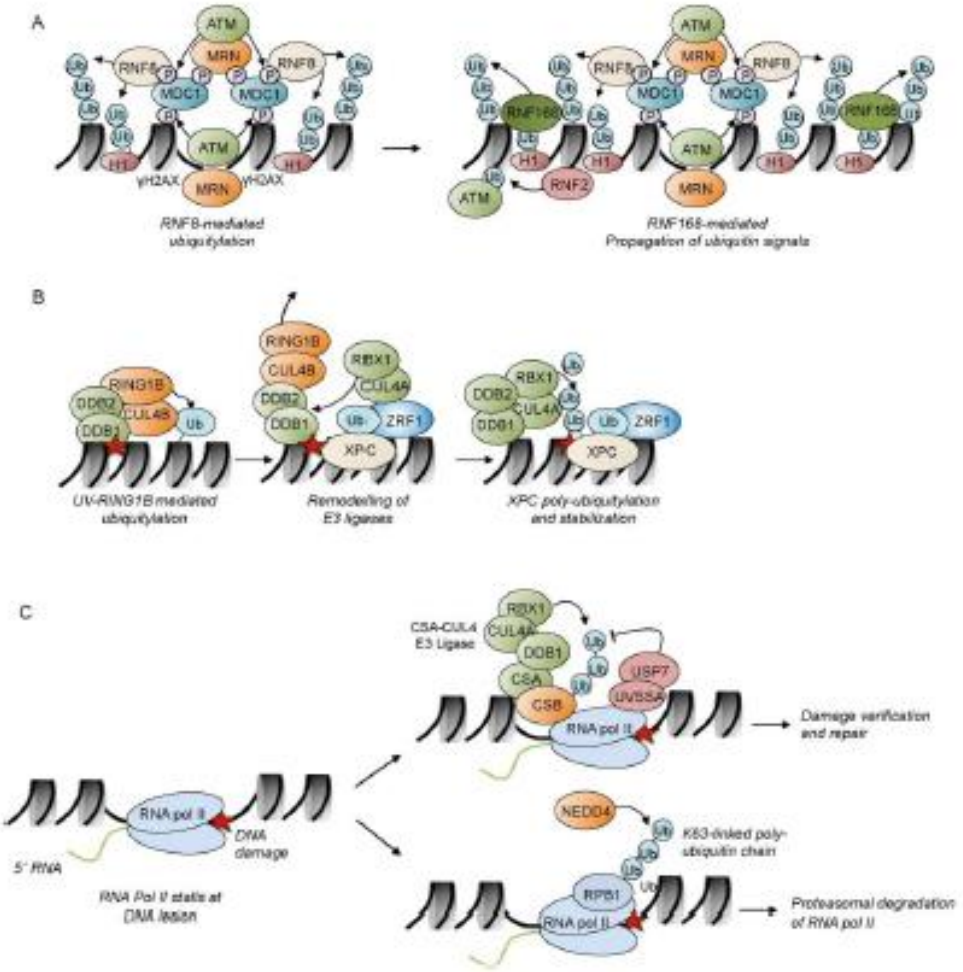

Figure 1. Ubiquitin signaling in both sub-pathways of nucleotide excision repair (NER), global genomic (GG-) and Transcription coupled NER (TC-NER), and double-strand break (DSB) repair. (**A**) Ubiquitin signaling at DSB sites. DSBs are recognized by the MRN (MRE11–RAD50–NBS1) complex, which recruits and activates the ATM kinase through association with its NBS1 subunit. ATM phosphorylates H2AX at S139 (γH2AX), thereby generating a binding platform for MDC1 (mediator of DNA damage checkpoint protein 1). The protein Casein kinase 2 (CK2) (not shown for clarity) constitutively phosphorylates residues within MDC1's SDT domain. Phosphorylated MDC1 is recognized by NBS1, a subunit of the aforementioned MRN complex. The MDC1-bound MRN subunit NSB1 attracts the ATM kinase, thereby promoting the spreading of γH2AX along the DNA. Phosphorylated MDC1 subsequently recruits the ubiquitin E3 ligase RNF8, which promotes K63-linked poly-ubiquitylation of histone H1 recognized by RNF168. RNF168, in concert with RNF8, ubiquitylates histones H2A and H2AX at K13 and K15 generating recruitment platforms for a range of ubiquitin-binding factors. Additionally, RNF168 can also recognize ubiquitylated forms of H2A, further supporting the efficient spreading of the DNA damage signal along the chromatin. Furthermore, the BMI1-RNF2 (shown as RNF2) module regulates the early initiation steps in the DNA damage response through association with H2AX and stimulating H2AX mono-ubiquitylation which serves as binding platform for ATM; (**B**) The UV-RING1B complex causes mono-ubiquitylation of histone H2A at lysine residue 119 in proximity to the DNA damage site (red star). ZRF1 is localized to the damage site both by interaction with XPC and by binding to H2A-ubiquitin via its ubiquitin binding domain. Furthermore, ZRF1 mediates remodeling of the UV RING1B E3 ligase complex by facilitating the release of the CUL4B-RING1B module and the incorporation of the CUL4A-RBX1 module. The newly-formed

DDB-CUL4A E3 ligase complex (green) catalyzes the poly-ubiquitylation of XPC, which is thereby stabilized at the damage site; (C) Ubiquitin signaling events during transcription coupled-NER (TC-NER) which either lead to the formation of a pre-incision TC-NER complex (upper part), or mediate proteasomal degradation of RNA pol II (lower part). Elongating RNA polymerase II is stalled after encountering a DNA lesion (indicated as red star). The stalled polymerase serves as a recruiting signal for the Cockayne Syndrome B (CSB) protein. CSB further recruits Cockayne Syndrome WD repeat protein A (CSA) which is part of a multiprotein complex consisting of DNA damage binding protein 1 (DDB1), the scaffold protein CUL4A or CUL4B, respectively, and the E3 ligase RBX1. The removal of CSB initiated by its poly-ubiquitylation is counteracted by the action of the deubiquitinase USP7 which is recruited to stalled RNA pol II by UV-stimulated scaffold protein A (UVSSA) and catalyzes the degradation of the poly-ubiquitin chain on CSB. An alternative pathway initiates subsequent proteasomal degradation of RNA pol II in case TC-NER fails to repair the DNA lesion. The E3 ubiquitin ligase NEDD4 mediates K63 linked poly-ubiquitylation of the RNA pol II component, termed the RNA pol II subunit B1 (RPB1). Poly-ubiquitylated RPB1 is further modified by deubiquitinases and by the elongin A (ELOA)-ELOB-ELOC-CUL5-RING-box protein 2 (RBX2) E3 ligase complex (not shown), which trigger its extraction by the valosin-containing protein (VCP)/p97 ATPase complex followed by proteasomal degradation.

5. Impact of Chromatin Remodeling and PARylation on DNA Repair

PARylation is catalyzed by poly (ADP-ribose) polymerases (PARPs) and constitutes probably one of the earliest post-translational modifications at DNA damage sites. The activity of PARP1 is triggered by DNA damage. PARP generates ADP-ribose polymers by consuming NAD^+ to modify DNA repair factors and other ancillary proteins involved in DNA repair events and recombination [70,71]. PARP1 elicits the recruitment and regulation of many DNA damage response proteins and has been linked to chromatin remodeling. Remodelers seem to play an essential role during DNA repair, however, the function of many remodelers still remains mysterious. The chromatin surrounding DSBs is rapidly and transiently PARylated (Figure 2) causing the recruitment of the NuRD complex [72,73], which harbors both ATP-dependent chromatin remodeling and histone deacetylase activities. The NuRD subunit CHD4 was found to contain PAR-binding motifs in its amino-terminal region explaining the aforementioned recruitment [74]. At the damage site, NuRD appears to be essential for the localization of DNA repair and checkpoint factors to the damage site and, moreover, it seems to promote transcriptional silencing to support the repair process [75,76] (Figure 2). Likewise, the remodeling ATPase ALC1 (amplified in liver cancer protein 1) that repositions nucleosomes on chromatin is rapidly localized to DSBs by direct interaction with PAR chains on chromatin [77,78]. Only after these PARP1-mediated PARylation events and the following recruitment of the MRN complex and remodeling machineries in response to DSB signaling (Figure 2), ATM activation, and concomitant γH2AX occur. Hence, PARylation at DSBs is a critical event early in the DNA-damage response. Remodeling complexes cause the opening of the condensed chromatin conformation, which allows for the ordered recruitment of DNA repair factors. Chromatin is temporarily locked in a decondensed state, which is also evidenced by the setting of acetylation marks at histones [79,80]. Acetylation, like the spreading of γH2AX, propagates for hundreds of kilo-bases away from the DSB [79,81]. One important acetyltransferase during DSB repair is TIP60, which operates as a subunit of the human NuA4 remodeling complex and catalyzes acetylation of histones H2A, H4, and other DNA repair factors at DSBs [82–84]. NuA4 is recruited to chromatin via binding to MDC1, hence, at a later time point than the aforementioned PARylation-dependent remodeling enzymes NuRD and ALC1.

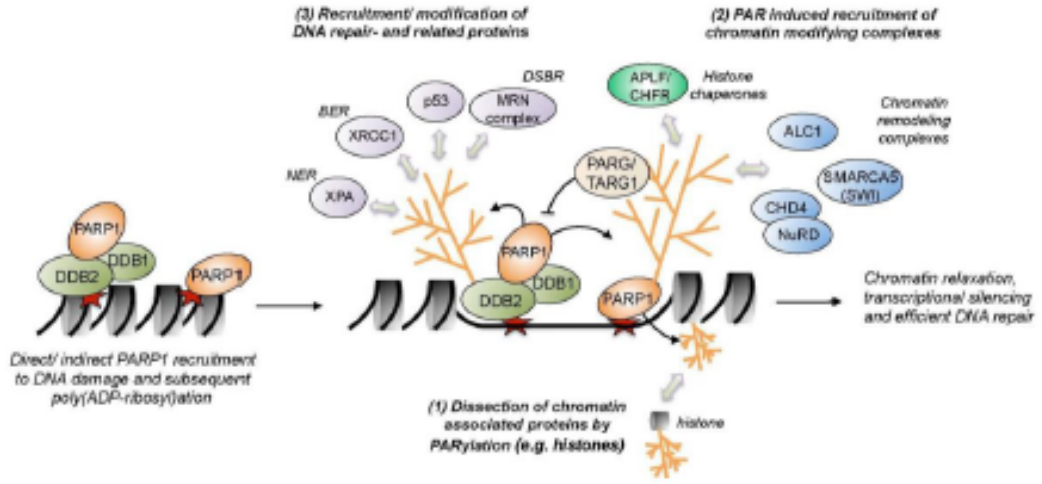

Figure 2. Chromatin re-organization processes mediated by PARylation. Amongst other stimuli, poly (ADP-ribose) polymerases (PARP1) activity is triggered by directly binding to DNA single and double strand breaks (indicated as red star), by post-translational modifications of PARP (e.g., phosphorylation), or by attraction by other DNA damage recognition factors (e.g., DDB2). PARP1-mediated PARylation results in a drastic chromatin re-structuring and decompaction by: (1) dissection of chromatin-associated proteins; (2) stimulation of chromatin re-organization and relaxation by the recruitment of chromatin-modifying complexes; and (3) the recruitment and repair of DNA repair factors. Amongst the proteins recruited to the damage site are the chromatin remodelers amplified in liver cancer 1 (ALC1), SMARCA5, and the NuRD complex, as well as the histone chaperones APLF and CHFR. Furthermore, the PAR-hydolyzing enzmyes poly(ADP-ribose) glycohydrolase (PARG) and terminal ADP-ribose glycohydolase TARG1 are also attracted to chromatin by PAR chains. In addition, PARP1-mediated PARylation plays an important role for the direct recruitment of DNA repair proteins from a wide variety of DNA repair or DDR signaling pathways, such as p53, XRCC1, XPA, and the MRN complex.

PARylation-mediated chromatin remodeling also plays an essential role within both NER sub-pathways. In GG-NER, the damage recognition factors XPC and DDB2 are targeted by PARP1. PARP1 parylates DDB2 and this causes the recruitment of XPC, thereby promoting efficiency of the NER pathway [71]. PARylation of DDB2 impedes its K48-linked poly-ubiquitylation and subsequent proteasomal degradation and thereby stabilizes DDB2 at the damage site. DDB2 associates with PARP1 and promotes PARylation of chromatin which, in turn, leads to the recruitment of the SWI/SNF chromatin remodeler ALC1 and, hence, chromatin remodeling [85] (Figure 2). Further, both XPC and RAD23B are parylated by PARP1 in response to UV irradiation [86]. XPA, a key factor involved in damage verification within both sub-pathways of NER (Figure 2), shows a high affinity for PAR chains [87], suggesting that PARylation might also play a role at later stages of NER. This non-covalent interaction with PAR chains lowers the DNA binding affinity of XPA. PARP1 also parylates Cockayne syndrome protein CSB after oxidative DNA damage, which inhibits the ATP hydrolysis activity of CSB [88]. CSB itself engages in chromatin remodeling. It remodels nucleosomes in vitro in conjunction with NAP1L1 and NAP1L4 (histone chaperone nucleosome assembly protein 1-like 1/4). CSB also recruits the histone acetyltransferase p300 and the high mobility group nucleosome binding domain-containing protein 1 (HMGN1), further linking lesion recognition in TC-NER to chromatin remodeling [89]. Furthermore, the histone chaperones FACT (facilitates chromatin transcription) [90] and HIRA [13] facilitate transcription restart after lesion-induced transcriptional arrest. Chromatin remodelers from the SWI/SNF family also operate during NER. In baker's yeast, Rad16 forms part of the NEF4 complex and its SWI/SNF-related ATPase activity is essential for efficient

NER [91]. Additionally, NEF4 mediates Gcn5-dependent histone H3 acetylation, which contributes to a decondensed chromatin conformation during the repair process [92]. Further, the damage recognition factors Rad4 (XPC) and Rad23 (RAD23B) associate with the SWI/SNF chromatin remodeling complex subunits Snf6 and Snf5 [93] and the INO80 ATPase or the INO80 complex, respectively, is important for the repair of UV-damaged chromatin likely by enabling the recruitment of XPA and XPC to the damage site [94]. Taken together, chromatin remodeling is an essential feature of DNA damage repair pathways and the loading of nucleosome remodeling complexes on damaged chromatin may be regulated by PARylation of chromatin or DNA repair factors.

6. Role of ncRNAs and DICER

Small RNAs have emerged as key players in various aspects of biology. Eukaryotes have evolved intricate mechanisms to repair DNA double-strand breaks (DSBs) through well-timed actions of DNA repair factors involving the function of ncRNAs (non-coding RNAs). One factor that processes ncRNAs to control gene expression and genome integrity is the endoribonuclease DICER. DICER chops double-stranded RNA into short RNA fragments, miRNAs, which are crucial to degrade mRNAs in the cytoplasm, and siRNAs, which contribute to the formation of heterochromatin to induce gene silencing [95]. RNA transcribed from a genomic locus is shaped into dsRNA by RDRP (RNA-dependent RNA polymerase) and the resulting dsRNA is concomitantly processed by DICER. siRNAs generated by DICER are assembled into the RITS (RNA-induced transcriptional silencing) complex, which is recruited by chromatin and causes the propagation of H3K9 methylation, a histone mark intimately linked with condensed chromatin states along the chromatin fiber [95]. DICER also contributes to repair of DSBs by generating small ncRNAs which comprise the sequence of the damaged locus [96–99] (Figure 3A). At DSBs, DICER is of paramount importance for the activation of the DNA damage response and DNA damage checkpoints [96]. Antisense transcripts at the DSB cause the generation of small dsRNAs, which are subsequently processed by the DROSHA-DICER-AGO complex. AGO-bound ncRNAs are localized to the DSB and cause the recruitment of MDC1 and 53BP1 [100]. However, the molecular mechanism of ncRNAs at DSBs is still far from being understood.

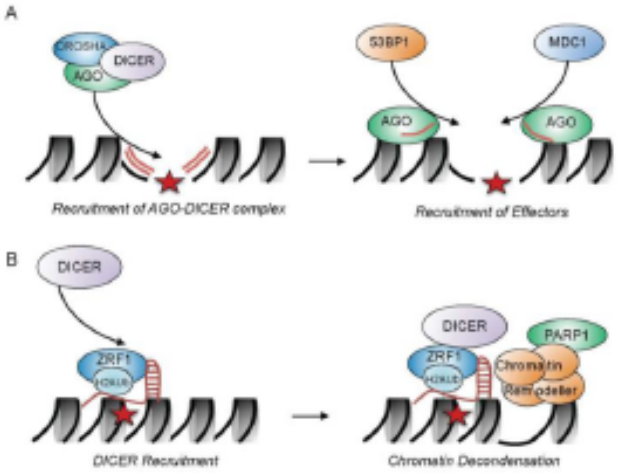

Figure 3. DICER dependent functions in NER and DSB repair. (**A**) Double-stranded RNAs (dsRNAs) are generated from antisense transcripts at the DSB and are subsequently processed by the DROSHA-DICER-AGO complex. AGO-bound ncRNAs localize at the DSB site (indicated as red star) and cause the recruitment of effectors, like 53BP1 and MDC1, by a yet-unknown mechanism; and (**B**) during GG-NER, H2A-ubiquitin-bound ZRF1 provides a binding platform for DICER. Multiprotein complexes consisting of DICER, ZRF1, PARP1 and, potentially, proteins from the SWI/SNF family of remodeling chromatin complexes cause a local decondensation of chromatin.

Very recently, another role for DICER was identified that deviates from its conventional RNA-dependent function in regulating chromatin conformation [101]. Contrary to its function in generating heterochromatin, DICER also mediates the de-condensation of the chromatin conformation at DNA damage sites during NER (Figure 3B). This unanticipated role for DICER is independent of its ribonuclease activity. DICER is localized to chromatin via the H2A-ubiquitin binding protein ZRF1, which operates during damage lesion recognition in GG-NER. ZRF1 associates to chromatin by both binding to the epigenetic H2A-ubiquitin mark and by interacting with RNA through its SANT domains [102]. ZRF1 and DICER interact with PARP1 and SWI/SNF chromatin remodeling complexes [101], which likely contribute to the decondensation of chromatin structures in GG-NER. Hence, DICER represents a versatile factor that alters the chromatin conformation. Employing its catalytic activity, DICER is involved in chromatin condensation supporting DSB repair in contrast to its contribution to chromatin decondensation in the context of NER where DICER associates with chromatin remodeling factors.

7. Concluding Remarks

Chromatin conformation regulates many essential processes, such as replication, transcription, and DNA repair. Hence, components that affect the chromatin state, such as chromatin remodeling complexes and specific chromatin marks, are at the heart of the DNA repair mechanisms. Chromatin marks and modifications of chromatin-associated proteins either cause the recruitment of DNA repair factors or regulate their activity. The interplay of these marks and remodeling activities form the basis of a chromatin signaling network that we are just starting to understand. Future work certainly needs to further address the intricacies and interactions within this chromatin network to better understand how the chromatin environment regulates DNA repair mechanisms.

Acknowledgments: Holger Richly is supported by grants from the Boehringer Ingelheim Foundation. We thank members of the Richly laboratory for critical reading of the manuscript. We apologize to colleagues for being unable to cite their work due to space limitations.

Author Contributions: Jens Stadler and Holger Richly contributed equally to the preparation of the manuscript.

Conflicts of Interest: The authors declare no conflict of interest.

References

1. Ciccia, A.; Elledge, S.J. The DNA Damage Response: Making It Safe to Play with Knives. *Mol. Cell* **2010**, *40*, 179–204. [CrossRef] [PubMed]
2. Jackson, S.P.; Bartek, J. The DNA-damage response in human biology and disease. *Nature* **2009**, *461*, 1071–1078. [CrossRef] [PubMed]
3. De Graaf, C.A.; van Steensel, B. Chromatin organization: Form to function. *Curr. Opin. Genet. Dev.* **2013**, *23*, 185–190. [CrossRef] [PubMed]
4. Smerdon, M.J. DNA repair and the role of chromatin structure. *Curr. Opin. Cell Biol.* **1991**, *3*, 422–428. [CrossRef]
5. Soria, G.; Polo, S.E.; Almouzni, G. Prime, repair, restore: The active role of chromatin in the DNA damage response. *Mol. Cell* **2012**, *46*, 722–734. [CrossRef] [PubMed]
6. Cleaver, J.E. Nucleosome structure controls rates of excision repair in DNA of human cells. *Nature* **1977**, *270*, 451–453. [CrossRef] [PubMed]
7. Smerdon, M.J.; Lieberman, M.W. Nucleosome rearrangement in human chromatin during UV-induced DNA-reapir synthesis. *Proc. Natl. Acad. Sci. USA* **1978**, *75*, 4238–4241. [CrossRef] [PubMed]
8. Adam, S.; Dabin, J.; Polo, S.E. Chromatin plasticity in response to DNA damage: The shape of things to come. *DNA Repair* **2015**, *32*, 120–126. [CrossRef] [PubMed]
9. Clapier, C.R.; Iwasa, J.; Cairns, B.R.; Peterson, C.L. Mechanisms of action and regulation of ATP-dependent chromatin-remodelling complexes. *Nat. Rev. Mol. Cell Biol.* **2017**, *18*, 407–422. [CrossRef] [PubMed]
10. Kouzarides, T. Chromatin modifications and their function. *Cell* **2007**, *128*, 693–705. [CrossRef] [PubMed]

11. De Laat, W.L.; Jaspers, N.G.; Hoeijmakers, J.H. Molecular mechanism of nucleotide excision repair. *Genes Dev.* **1999**, *13*, 768–785. [CrossRef] [PubMed]
12. Fousteri, M.; Mullenders, L.H. Transcription-coupled nucleotide excision repair in mammalian cells: Molecular mechanisms and biological effects. *Cell Res.* **2008**, *18*, 73–84. [CrossRef] [PubMed]
13. Marteijn, J.A.; Lans, H.; Vermeulen, W.; Hoeijmakers, J.H. Understanding nucleotide excision repair and its roles in cancer and ageing. *Nat. Rev. Mol. Cell Biol.* **2014**, *15*, 465–481. [CrossRef] [PubMed]
14. Marnef, A.; Legube, G. Organizing DNA repair in the nucleus: DSBs hit the road. *Curr. Opin. Cell Biol.* **2017**, *46*, 1–8. [CrossRef] [PubMed]
15. Meek, K.; Dang, V.; Lees-Miller, S.P. DNA-PK: The means to justify the ends? *Adv. Immunol.* **2008**, *99*, 33–58. [PubMed]
16. Mari, P.O.; Florea, B.I.; Persengiev, S.P.; Verkaik, N.S.; Brüggenwirth, H.T.; Modesti, M.; Giglia-Mari, G.; Bezstarosti, K.; Demmers, J.A.; Luider, T.M. Dynamic assembly of end-joining complexes requires interaction between Ku70/80 and XRCC4. *Proc. Natl. Acad. Sci. USA* **2006**, *103*, 18597–18602. [CrossRef] [PubMed]
17. Davis, A.J.; Chen, D.J. DNA double strand break repair via non-homologous end-joining. *Transl. Cancer Res.* **2013**, *2*, 130–143. [PubMed]
18. Lieber, M.R. The mechanism of double-strand DNA break repair by the nonhomologous DNA end-joining pathway. *Annu. Rev. Biochem.* **2010**, *79*, 181–211. [CrossRef] [PubMed]
19. Kakarougkas, A.; Jeggo, P.A. DNA DSB repair pathway choice: An orchestrated handover mechanism. *Br. J. Radiol.* **2014**, *87*, 20130685. [CrossRef] [PubMed]
20. Ceccaldi, R.; Rondinelli, B.; D'Andrea, A.D. Repair Pathway Choices and Consequences at the Double-Strand Break. *Trends Cell Biol.* **2016**, *26*, 52–64. [CrossRef] [PubMed]
21. Bothmer, A.; Robbiani, D.F.; Feldhahn, N.; Gazumyan, A.; Nussenzweig, A.; Nussenzweig, M.C. 53BP1 regulates DNA resection and the choice between classical and alternative end joining during class switch recombination. *J. Exp. Med.* **2010**, *207*, 855–865. [CrossRef] [PubMed]
22. Marechal, A.; Zou, L. DNA damage sensing by the ATM and ATR kinases. *Cold Spring Harb. Perspect. Biol.* **2013**, *5*, a012716. [CrossRef] [PubMed]
23. Paull, T.T.; Deshpande, R.A. The Mre11/Rad50/Nbs1 complex: Recent insights into catalytic activities and ATP-driven conformational changes. *Exp. Cell Res.* **2014**, *329*, 139–147. [CrossRef] [PubMed]
24. Haince, J.F.; McDonald, D.; Rodrigue, A.; Déry, U.; Masson, J.Y.; Hendzel, M.J.; Poirier, G.G. PARP1-dependent kinetics of recruitment of MRE11 and NBS1 proteins to multiple DNA damage sites. *J. Biol. Chem.* **2008**, *283*, 1197–1208. [CrossRef] [PubMed]
25. Stucki, M.; Clapperton, J.A.; Mohammad, D.; Yaffe, M.B.; Smerdon, S.J.; Jackson, S.P. MDC1 directly binds phosphorylated histone H2AX to regulate cellular responses to DNA double-strand breaks. *Cell* **2005**, *123*, 1213–1226. [CrossRef] [PubMed]
26. Melander, F.; Bekker-Jensen, S.; Falck, J.; Bartek, J.; Mailand, N.; Lukas, J. Phosphorylation of SDT repeats in the MDC1 N terminus triggers retention of NBS1 at the DNA damage-modified chromatin. *J. Cell Biol.* **2008**, *181*, 213–226. [CrossRef] [PubMed]
27. Bonner, W.M.; Redon, C.E.; Dickey, J.S.; Nakamura, A.J.; Sedelnikova, O.A.; Solier, S.; Pommier, Y. GammaH2AX and cancer. *Nat. Rev. Cancer* **2008**, *8*, 957–967. [CrossRef] [PubMed]
28. Doil, C.; Mailand, N.; Bekker-Jensen, S.; Menard, P.; Larsen, D.H.; Pepperkok, R.; Ellenberg, J.; Panier, S.; Durocher, D.; Bartek, J. RNF168 binds and amplifies ubiquitin conjugates on damaged chromosomes to allow accumulation of repair proteins. *Cell* **2009**, *136*, 435–446. [CrossRef] [PubMed]
29. Jackson, S.P.; Durocher, D. Regulation of DNA Damage Responses by Ubiquitin and SUMO. *Mol. Cell* **2013**, *49*, 795–807. [CrossRef] [PubMed]
30. Yazinski, S.A.; Zou, L. Functions, Regulation, and Therapeutic Implications of the ATR Checkpoint Pathway. *Annu. Rev. Genet.* **2016**, *50*, 155–173. [CrossRef] [PubMed]
31. Chen, H.; Lisby, M.; Symington, L.S. RPA coordinates DNA end resection and prevents formation of DNA hairpins. *Mol. Cell* **2013**, *50*, 589–600. [CrossRef] [PubMed]
32. Zou, L.; Elledge, S.J. Sensing DNA damage through ATRIP recognition of RPA-ssDNA complexes. *Science* **2003**, *300*, 1542–1548. [CrossRef] [PubMed]
33. Branzei, D.; Foiani, M. Regulation of DNA repair throughout the cell cycle. *Nat. Rev. Mol. Cell Biol.* **2008**, *9*, 297–308. [CrossRef] [PubMed]

34. Auclair, Y.; Rouget, R.; Affar el, B.; Drobetsky, E.A. ATR kinase is required for global genomic nucleotide excision repair exclusively during S phase in human cells. *Proc. Natl. Acad. Sci. USA* **2008**, *105*, 17896–17901. [CrossRef] [PubMed]
35. Heffernan, T.P.; Simpson, D.A.; Frank, A.R.; Heinloth, A.N.; Paules, R.S.; Cordeiro-Stone, M.; Kaufmann, W.K. An ATR- and Chk1-dependent S checkpoint inhibits replicon initiation following UVC-induced DNA damage. *Mol. Cell. Biol.* **2002**, *22*, 8552–8561. [CrossRef] [PubMed]
36. Yajima, H.; Lee, K.J.; Zhang, S.; Kobayashi, J.; Chen, B.P. DNA double-strand break formation upon UV-induced replication stress activates ATM and DNA-PKcs kinases. *J. Mol. Biol.* **2009**, *385*, 800–810. [CrossRef] [PubMed]
37. Ray, A.; Milum, K.; Battu, A.; Wani, G.; Wani, A.A. NER initiation factors, DDB2 and XPC, regulate UV radiation response by recruiting ATR and ATM kinases to DNA damage sites. *DNA Repair* **2013**, *12*, 273–283. [CrossRef] [PubMed]
38. Wakasugi, M.; Sasaki, T.; Matsumoto, M.; Nagaoka, M.; Inoue, K.; Inobe, M.; Horibata, K.; Tanaka, K.; Matsunaga, T. Nucleotide excision repair-dependent DNA double-strand break formation and ATM signaling activation in mammalian quiescent cells. *J. Biol. Chem.* **2014**, *289*, 28730–28737. [CrossRef] [PubMed]
39. Glickman, M.H.; Ciechanover, A. The ubiquitin-proteasome proteolytic pathway: Destruction for the sake of construction. *Physiol. Rev.* **2002**, *82*, 373–428. [CrossRef] [PubMed]
40. Schnell, J.D.; Hicke, L. Non-traditional functions of ubiquitin and ubiquitin-binding proteins. *J. Biol. Chem.* **2003**, *278*, 35857–35860. [CrossRef] [PubMed]
41. Mukhopadhyay, D.; Riezman, H. Proteasome-independent functions of ubiquitin in endocytosis and signaling. *Science* **2007**, *315*, 201–205. [CrossRef] [PubMed]
42. Mailand, N.; Bekker-Jensen, S.; Faustrup, H.; Melander, F.; Bartek, J.; Lukas, C.; Lukas, J. RNF8 ubiquitylates histones at DNA double-strand breaks and promotes assembly of repair proteins. *Cell* **2007**, *131*, 887–900. [CrossRef] [PubMed]
43. Pan, M.R.; Peng, G.; Hung, W.C.; Lin, S.Y. Monoubiquitination of H2AX protein regulates DNA damage response signaling. *J. Biol. Chem.* **2011**, *286*, 28599–28607. [CrossRef] [PubMed]
44. Thorslund, T.; Ripplinger, A.; Hoffmann, S.; Wild, T.; Uckelmann, M.; Villumsen, B.; Narita, T.; Sixma, T.K.; Choudhary, C.; Bekker-Jensen, S. Histone H1 couples initiation and amplification of ubiquitin signalling after DNA damage. *Nature* **2015**, *527*, 389–393. [CrossRef] [PubMed]
45. Mattiroli, F.; Vissers, J.H.; van Dijk, W.J.; Ikpa, P.; Citterio, E.; Vermeulen, W.; Marteijn, J.A.; Sixma, T.K. RNF168 ubiquitinates K13–15 on H2A/H2AX to drive DNA damage signaling. *Cell* **2012**, *150*, 1182–1195. [CrossRef] [PubMed]
46. Sobhian, B.; Shao, G.; Lilli, D.R.; Culhane, A.C.; Moreau, L.A.; Xia, B.; Livingston, D.M.; Greenberg, R.A. RAP80 targets BRCA1 to specific ubiquitin structures at DNA damage sites. *Science* **2007**, *316*, 1198–1202. [CrossRef] [PubMed]
47. Kim, H.; Chen, J.; Yu, X. Ubiquitin-binding protein RAP80 mediates BRCA1-dependent DNA damage response. *Science* **2007**, *316*, 1202–1205. [CrossRef] [PubMed]
48. Wang, B.; Matsuoka, S.; Ballif, B.A.; Zhang, D.; Smogorzewska, A.; Gygi, S.P.; Elledge, S.J. Abraxas and RAP80 form a BRCA1 protein complex required for the DNA damage response. *Science* **2007**, *316*, 1194–1198. [CrossRef] [PubMed]
49. Panier, S.; Boulton, S.J. Double-strand break repair: 53BP1 comes into focus. *Nat. Rev. Mol. Cell Biol.* **2014**, *15*, 7–18. [CrossRef] [PubMed]
50. Fradet-Turcotte, A.; Canny, M.D.; Escribano-Díaz, C.; Orthwein, A.; Leung, C.C.; Huang, H.; Landry, M.C.; Kitevski-LeBlanc, J.; Noordermeer, S.M.; Sicheri, F. 53BP1 is a reader of the DNA-damage-induced H2A Lys 15 ubiquitin mark. *Nature* **2013**, *499*, 50–54. [CrossRef] [PubMed]
51. Pesavento, J.J.; Yang, H.; Kelleher, N.L.; Mizzen, C.A. Certain and progressive methylation of histone H4 at lysine 20 during the cell cycle. *Mol. Cell. Biol.* **2008**, *28*, 468–486. [CrossRef] [PubMed]
52. Pei, H.; Zhang, L.; Luo, K.; Qin, Y.; Chesi, M.; Fei, F.; Bergsagel, P.L.; Wang, L.; You, Z.; Lou, Z. MMSET regulates histone H4K20 methylation and 53BP1 accumulation at DNA damage sites. *Nature* **2011**, *470*, 124–128. [CrossRef] [PubMed]
53. Ismail, I.H.; Andrin, C.; McDonald, D.; Hendzel, M.J. BMI1-mediated histone ubiquitylation promotes DNA double-strand break repair. *J. Cell Biol.* **2010**, *191*, 45–60. [CrossRef] [PubMed]

54. Ginjala, V.; Nacerddine, K.; Kulkarni, A.; Oza, J.; Hill, S.J.; Yao, M.; Citterio, E.; van Lohuizen, M.; Ganesan, S. BMI1 is recruited to DNA breaks and contributes to DNA damage-induced H2A ubiquitination and repair. *Mol. Cell. Biol.* **2011**, *31*, 1972–1982. [CrossRef] [PubMed]
55. Chagraoui, J.; Hebert, J.; Girard, S.; Sauvageau, G. An anticlastogenic function for the Polycomb Group gene Bmi1. *Proc. Natl. Acad. Sci. USA* **2011**, *108*, 5284–5289. [CrossRef] [PubMed]
56. Ui, A.; Nagaura, Y.; Yasui, A. Transcriptional elongation factor ENL phosphorylated by ATM recruits polycomb and switches off transcription for DSB repair. *Mol. Cell* **2015**, *58*, 468–482. [CrossRef] [PubMed]
57. Bergink, S.; Salomons, F.A.; Hoogstraten, D.; Groothuis, T.A.; de Waard, H.; Wu, J.; Yuan, L.; Citterio, E.; Houtsmuller, A.B.; Neefjes, J. DNA damage triggers nucleotide excision repair-dependent monoubiquitylation of histone H2A. *Genes Dev.* **2006**, *20*, 1343–1352. [CrossRef] [PubMed]
58. Kapetanaki, M.G.; Guerrero-Santoro, J.; Bisi, D.C.; Hsieh, C.L.; Rapić-Otrin, V.; Levine, A.S. The DDB1-CUL4ADDB2 ubiquitin ligase is deficient in xeroderma pigmentosum group E and targets histone H2A at UV-damaged DNA sites. *Proc. Natl. Acad. Sci. USA* **2006**, *103*, 2588–2593. [CrossRef] [PubMed]
59. Marteijn, J.A.; Bekker-Jensen, S.; Mailand, N.; Lans, H.; Schwertman, P.; Gourdin, A.M.; Dantuma, N.P.; Lukas, J.; Vermeulen, W. Nucleotide excision repair-induced H2A ubiquitination is dependent on MDC1 and RNF8 and reveals a universal DNA damage response. *J. Cell Biol.* **2009**, *186*, 835–847. [CrossRef] [PubMed]
60. Guerrero-Santoro, J.; Kapetanaki, M.G.; Hsieh, C.L.; Gorbachinsky, I.; Levine, A.S.; Rapić-Otrin, V. The cullin 4B-based UV-damaged DNA-binding protein ligase binds to UV-damaged chromatin and ubiquitinates histone H2A. *Cancer Res.* **2008**, *68*, 5014–5022. [CrossRef] [PubMed]
61. Gracheva, E.; Chitale, S.; Wilhelm, T.; Rapp, A.; Byrne, J.; Stadler, J.; Medina, R.; Cardoso, M.C.; Richly, H. ZRF1 mediates remodeling of E3 ligases at DNA lesion sites during nucleotide excision repair. *J. Cell Biol.* **2016**, *213*, 185–200. [CrossRef] [PubMed]
62. Sugasawa, K.; Okuda, Y.; Saijo, M.; Nishi, R.; Matsuda, N.; Chu, G.; Mori, T.; Iwai, S.; Tanaka, K.; Tanaka, K. UV-induced ubiquitylation of XPC protein mediated by UV-DDB-ubiquitin ligase complex. *Cell* **2005**, *121*, 387–400. [CrossRef] [PubMed]
63. Chitale, S.; Richly, H. Timing of DNA lesion recognition: Ubiquitin signaling in the NER pathway. *Cell cycle* **2017**, *16*, 163–171. [CrossRef] [PubMed]
64. Marnef, A.; Cohen, S.; Legube, G. Transcription-Coupled DNA Double-Strand Break Repair: Active Genes Need Special Care. *J. Mol. Biol.* **2017**, *429*, 1277–1288. [CrossRef] [PubMed]
65. Zhang, X.; Horibata, K.; Saijo, M.; Ishigami, C.; Ukai, A.; Kanno, S.I.; Tahara, H.; Neilan, E.G.; Honma, M.; Nohmi, T. Mutations in UVSSA cause UV-sensitive syndrome and destabilize ERCC6 in transcription-coupled DNA repair. *Nat. Genet.* **2012**, *44*, 593–597. [CrossRef] [PubMed]
66. Schwertman, P.; Lagarou, A.; Dekkers, D.H.; Raams, A.; van der Hoek, A.C.; Laffeber, C.; Hoeijmakers, J.H.; Demmers, J.A.; Fousteri, M.; Vermeulen, W. UV-sensitive syndrome protein UVSSA recruits USP7 to regulate transcription-coupled repair. *Nat. Genet.* **2012**, *44*, 598–602. [CrossRef] [PubMed]
67. Sarasin, A. UVSSA and USP7: New players regulating transcription-coupled nucleotide excision repair in human cells. *Genome Med.* **2012**, *4*, 44. [CrossRef] [PubMed]
68. Yasukawa, T.; Kamura, T.; Kitajima, S.; Conaway, R.C.; Conaway, J.W.; Aso, T. Mammalian Elongin A complex mediates DNA-damage-induced ubiquitylation and degradation of Rpb1. *EMBO J.* **2008**, *27*, 3256–3266. [CrossRef] [PubMed]
69. Wilson, M.D.; Harreman, M.; Svejstrup, J.Q. Ubiquitylation and degradation of elongating RNA polymerase II: The last resort. *Biochim. Biophys. Acta Gene Regul. Mech.* **2013**, *1829*, 151–157. [CrossRef] [PubMed]
70. De Vos, M.; Schreiber, V.; Dantzer, F. The diverse roles and clinical relevance of PARPs in DNA damage repair: Current state of the art. *Biochem. Pharmacol.* **2012**, *84*, 137–146. [CrossRef] [PubMed]
71. Robu, M.; Shah, R.G.; Petitclerc, N.; Brind'Amour, J.; Kandan-Kulangara, F.; Shah, G.M. Role of poly(ADP-ribose) polymerase-1 in the removal of UV-induced DNA lesions by nucleotide excision repair. *Proc. Natl. Acad. Sci. USA* **2013**, *110*, 1658–1663. [CrossRef] [PubMed]
72. Chou, D.M.; Adamson, B.; Dephoure, N.E.; Tan, X.; Nottke, A.C.; Hurov, K.E.; Gygi, S.P.; Colaiácovo, M.P.; Elledge, S.J. A chromatin localization screen reveals poly (ADP ribose)-regulated recruitment of the repressive polycomb and NuRD complexes to sites of DNA damage. *Proc. Natl. Acad. Sci. USA* **2010**, *107*, 18475–18480. [CrossRef] [PubMed]

54. Ginjala, V.; Nacerddine, K.; Kulkarni, A.; Oza, J.; Hill, S.J.; Yao, M.; Citterio, E.; van Lohuizen, M.; Ganesan, S. BMI1 is recruited to DNA breaks and contributes to DNA damage-induced H2A ubiquitination and repair. *Mol. Cell. Biol.* **2011**, *31*, 1972–1982. [CrossRef] [PubMed]
55. Chagraoui, J.; Hebert, J.; Girard, S.; Sauvageau, G. An anticlastogenic function for the Polycomb Group gene Bmi1. *Proc. Natl. Acad. Sci. USA* **2011**, *108*, 5284–5289. [CrossRef] [PubMed]
56. Ui, A.; Nagaura, Y.; Yasui, A. Transcriptional elongation factor ENL phosphorylated by ATM recruits polycomb and switches off transcription for DSB repair. *Mol. Cell* **2015**, *58*, 468–482. [CrossRef] [PubMed]
57. Bergink, S.; Salomons, F.A.; Hoogstraten, D.; Groothuis, T.A.; de Waard, H.; Wu, J.; Yuan, L.; Citterio, E.; Houtsmuller, A.B.; Neefjes, J. DNA damage triggers nucleotide excision repair-dependent monoubiquitylation of histone H2A. *Genes Dev.* **2006**, *20*, 1343–1352. [CrossRef] [PubMed]
58. Kapetanaki, M.G.; Guerrero-Santoro, J.; Bisi, D.C.; Hsieh, C.L.; Rapić-Otrin, V.; Levine, A.S. The DDB1-CUL4A DDB2 ubiquitin ligase is deficient in xeroderma pigmentosum group E and targets histone H2A at UV-damaged DNA sites. *Proc. Natl. Acad. Sci. USA* **2006**, *103*, 2588–2593. [CrossRef] [PubMed]
59. Marteijn, J.A.; Bekker-Jensen, S.; Mailand, N.; Lans, H.; Schwertman, P.; Gourdin, A.M.; Dantuma, N.P.; Lukas, J.; Vermeulen, W. Nucleotide excision repair-induced H2A ubiquitination is dependent on MDC1 and RNF8 and reveals a universal DNA damage response. *J. Cell Biol.* **2009**, *186*, 835–847. [CrossRef] [PubMed]
60. Guerrero-Santoro, J.; Kapetanaki, M.G.; Hsieh, C.L.; Gorbachinsky, I.; Levine, A.S.; Rapić-Otrin, V. The cullin 4B-based UV-damaged DNA-binding protein ligase binds to UV-damaged chromatin and ubiquitinates histone H2A. *Cancer Res.* **2008**, *68*, 5014–5022. [CrossRef] [PubMed]
61. Gracheva, E.; Chitale, S.; Wilhelm, T.; Rapp, A.; Byrne, J.; Stadler, J.; Medina, R.; Cardoso, M.C.; Richly, H. ZRF1 mediates remodeling of E3 ligases at DNA lesion sites during nucleotide excision repair. *J. Cell Biol.* **2016**, *213*, 185–200. [CrossRef] [PubMed]
62. Sugasawa, K.; Okuda, Y.; Saijo, M.; Nishi, R.; Matsuda, N.; Chu, G.; Mori, T.; Iwai, S.; Tanaka, K.; Tanaka, K. UV-induced ubiquitylation of XPC protein mediated by UV-DDB-ubiquitin ligase complex. *Cell* **2005**, *121*, 387–400. [CrossRef] [PubMed]
63. Chitale, S.; Richly, H. Timing of DNA lesion recognition: Ubiquitin signaling in the NER pathway. *Cell cycle* **2017**, *16*, 163–171. [CrossRef] [PubMed]
64. Marnef, A.; Cohen, S.; Legube, G. Transcription-Coupled DNA Double-Strand Break Repair: Active Genes Need Special Care. *J. Mol. Biol.* **2017**, *429*, 1277–1288. [CrossRef] [PubMed]
65. Zhang, X.; Horibata, K.; Saijo, M.; Ishigami, C.; Ukai, A.; Kanno, S.I.; Tahara, H.; Neilan, E.G.; Honma, M.; Nohmi, T. Mutations in UVSSA cause UV-sensitive syndrome and destabilize ERCC6 in transcription-coupled DNA repair. *Nat. Genet.* **2012**, *44*, 593–597. [CrossRef] [PubMed]
66. Schwertman, P.; Lagarou, A.; Dekkers, D.H.; Raams, A.; van der Hoek, A.C.; Laffeber, C.; Hoeijmakers, J.H.; Demmers, J.A.; Fousteri, M.; Vermeulen, W. UV-sensitive syndrome protein UVSSA recruits USP7 to regulate transcription-coupled repair. *Nat. Genet.* **2012**, *44*, 598–602. [CrossRef] [PubMed]
67. Sarasin, A. UVSSA and USP7: New players regulating transcription-coupled nucleotide excision repair in human cells. *Genome Med.* **2012**, *4*, 44. [CrossRef] [PubMed]
68. Yasukawa, T.; Kamura, T.; Kitajima, S.; Conaway, R.C.; Conaway, J.W.; Aso, T. Mammalian Elongin A complex mediates DNA-damage-induced ubiquitylation and degradation of Rpb1. *EMBO J.* **2008**, *27*, 3256–3266. [CrossRef] [PubMed]
69. Wilson, M.D.; Harreman, M.; Svejstrup, J.Q. Ubiquitylation and degradation of elongating RNA polymerase II: The last resort. *Biochim. Biophys. Acta Gene Regul. Mech.* **2013**, *1829*, 151–157. [CrossRef] [PubMed]
70. De Vos, M.; Schreiber, V.; Dantzer, F. The diverse roles and clinical relevance of PARPs in DNA damage repair: Current state of the art. *Biochem. Pharmacol.* **2012**, *84*, 137–146. [CrossRef] [PubMed]
71. Robu, M.; Shah, R.G.; Petitclerc, N.; Brind'Amour, J.; Kandan-Kulangara, F.; Shah, G.M. Role of poly(ADP-ribose) polymerase-1 in the removal of UV-induced DNA lesions by nucleotide excision repair. *Proc. Natl. Acad. Sci. USA* **2013**, *110*, 1658–1663. [CrossRef] [PubMed]
72. Chou, D.M.; Adamson, B.; Dephoure, N.E.; Tan, X.; Nottke, A.C.; Hurov, K.E.; Gygi, S.P.; Colaiácovo, M.P.; Elledge, S.J. A chromatin localization screen reveals poly (ADP ribose)-regulated recruitment of the repressive polycomb and NuRD complexes to sites of DNA damage. *Proc. Natl. Acad. Sci. USA* **2010**, *107*, 18475–18480. [CrossRef] [PubMed]

91. Ramsey, K.L.; Smith, J.J.; Dasgupta, A.; Maqani, N.; Grant, P.; Auble, D.T. The NEF4 complex regulates Rad4 levels and utilizes Snf2/Swi2-related ATPase activity for nucleotide excision repair. *Mol. Cell. Biol.* **2004**, *24*, 6362–6378. [CrossRef] [PubMed]
92. Jin, Q.; Yu, L.R.; Wang, L.; Zhang, Z.; Kasper, L.H.; Lee, J.E.; Wang, C.; Brindle, P.K.; Dent, S.Y.; Ge, K. Distinct roles of GCN5/PCAF-mediated H3K9ac and CBP/p300-mediated H3K18/27ac in nuclear receptor transactivation. *EMBO J.* **2011**, *30*, 249–262. [CrossRef] [PubMed]
93. Gong, F.; Fahy, D.; Smerdon, M.J. Rad4-Rad23 interaction with SWI/SNF links ATP-dependent chromatin remodeling with nucleotide excision repair. *Nat. Struct. Mol. Biol.* **2006**, *13*, 902–907. [CrossRef] [PubMed]
94. Jiang, Y.; Wang, X.; Bao, S.; Guo, R.; Johnson, D.G.; Shen, X.; Li, L. INO80 chromatin remodeling complex promotes the removal of UV lesions by the nucleotide excision repair pathway. *Proc. Natl. Acad. Sci. USA* **2010**, *107*, 17274–17279. [CrossRef] [PubMed]
95. Holoch, D.; Moazed, D. RNA-mediated epigenetic regulation of gene expression. *Nat. Rev. Genet.* **2015**, *16*, 71–84. [CrossRef] [PubMed]
96. Francia, S.; Michelini, F.; Saxena, A.; Tang, D.; de Hoon, M.; Anelli, V.; Mione, M.; Carninci, P.; di Fagagna, F.D.A. Site-specific DICER and DROSHA RNA products control the DNA-damage response. *Nature* **2012**, *488*, 231–235. [CrossRef] [PubMed]
97. Wei, W.; Ba, Z.; Gao, M.; Wu, Y.; Ma, Y.; Amiard, S.; White, C.I.; Danielsen, J.M.R.; Yang, Y.G.; Qi, Y. A role for small RNAs in DNA double-strand break repair. *Cell* **2012**, *149*, 101–112. [CrossRef] [PubMed]
98. Michalik, K.M.; Bottcher, R.; Forstemann, K. A small RNA response at DNA ends in Drosophila. *Nucleic Acids Res.* **2012**, *40*, 9596–9603. [CrossRef] [PubMed]
99. Gao, M.; Wei, W.; Li, M.M.; Wu, Y.S.; Ba, Z.; Jin, K.X.; Li, M.M.; Liao, Y.Q.; Adhikari, S.; Chong, Z. Ago2 facilitates Rad51 recruitment and DNA double-strand break repair by homologous recombination. *Cell Res.* **2014**, *24*, 532–541. [CrossRef] [PubMed]
100. Francia, S.; Cabrini, M.; Matti, V.; Oldani, A.; di Fagagna, F.D.A. DICER, DROSHA and DNA damage response RNAs are necessary for the secondary recruitment of DNA damage response factors. *J. Cell Sci.* **2016**, *129*, 1468–1476. [CrossRef] [PubMed]
101. Chitale, S.; Richly, H. DICER and ZRF1 contribute to chromatin decondensation during nucleotide excision repair. *Nucleic Acids Res.* **2017**, *45*, 5901–5912. [CrossRef] [PubMed]
102. Papadopoulou, T.; Kaymak, A.; Sayols, S.; Richly, H. Dual role of Med12 in PRC1-dependent gene repression and ncRNA-mediated transcriptional activation. *Cell Cycle* **2016**, *15*, 1479–1493. [CrossRef] [PubMed]

Gracheva E, Chitale S, Wilhelm T, Rapp A, Byrne J, Stadler J, Medina R, Cardoso MC,Richly H.
ZRF1 mediates remodeling of E3 ligases at DNA lesion sites during nucleotide excision repair. J Cell Biol. 2016 Apr 25;213(2):185-200.
PubMed PMID: 27091446

ZRF1 mediates remodeling of E3 ligases at DNA lesion sites during Nucleotide excision repair.

Author Contribution

J. M. Stadler performed the following experiments (including cell culture, transfection, IP and analysis by immunoblotting:

1. HA-ubi pulldown in control, shZRF1 and shRING1B knockdown cells (Figure 8B).
2. XPC-GFP pulldown in control, shZRF1 and shRING1B (Figure 8C).

J Cell Biol. 2016 Apr 25;213(2):185-200.

ZRF1 mediates remodeling of E3 ligases at DNA lesion sites during nucleotide excision repair

Ekaterina Gracheva,[1]* Shalaka Chitale,[1]* Thomas Wilhelm,[1] Alexander Rapp,[2] Jonathan Byrne,[1] **Jens Stadler**,[1] Rebeca Medina,[1] M. Cristina Cardoso,[2] and Holger Richly[1]

[1]*E. Gracheva and S. Chitale contributed equally to this paper.

Correspondence to Holger Richly: h.richly@imb-mainz.de

Abbreviations used in this paper: CPD, cyclobutane pyrimidine dimer; DSB, double-strand break; GG, global genome; NER, nucleotide excision repair; TC, transcription coupled; UDS, unscheduled DNA synthesis.

Laboratory of Molecular Epigenetics, Institute of Molecular Biology, 55128 Mainz, Germany [2]Department of Biology, Technische Universität Darmstadt, 64287 Darmstadt, Germany

Faithful DNA repair is essential to maintain genome integrity. Ultraviolet (UV) irradiation elicits both the recruitment of DNA repair factors and the deposition of histone marks such as monoubiquitylation of histone H2A at lesion sites. Here, we report how a ubiquitin E3 ligase complex speci c to DNA repair is remodeled at lesion sites in the global genome nucleotide excision repair (GG-NER) pathway. Monoubiquitylation of histone H2A (H2A-ubiquitin) is catalyzed pre- dominantly by a novel E3 ligase complex consisting of DDB2, DDB1, CUL4B, and RING1B (UV–RING1B complex) that acts early during lesion recognition. The H2A-ubiquitin binding protein ZRF1 mediates remodeling of this E3 ligase complex directly at the DNA lesion site, causing the assembly of the UV–DDB–CUL4A E3 ligase complex (DDB1–DDB2– CUL4A-RBX1). ZRF1 is an essential factor in GG-NER, and its function at damaged chromatin sites is linked to damage recognition factor XPC. Overall, the results shed light on the interplay between epigenetic and DNA repair recognition factors at DNA lesion sites.

Introduction

Nucleotide excision repair (NER) constitutes one of the major DNA repair pathways. It handles various helix-distorting DNA lesions such as 6–4 photoproducts and cyclobutane pyrimidine dimers (CPDs), arising after exposure to UV light (de Laat et al., 1999).

Impaired NER activity is associated with several ge- netic disorders such as *Xeroderma pigmentosum*, which is char- acterized by hypersensitivity to sunlight and a predisposition for skin cancer (Friedberg, 2001). Mammalian NER comprises two pathways that differ in the nature of recognizing DNA lesions. Transcription-coupled (TC) NER is con ned to regions of ac- tive transcription, where stalled RNA polymerase II triggers the DNA damage response. In contrast, global genome (GG) NER represents the transcription- independent recognition of lesions. The recognition step is followed by veri cation of the

lesion by the repair factor XPA and by the formation of the preexcision complex involving TFIIH and its helicase subunits XPB and XPD. Subsequently, the DNA lesion is excised by the endo- nucleases XPF and XPG, and the gap is lled by DNA poly- merases. (Fousteri and Mullenders, 2008; Marteijn et al., 2014).

In GG-NER DNA lesions are recognized by two well- described factors: XPC and DDB2. XPC represents a struc- ture speci c DNA binding factor, which speci cally binds helix-distorting structures (Sugasawa et al., 1998; Riedl et al., 2003). XPC forms a stable complex with the Rad23 homologs RAD23A or RAD23B, respectively, and centrin2 (Masutani et al., 1994; Araki et al., 2001). This trimeric complex binds to a variety of lesions, triggers NER activity, and rapidly dissoci- ates after binding damaged DNA (Sugasawa et al., 2001; Hoog- straten et al., 2008; Bergink et al., 2012). Ef cient recognition of CPDs and 6–4 photoproducts also requires the presence of DDB2 (XPE; Tang et al., 2000; Fitch et al., 2003; Moser et al., 2005; Luijsterburg et al., 2007; Nishi et al., 2009). Loss of func- tional DDB2 causes defective repair of CPDs, reduced repair of 6–4 photoproducts, and hypersensitivity to UV-induced skin cancer (Rapić-Otrin et al., 2003; Alekseev et al., 2005). DDB2 along with DDB1, the RING-domain protein RBX1, and either of the scaffold proteins CUL4A or CUL4B forms E3 ubiqui- tin ligase complexes (UV–DDB–CUL4A/B) that catalyze the monoubiquitylation of histones H2A, H3, and H4 (Shiyanov et al., 1999; Groisman et al., 2003; Angers et al., 2006; Wang et al., 2006; Guerrero-Santoro et al., 2008). Importantly, the UV–DDB–CUL4A complex catalyzes the polyubiquitylation of XPC, thereby increasing its af nity for DNA in vitro and contributing to recognition and stable binding of photolesions (Sugasawa et al., 2005).

A prominent histone modi cation present at DNA damage sites is ubiquitylation of histones H2A, H2AX, and H1 (Bergink et al., 2006; Mailand et al., 2007; Pan et al., 2011; Thorslund et al., 2015). At double-strand breaks (DSBs), ubiquitylation histones is catalyzed by the E3 ligases RNF168, RNF8, and RING1B (Doil et al., 2009; Pan et al., 2011; Mattiroli et al., 2012; Ui et al., 2015). During NER, H2A ubiquitylation is cat- alyzed by the E3 ligase RNF8 and the UV–DDB–CUL4A/B complexes (Bergink et al., 2006; Kapetanaki et al., 2006; Guer- rero-Santoro et al., 2008; Marteijn et al., 2009).
Further, it was demonstrated that H2A ubiquitylation after UV irradiation de- pends on RING1B (Bergink et al., 2006). RING1B constitutes a subunit of the Polycomb group repressive complex 1 (PRC1), which catalyzes the monoubiquitylation of histone H2A at lysine 119 to silence genes during pluripotency (Wang et al., 2004; Morey and Helin, 2010). Interestingly, at DSBs, H2A ubiquitylation is dependent on the PRC1 subunits BMI-1 and RING1B (Ismail et al., 2010; Chagraoui et al., 2011; Ginjala et al., 2011; Pan et al., 2011). More recently, it was reported that PRC1 mediates DSB-induced gene silencing, linking PRC1 strongly to DSB repair (Ui et al., 2015). Still, it remains unclear how the E3 ligases cross talk and in which sequence they act during DNA repair.

We have previously shown that Zuotin-related factor 1 (ZRF1) binds monoubiquitylated histone H2A via its ubiqui- tin-binding domain and removes PRC1 from chromatin during

cellular differentiation (Richly et al., 2010). Given the signi - cance of H2A ubiquitylation in DNA repair, we have set out to study the roles of RING1B and ZRF1 in NER. Our results reveal that RING1B is the catalytic subunit of a novel DDB–cullin–E3 ligase complex, which ubiquitylates histone H2A early during NER. Further, we discovered that ZRF1 is a switch protein that remodels chromatin-bound E3 ligases during lesion recogni- tion. Hence, our study sheds new light on the interplay of epi- genetic and DNA repair recognition factors at DNA lesion sites.

Results

RING1B mediates ubiquitylation of histone H2A after UV irradiation To distinguish the functions of E3 ligases functioning after UV irradiation, we performed knockdown of RING1B (shRING1B), RNF168 (siRNF168), and the scaffold protein CUL4A (siCUL4A), which is a component of the UV–DDB–CUL4A E3 complex, in HEK293T cells. To assess the recruitment of the respective E3 ligases to chromatin, we cross-linked cells at the given time points after UV irradiation and isolated the chromatin fraction. We measured the relative intensities of H2A ubiquitin and H2A after probing Western blots with H2A antibodies. We observed that the reduction of RING1B hampered the increase of H2A ubiquitylation, whereas knockdown of the other E3 li- gases did not signi cantly alter H2A ubiquitin levels (Fig. 1 A; representative Western blots of the analysis: Figs. 1 B and S1, A and B). We also con rmed that RING1B speci cally catalyzes monoubiquitylation of lysine 119 at histone H2A after UV ir- radiation (Figs. 1 B and S1 C). Additionally, we con rmed that knockdown of CUL4A renders the UV–DDB–CUL4A E3 li- gase inactive (Fig. S1 A). To further assess whether RING1B is recruited to DNA damage sites, we performed microirradiation experiments with a 405-nm laser in cells expressing DDB2-GFP and RING1B-YFP fusion proteins (Fig. S1, D–F). We observed that both DDB2 and RING1B show a relatively weak, but sig- ni cant accumulation to sites of DNA damage, consistent with a previous observation demonstrating RING1B- mediated accu- mulation of H2A-ubiquitylation at DNA damage sites (Bergink

et al., 2006). Further, we did not observe any major difference in cellular ubiquitylation levels upon depletion of RING1B (Fig. S1, G and H) as suggested previously (Bergink et al., 2006). To link RING1B to the NER pathway, we investigated its func- tion performing UV irradiation experiments with the nematode *Caenorhabditis elegans* (Lans and Vermeulen, 2011; Craig et al., 2012). Compared with wild-type animals treated with a con- trol RNAi (N2/control), we observed a reduction of viability after UV irradiation of the RING1B mutant treated with control RNAi (VC31/control) and upon RNAi- mediated depletion of the NER factor XPC in wild-type worms (N2/*xpc-1*; Fig. 1 C).
Knockdown of XPC in RING1B mutant strains (VC31/*xpc-1*) did not exhibit further reduction of viability, suggesting that RING1B is epistatic to XPC.

Given the function of PRC1 at DSBs, we next determined whether PRC1 plays a role in H2A ubiquitylation after UV irradiation. Knockdown of BMI-1 displayed only a slight ef- fect on the recruitment of RING1B and the deposition of H2A ubiquitin (Fig. 1 D), which is likely a consequence of reduced RING1B and H2A-ubiquitin basal levels. A colony

formation assay showed that knockdown of either RING1B or BMI-1 ex- hibits a mild reduction of the colony formation potential. In- terestingly, simultaneous knockdown of both proteins showed additive reduction of the colony formation potential, suggesting that BMI-1 and RING1B likely exert different functions in the repair of UV-mediated DNA lesions (Fig. 1 E). Notably, we ob- served a similar relationship performing an epistasis analysis with the *C. elegans* orthologs of BMI-1 (*mig-32*) and RING1B (*spat-3*; Karakuzu et al., 2009; Fig. S1 I).

Collectively, these data suggest a critical role for RING1B in H2A-ubiquitylation in the NER pathway. Opposed to its function at DSBs, RING1B seems to catalyze the ubiquitylation reaction without its PRC1 binding partner BMI-1.

RING1B and DDB2 cooperate in the ubiquitylation of histone H2A Intrigued by the epistatic relationship of XPC and RING1B, we sought to nd out whether RING1B is linked to the NER machinery. We expressed ^{FLAG}RING1B in HEK293T cells and performed af nity puri cations. As expected, RING1B binds the PRC1 subunit BMI-1 (Wang et al., 2004; Fig. 2 A). Inter- estingly, RING1B interacts robustly with DDB2, but not with other selected factors of the NER pathway (Figs. 2 A and S2 A). Immunoprecipitation of endogenous RING1B further veri ed the interaction of DDB2 with RING1B (Fig. 2 B). Likewise, pu- ri cations performed with ^{FLAG}DDB2 displayed strong binding of RING1B and interaction with its well-characterized binding partners DDB1 and CUL4A (Shiyanov et al., 1999; Fig. 2 C).

Next, we examined whether DDB2 and BMI-1 interact with RING1B in a mutually exclusive manner. Immunoprecip- itating BMI-1 we observed binding of RING1B, but not DDB2 (Fig. S2 B). Overexpression of BMI-1 caused a slight increase in the BMI-1–RING1B interaction but a complete loss of DDB2-RING1B binding (Fig. S2 C). Depletion of BMI-1 had only a slight effect on the DDB2–RING1B interaction (Fig. S2 D). These data suggest that the majority of RING1B is associ- ated with BMI-1 rather than DDB2, which is in agreement with the general function of PRC1 in gene silencing.

To investigate a joint function of DDB2 and RING1B in DNA repair, we performed colony formation assays (Fig. 2 D). After depletion of DDB2 we observed reduced colony forma- tion potential, which is in agreement with a previous study

showing impaired survival of XPE patient fibroblasts after UV irradiation (Rapić-Otrin et al., 2003). Similarly, deple- tion of RING1B exhibited reduced colony formation po- tential. Simultaneous depletion of both proteins showed no further reduction of colony formation potential, suggesting that RING1B and DDB2 likely act in a common DNA re- pair pathway. To further support this finding, we analyzed skin biopsy specimens after staining with DDB2 and H2A ubiquitin or RING1B antibodies, respectively (Fig. S2, E, G, and I). We observed a clear correlation of DDB2 with both RING1B and H2A-

ubiquitin only in UV exposed skin sections as judged by single cell quantification of staining intensities (Fig. S2, F and H). Depletion of RING1B did not hamper the recruitment of DDB2 or BMI-1 to chroma- tin after UV irradiation (Fig. 2 E), implying divergent roles for RING1B and BMI-1 in UV-triggered DNA repair. Cells depleted of DDB2 as well as XPE patient fibroblasts exhib- ited reduced H2A ubiquitylation consistent with a previous study (Kapetanaki et al., 2006) and diminished recruitment of RING1B to chromatin (Figs. 2 F, 4 G, and S2 K). Nota- bly, knockdown of DDB2 did not impair BMI-1 recruitment to chromatin, further uncoupling BMI-1 from H2A ubiqui- tylation in NER (Figs. 2 F and S2 J).

In sum, these data suggest a functional interplay of DDB2 and RING1B in H2A ubiquitylation during NER.

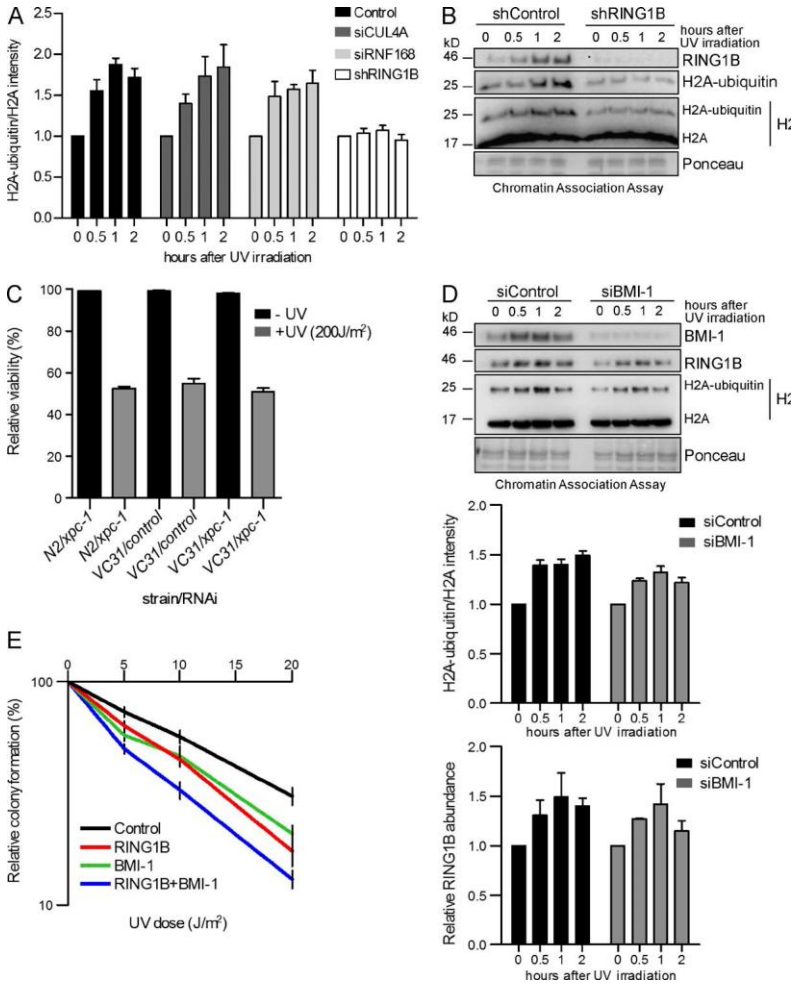

Figure 1. **Dissection of E3 ligase functions in UV-medi- ated DNA damage repair.** (A) Quantitative analysis of H2A-ubiquitylation levels. Immunoblots (as in B and Fig. S1, A and B) were probed with histone H2A antibody. The intensities of H2A and H2A-ubiquitin bands were quanti- ed by the ImageJ software. The graphs illustrate the relative H2A ubiquitylation calculated as (H2A ubiquitin)/ (H2A +

H2A ubiquitin), normalized to Ponceau staining intensity after knockdown of the respective proteins (H2A ubiquitin/H2A). Values are normalized to the value from nonirradiated cells and are given as mean ± SEM (n = 4). (B) Monoubiquitylation of histone H2A at lysine 119 after UV irradiation is mainly catalyzed by RING1B. Chroma- tin association assays of control and RING1B knockdown HEK293T cells after UV irradiation. De–cross-linked mate- rial of the respective time points was subjected to Western blotting and probed with the indicated antibodies. The speci city of the H2A-ubiquitin antibody was veri ed (Fig. S1 C). (C) Epistatic relationship of *xpc-1* and *spat- 3.* Wild-type nematodes (N2) or *spat- 3* mutants (VC31) were fed with either control or *xpc-1* RNAi–producing bacteria. The relative viability was analyzed after UV irradiation (200 J/m^2). Values are given as mean ± SEM (n = 3). (D) Impact of BMI-1 on RING1B-mediated H2A ubiquitylation after UV irradiation. Chromatin association assays of UV-irradiated HEK293T cells treated with siRNAs (control, *BMI-1*). De–cross-linked material of the respective time points was subjected to Western blotting and probed with the indicated antibodies.
Relative intensities of H2A ubiquitin/H2A and RING1B abundance after BMI-1 de- pletion were measured. Values are given as mean ± SEM (n = 4). (E) Epistatic relationship of RING1B and BMI-1 in response to UV irradiation. Relative colony formation po- tential of control or RING1B knockdown cell lines treated with siRNA was analyzed at different UV doses. Control cells were transfected with either control siRNA (control) or BMI-1 siRNA (*BMI-1*). RING1B knockdown cell lines were transfected with either control siRNA (*RING1B*) or BMI-1 siRNA (*RING1B* + *BMI-1*). Gene knockdown was con rmed by Western blots (not depicted). Values are given as mean ± SEM (n = 9).

RING1B forms a stable protein complex with CUL4B, DDB1, and DDB2. To reveal the composition of the putative RING1B-DDB2 E3 ligase complex, we expressed ^{FLAG}DDB2 in HEK293T cells and performed puri cations in UV-irradiated and untreated cells (Fig. 3 A and Table S5). After elution of ^{FLAG}DDB2 containing protein complexes with FLAG peptide, we subsequently used the eluate in immunoprecipitations with RING1B antibodies to speci cally purify RING1B-DDB2 containing protein com- plexes. The puri ed material was subjected to mass spectrom- etry, identifying DDB1 and CUL4B as the main interactors of RING1B and DDB2 (UV–RING1B complex in Fig. 3 A and Table S5). Furthermore, immunoprecipitations of endogenous DDB1 or RING1B as well as pull-downs with recombinant GST–RING1B and puri ed DDB1–DDB2 complexes con- rmed our ndings (Fig. S3, A–D). To verify the assembly of the UV–RING1B E3 ligase complex, we overexpressed ^{FLAG}DDB1, ^{FLAG}DDB2, and ^{FLAG}RING1B with or without $^{FLAG\text{-}STREP}$CUL4B in HEK293T cells (Fig. 3 B). Af nity puri cations of CUL4B revealed speci c binding of DDB1, DDB2, and RING1B. We further analyzed the interactions of the subunits of the UV– RING1B complex in vitro by pull-down experiments with puri ed proteins (Fig. S3 E). Collectively, these experiments revealed that RING1B speci cally binds to CUL4B and DDB2 but shows no direct interaction with either CUL4A or DDB1

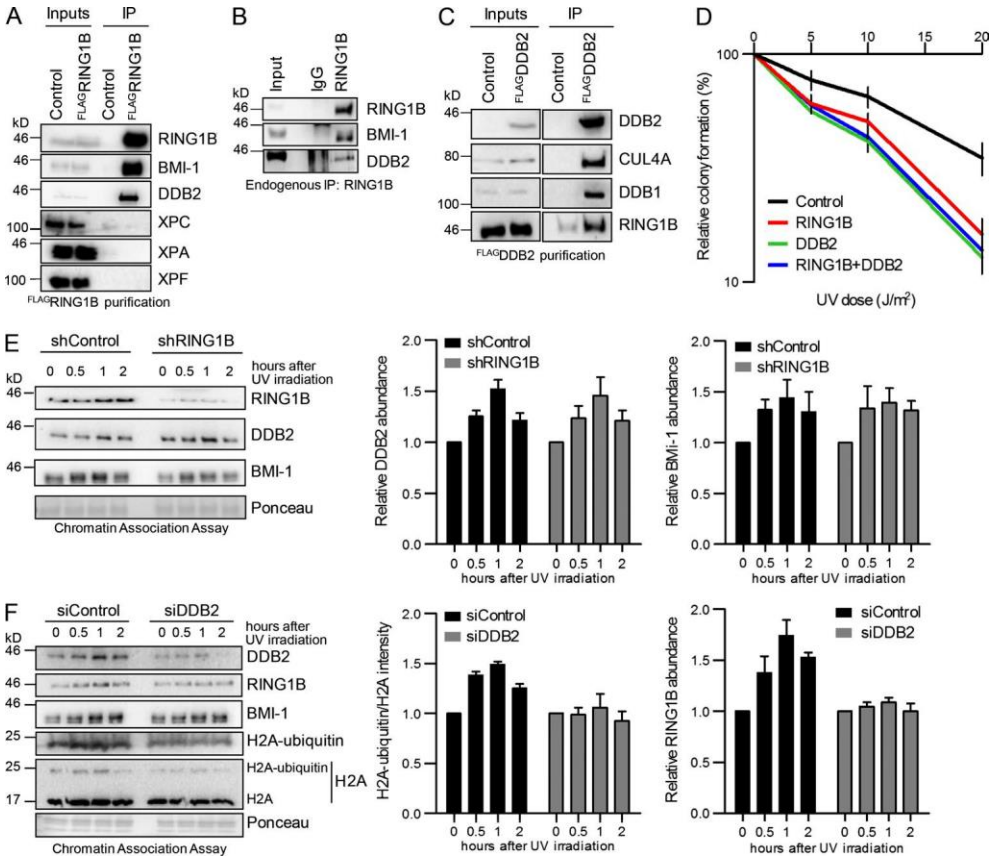

Figure 2. **RING1B and DDB2 cooperate in H2A ubiquitylation.** (A) RING1B interacts with DDB2. Control cells and cells expressing FLAGRING1B were irra- diated with UV light. After immunoprecipitation with FLAG-M2-Agarose the puri ed material was subjected to Western blotting and blots were incubated with the indicated antibodies. Inputs correspond to 3%. (B) Endogenous immunoprecipitations with RING1B antibodies after UV irradiation. Western blots of the precipitated material were incubated with the indicated antibodies. IgG lanes show unspeci c staining of the IgG heavy chains. (C) DDB2 associates with RING1B. Control cells and cells expressing FLAGDDB2 were irradiated with UV light. After immunoprecipitation with FLAG-M2-agarose, the puri ed material was subjected to Western blotting and blots were incubated with the indicated antibodies. Inputs correspond to 3%. (D) Epistatic relationship of RING1B and DDB2 in response to UV irradiation. Relative colony formation potential of control or RING1B knockdown cell lines treated with siRNA was analyzed at different UV dosages. Control cells were transfected with either control siRNA (control) or DDB2 siRNA (*DDB2*).

RING1B knockdown cell lines were transfected with either control siRNA (*RING1B*) or DDB2 siRNA (*RING1B* + *DDB2*). Gene knockdown was con rmed by Western blots (not depicted). Values are given as mean ± SEM (n = 6). (E) Knockdown of RING1B does not impair DDB2 recruitment. Chromatin association assays of control and RING1B knockdown HEK293T cells after UV irradiation. De–cross- linked material of the respective time points was subjected to Western blotting and probed with the indicated antibodies. The relative DDB2 and BMI-1 abundance was calculated. Values are given as mean

± SEM (n = 3). (F) Knockdown of DDB2 shows reduced H2A-ubiquitylation but unaltered BMI-1 recruitment. Chromatin association assays of UV-irradiated HEK293T cells treated with siRNAs (control, *DDB2*). De–cross-linked material of the respective time points was subjected to Western blotting and probed with the indicated antibodies. The relative H2A-ubiquitylation and RING1B abundance was calculated. Values are given as mean ± SEM (n = 4).

(Fig. S3, F–I). Additionally, to distinguish the UV–RING1B complex from the UV– DDB–CUL4B complex, we performed competition experiments. The E3 ligases RING1B and RBX1 compete for binding to CUL4B as judged by in vitro pull-down experiments with CUL4B (Fig. S3 J). Similarly, in pull-downs with recombinant RBX1 (Fig. S3, K and L) and in immunoprecipitations of endogenous RBX1 after RING1B overexpression (Fig. S3 M), excess RING1B disrupted CUL4B-RBX1 binding.

Next, we set out to purify the UV–RING1B complex to test its ubiquitylation capacity in vitro. To this end, we over- expressed ^{FLAG}DDB1, ^{FLAG}DDB2, ^{FLAG}RING1B, and $^{FLAG\text{-}STREP}$CUL4B in HEK293T cells (Fig. S3 N). After enriching for the FLAG-tagged proteins, we selectively puri ed the UV– RING1B complex. We subjected the puri ed material to col-loidal Coomassie staining (Fig. 3 C) and mass spectrometry (Table S4), which con rmed the speci c assembly of the UV– RING1B complex. Importantly, no contamination with chroma- tin components was found in the puri cation, ruling out that the assembly of the UV–RING1B complex was generated indirectly through association with chromatin (Tables S5 and S6). Likewise, no other E3 ligases were identi ed in the af nity pu- ri cation, excluding unspeci c ubiquitylation events when test- ing the UV–RING1B complex in vitro. To explore whether the puri ed UV–RING1B complex catalyzes H2A ubiquitylation, we performed in vitro ubiquitylation assays with histone H2A (Fig. 3 D). Compared with control reactions, the UV–RING1B complex strongly increased the speci c monoubiquitylation of histone H2A over time. Similarly, the UV–RING1B complex caused monoubiquitylation of nucleosomes at histone H2A in ubiquitylation assays (Fig. 3 E).

In conclusion, we have identified a novel RING1B-contain- ing complex that catalyzes monoubiquitylation of histone H2A.

ZRF1 tethers to the H2A-ubiquitin mark during UV-triggered DNA repair

Monoubiquitylated H2A is bound by ZRF1 during cellular dif- ferentiation (Richly et al., 2010). Interestingly, we observed that ZRF1 is recruited to chromatin after UV irradiation and its recruitment is dependent on RING1B (Fig. 4 A). Furthermore, the ubiquitin- binding domain of ZRF1 is required for its asso- ciation with chromatin after UV irradiation (Fig. 4 B). When inducing local UV damage by irradiation through a microp- ore membrane, we observed ZRF1 localizing to DNA lesions, which are marked by XPC and XPA (Fig. 4, C and D; and Fig. S4 A), further supporting a role for ZRF1 in UV- mediated DNA repair. We next addressed the association of ZRF1 with DNA lesions in the presence of the RING1B inhibitor PRT4165 (Is- mail et al., 2013). Under control conditions, we observed ZRF1 at DNA lesions (Fig. 4 E), whereas administration of the drug abolished H2A ubiquitylation (Fig. S4 B), unscheduled DNA synthesis (UDS) after UV irradiation (Fig. S4 C), and, most importantly, the presence of ZRF1 at the damage site (Figs. 4 E and S4 D). Similarly, ZRF1 recruitment to chromatin was hampered after depletion of the UV–RING1B complex sub-unit CUL4B or in XPE patient broblasts (Fig. 4, F and G). To investigate ZRF1 function in vivo, we analyzed human skin biopsy

specimens. ZRF1 and CPD antibody staining signals colocalized only when the skin was exposed to UV light (Fig. S4 E). In addition, single-cell analysis revealed that the relative ZRF1 intensities correlate with the relative intensities of CPDs upon irradiation (Fig. S4, E and F).

Collectively, these data suggest that ZRF1 plays a role in UV-triggered DNA repair and that it localizes to the damage site via binding of H2A-ubiquitin.

ZRF1's function in NER is dependent on XPC

To explore whether ZRF1 interacts with NER factors, we performed affinity purifications after expressing ^{FLAG}ZRF1 in

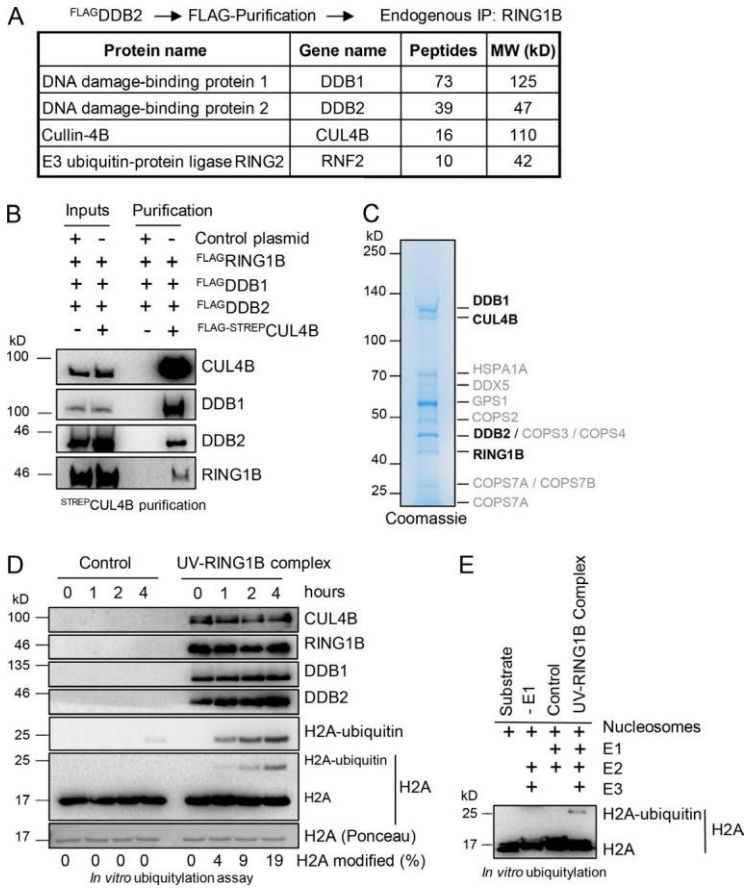

Figure 3. **H2A ubiquitylation after UV irradiation is performed by the UV–RING1B complex.** (A) Protein interaction partners of RING1B and DDB2. Mass spectrometry analysis after sequen- tial immunoprecipitations with FLAG and RING1B antibodies revealed DDB1 and CUL4B as main interaction partners of DDB2 and RING1B. A comprehensive list of the identi ed unique peptides after RING1B and control immunoprecipitations (with or without UV irradiation) is provided in Table S5. (B) Assem- bly of the UV–RING1B complex. Plasmids expressing ^{FLAG}DDB1, ^{FLAG}DDB2, and ^{FLAG}RING1B were cotransfected in combination with either control plasmid or a plasmid encoding $^{FLAG\text{-}STREP}$CUL4B. After immunoprecipitation with STREP-Tactin beads, the puri ed material was subjected to Western

blotting and blots were incu- bated with the indicated antibodies. Inputs correspond to 5%. (C) Visualization of the UV–RING1B complex. Puri ed UV– RING1B complex was subjected to SDS gel electrophoresis and colloidal Coomassie staining. Mass spectrometry analysis revealed the presence of all four subunits (bold). A compre- hensive list of unique peptides is provided in Table S6. (D) The UV– RING1B complex catalyzes ubiquitylation of H2A in vitro. Ubiquitylation assays were performed with recombinant H2A, E1 (UBA1), E2 (UBCH5), and either GST (control) or the UV–RING1B complex.
Reactions were performed at 37°C, and samples were taken at the indicated time points. Material of the respective time points was subjected to Western blotting and probed with the indicated antibodies. (E) The UV–RING1B complex catalyzes monoubiquitylation of nucleosomal H2A. Ubiquitylation assays were performed with recombinant nucleosomes, E1 (UBA1), E2 (UBCH5), and either GST (control) or UV-RING1B complex. Re- actions lacking E1 (−E1) were performed as additional controls. The ubiquitylation assays were performed at 37°C for 5 h, and samples or pure substrate (Substrate) were subjected to Western blotting and probed with H2A antibodies.

HEK293T cells (Fig. 5 A). We found the DNA lesion recogni- tion factor XPC interacting with ZRF1, but we did not observe binding of other selected NER factors. Likewise, we found XPC associated with ZRF1 in endogenous immunoprecipita- tions, con rming the interaction of both proteins (Fig. 5 B). To investigate the interplay between XPC and ZRF1, we analyzed the localization of ZRF1 to lesions sites using DDB2 as a dam- age marker. Interestingly, we observed reduced colocalization of ZRF1 and DDB2 in XPC patient broblasts (Figs. 5 C and S5 A). Next, we analyzed chromatin from XPC patient bro- blasts and control broblasts after UV irradiation (Fig. 5 D). We observed reduced levels of ZRF1 despite enhanced RING1B and H2A-ubiquitin levels. Accordingly, siRNA-mediated knockdown of XPC caused a drastic reduction of ZRF1 lev- els at chromatin after UV irradiation (Fig. S5 B). In contrast, chromatin isolated from XPA patient broblasts exhibited no reduction in H2A ubiquitylation, RING1B, and ZRF1 levels as compared with control broblasts (Fig. 5 E). These data sug- gest that H2A ubiquitylation via the UV–RING1B complex and subsequent ZRF1 recruitment predominantly occurs early during DDB2-mediated lesion recognition and likely before the assembly of the DNA incision complex (de Laat et al., 1999; Wakasugi and Sancar, 1999).

Next, we performed an epistasis analysis addressing the common functions of ZRF1 and XPC in NER. We observed a strong reduction in the colony formation potential after irradiat- ing ZRF1 knockdown cells or cells treated with siRNA directed against XPC, respectively (Fig. 5 F), consistent with previous observations in XPC patient broblasts (Bohr et al., 1986). Simultaneous knockdown of both factors did not signi cantly alter the colony formation potential compared with a single

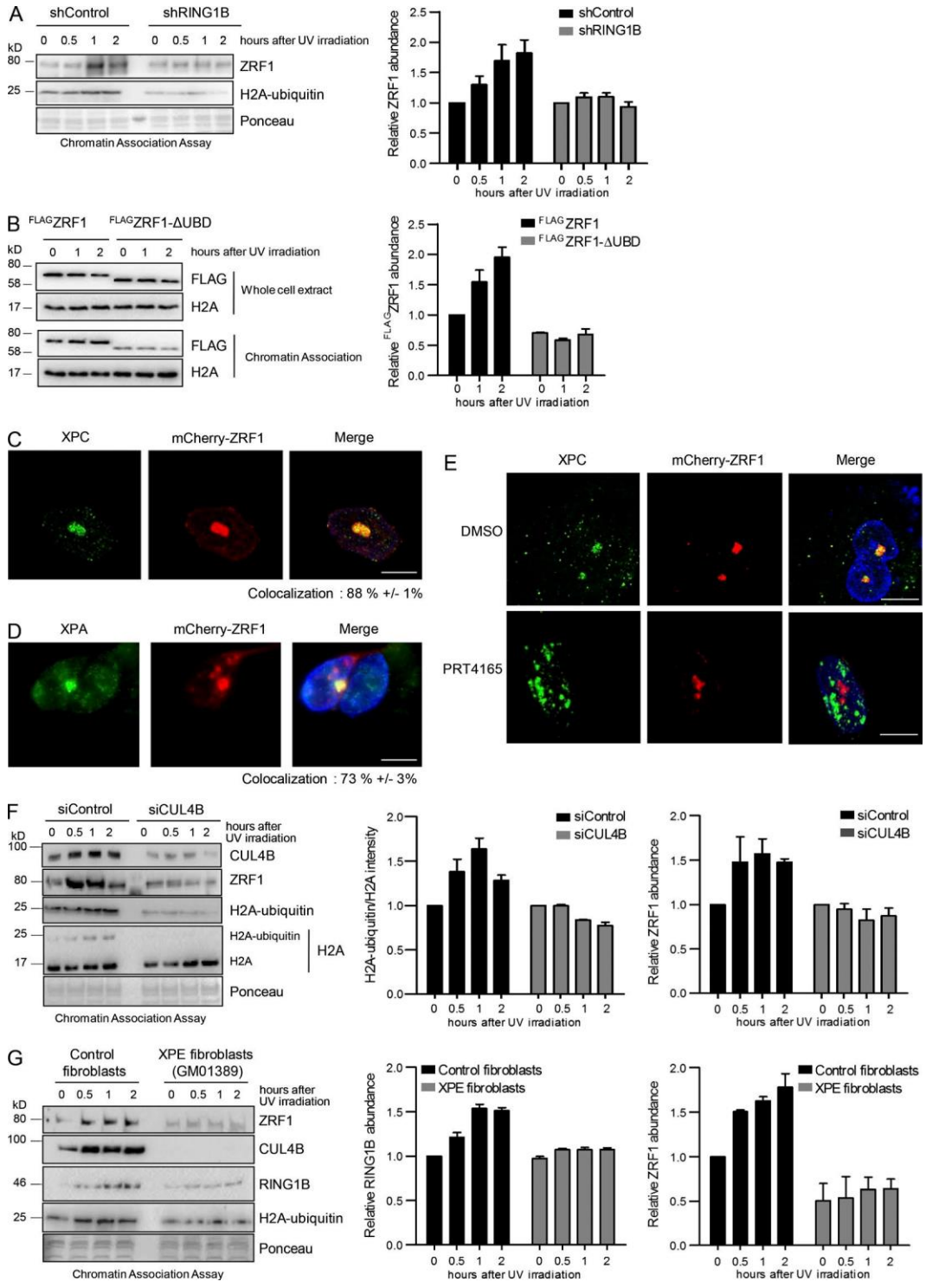

Figure 4. **Function of ZRF1 in UV-mediated DNA repair.** (A) ZRF1 is tethered to chromatin in a RING1B-dependent manner. Chromatin association assays of control and RING1B knockdown HEK293T cell lines after UV irradiation. De–cross-linked material of the respective time points was subjected to West- ern blotting and probed with the indicated antibodies. The relative ZRF1 abundance was calculated. Values are given as mean ± SEM (n = 3). (B) The ubiquitin-binding domain (UBD) is important for tethering ZRF1 to chromatin after UV irradiation. HEK293T cells expressing FLAGZRF1 and FLAGZRF1-

ΔUBD were irradiated with UV light, and chromatin was isolated at the indicated time points. De-cross- linked material was subjected to Western blotting and blots were incubated with FLAG-antibody. The relative ^{FLAG}ZRF1 abundance was calculated. Values are given as mean ± SEM (n = 4). (C and D) ZRF1 localizes to DNA damage sites after UV irradiation. MRC5 broblasts expressing mCherry-ZRF1 were UV irradiated (100 J/m^2) through a micropore membrane (+ UV) 24 h after transfection. 30 min after irradiation, cells were preextracted and xed. DNA damage sites were visualized by staining with XPC (C) or XPA (D) antibody. The colocalization of ZRF1 with XPC amounts to 88% ± 1%. The colocalization of ZRF1 with XPA amounts to 73% ± −3%. Nonirradiated control and quanti cation of the ZRF1 localization at the damage sites are represented in Fig. S4 A. Bar, 10 µm. (E) Inhibition of RING1B affects recruitment of ZRF1 to DNA damage sites. MRC5 broblasts expressing mCherry-ZRF1 were treated with PRT4165 or DMSO. Cells were UV-irradiated (100 J/m^2) through a micropore membrane. 30 min after irradiation cells were preextracted and xed. DNA damage sites were visualized by XPC antibody staining. ZRF1 localization to DNA lesions after treatment with DMSO or PRT4165 was quanti ed (Fig. S4 B). Bar, 10 µm. (F) Depletion of CUL4B impacts H2A knockdown, suggesting that ZRF1 and XPC are likely epistatic in human cells. Additionally, we made similar observations in epistasis experiments using *C. elegans* (Fig. S5 C). To estimate the contribution of RING1B and ZRF1 in repairing UV-mediated DNA damage, we measured unscheduled DNA synthesis after UV irradiation and removal of CPDs in control broblasts, knockdown broblasts, and XPA broblasts (Fig. 6, A–C). In ZRF1 and RING1B knockdown cells, EdU incorporation was reduced to ∼40% when compared with control cells (Fig. 6 A). Similarly, the removal of CPDs was compromised in ZRF1 and RING1B knockdown broblasts (Fig. 6 B).

Further analysis of the DNA damage response in the *C. el- egans* germline, which is regarded a measure for GG-NER (Lans and Vermeulen, 2011; Craig et al., 2012), showed that RING1B (*spat-3*) and XPC (*xpc-1*) mutants were affected by UV irra- diation to a similar extent (Fig. 6 D). ZRF1 mutants (*dnj-11*) showed a stronger phenotype than XPC mutants (*xpc-1*), which is only surpassed by XPA mutants (xpa-1). We used a CSB mu- tant (*csb-1*) as a control strain, which is defective in TC-NER, but not in GG-NER. This mutant showed UV sensitivity com- parable to wild-type animals. We made similar ndings using RNAi-mediated knockdown of NER factors RING1B (*spat-3*) and ZRF1 (*dnaj-11*; Fig. S5 D). To analyze a potential function of RING1B and ZRF1 in TC-NER, we analyzed the relative lar- val stage stalling (L1 arrest; Lans and Vermeulen, 2011; Craig et al., 2012). After irradiation with increasing doses of UV light, worms were analyzed microscopically and by sorting on a large-particle sorter (Fig. 6 E; Fig. S5, E and F; and Table S1). Wild-type worms and XPC (*xpc-1*) and ZRF1 (*dnj-11*) mutants show larval arrest only at high doses of UV light, whereas CSB (*csb-1*) and XPA (*xpa-1*) mutants exhibit very strong pheno- types already at a low UV doses, in line with their defects in the TC-NER pathway (Fig. 6 E).

Collectively, we have identifed ZRF1 and RING1B as potential players of GG-NER. ZRF1 recruitment to damaged chromatin is regulated by both its binding partner XPC and H2A ubiquitylation via the UV–RING1B complex.

ZRF1 remodels E3 ligase complexes at the lesion site

To explore the function of ZRF1 at damaged chromatin, we analyzed chromatin from ZRF1 knockdown cells after UV irradiation (Fig. 7 A). Upon depletion of ZRF1, we found enhanced RING1B and H2A-ubiquitylation levels at chromatin consistent with a function of ZRF1 in dislocating RING1B from chromatin (Richly et al., 2010). We next addressed its potential role in dislodging other subunits of the UV–RING1B complex from chromatin. We noticed that depletion of ZRF1 did not alter the recruitment of DDB2 to chromatin (Fig. 7 B). Impor- tantly, however, we observed retention of CUL4B at chromatin, whereas recruitment of CUL4A was impaired. To determine the CUL4A levels at chromatin in control and ZRF1 knockdown cells, we expressed ^{FLAG}H2AX and performed af nity puri - cations (Fig. 7 C). We observed constant levels of DDB2 but reduced levels of CUL4A in the coprecipitate puri ed from ZRF1 knockdown cells.
Similarly, ^{FLAG}DDB2 showed dimin- ished association with CUL4A when puri ed from ZRF1 knockdown cells (Fig. 7 D). These data suggest a potential function for ZRF1 in remodeling the UV–RING1B complex at the DNA damage sites. To follow up on this idea, we ana- lyzed whether the assembly of the UV–DDB–CUL4A com- plex was compromised in ZRF1 knockdown cells. To that end, we immunoprecipitated ^{HA}RBX1 in control and ZRF1 knockdown cells (Fig. 7 E). In the coprecipitate, we noticed diminished levels of DDB2 and DDB1 but unaltered CUL4A binding upon ZRF1 knockdown, suggesting that ZRF1 me- diates the association of CUL4A–RBX1 with DDB1–DDB2.
Next, we tested a function for ZRF1 in remodeling the UV– RING1B complex in vitro. In pull-down experiments with puri ed proteins, we had noticed that ZRF1, like CUL4B and RING1B, speci cally binds DDB2 (Fig. S3, F and G). Hence, we addressed whether ZRF1 competed with CUL4B, DDB1, and RING1B for binding to DDB2 (Fig. 7 F). In pull- downs with GFP-DDB2, we observed that increasing amounts of ZRF1 competes with CUL4B and RING1B bind- ing, whereas the DDB1–DDB2 interaction was unaltered.
Experiments using similar amounts of CUL4A, RBX1, and DDB1 showed that ZRF1 did not hamper the interaction of CUL4A and RBX1 with DDB2 (Fig. 7 G).

Finally, to study ZRF1-mediated remodeling in vitro, we assembled the UV–RING1B complex and analyzed the replace- ment of CUL4B–RING1B with CUL4A–RBX1 (Fig. 7 H). The addition of puri ed CUL4A–RBX1 to immobilized UV– RING1B complexes (Fig. 7 H, lane 2) or GFP-loaded beads (lane 1) showed only minimal or no incorporation of CUL4A and RBX1 into the E3 ligase complex. In contrast, in the pres- ence of ZRF1, we noticed a signi cant replacement of CUL4B– RING1B by CUL4A–RBX1 (lane 3).

In sum, our data suggest that ZRF1 remodels E3 ligase complexes at the lesion site and that it mediates the assembly of the UV–DDB–CUL4A E3 ligase complex.

ZRF1 regulates ubiquitylation of XPC

To confirm that ZRF1 mediates the assembly of the UV– DDB–CUL4A E3 ligase complex, we analyzed the poly- ubiquitylation of its substrate, XPC (Sugasawa et al., 2005). After UV irradiation of ZRF1 knockdown cells, we observed diminished polyubiquitylation of XPC when compared with control cells (Fig. 8 A). Similarly,

immunoprecipitations of ubiquitylated proteins after expressing ^{HA}Ubiquitin in control, RING1B, and ZRF1 knockdown cells showed a signi cant re- duction of ubiquitylated XPC in knockdowns compared with control (Fig. 8 B). After expression of ^{HA}XPC and ^{HIS}Ubiq- uitin, we immunoprecipitated ^{HA}XPC and analyzed its ubiq- uitylation status (Fig. 8 C). In agreement with our previous data, we observed a signi cant reduction of XPC ubiquityl- ation in both knockdown cell lines. Moreover, we expressed ^{HIS}Ubiquitin in control, RING1B, and ZRF1 knockdown cell

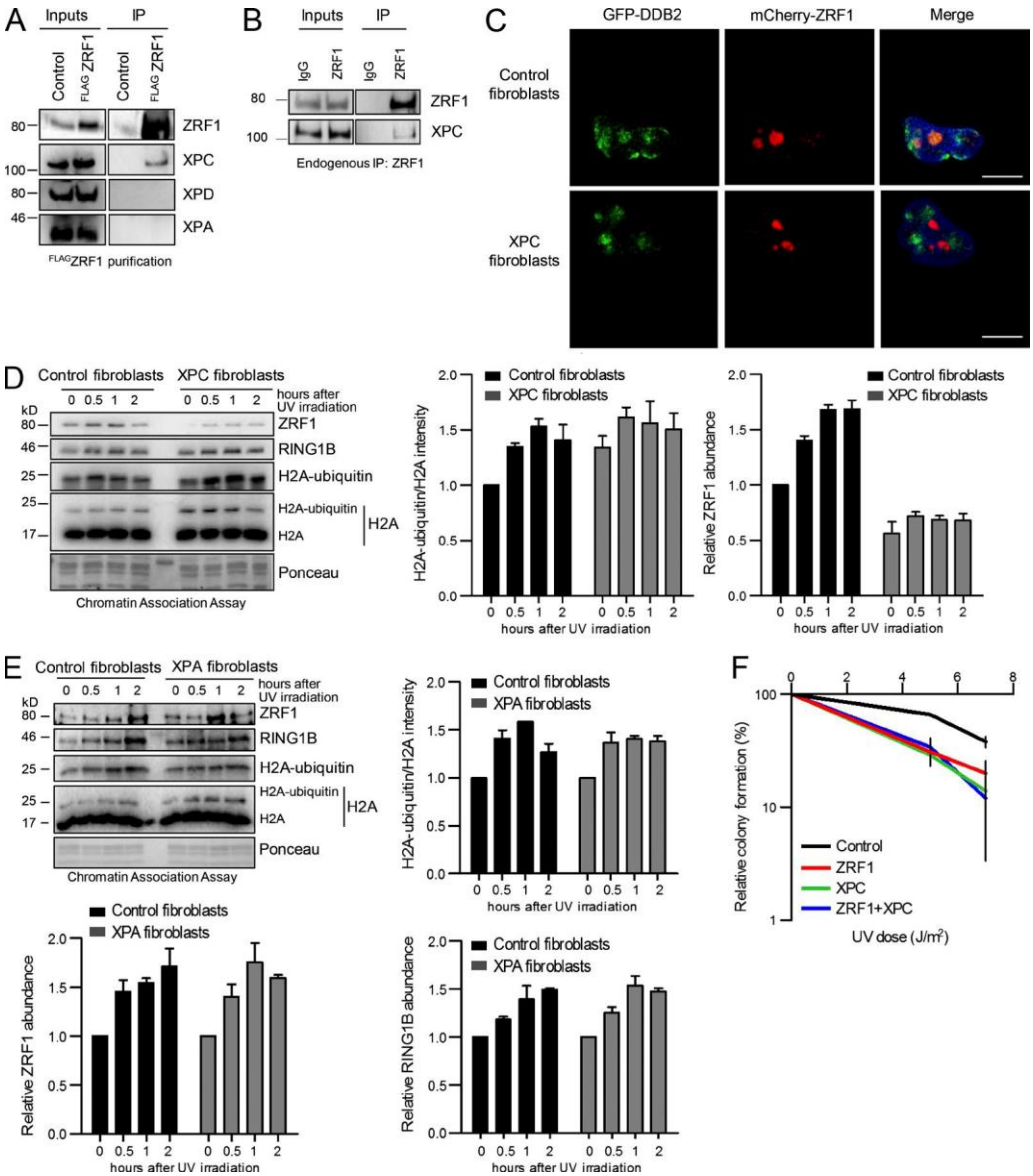

Figure 5. **ZRF1 interacts with XPC during UV-mediated DNA repair.** (A) ZRF1 speci cally binds to XPC. Control and ^{FLAG}ZRF1-expressing cells were irra- diated with UV light. After immunoprecipitation with FLAG-M2-agarose, the puri ed material was subjected to Western blotting and blots were incubated

with the indicated antibodies. Inputs correspond to 4%. (B) Endogenous immunopreciptiations with ZRF1 antibodies. Precipitates were subjected to Western blotting, and blots were incubated with the indicated antibodies. Inputs correspond to 3%. (C) ZRF1 localization to DNA damage sites is dependent on XPC. Control broblasts and XPC patient broblasts expressing both mCherry-ZRF1 and DDB2-GFP were UV irradiated (100 J/m^2) through a micropore membrane. Thirty minutes after irradiation, cells were preextracted and xed. DNA damage sites were visualized by DDB2-GFP. (D) ZRF1 enriches at chromatin after UV irradiation in a XPC-dependent manner. Chromatin association assays with control broblasts (GM16248) and XPC patient broblasts (GM15983) after UV irradiation. De–cross-linked material of the respective time points was subjected to Western blotting and probed with the indicated antibodies. The relative H2A-ubiquitin and ZRF1 abundance was calculated. Values are given as mean ± SEM (*n* = 3). (E) H2A ubiquitylation is not al- tered in XPA patient broblasts. Chromatin association assays with control broblasts (GM15876) and XPA broblasts (GM04312) after UV irradiation. De–cross-linked material of the respective time points was subjected to Western blotting and probed with the indicated antibodies.
Relative intensities of H2A-ubiquitin/H2A, ZRF1 and RING1B abundance were measured. Values are given as mean ± SEM (*n* = 3). (F) Epistasis analysis of ZRF1 and XPC. The relative colony formation potential of control or ZRF1 knockdown cell lines treated with control (Control; *ZRF1*) or XPC siRNA (*XPC*; *ZRF1+XPC*) was analyzed at different UV doses. Gene knockdown was con rmed by Western blots (not depicted). Values are given as mean ± SEM (*n* = 3). ubiquitylation and ZRF1 recruitment. Chromatin association assays of UV irradiated HEK293T cells treated with siRNAs (control, *CUL4B*). De–cross- linked material of the respective time points was subjected to Western blotting and probed with the indicated antibodies. The relative H2A-ubiquitin and ZRF1 abundance was calculated. Values are given as mean ± SEM (*n* = 3). (G) Tethering of ZRF1 to chromatin depends on DDB2 during NER. Chromatin asso- ciation assays in control broblasts (GM15876) and XPE (DDB2) broblasts (GM01389) after UV irradiation. De–cross-linked material of the respective time points was subjected to Western blotting and probed with the indicated antibodies. The relative RING1B and ZRF1 abundance was calculated. Values are given as mean ± SEM (*n* = 3).

lines (Fig. 8 D). After UV irradiation of cells, we performed NiNTA pull-down experiments under denaturing conditions to enrich for ubiquitylated proteins. We observed strong ubiquitylation of XPC only in control cells, whereas XPC ubiqui- tylation levels in ZRF1 and RING1B knockdown cells were reduced. Collectively these experiments suggest that ZRF1 likely regulates XPC ubiquitylation by facilitating the as- sembly of the UV–DDB–CUL4A complex. RING1B in turn provides a tethering platform for ZRF1, thereby indirectly affecting the remodeling process.

Based on our results, we propose that H2A ubiquitylation by the UV–RING1B complex is catalyzed early during damage recognition (Fig. 8 E). Our data illustrate for the rst time how E3 ligase complexes are remodeled at the DNA lesion site. The pre- sented results suggest that ZRF1 acts as a switch protein that re- models E3 ligases at or close to the DNA damage site (Fig. 8 E).

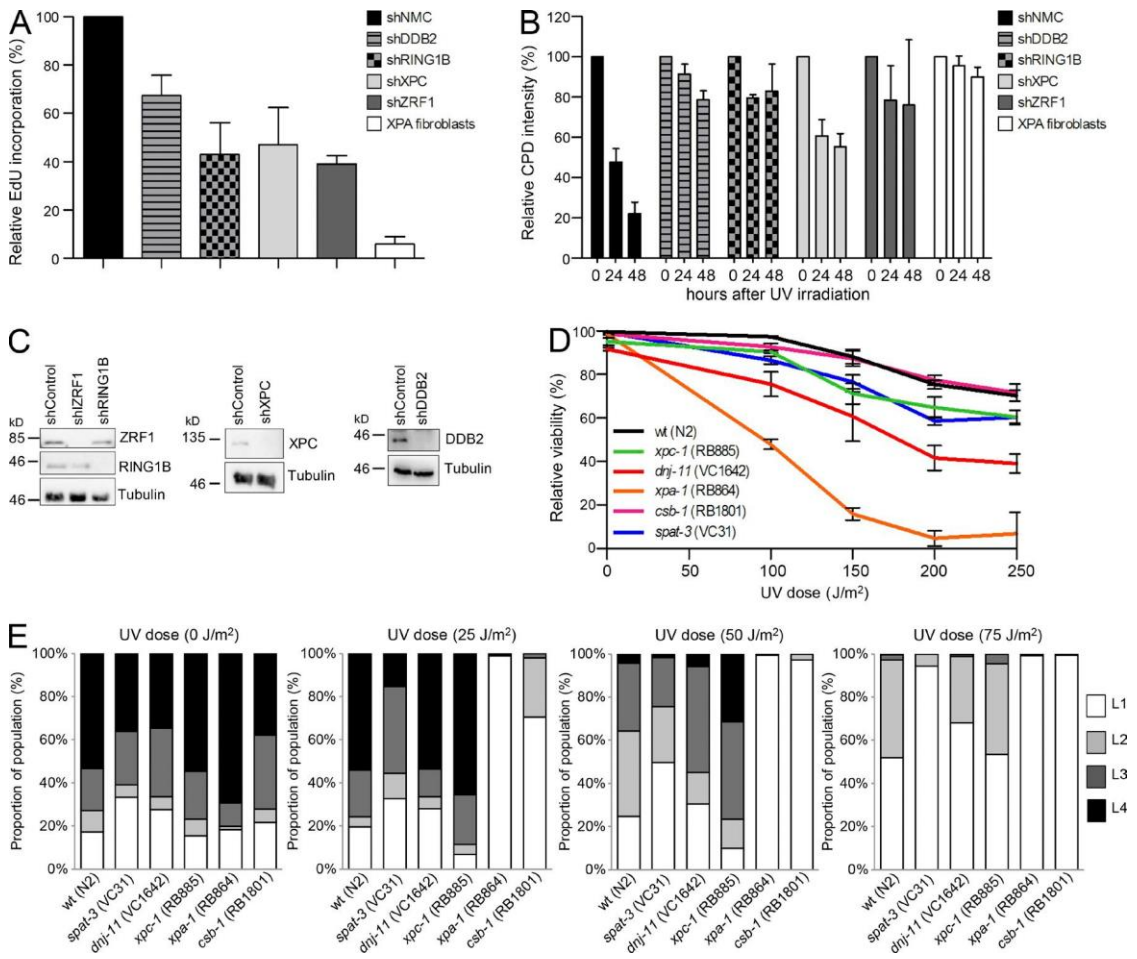

Figure 6. **ZRF1 and RING1B contribute to GG-NER.** (A) RING1B and ZRF1 knockdown broblasts are defective in UDS after UV irradiation. UDS was measured by EdU incorporation after UV treatment in MRC5 broblasts with shRNA-mediated knockdown of the indicated proteins. XPA broblasts were used as a positive control. Values are given as mean ± SEM. Data were acquired from three independent experiments (150–300 nuclei per sample). (B) RING1B and ZRF1 knockdown broblasts are defective in the removal of CPDs. The CPD removal was analyzed in MRC5 broblasts after knockdown of the indicated proteins in MRC5 broblasts and in XPA broblasts. Cells were irradiated with 10 J/m^2 and xed immediately or 24 or 48 h after irradiation and stained with CPD antibodies. The relative uorescence intensity was determined. Values are given as mean ± SEM. Data were acquired from three independent experiments (100–200 nuclei per sample). (C) MRC5 broblasts were treated with lentiviral particles containing the respective shRNA. Knock- down of the proteins levels was analyzed 48h after infection by Western blotting and incubation with the indicated antibodies. (D) *C. elegans* knockout mutants for ZRF1 (*dnj-11*) and RING1B (*spat-3*) show increased sensitivity toward UV irradiation. Late-L4 larval wild-type worms and the indicated mutants were irradiated with UV light at different doses, and the relative viability was determined by comparing hatched versus dead embryos (unhatched eggs). Values are given as mean ± SEM (n = 3). (E) *C. elegans* knockout mutants for dnj-11 and for spat-3 show only weak developmental arrest upon somatic UV irradiation. L1 larval worms were irradiated with UV light at different doses.
Relative larval-stage stalling was determined after 60 h by using a large particle ow cytometer (BioSorter platform; Union Biometrica), assaying at least 1,000 worms per condition

DISCUSSION

Monoubiquitylation of histone H2A is a hallmark of various DNA repair pathways. Nevertheless, it is still a matter of de- bate how and when different E3 ligases contribute to H2A ubiquitylation during the DNA damage response. Here, we have examined selected E3 ligases involved in UV-induced DNA damage repair. Our data point to RING1B as the main E3 ligase involved in H2A ubiquitylation at lysine 119 early during damage recognition in NER. Depletion of RNF168 or abrogation of UV–DDB–CUL4A E3 ligase function did not cause any signi cant changes in H2A ubiquitylation after UV irradiation. The UV–DDB–CUL4A E3 complex was previously shown to catalyze ubiquitylation of histone H2A (Kapetanaki et al., 2006). Our data show that the UV– DDB–CUL4A E3 ligase complex functions downstream of ZRF1, suggesting that it might ubiquitylate histone H2A at a later stage in the NER pathway (Fig. 7 D). Hence, we propose that the timing of E3 ligase action is an important feature of NER and other DNA repair pathways. In the same vein, it was demonstrated that RNF8-mediated H2A ubiquitylation is a relatively late event during NER (Marteijn et al., 2009). Our data extend this obser- vation, proposing that E3 ligases operate successively during the DNA damage response. In addition, E3 ligases target differ- ent lysines of histone H2A, adding another layer of complexity. For instance, at DSBs, RNF168 catalyzes the ubiquitylation of lysines 13 and 15 (Mailand et al., 2007; Mattiroli et al., 2012), whereas RING1B targets lysine 119 of histone H2A in both DSB repair and NER (Ui et al., 2015).

However, understanding the concerted action and the substrate speci city of E3 ligases in DNA repair needs further investigation.

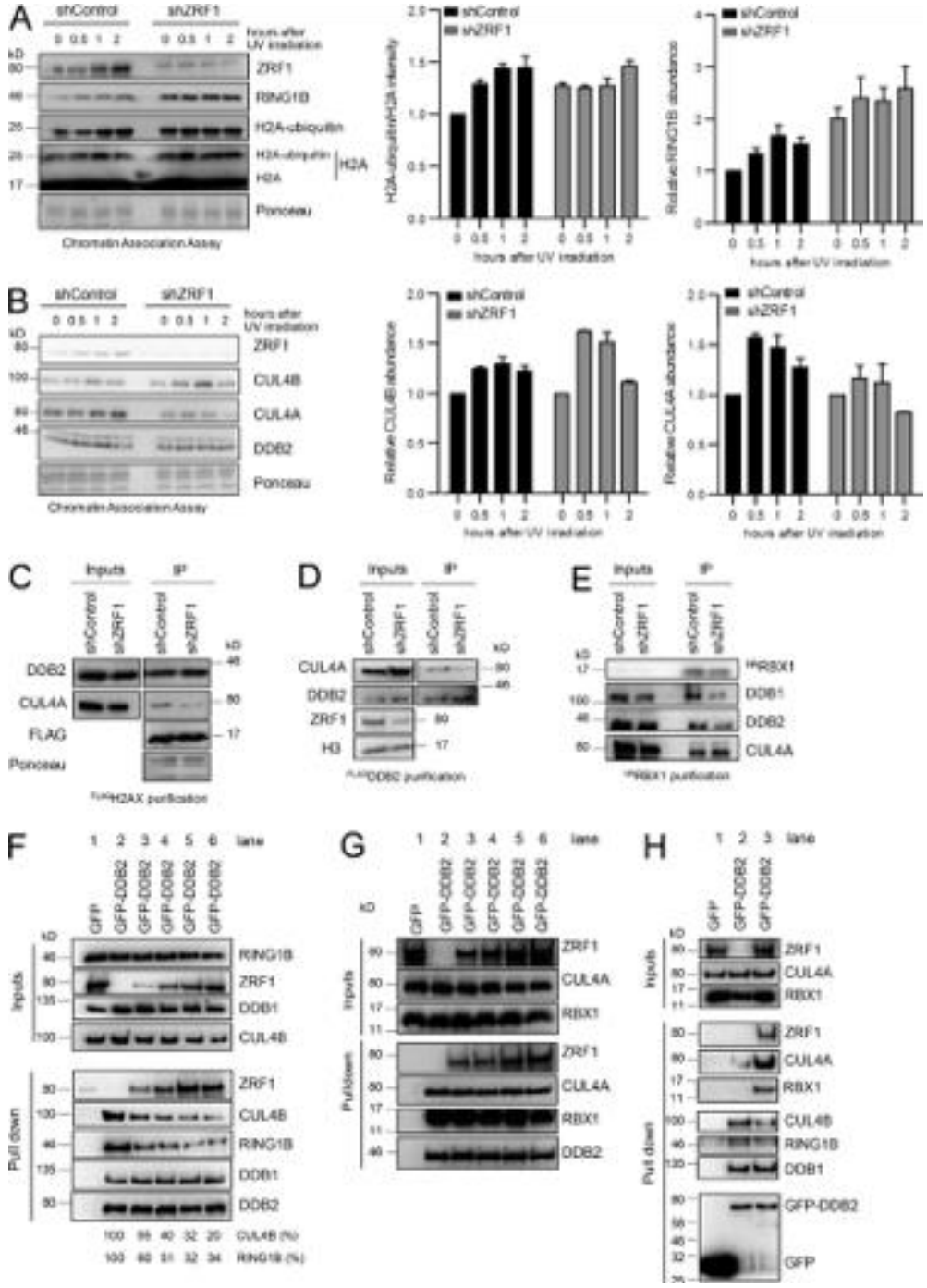

Figure 7. **ZRF1 facilitates the assembly of the UV–DDB–CUL4A E3 ligase complex.** (A) ZRF1 displaces RING1B from chromatin during NER. Chromatin association assays of control and ZRF1 knockdown HEK293T cell lines after UV irradiation. De–cross-linked material of the respective time points was subjected to Western blotting and probed with the indicated antibodies. The relative H2A ubiquitin and RING1B abundance was calculated. Values are given as mean ± SEM (n = 3). (B) ZRF1 regulates chromatin association of CUL4A and CUL4B. Chromatin association assays of control and ZRF1 knockdown HEK293T cell lines after UV irradiation. De–cross-linked material of the respective time points was subjected to Western blotting and probed with the indi- cated antibodies. The relative CUL4B and CUL4A abundance was calculated. Values are given as mean ± SEM (n = 3). (C) ZRF1 regulates CUL4A association with H2AX containing nucleosomes. Control cells and ZRF1 knockdown cells expressing ^{FLAG}H2AX were irradiated with UV. After immunoprecipitation with FLAG-M2-agarose,

the puri ed material was subjected to Western blotting and blots were incubated with the indicated antibodies. Inputs correspond to 3%. (D) Knockdown of ZRF1 modulates CUL4A association with DDB2. Control cells and ZRF1 knockdown cells expressing ^{FLAG}DDB2 were irradiated with UV light. After immunoprecipitation with FLAG-M2-agarose, the puri ed material was subjected to Western blotting and blots were incubated with the indicated antibodies. Inputs correspond to 3%. (E) Assembly of the UV–DDB–CUL4A E3 ligase is facilitated by ZRF1. Control cells and ZRF1 knockdown HEK293T cells expressing ^{HA}RBX1 were irradiated with UV light. After immunoprecipitation with HA-speci c antibodies the precipitated material was subjected to Western blotting, and blots were incubated with the indicated antibodies. Inputs correspond to 5%. (F) ZRF1 competes with CUL4B and RING1B for DDB2 binding in vitro. GFP and GFP-DDB2 immobilized on beads were incubated with equimolar amounts of puri ed DDB1, CUL4B, and RING1B and increasing amounts of ZRF1. ZRF1 levels were doubled stepwise reaching an eightfold molar excess of ZRF1 over the other components (relative molarity ZRF1: DDB1–CUL4B–RING1B; lane 3, 1:1; lane 4, 2:1; lane 5, 4:1; lane 6, 8:1). Precipitated material was subjected to Western blotting and blots were blots were incubated with the indicated antibodies. Inputs correspond to 5%.

RING1B and H2A ubiquitylation have been implicated in UV-mediated DNA damage repair about a decade ago (Bergink et al., 2006). However, the molecular mechanism of RING1B function still remained unclear. RING1B controls the basal levels of the highly abundant H2A-ubiquitin mark (Matsui et al., 1979; Wang et al., 2004). Thus, it might affect the nuclear pool of free ubiquitin and thereby indirectly ubiquitin signaling during DNA repair (Dantuma et al., 2006). Additionally, it was reported that knockdown of RING1B decreases nuclear ubiquitin levels and thus indirectly reduces histone ubiquitylation at damaged chromatin (Bergink et al., 2006). Our data refute these ideas, as we observe no global changes in the levels of ubiquitylated proteins in RING1B knockdown cells (Fig. S1, G and H). Thus, we rule out an indirect effect of RING1B knockdown, implying a DNA damage–speci c role of RING1B in H2A ubiquitylation. In particular, we provide evidence that RING1B constitutes a DNA damage–speci c E3 ligase, as it is speci cally recruited to DNA lesion sites induced by irradiation with a 405- nm laser (Fig. S1, D–F). This observation is also in agreement with a recent study demonstrating that RING1B is recruited to DSBs to promote local gene silencing (Ui et al., 2015). In light of these ndings, we addressed how RING1B interacts with the NER pathway, which is an essential DNA repair pathway implicated in repair of UV-mediated DNA damage. Previously, RING1B had been shown to mediate ubiquitylation of histones H2A and H2AX at DSBs together with its PRC1 binding partner, BMI-1 (Pan et al., 2011; Ui et al., 2015). After UV irradiation, RING1B seems to catalyze H2A ubiquitylation at lysine 119 independent of BMI-1, contrasting its function in DSB repair and during gene silencing. Our data indicate that RING1B binds to the DNA damage rec- ognition factor DDB2. Importantly, DDB2 determines whether RING1B is recruited to chromatin after UV irradiation, sug- gesting that DDB2 tethers RING1B to the damage site. DDB2 and RING1B represent subunits of a novel E3 ligase complex (UV–RING1B). In this complex, RING1B directly interacts with CUL4B (Fig. S3, E–I), which is in agreement with the common modular composition of cullin-RING E3 ligases (Petroski and Deshaies, 2005). The UV–RING1B complex is reminiscent of the well-described UV–DDB– CUL4A complex consisting of DDB1, DDB2, CUL4A, and RBX1 (Groisman et al., 2003). Our study suggests that DDB1–DDB2 might act as a platform that can either

accommodate CUL4B–RING1B or CUL4A– RBX1 modules, respectively. We have demonstrated that the UV–RING1B complex dramatically enhances ubiquitylation of histone H2A in vitro and in vivo. Hence, RING1B mediated monoubiquitylation at lysine 119 in DNA repair is performed by either the PRC1 complex or the UV–RING1B complex.

Because ZRF1 is one of the few known readers of H2A ubiquitin, we hypothesized that it would play a similar role in UV-mediated DNA repair as in cellular differentiation (Richly et al., 2010). In accordance, we observed that binding of ZRF1 to chromatin after UV irradiation depends both on presence of RING1B and its ability to bind H2A ubiquitin. More importantly, ZRF1 localizes to XPA and XPC foci after local irra- diation and knockdown of ZRF1 compromises DNA repair as seen by UDS and removal of CPD, describing ZRF1 as a new player in UV-mediated DNA repair. Drug-mediated inhibition of the RING1B activity signi cantly reduced ZRF1 colocaliza- tion with XPC, supporting a role for H2A ubiquitin in tethering ZRF1 to the damage site. On the other hand, UV irradiation– triggered recruitment of ZRF1 to chromatin depends on XPC. This close interplay between ZRF1 and XPC is further re ected by the interaction of both proteins and the epistasis analysis performed with either human cells or *C. elegans*, supporting a role for ZRF1 in GG-NER. In light of these ndings, we specu- late that XPC is probably involved in ZRF1's recruitment to the DNA damage site, whereas the H2A-ubiquitin mark is poten- tially needed to stably tether ZRF1 to chromatin. Most impor- tantly, ZRF1 mediates the remodeling of E3 ligase complexes at DNA damage sites (Fig. 7 D). Upon recruitment to chroma- tin, ZRF1 causes the exchange of the cullin-E3 ligase module, whereas DDB1 and DDB2 most probably remain bound to the lesion site. This observation does not exclude that UV–CUL4A complexes are generated independent of ZRF1. Still, our data re ect one plausible succession of events that take place at dam- aged chromatin. This function of ZRF1 is reminiscent of the Cand1 protein, which promotes the exchange of subunits from cullin–RING complexes (Pierce et al., 2013). We propose that ZRF1 acts in concert with other remodeling complexes or chap- erones at chromatin. In fact, ZRF1 was shown to cooperate with the HSP70 chaperone network during protein quality control (Qiu et al., 2006; Jaiswal et al., 2011). It remains to be tested whether ZRF1 cooperates with the HSP70 system, Cand1, or chromatin remodeling complexes during NER.

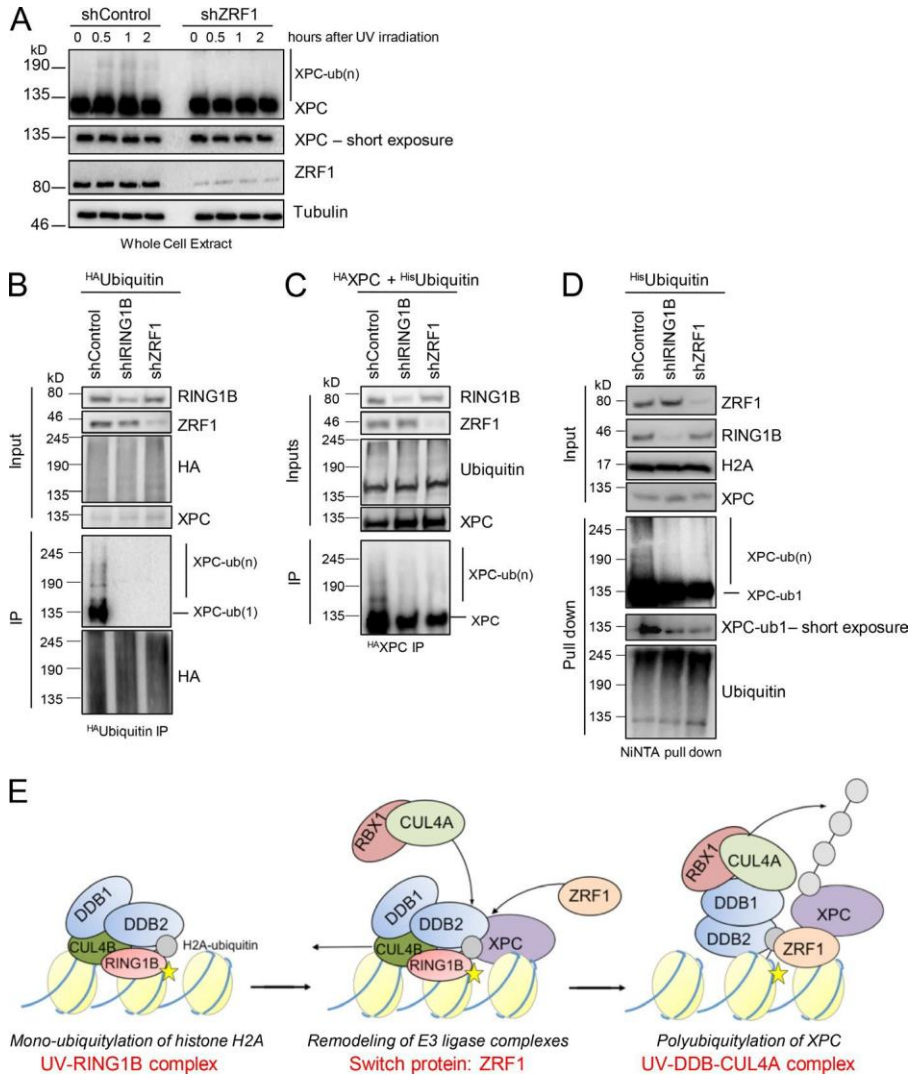

Figure 8. **ZRF1 regulates XPC ubiquitylation.** (A) ZRF1 facilitates XPC ubiquitylation after UV irradiation. Whole-cell extracts of control and ZRF1 knockdown HEK293T cells from the stated time points were subjected to Western blotting and probed with the indicated anti- bodies. (B) Role of RING1B and ZRF1 in XPC ubiquitylation. Control cells and RING1B and ZRF1 knockdown HEK293T cells expressing ^{HA}Ubiquitin were irradiated with UV light. After immunoprecipitation with HA-speci c an- tibody, the precipitated material was subjected to Western blotting and blots were incubated with the indicated antibodies. Inputs corre- spond to 5%. (C) Control cells and RING1B and ZRF1 knockdown HEK293T cells express- ing ^{HA}XPC and ^{HIS}Ubiquitin were irradiated with UV light. After immunoprecipitation with HA-speci c antibody, the precipitated material was subjected to Western blotting and blots were incubated with the indicated antibodies. Inputs correspond to 5%. (D) Control cells and RING1B and ZRF1 knockdown HEK293T cells expressing HISUbiquitin were irradiated with UV and harvested 1 h after UV exposure. Ubiquitylated proteins were puri ed by NiNTA agarose under denaturing conditions, and Western blots of the puri ed material were in- cubated with the indicated antibodies. (E) The UV–RING1B complex and ZRF1 cooperate during NER. DNA lesions (yellow star) are rec- ognized by the UV-RING1B complex (DDB1–DDB2–CUL4B–RING1B), which catalyzes ubiquitylation of histone H2A (gray sphere). ZRF1 is recruited to the lesion site by XPC and tethers to the

H2A-ubiquitin mark. ZRF1 causes the assembly of the UV–DDB–CUL4A complex, which subsequently catalyzes ubiquitylation of XPC. incubated with the indicated antibodies. Inputs correspond to 10%. (G) ZRF1 does not compete with CUL4A and RBX1 for binding to DDB1–DDB2. GFP and GFP-DDB2 immobilized on beads were incubated with equimolar amounts of puri ed DDB1, CUL4A and RBX1 and increasing amounts of ZRF1. ZRF1 levels were doubled stepwise reaching an eightfold molar excess of ZRF1 (relative molarity ZRF1: DDB1–CUL4A–RBX1; lane 3, 1:1; lane 4, 2:1; lane 5, 4:1; lane 6, 8:1). Precipitated material was subjected to Western blotting and blots were incubated with the indicated antibodies. Inputs correspond to 10%. (H) ZRF1 mediates the formation of the UV-DDB-CUL4A complex in vitro. GFP and GFP-DDB2 were coupled to beads and incubated with CUL4B, DDB1 and RING1B. After washing, GFP and GFP-DDB2 (UV–RING1B complex) beads were incubated with an estimated vefold excess of puri ed CUL4A and RBX1 (lanes 1–3) over the retained UV–RING1B complex. Simultaneously, ZRF1 (lanes 1 and 3) or GST (lane 2) was added to the incubations in equim- olar amounts. The precipitated material was subjected to Western blotting and blots were incubated with the indicated antibodies. Inputs correspond to 5%.

Materials and Methods

Cell lines and transfections

HEK293T and HEK293 cells were cultured in DMEM supple- mented with 10% FBS at 37°C and 5% CO_2. HeLa Kyoto cells sta- bly expressing cherry-PCNA were cultured in DMEM supplemented with 10% FCS and 1 μM/ml gentamycin and 2.5 μg/ml blastici- din. MRC5 (AG05965), normal skin broblasts (GM15876), XPE (GM01389), XPE (GM02415), XPC-complemented (GM16248), XPC (GM15983), XPA-complemented (GM15876), and XPA (GM04312 and GM00710) broblasts were purchased from Coriell Cell Repositories and cultured in DMEM, supplemented with 15% FBS. To generate cells stably expressing ^{FLAG}RING1B, HEK293 cells were transfected with a pCMV-2b-RING1B-FLAG plasmid and selected with G148 for 14 d. The expression of ^{FLAG}RING1B was veri ed by Western blot.

Transfection of HEK293T cells was either performed by the calcium phosphate coprecipitation method as described previously (Richly et al., 2010) or by Lipofectamine (Invitrogen) transfection. In- formation on the plasmids used is provided in Table S2.

UV irradiation and drug treatment

Cells were irradiated with 10 J/m^2 UV-C using a CL-1000 UV cross- linker (UVP) unless stated otherwise. PRT4165 (Abcam) was used at a concentration of 50 μM as described in Ismail et al. (2013).

Gene inactivation by shRNA/siRNA

HEK293T-shControl, HEK293T-shZRF1, and HEK293T-shRING1B were described previously and generated by transduction of HEK293T cells with retrovirus vector, containing shRNA against ZRF1 or RING1B (Richly et al., 2010). Gene knockdown in MRC5 broblasts was performed by introduction of MISSION pLKO.1-shRNA plas- mids (Sigma-Aldrich) targeting the respective gene using third gen- eration lentivirus system. Plasmids contained the following

sequences (Sigma-Aldrich): control (TRC1/1.5), ZRF1 (TRCN0000254058), RING1B (TRCN0000033697), DDB2 (TRCN0000083995), and XPC (TRCN0000307193).

The siRNA transfections were performed using Lipofect- amine 2000 according to the manufacturer's instructions (Invitro- gen). The following siRNAs were used in this study: control (SIC001; Sigma-Aldrich), CUL4A (esiRNA EHU011891; Sigma-Aldrich), RNF168 (SMARTpool D-011-22-(01–04); GE Healthcare), DDB2 (SASI_Hs01_00101645, SASI_Hs01_00101647; Sigma-Aldrich), BMI-1 (esiRNA EHU004421; Sigma-Aldrich), CUL4B (esiRNA EHU064911; Sigma-Aldrich), XPC (SASI_Hs01_00086530, SASI_

Chromatin association assays

HEK293T cells (unless stated otherwise) were irradiated with UV and cross-linked by formaldehyde at the indicated time points after UV irra- diation. Assays were essentially performed as published (Richly et al., 2010). In brief, cell pellets were resuspended in buffer A (100 mM Tris, pH 7.5, 5 mM $MgCl_2$, 60 mM KCl, 125 mM NaCl, 300 mM sucrose, 1% NP-40, and 0.5 mM DTT) and kept on ice for 10 min. After cen- trifuging nuclei pellet was lysed in a hypotonic solution (3mM EDTA, 0.2 mM EGTA, and 1 mM DTT) twice. The chromatin-containing pellet was solubilized in 2× Laemmli buffer, sonicated, and boiled to reverse cross-linking. Information on antibodies used for Western blots is provided in Table S4. All experiments were repeated at least three times. Band intensities from Western blots were measured as stated in the gure legends using ImageJ or ImageLab (Bio-Rad) software.

Immunoprecipitations and af nity puri cations

Cells were treated with UV and harvested 1 h after exposure unless stated otherwise. Cells were resuspended in buffer A (10 mM Hepes, pH 7.9, 1.5 mM $MgCl_2$, 10 mM KCl and 0.5 mM DTT, 1 mM PMSF, and protease inhibitors; Roche) and homogenized by 10 strokes in a Dounce homogenizer with a B-type pestle. After centrifugation, nuclei were resuspended in lysis buffer (20 mM Hepes, 150 mM NaCl, 2.5 mM EGTA, 2 mM EDTA, 0.1% Triton X-100, 0.5 mM DTT, 1 mM PMSF, and protease inhibitors; Roche) and soni ed using a Diagenode Bioruptor for 20 min on the high setting. To verify soni cation ef - ciency, DNA from the extracts analyzed by agarose gel electrophore- sis. Only samples containing DNA of 300 bp or smaller were used in the experiments. Protein extracts were then subjected to centrifugation (21,000 *g*, 4°C, 15 min), and the supernatant was incubated with anti- bodies overnight at 4°C. After incubation with protein A agarose beads for 2 h at 4°C, the immune complexes were washed extensively in lysis buffer and material retained on the beads was subjected to Western blotting. Information on antibodies used for immunoprecipitations and Western blots is provided in Table S4.

Af nity puri cations using FLAG-M2 agarose beads (Sigma- Aldrich) and Anti-HA Agarose beads (Sigma-Aldrich) were per- formed using the protocol stated for immunoprecipitations. Puri ca- tions involving the STREP tag were performed with STREP-Tactin beads (Iba LifeSciences) and Desthiobiotin (Sigma-Aldrich) accord- ing to the manufacturer's instructions. Puri cations involving the GFP tag were performed with GFP-Trap agarose beads (Chromo- Tek) according to the manufacturer's instructions. For puri cation of the proteins used in the in vitro experiments (Fig. S3 E: $^{\text{FLAG-STR EP}}$CUL4B, $^{\text{FLAG}}$DDB1, $^{\text{FLAG}}$RING1B, $^{\text{FLAG}}$ZRF1, $^{\text{FLAG}}$ZRF1, $^{\text{HA}}$RBX1, and

^{HA}CUL4A), the proteins were washed extensively on the beads with lysis buffer containing 1 M NaCl before elution with FLAG or HA peptide (Sigma-Aldrich).

In vitro ubiquitylation assays

In vitro ubiquitylation reactions were performed with 3 µg puri ed histone H2A (New England Biolabs, Inc.) or 5 µg recombinant nucle- osomes (Active Motif), 200 ng puri ed HIS-UBA1 (E1), 20 ng pu- ri ed GST-UBC5H (E2), 150 ng puri ed UV-RING1B (E3), or 150 ng GST (control) in UBAB buffer (25 mM Tris/HCl, pH 7.5, 50 mM NaCl, and 10 mM $MgCl_2$) supplemented with 20 mM ATP, 1.5 mg/ml ubiquitin, 10 mM DTT, and 1 U creatine phosphokinase. Reactions were kept at 37°C for the indicated times and subsequently sub- jected to Western blotting.

Purification of recombinant proteins

Proteins were puri ed as suggested by GE Healthcare (GST-tagged pro- teins) or QIAGEN (His-tagged proteins) after inducing BL21 bacterial strains transformed with the respective plasmids at an OD = 0.5 with 0.2 mM isopropyl-β-D-thiogalactoside for 4 h at 37°C or at 20°C for 14 h. The following recombinant proteins were purchased: H2A (New England Biolabs), Ubiquitin (Boston Biochem), nucleosomes (Active Motif), GST-RBX1 (Novus Biologicals), and RAD23A (Abcam).

GST pull-downs

Puri ed GST–proteins were bound in equimolar amounts to glutathi- one beads (Amersham) in binding buffer (20 mM Tris, pH 7.4, 150 mM NaCl, and 0.1% Triton X-100). Loaded beads were washed in the same buffer and used for incubation with puri ed proteins for 2 h at 4°C. After extensive washing in binding buffer, the retained material was subjected to Western blotting.

Purification of ubiquitin conjugates from cells

Cells expressing HIS-tagged ubiquitin were lysed in lysis buffer (8 M urea, 100 mM NaH_2PO_4, and 10 mM Tris, pH 8.0) 1 h after UV irra- diation. Ubiquitylated proteins were retained on NiNTA agarose after washing with wash buffer (8 M urea, 100 mM NaH_2PO_4, 10 mM Tris, pH 6.3, 300 mM NaCl, and 0.1% Triton X-100) and detected by West- ern blotting using the indicated antibodies.

Fractionation of cell extracts

HEK293T cells were harvested by trypsinization and the cell pellet was divided in two equal parts. One part was resuspended in Laemmli buf- fer and sonicated (whole-cell extract), and the other was washed twice with PBS and resuspended in buffer A (10 mM Hepes, pH 7.9, 10 mM KCl, 1.5 mM $MgCl_2$, 0.34 M sucrose, 10% glycerol, 1 mM DTT, pro- tease inhibitors, and 0.1% Triton X-100) and cells were incubated for 8 min on ice. Subsequently, cells were spun down (4°C, 1,300 *g*, 5 min). The supernatant (cytoplasmic fraction) was collected, precipitated with TCA, and resuspended in Laemmli buffer. Nuclei were washed twice with buffer A, resuspended in Laemmli buffer, and sonicated. Whole- cell extract, cytoplasmic, and nuclear fractions were subjected to West- ern blotting as indicated.

Mass spectrometry analysis

Mass spectrometry sample preparation, measurement and database search were performed as described previously (Bluhm et al., 2016). Gradient lengths of 45 or 105 min were chosen depending on the im- munoprecipitated material obtained. Raw les were processed with MaxQuant (version 1.5.2.8) and searched against the *Homo sapiens* UniProt database (February 25, 2012) using the Andromeda search en- gine integrated into MaxQuant and default settings were applied. Pro- teins with at least two peptides, one of them unique, count as identi ed.

Fluorescence microscopy

Experiments were performed with MRC5 broblasts and patient- derived broblasts. Cells were transfected with mCherry-ZRF1 and GFP-DDB2 expressing plasmids. Cells were exposed to localized UV damage (100 J/m^2) using a micropore membrane with 5-μm pore size as described previously (Katsumi et al., 2001). Preextraction was per- formed with CSK supplemented with 0.2% Triton X-100 at 30 min after UV and then xed in 4% PFA. Cells were stained with XPA (Novus Biologicals) or XPC (Cell Signaling Technology) antibodies overnight at 4°C. After washing, coverslips were incubated with Alexa Fluor 488 uorophore–conjugated secondary antibodies (Thermo Fisher Scienti c) and mounted in Vectashield with DAPI. Images were acquired with the LAS AF software (Leica Biosystems) using a TCS SP5 confocal microscope (Leica Biosystems) with a 63×/1.4 oil-immersion objective. For colocalization studies, ∼100 lesions were counted per condition.

Imaging and microirradiation experiments

For microirradiation, HeLa-Kyoto Cherry-PCNA cells were grown on cover slide dishes and transfected with the indicated constructs using polyethylenimine. Imaging and microirradiation experiments were performed using an UltraVIEW VoX spinning-disc confocal system (PerkinElmer) in a closed live-cell microscopy chamber (ACU; Perkin- Elmer) at 37°C with 5% CO_2 and 60% humidity, mounted on a Nikon TI microscope (Nikon). Images were taken with a CFI Apochromat 60×/1.45 NA oil immersion objective. GFP and Cherry or mRFP were imaged with 488 and 561 nm laser excitation and 527 ± 55 and 612 ± 70 nm (full width at half maximum) emission lters, respectively. For microirradiation, a preselected spot (1 μm diameter) within the nucleus was microirradiated for 1,200 ms with the 405-nm laser resulting in 1 mJ. Before and after microirradiation, confocal image series of one midnucleus z section were recorded in 2-s intervals. For evaluation of the accumulation kinetics between 4 and 12 cells were analyzed. Im- ages were rst corrected for cell movement (ImageJ plugin StackReg and transformation mode Rigid body), and mean intensity of the irradi- ated region was divided by mean intensity of the whole nucleus (both corrected for background) using ImageJ software.
Maximal accumula- tion represents the highest ratio from each experiment.

Microscopy on skin biopsy specimens

Human skin sections were taken from material biopsied from patients who had given their written consent and were provided by R. Greinert and B. Volkmer (Dermatology Center Buxtehude, Buxtehude, Ger- many). Biopsy specimens were taken from either the cheek (UV ex- posed) or

groin (not exposed), and 7-µm cryosections were prepared after freezing in liquid nitrogen. The sections were mounted on glass slides and xed in 100% MeOH and 100% acetone for 10 min, each at −20°C. For immunostaining, the sections were rehydrated in PBS, and antigen retrieval was performed at 80°C in sodium citrate buffer (10 mM sodium citrate, pH 6.0) overnight. Then the sections were blocked in 4% BSA in PBS for 30 min before the rst antibody was applied in 1% BSA, 0.1% Triton X-100 in PBS (ZRF1; self-made), H2A ubiquitin (Cell Signaling Technology), RING1B (self-made; all diluted 1:100), and mouse DDB2 (1:20; Abcam). For CPD detection, DNA was additionally denatured for 3 min in 0.1 N NaOH/70% ethanol after the antigen retrieval followed by dehydration in 70%, 90%, and 100% ethanol. The CPD antibody (Kamiya) was used at a dilution of 1:100. Primary antibodies were incubated for 3 h at room temperature, followed by three washes in PBS. Secondary antibodies (anti–mouse IgG Alexa Fluor 488; Invitrogen; and anti–rabbit IgG-Cy3 and anti– rabbit IgG TexasRed; Jackson ImmunoResearch Laboratories, Inc.) were added at 1:500 for 1 h at room temperature. Sections were then washed three times in PBS and stained with 10 µM DAPI for 10 min before being mounted in Vectashield. Skin sections were imaged using an Axiovert 200 (ZEISS) equipped with a 40× Planneo uar 1.3 NA ob- jective lens and single channels were recorded with a black and white Axicam mRM (ZEISS). Quanti cation of signals on the single-cell level was performed using ImageJ. After selecting random nuclei in the DAPI channel, the mean and integrated intensities of the red and green channels were measured. All intensities are normalized to the DNA content of the corresponding nucleus. At least 200 nuclei were analyzed in at least three sections.

Colony formation assay

HEK293T control and knockdown cell lines were transfected with the respective siRNAs with Lipofectamine (Invitrogen) according to the manufacturer's protocol. Details on the respective transfections are given in the gure legends. Cells were plated on tissue culture plates at a density of 1,000 cells per plate 24 h after transfection. Cells were irradiated with the indicated UV dose 48 h after transfection. Colonies were counted 7 d after irradiation. Numbers of colonies formed after UV irradiation were normalized against the non-UV–treated control.

UDS

UDS experiments were performed as described previously (Jia et al., 2015). In brief, MRC5 broblasts were transduced with lentiviral par- ticles expressing the respective shRNAs. XPA broblasts were used as a positive control. After viral transduction, the cells were serum starved for 24 h, irradiated with UV light (20 J/m^2), and incubated with 10 µM EdU (Thermo Fisher Scienti c) for 2 h. Alexa Fluor 555 azide (Thermo Fisher Scienti c) was conjugated to EdU using the Click-reaction. The coverslips were mounted in Vectashield with DAPI. Images were acquired with the LAS AF software (Leica Bio- systems) using a AF-7000 wide eld microscope (Leica Biosystems) with a 63×/1.4 oil immersion objective and an ORCA CCD camera (Hamamatsu). Images were analyzed using ImageJ. DAPI was used to de ne nuclei, and EdU intensity within nuclei was measured after background subtraction. A total of 150–300 nuclei were analyzed per sample. Mean intensities of +UV and −UV conditions for all cells were calculated and used to estimate the DNA repair occurring in the particular sample.

Removal of CPDs

MRC5 broblasts were transduced with lentiviral particles express- ing the respective shRNAs. XPA broblasts were used as a positive control. 24 h after viral transduction, cells were replated on cover- slips, exposed to UV light, and xed at the indicated time points. Cells were stained with CPD antibody (Cosmo Bio) using the man- ufacturer's protocol, followed by incubation with Alexa Fluor 488 uorophore–conjugated secondary antibodies (Thermo Fisher Sci- enti c). The cells were mounted in Vectashield with DAPI, and im- ages were acquired with the LAS AF software (Leica Biosystems) using an AF-7000 wide eld microscope (Leica Biosystems) with a 63×/1.4 oil-immersion objective and an ORCA CCD camera (Ham- amatsu Photonics). Images were analyzed using ImageJ. DAPI was used to de ne nuclei, and CPD intensity within nuclei was mea- sured after background subtraction. 100–200 nuclei were analyzed per sample. Mean intensities of +UV and −UV conditions for all cells were calculated and used to estimate the DNA repair occurring in the particular sample.

C. elegans culture

Nematodes were cultured on agar plates at 20°C according to standard procedures. Strains were provided by the Caenorhabditis Genetics Cen- ter, which is funded by National Institutes of Health Of ce of Research Infrastructure Programs (P40 OD010440). The following strains were used: wild type (N2 Bristol), VC31/*spat-3* (gk22; WBGene00020496), DL74/*mig-32* (n4275; WBGene00008684), VC1642/*dnj-11* (gk1025; WBGene00001029), RB885/*xpc-1*(ok734; WBGene00022296), RB1801/*csb-1*(ok2335; WBGene00000803), and RB864/*xpa-1* (ok698; WBGene00006963). Mutant strains were outcrossed at least three times to the wild-type strain (N2).

Measuring DNA damage response in the C. elegans germline

The L4 survival assay was performed as described previously (Craig et al., 2012). In brief, late-L4 larval hermaphrodites were ir- radiated with different doses of UV light. The damage sensitivity of the meiotic pachytene cells of the germline was measured by de- termining the survival of embryos produced between 24 and 30 h after L4-stage irradiation.

Measuring DNA damage response in the C. elegans soma via developmental arrest The L1 development arrest assay was performed as described previ- ously (Craig et al., 2012). In brief, L1-stage worms were synchronized via starvation and irradiated with different doses of UV light. Relative larval-stage stalling was determined after 60 h, when control worms were fully fertile.
Larval-stage scoring was done using a large-particle ow cytometer (BioSorter platform; Union Biometrica).

RNAi via feeding

Worms were fed at L1 larval stage with *Escherichia coli* feeding clones (HT115), which express dsRNAi targeted against a gene of interest. In brief a single colony of a clone was grown overnight in LB contain- ing 100 μg/ml ampicillin (37°C, 200 rpm). Subsequently the clone was induced for 1 h by adding 4 mM IPTG to the LB media. The induced bacteria then was spun down at room temperature and resuspended in nematode growth medium with 4 mM IPTG. L1 larval worms were directly grown in this medium at 20°C until they reached late L4 stage or early adulthood (50–60 h).

Online supplemental material

Fig. S1 shows the function of RING1B in H2A ubiquitylation during UV-triggered DNA repair and recruitment of RING1B to UV-mediated

DNA damage sites. Fig. S2 shows the BMI-1 independent interaction of RING1B–DDB2. RING1B, H2A ubiquitin, and DDB2 staining in human skin sections and H2A ubiquitin accumulation after UV irradiation in GM02415 broblasts. Fig. S3 shows interactions of UV– RING1B subunits and competition of RING1B and RBX-1 for binding to CUL4B. Fig. S4 shows a quanti cation of ZRF1 localization to DNA damage sites and its dependency on H2A ubiquitin. Fig. S5 shows the ZRF1 and XPC interplay and effect on UV sensitivity assays in *C. elegans*.
Table S1 shows a data summary of developmental arrest assay in mutant strains. Table S2 lists plasmids used in this study. Table S3 lists the shRNA and siRNA sequences used for this study. Table S4 lists antibodies used in this study. Table S5 provides peptide numbers and protein names for all proteins identi ed in the mass spectrometry analysis after sequential immunoprecipitations with FLAG and RING1B antibodies. Table S6 provides peptide numbers and protein names for all proteins identi ed in the mass spectrometry analysis of puri ed UV– RING1B complex. Online supplemental material is available at http://www.jcb.org/cgi/content/full/jcb.201506099/DC1.

Acknowledgments

We thank the members of the Richly laboratory for comments on the manuscript. We thank M. Hanulova for help with processing data for UDS experiments. We thank S. Papaefstathiou, S. Schaffer, and S. Meyer for excellent technical work.

This work was supported by grants from the Boehringer Ingelheim Foun- dation and the Deutsche Forschungsgemeinschaft (RI-2413/1-1). M.C. Cardoso was supported by a grant from the Bundesministerium für Bildung und Forschung (02NUK017D). We thank the Institute of Molecu- lar Biology Proteomics and Microscopy core facilities for their expert as- sistance. *C. elegans* strains were kindly provided by the Caenorhabditis Genetics Center, which is funded by the National Institutes of Health Office of Research Infrastructure Programs (P40 OD010440).

The authors declare no competing financial interests. Submitted:

22 June 2015 Accepted: 16 March 201

Alekseev, S., H. Kool, H. Rebel, M. Fousteri, J. Moser, C. Backendorf, F.R. de Gruijl, H. Vrieling L.H. Mullenders. 2005. Enhanced DDB2 expression protects mice from carcinogenic effects of chronic UV-B irradiation. *Cancer Res.* 65:10298–10306. http://dx.doi.org/10.1158 /0008-5472.CAN-05-2295

Angers, S., T. Li, X. Yi, M.J. MacCoss, R.T. Moon, and N. Zheng. 2006. Molecular architecture and assembly of the DDB1-CUL4A ubiquitin li- gase machinery. *Nature.* 443:590–593.

Araki, M., C. Masutani, M. Takemura, A. Uchida, K. Sugasawa, J. Kondoh, Y. Ohkuma, and F. Hanaoka. 2001. Centrosome protein centrin 2/ caltractin 1 is part of the xeroderma pigmentosum group C complex that initiates global genome nucleotide excision repair. *J. Biol. Chem.* 276:18665–18672. http://dx.doi.org/10.1074/jbc.M100855200

Bergink, S., F.A. Salomons, D. Hoogstraten, T.A. Groothuis, H. de Waard, J. Wu, L. Yuan, E. Citterio, A.B. Houtsmuller, J. Neefjes, et al. 2006. DNA damage triggers nucleotide excision repair-dependent monoubiquitylation of histone H2A. *Genes Dev.* 20:1343–1352. http://dx.doi.org/10.1101/ gad.373706

Bergink, S., W. Toussaint, M.S. Luijsterburg, C. Dinant, S. Alekseev, J.H. Hoeijmakers, N.P. Dantuma, A.B. Houtsmuller, and W. Vermeulen. 2012. Recognition of DNA damage by XPC coincides with disruption of the XPC-RAD23 complex. *J. Cell Biol.* 196:681–688. http://dx.doi.org /10.1083/jcb.201107050

Bluhm, A., N. Casas-Vila, M. Scheibe, and F. Butter. 2016. Reader interactome of epigenetic histone marks in birds. *Proteomics.* 6:427-436. http://dx.doi .org/10.1002/pmic.201500217

Bohr, V.A., D.S. Okumoto, and P.C. Hanawalt. 1986. Survival of UV-irradiated mammalian cells correlates with ef cient DNA repair in an essential gene. *Proc. Natl. Acad. Sci. USA.* 83:3830–3833. http://dx.doi.org/10 .1073/pnas.83.11.3830

Chagraoui, J., J. Hébert, S. Girard, and G. Sauvageau. 2011. An anticlastogenic function for the Polycomb Group gene Bmi1. *Proc. Natl. Acad. Sci. USA.* 108:5284–5289. http://dx.doi.org/10.1073/pnas.1014263108

Craig, A.L., S.C. Moser, A.P. Bailly, and A. Gartner. 2012. Methods for studying the DNA damage response in the Caenorhabdatis elegans germ line. *Methods Cell Biol.* 107:321–352. http://dx.doi.org/10.1016/B978-0-12 -394620-1.00011-4

Dantuma, N.P., T.A. Groothuis, F.A. Salomons, and J. Neefjes. 2006. A dynamic ubiquitin equilibrium couples proteasomal activity to chromatin remodeling. *J. Cell Biol.* 173:19–26. http://dx.doi.org/10.1083/jcb .200510071

de Laat, W.L., N.G. Jaspers, and J.H. Hoeijmakers. 1999. Molecular mechanism of nucleotide excision repair. *Genes Dev.* 13:768–785. http://dx.doi.org /10.1101/gad.13.7.768

Doil, C., N. Mailand, S. Bekker-Jensen, P. Menard, D.H. Larsen, R. Pepperkok, J. Ellenberg, S. Panier, D. Durocher, J. Bartek, et al. 2009. RNF168 binds and ampli es ubiquitin conjugates on damaged chromosomes to allow accumulation of repair proteins. *Cell.* 136:435–446. http://dx.doi.org/10 .1016/j.cell.2008.12.041

Fitch, M.E., S. Nakajima, A. Yasui, and J.M. Ford. 2003. In vivo recruitment of XPC to UV-induced cyclobutane pyrimidine dimers by the DDB2 gene product. *J. Biol. Chem.* 278:46906–46910. http://dx.doi.org/10.1074/jbc .M307254200

Fousteri, M., and L.H. Mullenders. 2008. Transcription-coupled nucleotide excision repair in mammalian cells: molecular mechanisms and biological effects. *Cell Res.* 18:73–84. http://dx.doi.org/10.1038/cr.2008.6

Friedberg, E.C. 2001. How nucleotide excision repair protects against cancer. *Nat. Rev. Cancer.* 1:22–33. http://dx.doi.org/10.1038/35094000

Ginjala, V., K. Nacerddine, A. Kulkarni, J. Oza, S.J. Hill, M. Yao, E. Citterio, M. van Lohuizen, and S. Ganesan. 2011. BMI1 is recruited to DNA breaks and contributes to DNA damage-induced H2A ubiquitination and repair. *Mol. Cell. Biol.* 31:1972–1982. http://dx.doi.org/10.1128/MCB .00981-10

Groisman, R., J. Polanowska, I. Kuraoka, J. Sawada, M. Saijo, R. Drapkin, A.F. Kisselev, K. Tanaka, and Y. Nakatani. 2003. The ubiquitin ligase activity in the DDB2 and CSA complexes is differentially regulated by the COP9 signalosome in response to DNA damage. *Cell.* 113:357–367. http://dx.doi.org/10.1016/S0092-8674(03)00316-7

Guerrero-Santoro, J., M.G. Kapetanaki, C.L. Hsieh, I. Gorbachinsky, A.S. Levine, and V. Rapić-Otrin. 2008. The cullin 4B-based UV-damaged DNA-binding protein ligase binds to UV-damaged chromatin and ubiquitinates histone H2A. *Cancer Res.* 68:5014–5022. http://dx.doi.org /10.1158/0008-5472.CAN- 07-6162

Hoogstraten, D., S. Bergink, J.M. Ng, V.H. Verbiest, M.S. Luijsterburg, B. Geverts, A. Raams, C. Dinant, J.H. Hoeijmakers, W. Vermeulen, and A.B. Houtsmuller. 2008. Versatile DNA damage detection by the global genome nucleotide excision repair protein XPC. *J. Cell Sci.* 121:2850– 2859. http://dx.doi.org/10.1242/jcs.031708

Ismail, I.H., C. Andrin, D. McDonald, and M.J. Hendzel. 2010. BMI1-mediated histone ubiquitylation promotes DNA double-strand break repair. *J. Cell Biol.* 191:45–60. http://dx.doi.org/10.1083/jcb.201003034

Ismail, I.H., D. McDonald, H. Strickfaden, Z. Xu, and M.J. Hendzel. 2013. A small molecule inhibitor of polycomb repressive complex 1 inhibits ubiquitin signaling at DNA double-strand breaks. *J. Biol. Chem.* 288:26944–26954. http://dx.doi.org/10.1074/jbc.M113.461699

Jaiswal, H., C. Conz, H. Otto, T. Wöl e, E. Fitzke, M.P. Mayer, and S. Rospert. 2011. The chaperone network connected to human ribosome-associated complex. *Mol. Cell. Biol.* 31:1160–1173. http://dx.doi.org/10.1128/MCB .00986-10

Jia, N., Y. Nakazawa, C. Guo, M. Shimada, M. Sethi, Y. Takahashi, H. Ueda, Y. Nagayama, and T. Ogi. 2015. A rapid, comprehensive system for assaying DNA repair activity and cytotoxic effects of DNA-damaging reagents. *Nat. Protoc.* 10:12–24. http://dx.doi.org/10.1038/nprot.2014 .194

Kapetanaki, M.G., J. Guerrero-Santoro, D.C. Bisi, C.L. Hsieh, V. Rapić-Otrin, and A.S. Levine. 2006. The DDB1-CUL4ADDB2 ubiquitin ligase is de cient in xeroderma pigmentosum group E and targets histone H2A at UV-damaged DNA sites. *Proc. Natl. Acad. Sci. USA.* 103:2588–2593. http://dx.doi.org/10.1073/pnas.0511160103

Karakuzu, O., D.P. Wang, and S. Cameron. 2009. MIG-32 and SPAT-3A are PRC1 homologs that control neuronal migration in Caenorhabditis elegans. *Development.* 136:943–953.

http://dx.doi.org/10.1242/dev.029363

Katsumi, S., N. Kobayashi, K. Imoto, A. Nakagawa, Y. Yamashina, T. Muramatsu, T. Shirai, S. Miyagawa, S. Sugiura, F. Hanaoka, et al.. 2001. In situ visualization of ultraviolet-light-induced DNA damage repair in locally irradiated human broblasts. *J. Invest. Dermatol.* 117:1156–1161. http://dx.doi.org/10.1046/j.0022-202x.2001.01540.x

Lans, H., and W. Vermeulen. 2011. Nucleotide excision repair in Caenorhabditis elegans. *Mol. Biol. Int.* 2011:542795. http://dx.doi.org/10.4061/2011/542795

Luijsterburg, M.S., J. Goedhart, J. Moser, H. Kool, B. Geverts, A.B. Houtsmuller, L.H. Mullenders, W. Vermeulen, and R. van Driel. 2007. Dynamic in vivo interaction of DDB2 E3 ubiquitin ligase with UV-damaged DNA is independent of damage-recognition protein XPC. *J. Cell Sci.* 120:2706– 2716. http://dx.doi.org/10.1242/jcs.008367

Mailand, N., S. Bekker-Jensen, H. Faustrup, F. Melander, J. Bartek, C. Lukas, and J. Lukas. 2007. RNF8 ubiquitylates histones at DNA double-strand breaks and promotes assembly of repair proteins. *Cell.* 131:887–900. http ://dx.doi.org/10.1016/j.cell.2007.09.040

Marteijn, J.A., S. Bekker-Jensen, N. Mailand, H. Lans, P. Schwertman, A.M. Gourdin, N.P. Dantuma, J. Lukas, and W. Vermeulen. 2009. Nucleotide excision repair-induced H2A ubiquitination is dependent on MDC1 and RNF8 and reveals a universal DNA damage response. *J. Cell Biol.* 186:835–847. http://dx.doi.org/10.1083/jcb.200902150

Marteijn, J.A., H. Lans, W. Vermeulen, and J.H. Hoeijmakers. 2014. Understanding nucleotide excision repair and its roles in cancer and ageing. *Nat. Rev. Mol. Cell Biol.* 15:465–481. http://dx.doi.org/10.1038/nrm3822

Masutani, C., K. Sugasawa, J. Yanagisawa, T. Sonoyama, M. Ui, T. Enomoto, K. Takio, K. Tanaka, P.J. van der Spek, D. Bootsma, et al. 1994. Puri cation and cloning of a nucleotide excision repair complex involving the xeroderma pigmentosum group C protein and a human homo- logue of yeast RAD23. *EMBO J.* 13:1831–1843.

Matsui, S.I., B.K. Seon, and A.A. Sandberg. 1979. Disappearance of a structural chromatin protein A24 in mitosis: implications for molecular basis of chromatin condensation. *Proc. Natl. Acad. Sci. USA.* 76:6386–6390. http://dx.doi.org/10.1073/pnas.76.12.6386

Mattiroli, F., J.H. Vissers, W.J. van Dijk, P. Ikpa, E. Citterio, W. Vermeulen, J.A. Marteijn, and T.K. Sixma. 2012. RNF168 ubiquitinates K13-15 on H2A/H2AX to drive DNA damage signaling. *Cell.* 150:1182–1195. http://dx.doi.org/10.1016/j.cell.2012.08.005

Morey, L., and K. Helin. 2010. Polycomb group protein-mediated repression of transcription. *Trends Biochem. Sci.* 35:323–332. http://dx.doi.org/10 .1016/j.tibs.2010.02.009

Moser, J., M. Volker, H. Kool, S. Alekseev, H. Vrieling, A. Yasui, A.A. van Zeeland, and L.H. Mullenders. 2005. The UV-damaged DNA binding protein mediates ef cient targeting of the nucleotide excision repair complex to UV-induced photo lesions. *DNA Repair (Amst.).* 4:571–582. http://dx.doi.org/10.1016/j.dnarep.2005.01.001

Nishi, R., S. Alekseev, C. Dinant, D. Hoogstraten, A.B. Houtsmuller, J.H. Hoeijmakers, W. Vermeulen, F. Hanaoka, and K. Sugasawa. 2009. UV-DDB-dependent regulation of nucleotide excision repair kinetics in

living cells. *DNA Repair (Amst.).* 8:767–776. http://dx.doi.org/10.1016/j .dnarep.2009.02.004

Pan, M.R., G. Peng, W.C. Hung, and S.Y. Lin. 2011. Monoubiquitination of H2AX protein regulates DNA damage response signaling. *J. Biol. Chem.* 286:28599–28607. http://dx.doi.org/10.1074/jbc.M111.256297

Petroski, M.D., and R.J. Deshaies. 2005. Function and regulation of cullin-RING ubiquitin ligases. *Nat. Rev. Mol. Cell Biol.* 6:9–20. http://dx.doi.org/10 .1038/nrm1547

Pierce, N.W., J.E. Lee, X. Liu, M.J. Sweredoski, R.L. Graham, E.A. Larimore, M. Rome, N. Zheng, B.E. Clurman, S. Hess, et al. 2013. Cand1 promotes assembly of new SCF complexes through dynamic exchange of F box proteins. *Cell.* 153:206–215. http://dx.doi.org/10.1016/j.cell .2013.02.024

Qiu, X.B., Y.M. Shao, S. Miao, and L. Wang. 2006. The diversity of the DnaJ/ Hsp40 family, the crucial partners for Hsp70 chaperones. *Cell. Mol. Life Sci.* 63:2560–2570. http://dx.doi.org/10.1007/s00018-006-6192-6

Rapić-Otrin, V., V. Navazza, T. Nardo, E. Botta, M. McLenigan, D.C. Bisi, A.S. Levine, and M. Stefanini. 2003. True XP group E patients have a defective UV-damaged DNA binding protein complex and mutations in DDB2 which reveal the functional domains of its p48 product. *Hum. Mol. Genet.* 12:1507–1522. http://dx.doi.org/10.1093/hmg/ddg174

Richly, H., L. Rocha-Viegas, J.D. Ribeiro, S. Demajo, G. Gundem, N. Lopez- Bigas, T. Nakagawa, S. Rospert, T. Ito, and L. Di Croce. 2010. Transcriptional activation of polycomb-repressed genes by ZRF1. *Nature.* 468:1124–1128. http://dx.doi.org/10.1038/nature09574

Riedl, T., F. Hanaoka, and J.M. Egly. 2003. The comings and goings of nucleotide excision repair factors on damaged DNA. *EMBO J.* 22:5293–5303. http:// dx.doi.org/10.1093/emboj/cdg489

Shiyanov, P., A. Nag, and P. Raychaudhuri. 1999. Cullin 4A associates with the UV-damaged DNA- binding protein DDB. *J. Biol. Chem.* 274:35309– 35312. http://dx.doi.org/10.1074/jbc.274.50.35309

Sugasawa, K., J.M. Ng, C. Masutani, S. Iwai, P.J. van der Spek, A.P. Eker, F. Hanaoka, D. Bootsma, and J.H. Hoeijmakers. 1998. Xeroderma pigmentosum group C protein complex is the initiator of global genome nucleotide excision repair. *Mol. Cell.* 2:223–232. http://dx.doi.org/10 .1016/S1097-2765(00)80132-X

Sugasawa, K., T. Okamoto, Y. Shimizu, C. Masutani, S. Iwai, and F. Hanaoka. 2001. A multistep damage recognition mechanism for global genomic nucleotide excision repair. *Genes Dev.* 15:507–521. http://dx.doi.org/10 .1101/gad.866301

Sugasawa, K., Y. Okuda, M. Saijo, R. Nishi, N. Matsuda, G. Chu, T. Mori, S. Iwai, K. Tanaka, K. Tanaka, and F. Hanaoka. 2005. UV-induced ubiquitylation of XPC protein mediated by UV-DDB-ubiquitin ligase complex. *Cell.* 121:387–400. http://dx.doi.org/10.1016/j.cell.2005.02.035

Tang, J.Y., B.J. Hwang, J.M. Ford, P.C. Hanawalt, and G. Chu. 2000. Xeroderma pigmentosum p48 gene enhances global genomic repair and suppresses UV-induced mutagenesis. *Mol. Cell.* 5:737–744. http://dx.doi.org/10 .1016/S1097-2765(00)80252-X

Thorslund, T., A. Ripplinger, S. Hoffmann, T. Wild, M. Uckelmann, B. Villumsen, T. Narita, T.K. Sixma, C. Choudhary, S. Bekker-Jensen, and N. Mailand. 2015. Histone H1 couples initiation and ampli cation of

ubiquitin signalling after DNA damage. *Nature.* 527:389–393. http://dx .doi.org/10.1038/nature15401

Ui, A., Y. Nagaura, and A. Yasui. 2015. Transcriptional elongation factor ENL phosphorylated by ATM recruits polycomb and switches off transcription for DSB repair. *Mol. Cell.* 58:468–482. http://dx.doi.org/10.1016/j .molcel.2015.03.023

Wakasugi, M., and A. Sancar. 1999. Order of assembly of human DNA repair excision nuclease. *J. Biol. Chem.* 274:18759–18768. http://dx.doi.org/10 .1074/jbc.274.26.18759

Wang, H., L. Wang, H. Erdjument-Bromage, M. Vidal, P. Tempst, R.S. Jones, and Y. Zhang. 2004. Role of histone H2A ubiquitination in Polycomb silencing. *Nature.* 431:873–878. http://dx.doi.org/10.1038/nature02985

Wang, H., L. Zhai, J. Xu, H.Y. Joo, S. Jackson, H. Erdjument-Bromage, P. Tempst, Y. Xiong, and Y. Zhang. 2006. Histone H3 and H4 ubiquitylation by the CUL4-DDB-ROC1 ubiquitin ligase facilitates cellular response to DNA damage. *Mol. Cell.* 22:383–394. http://dx.doi.org/10.1016/j.molcel.2006.